



Detection of Epileptic Seizures with Multi-modal Signal Processing

Conradsen, Isa

Publication date:
2013

Document Version
Publisher's PDF, also known as Version of record

[Link back to DTU Orbit](#)

Citation (APA):
Conradsen, I. (2013). *Detection of Epileptic Seizures with Multi-modal Signal Processing*. DTU Elektro.

General rights

Copyright and moral rights for the publications made accessible in the public portal are retained by the authors and/or other copyright owners and it is a condition of accessing publications that users recognise and abide by the legal requirements associated with these rights.

- Users may download and print one copy of any publication from the public portal for the purpose of private study or research.
- You may not further distribute the material or use it for any profit-making activity or commercial gain
- You may freely distribute the URL identifying the publication in the public portal

If you believe that this document breaches copyright please contact us providing details, and we will remove access to the work immediately and investigate your claim.

Isa Conradsen

Detection of Epileptic Seizures with Multi-modal Signal Processing

PhD thesis, March 2012

© Isa Conradsen, 2012

All rights reserved. No part of this publication may be reproduced or transmitted, in any form or by any means, without permission.

Technical University of Denmark
Department of Electical Engineering
DK-2800 Kgs. Lyngby
Denmark

Submitted in partial fulfillment of the requirements for the degree of Doctor of Philosophy at Technical University of Denmark.

PREFACE

The research providing the foundation of this PhD dissertation has been carried out in the Biomedical Engineering section at the Department of Electrical Engineering, Technical University of Denmark (DTU) in cooperation with the Department of Neurophysiology at the Danish Epilepsy Center, Dianalund, Denmark, in partial fulfillment of the requirements for the degree of Doctor of Philosophy in Engineering.

The research work presented in this dissertation have been carried out over a period of three years, along with other activities such as teaching biomedical signal processing, participating in conferences and supervising students through bachelor and master projects.

The dissertation consists of a summary report and seven research papers written during the period 2009-2012. Six of them are published, and the last one is submitted.

Isa Conradsen

Lyngby, March 2012

ACKNOWLEDGEMENTS

First of all, my deepest appreciation goes to my supervisors Associate Professor, PhD Helge B.D. Sørensen and Associate Professor, PhD Thomas Sams from the Technical University of Denmark and Associate Professor, PhD Sándor Beniczky from the Danish Epilepsy Center for providing continuous support and guidance throughout the project. Also, I want to thank Professor, MD, PhD Peter Wolf for letting me draw on his extensive knowledge within the field of epilepsy.

The staff at the EMU at the Danish Epilepsy Center and the EMU at the Danish University Hospital, Rigshospitalet deserve a thankful mentioning for welcoming me at the sites and for helping me acquire the data I needed for this research. Special thanks goes to Chief Physicians Sándor Beniczky and Troels W. Kjær for making it possible and to Daniella Terney, Edina Varga, Anne-Bodil Harrild, Minna Litman and Lennart Derm for help with the data collection and recordings.

Kim Gommesen (IctalCare A/S) deserves my deepest gratitude for establishing a fruitful cooperation with us and furthermore providing us with wireless sEMG data. Furthermore, Karsten Hoppe (DELTA) deserves thanks for his valuable contributions to discussions on sEMG signals.

I want to thank current and former colleagues. Especially my office mate Jonas Duun-Henriksen for the collaboration, wide discussions and reviewing part of this dissertation. Grateful appreciation as well goes to Marie S. Enevoldsen for reviewing this dissertation and at last these two along with my other fellow "Medtekkere" Joachim Hee Rasmussen and Michael Pihl deserve thanks for good spirit during my time as a PhD student. In addition, Elna Sørensen and Henrik Laursen, deserve many thanks for their always kind help.

Also I would like to thank all the PhD students in the Biomedical Signal Processing group for a joyful working environment and valuable discussions.

Finally, I would like to thank my very best friend and life companion Martin Erikshøj, first of all for proofreading this dissertation, but most of all for always being there to encourage and support me.

ABSTRACT

The main focus of this dissertation lies within the area of epileptic seizure detection. Medically refractory epileptic patients suffer from the unawareness of when the next seizure sets in, and what the consequences will be. A wearable device based on uni- or multi-modalities able to detect and alarm whenever a seizure starts is of great importance to these patients and their relatives, in the sense, that the alert of the seizure will make them feel more safe. Thus the objective of the project is to investigate the movements of convulsive epileptic seizures and design seizure detection algorithms for these based on uni- or multi-modalities. Regarding seizure detection, the highest potential clinical relevance is for the generalized tonic-clonic (GTC) seizures, as these are associated with an increased risk for sudden unexpected death in epilepsy (SUDEP) in unsupervised patients.

Several methods have been applied in different studies in order to achieve the goal of reliable seizure detection. In the first study we present a method where the support vector machine classifier is applied on features based on wavelet bands. This was used on multi-modal data from control subjects, with the result that the inclusion of more modalities provided a better performance. We succeeded in performing a multi-modal recording of a GTC seizure from an epileptic patient, and a visual analysis of the data showed that it was similar to the data from our control subjects, only more pronounced. Based on this we expected the algorithm to perform better on the patient data as well if more modalities were used. The presented algorithm proved to be able to detect epileptic tonic and GTC seizures based on one modality, surface electromyography (sEMG), but it did not prove to be sufficient for the other convulsive seizures tested.

Another study was performed, involving quantitative parameters in the time and frequency domain. The study showed, that there are several differences between tonic seizures and the tonic phase of GTC seizures and furthermore revealed differences of the epileptic (tonic and tonic phase of GTC) and simulated seizures. This was valuable information concerning a seizure detection algorithm, and the findings from this research provided evidence for a change in the definition of these seizures by the International League Against Epilepsy (ILAE).

Our final study presents a novel seizure detection algorithm for GTC seizures based on sEMG from a

single channel. The algorithm is simple, based on a high-pass filter and a count of zero-crossings, in order to ease the implementation into a small wireless sEMG device. The algorithm proved to be reliable, and was after minor changes implemented in a wireless sEMG device. A double-blind test on patients in the clinic, showed 100 % reliability for three of four patients, whereas it failed for the last patient, who had atypical GTC seizures.

RESUMÉ

Denne afhandlings hovedfokus er detektion af epileptiske anfald. Medicinsk refraktære epileptiske patienter lider under uvisheden om, hvornår det næste anfald starter, og eventuelle konsekvenser heraf. Disse patienter og deres pårørende vil derfor have stor gavn af et bærbart apparat, der ud fra et uni- eller multimodalt system, er i stand til at detektere og alarmere, når der opstår et epileptisk anfald. Bevistheden om at de pårørende vil blive advaret, når et anfald starter, vil bevirke, at såvel pårørende som patienter kan føle sig mere trygge i hverdagen. Formålet med projektet har været, at udforske bevægelserne under krampagtige epileptiske anfald og designe en algoritme til at detektere disse på baggrund af et uni- eller multimodalt system. Inden for anfaldsdetektion er det de generaliserede tonisk-kloniske (GTC) anfald, der har størst relevans, idet disse er forbundet med en øget risiko for *sudden unexpected death in epilepsy* (SUDEP) hos uovervågede patienter.

Undervejs har vi udviklet flere metoder for at opnå en pålidelig algoritme til anfaldsdetektion. I vores første studie præsenterer vi en algoritme, der anvender *support vector machine* (SVM) klassifikatoren på features baseret på wavelet bånd. Test på multimodale data fra kontrolpersoner viste, at inddragelsen af flere modaliteter gav bedre resultater. Vi havde succes med at optage et GTC anfald fra en epilepsipatient monteret med alle vores modaliteter. En visuel analyse af data viste, at de simulerede epileptiske anfald målt på vores kontrolpersoner var sammenlignelige med dette anfald. Den eneste forskel bestod i, at det epileptiske anfald var mere udtalt. Ud fra disse observationer forventer vi, at algoritmen også vil virke tilsvarende bedre på patient data, hvis der bliver inkluderet flere modaliteter. Den præsenterede algoritme er i stand til at detektere toniske og GTC anfald baseret på én modalitet, overflade elektromyografi (sEMG), men den er ikke tilstrækkelig i forhold til andre typer af krampagtige epileptiske anfald.

I vores andet studie sammenholdt vi kvantitative parametre fra både tids- og frekvensdomænet, og fandt flere forskelle imellem toniske anfald og den toniske fase af et GTC anfald. Desuden opdagede vi forskelle imellem epileptiske anfald (tonisk og den toniske fase af et GTC anfald) og simulerede anfald, der kan være værdifuld information i forhold til en algoritme til anfaldsdetektion. De opnåede resultater præsenterer ny viden, der opfordrer til en ændring i definitionen af de to typer epileptiske anfald af *International League Against Epilepsy* (ILAE).

Vores sidste studie præsenterer en ny algoritme til detektion af GTC anfald baseret alene på sEMG fra en enkelt kanal. Algoritmen er holdt enkelt og baseret på et højpas filter, samt en optælling af signalets nulgennemgange, for at muliggøre implementeringen af algoritmen i et lille trådløst sEMG device. En dobbelt blindtest udført på patienter i klinikken demonstrerede 100 % pålidelighed for tre af fire patienter. Devicet fejlede for den sidste patient, der havde atypiske GTC anfald og dermed må ses som en outlier.

NOMENCLATURE

A	is the approximation signal
C	is a trade-off factor
D	is the detail signal
G	is the cross-spectrum
L	is the number of samples in $u(l)$
R	is a reconstructed signal
S	is the coherence
U	is the discrete frequency spectrum
a	is the feature vector for ACM
b	is the feature vector for ANG
b	is a shifting constant
c	is the feature vector for EMG
f	is the frequencies
f_{MF}	is the median frequency
f_s	is the sampling frequency
g	is a low-pass filter
h	is a high-pass filter
j	is a resolution or scale parameter
k	is the translation parameter
m	is the window number

n is a time index

$u(l)$ is one window of the signal of a single channel (modality: EMG, ACM, ANG)

\mathbf{w} is a weight vector

\mathbf{x} is the combined feature vector

x is a single input in the feature vector

y is the target vector

z is the coherence after introducing Fisher's transform

z_{MA} is the coherence after introducing a moving average filter

ξ is a positive slack variable

φ is the scaling function

ψ is the wavelet function

ABBREVIATIONS

3D	3 dimensional
ACM	ACceleroMeter
ANG	ANGular velocity
ANN	Artificial Neural Network
CNS	Central Nervous System
CWT	Continuous Wavelet Transform
DWT	Discrete Wavelet Transform
EEG	ElectroEncephaloGraphy
ECG	ElectroCardioGraphy
EMG	ElectroMyoGraphy
EMU	Epilepsy Monitoring Unit
FDR	False Detection Rate
FFT	Fast Fourier Transform
FIR	Finite Impulse Response
FP	False Positive
GTC	Generalized Tonic-Clonic
ILAE	International League Against Epilepsy
LAT	LATency
MA	Moving Average
MF	Median Frequency
MU	Motor Unit

MUAP	Motor Unit Action Potential
REC	Regional Ethics Committee
RMS	Root Mean Square
RP	Relative Power
SD	Standard Deviation
sEMG	surface EMG
SEN	SENSitivity
STFT	Short Time Fourier Transformation
SUDEP	Sudden Unexpected Death in EPilepsy
SVM	Support Vector Machine
WPT	Wavelet Packet Transformation

CONTENTS

Preface	v
Acknowledgements	vii
Abstract	ix
Resumé	xi
Nomenclature	xiii
Abbreviations	xv
1 Introduction	1
1.1 Thesis outline and contributions	2
2 Preliminaries	5
2.1 Epilepsy	5
2.2 The modalities	6
2.3 Data acquisition	12
3 Detection of Epileptic Seizures with Multi-modal Signal Processing	15
3.1 Background	15
3.2 Recordings	16
3.3 Data presentation	19
3.4 Methods	22
3.5 Results	32
3.6 Discussion	36
3.7 Conclusion	37
4 Investigation of Generalized Tonic and Tonic-Clonic Seizures	39

4.1	Background	39
4.2	Methods	40
4.3	Results	44
4.4	Discussion	49
4.5	Conclusion	50
5	Detection of Generalized Tonic-Clonic Epileptic Seizures	53
5.1	Background	53
5.2	Recordings	54
5.3	Methods	56
5.4	Results	63
5.5	Discussion	67
5.6	Conclusion	71
6	Conclusion	73
6.1	Future perspectives	74
	Bibliography	75
A	Tutorial	83
B	Multi-modal Patient Data	107
C	sEMG Patient Data	115
D	Filter specifications	119
	Paper I	121
	Paper II	129
	Paper III	135
	Paper IV	151
	Paper V	161
	Paper VI	167
	Paper VII	177

INTRODUCTION

Epilepsy is a neurological disorder, with a world-wide prevalence of 0.5-1% [24]. It is a serious and comprehensive disorder, and several aspects of it is still not fully described or understood. The gold standard used for analysis and diagnosis is the electroencephalography (EEG) combined with simultaneous video surveillance. Many seizures consist of motor manifestations, but most of these are only vaguely described. More information on the exact activity in the implicated muscles might improve the understanding of the seizures, and furthermore ease the way to discriminate the seizures from normal activities.

About one third of epilepsy patients is medically refractory [29, 44, 70], meaning that they have to live with seizures in their everyday lives. For these patients and their relatives the development of a reliable epilepsy seizure detection device is of great importance. EEG is known to be reliable for seizure detection, but this is only an advantage in a hospitalized situation, where the patient is equipped with either intracranial electrodes or several scalp electrodes. In a home situation other devices for measurements of the pathological signals are more appropriate, such as the novel (with respect to epilepsy) methods measuring signals describing the movements of the patients.

Thus the goal of the project is to explore the potentials of automatic seizure classification based on one or multiple modalities, recording the movements of the patients, as stated in the thesis objective below. The process of designing the perfect algorithm for seizure detection is complex. Some of the possible ways to choose from are outlined in Fig. 1.1. This dissertation presents both a multi-modal and a uni-modal solution. Our multi-modal approach is marked by the blue boxes, whereas the uni-modal approach is marked by the orange boxes in Fig. 1.1.

<p>Objective - to investigate the movements of convulsive epileptic seizures and design seizure detection algorithms for these based on uni- or multi-modalities.</p>

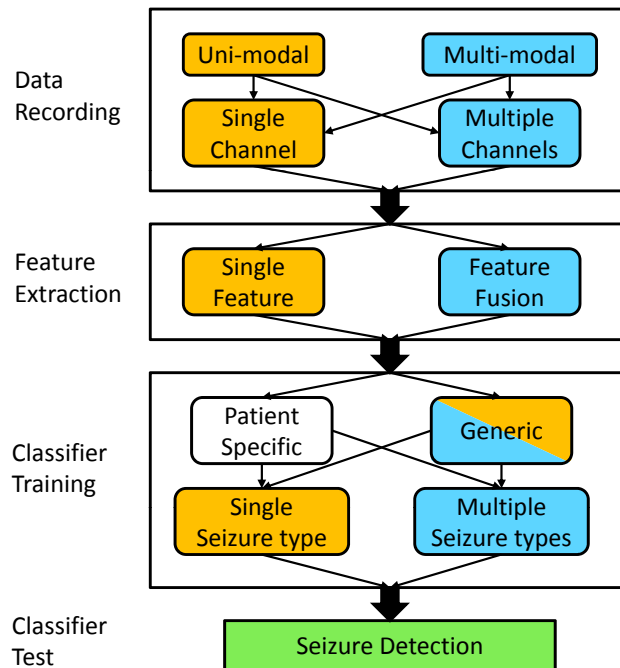


Figure 1.1: This figure presents a stepwise process toward seizure detection. We have engaged the process of seizure detection by dividing it into four steps. The four steps chosen are: data recording, feature extraction, classifier training and test of classifier (seizure detection). Within the first three steps different choices are available. Between the third and the last step it is possible to add an extra step called classifier fusion, where several classifiers, may be included to make the final decision (seizure versus non-seizure).

1.1 Thesis outline and contributions

This thesis is structured in three parts to illustrate the progress of the research that has been conducted. Besides this it contains an introduction, preliminaries and a conclusion. The accepted and submitted publications are found in the appendix.

Chapter 2 provide the theoretic basis of epilepsy and the used modalities, and presents the basics for the uni- and multi-modality recordings.

Chapter 3 presents the results of our algorithm for seizure detection based on multiple motion modalities. It compares the results for a uni- and multi-modal method. This work is presented in Paper I-III and is designed from the idea of following the blue path in Fig. 1.1.

Chapter 4 presents the results of Paper IV, which brings new knowledge of the muscle activation of the involved seizure types and furthermore the opportunities for use of the knowledge in a seizure detection algorithm.

Chapter 5 presents a uni-modal detection algorithm, which is developed based on the knowledge gained from Chapter 4. The design of the algorithm have at this point changed to the orange path in Fig. 1.1. Furthermore the results from the implementation of this algorithm into a wireless device is presented. This work is presented in Paper V-VII.

Chapter 6 encompasses the final conclusion on the results of the project and the ideas of where to proceed.

The contribution to the field of knowledge on epileptic seizures with motor manifestations and the devsign of seizure detection algorithms during this PhD project covers three published journal articles, three published conference papers, and one submitted conference paper, as well as two published co-authored conference papers. These are listed as follows:

Journal papers

- I. Conradsen, S. Beniczky, P. Wolf, T.W. Kjaer, T. Sams, and H.B.D. Sorensen, "*Automatic multi-modal intelligent seizure acquisition (MISA) system for detection of motor seizures from electromyographic data and motion data*", Computer Methods and Programs in Biomedicine, published online, July 2011.
- I. Conradsen, P. Wolf, T. Sams, H.B.D. Sorensen, and S. Beniczky, "*Patterns of muscle activation during generalized tonic and tonic-clonic epileptic seizures*", Epilepsia, 52(11):2125-2132, 2011.
- I. Conradsen, S. Beniczky, K. Hoppe, P. Wolf, and H.B.D. Sorensen, "*Automated Algorithm for Generalised Tonic-Clonic Epileptic Seizure Onset Detection based on sEMG Zero-Crossing Rate*", IEEE Transaction on Biomedical Engineering, 59(2):579-585, 2012.

Conference papers

- I. Conradsen, S. Beniczky, P. Wolf, D. Terney, T. Sams, and H.B.D. Sorensen, "*Multi-modal Intelligent Seizure Acquisition (MISA) system - A new approach towards seizure detection based on full body motion measures*", Engineering in Medicine and Biology Society (EMBC), 2009 Annual International Conference of the IEEE, 1:2591-2595, 2009.
- I. Conradsen, S. Beniczky, P. Wolf, J. Henriksen, T. Sams, and H.B.D. Sorensen, "*Seizure Onset Detection based on a Uni-or Multi-modal Intelligent Seizure Acquisition (UISA/MISA) system*", Engineering in Medicine and Biology Society (EMBC), 2010 Annual International Conference of the IEEE, 1:3269-3272, 2010.
- I. Conradsen, S. Beniczky, K. Hoppe, P. Wolf, T. Sams, and H.B.D. Sorensen, "*Seizure Onset Detection based on one sEMG channel*", Engineering in Medicine and Biology Society (EMBC), 2011 Annual International Conference of the IEEE, 1:7715-7718, 2011.

- I. Conradsen, S. Beniczky, P. Wolf, P. Jennum, and H.B.D. Sorensen, "Evaluation of novel algorithm embedded in a wearable sEMG device for seizure detection", Submitted to Engineering in Medicine and Biology Society (EMBC), 2012 Annual International Conference of the IEEE.

Co-authored papers

- T.L. Sorensen, U.L. Olsen, I. Conradsen, J. Henriksen, T.W. Kjaer, C.E. Thomsen, and H.B.D. Sorensen, "Automatic epileptic seizure onset detection using Matching Pursuit: A case study", Engineering in Medicine and Biology Society (EMBC), 2010 Annual International Conference of the IEEE, 1:3277-3280, 2010.
- J. Henriksen, L.S. Remvig, R.E. Madsen, I. Conradsen, T.W. Kjaer, C.E. Thomsen, and H.B.D. Sorensen, "Automatic seizure detection: going from sEEG to iEEG", Engineering in Medicine and Biology Society (EMBC), 2010 Annual International Conference of the IEEE, 1:2431-2434, 2010.

PRELIMINARIES

Objective *Epilepsy is a neurological disorder defined as a property of the central nervous system (CNS) to produce seizures. There are many different kinds of epileptic seizures, where both the cause, the origin and the symptoms may be very different. Though EEG recordings and video surveillance is the gold standard, other modalities have been used to gain more information about these seizures. However, there are still parts of the seizures, which are not fully understood, and which may be more clear if more information is provided from novel modalities. This may furthermore lead to promising features for a seizure detection system. Thus, this chapter will present the basic knowledge on epilepsy together with the modalities used in this project and the basic setup of the data acquisitions.*

2.1 Epilepsy

Epilepsy is the second most common acute neurological disorder, where the severeness of epilepsy spans from trivial to life-threatening [61]. The diagnosis of epilepsy is very strict, and requires a least two seizures in the patients history, which cannot reasonably well be explained by other diseases. Epileptic seizures are caused by an abnormal excessive or synchronous neural activity in the brain [28]. This may produce impaired consciousness, abnormalities of sensation or mental functioning, or convulsive movements.

Epileptic seizures are grouped in two major types: partial and generalized seizures. Partial seizures are characterized by an abnormal discharge from a relatively limited area of the brain structure. Thus, they are also known as focal or local seizures. These seizures only have limited behavioral, mental, sensory or motor expressions. Contrary to this, generalized seizures involves more widespread parts of the brain and both hemispheres simultaneously. Furthermore, they are characterized by a loss of consciousness. The partial seizures can be divided into simple and complex partial seizures, depending on whether the consciousness of the patient is retained or affected. Furthermore, partial seizures may lead to generalized

seizures, which is referred to as a secondary generalization.

Generalized seizures are divided in six general types:

Absences are seizures where the patients become absent. It may be visualized by a blank stare or other facial signs, indicating the impaired consciousness. The intentional behavior or memory is disrupted, but the posture and muscle tone is usually unaffected [61].

Myoclonia are twitches of one or more body parts which last shorter than 100 milliseconds. These are caused by a synchronous activity of the motor units. Myoclonia can occur alone or in sequences, where the consciousness is usually preserved. Often the sequences end up in generalized cramps [1].

Tonic seizures are characterized by a universal increase of tonus in the body and the extremities lasting about 5-10 seconds [1].

Clonic seizures are repeated rhythmically muscle contractions. Normally they repeat themselves about 0.2 to 5 times per second [1].

Tonic-Clonic (GTC) seizures have two sequential phases: the tonic phase (10-20 seconds) followed by a clonic phase (1/2-2 minutes) [61].

Astatic/atonic seizures are extremely short loss of axial tonus [1].

All epileptic seizures are sketched and grouped in Fig. 2.1. For this project the topic was to detect epileptic seizures based on data from movement modalities. Based on this, only the convulsive seizures (see Fig. 2.1) has been taken into account, when selecting criteria for the inclusion of patients for our recordings. In cases where a patient has more than one type of seizures, only the convulsive seizures are assessed.

2.2 The modalities

Several modalities have been examined during the years when investigating epilepsy. Where EEG and video surveillance are the gold standard, also electrocardiography (ECG) is recorded in most surveillance sessions of epilepsy patients. The more novel modalities in the field of epilepsy are surface electromyography (sEMG), accelerometers and gyroscopes, which all represent part of the patients movements during and between seizures.

The focus of this project has been to design algorithms for detection of epileptic seizures with motor manifestations based on these three novel modalities (sEMG, accelerometers and gyroscopes) outlining the movements of the patients. sEMG data were easy to obtain since this modality was already included as part of the recording on patients in the epilepsy monitoring unit (EMU) in Dianalund, in cases where

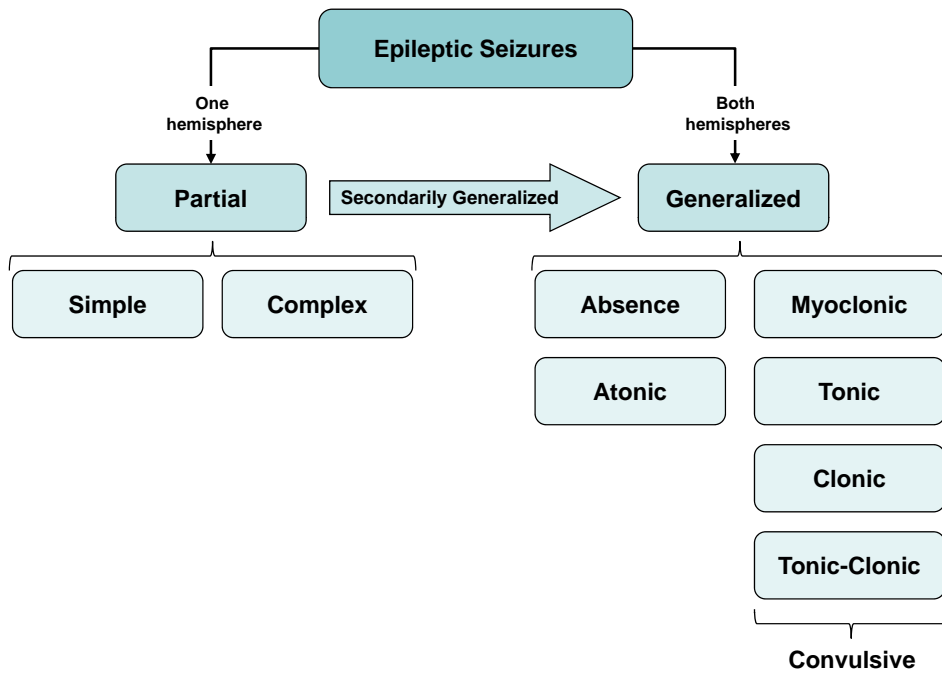


Figure 2.1: The division of epileptic seizures into partial and generalized seizures. Furthermore the group of convulsive seizures, which we focus on, is displayed.

it was expected to add valuable information (patients with seizures with motor manifestations). For the other two modalities Assoc. Professor H.B.D. Sørensen advised to acquire the Moven system from Xsens Technologies B.V., which we did early in the project period. This section briefly describes these modalities.

2.2.1 Electromyography

Electromyography (EMG) is a technique for measuring the electrical potential generated by the muscle cells during contractions. The amplitude of the signal is related to the force developed in the muscle. The size of this force is dependent on the amount of motor units (MU)s recruited in the muscle and the number of muscle fibers in each MU. An MU consists of a motor nerve and the corresponding muscle fibers it innervates [75].

The motor nerve provides a signal, which at the innervation point of each muscle fiber can trigger the release of an action potential. The sum of these action potentials for an MU is called motor unit action potential (MUAP). The sEMG signal, which we are measuring in this project is then a sum of all MUAPs in the muscle [75].

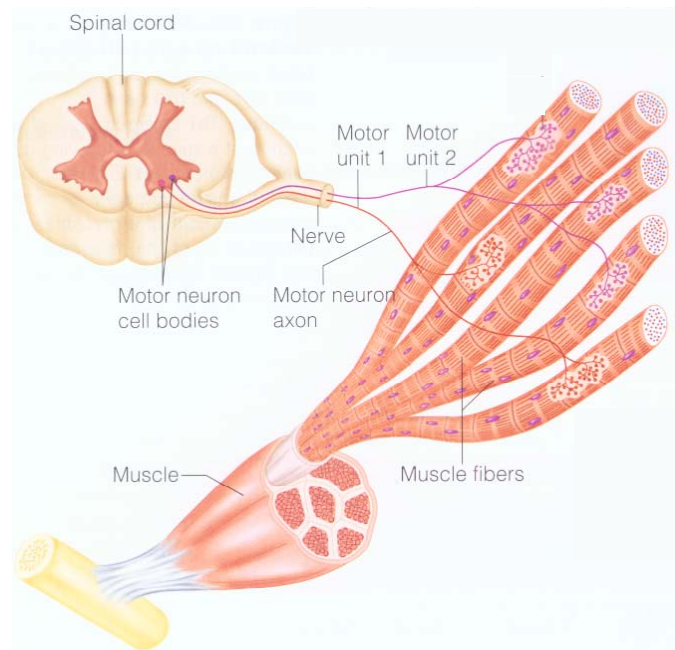


Figure 2.2: Illustration of the components involved in the generation of the EMG signal. The figure is from [50].

The force development in a muscle is controlled by the nervous system by three mechanisms:

- Change in the number of active MUs (recruitment), where the smallest MUs are recruited first.
- Change in the firing rate (the time between the release of MUAPs).
- Synchronizing the MUs. This makes the contraction stronger. Normally, the MUs are desynchronized to make the movement more smooth.

The components involved in the generation of the EMG signal are illustrated in Fig. 2.2.

Before the signal is registered by the sEMG electrode it has been dampened by the connective tissue in the muscle, fat and skin, which it has been traveling through. Furthermore, the biological tissue functions as a low-pass filter, which means that the higher frequencies have been dampened more than the lower frequencies in the signal [75].

The sEMG signals are measured by 9 mm silver/silver chloride (Ag^+/AgCl) surface electrodes from Ambu (Ambu®Neuroline 720 15-K). An example is shown in Fig. 2.3. The electrodes have standard sockets, making it possible to measure the sEMG signals along with the EEG signals in the EEG-amplifier, which we have done for the recordings in this project.

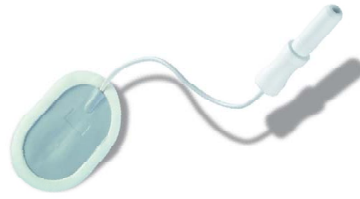


Figure 2.3: The 9 mm silver/silver chloride surface electrode, Ambu®Neuroline 720 15-K, used to measure sEMG signals in our project [4].

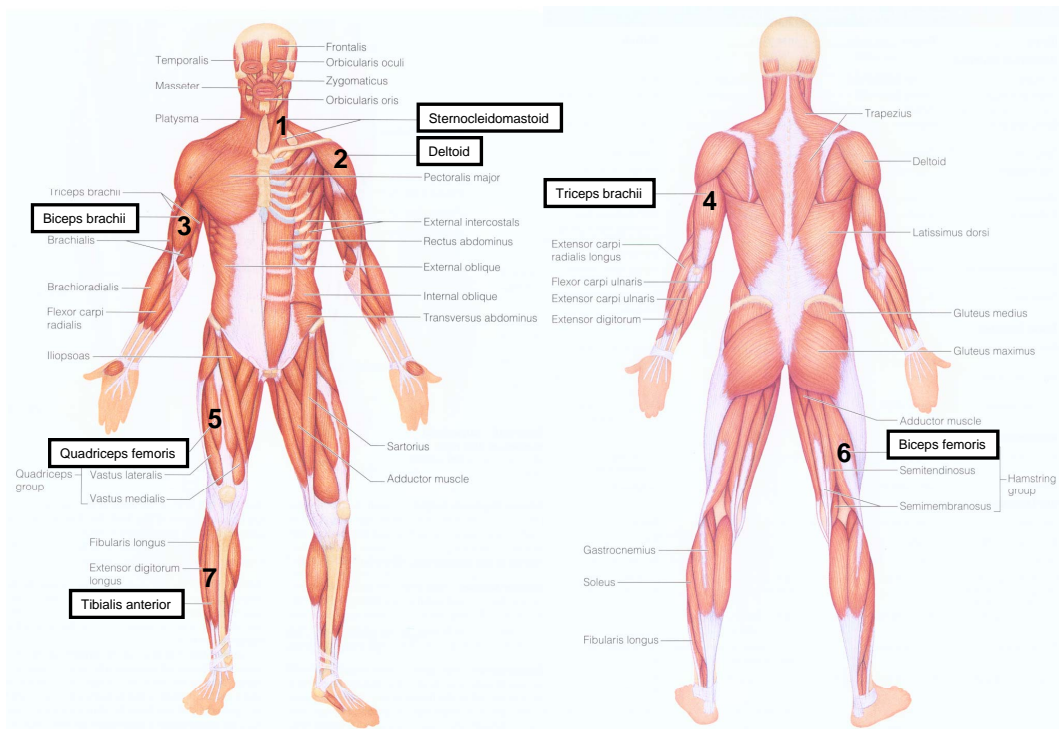


Figure 2.4: The placements of sEMG electrodes used in recordings associated with this project. Modified from [50].

Depending on the patients capability to cooperate on wearing the electrodes, we used more or less sEMG electrodes. The included muscles were chosen by a physician based on the knowledge on which parts of the body are most active during seizures, and to ensure full body coverage. The placements of the electrodes are visualized in Fig. 2.4. If possible, electrodes were placed on the 7 places marked on both the left and right side of the body (14 placements in total). If this was not possible, only placement 2 and 7 were used on both sides of the body (4 placements in total).

The sEMG electrodes were placed on the muscles in a monopolar setting (the active electrode was placed



Figure 2.5: The Movensuit, with all sensors placed in the associated small pockets [89].

on the midpoint of the muscle belly, whereas the reference electrode was placed on bone as close to the muscle as possible. We opted for this setting to circumvent the effects of phase-cancellation that occur in the bipolar setting, when both electrodes are placed on the muscle [8, 51, 79].

2.2.2 Acceleration and angular velocity using the Movens system

The Movens system (MOVEN Full-Body, MVN1, SN:00900077) is a suit (see Fig. 2.5) containing 16 sensors, each containing both 3D accelerometer (ACM), 3D magnetometer and 3D rate of turn sensors (gyroscopes), able to measure full-body movements. The 3D acceleration is measured in the x, y and z direction as showed in Fig. 2.6, whereas the angular velocity (ANG) is measured as the rotation around the three axes as indicated in Fig. 2.6 by the curved arrows. Advanced sensor fusion is applied using the magnetometer data to orientate the acceleration and angular velocity data to a global coordinate system (magnetic north) instead of the ones of each sensor. This makes the x-axis point in the north-south direction, the y-axis in the east-west direction and the z-axis points toward the center of the earth. An advanced articulated body model is used in the Movens system software, which implements constraints of the joints, and lengths of the limbs to estimate 7 extra placements (shown as position 2, 3, 4, 5, 6, 19 and 23 in Fig. 2.7). This gives a total of 23 sensor placements, see Fig. 2.7, and thus the possibility of a full body description of the movement of the subject. This is however not the focus in this project. From each placement we are able to extract 6 channels of data, since each of the two modalities are in three dimensions.

We focus on the raw transformed (into the coordinate system with magnetic north) signals (3D ACM data and 3D ANG), which we could extract. This provided 138 ($2 \times 3 \times 23$) channels, which is a lot when

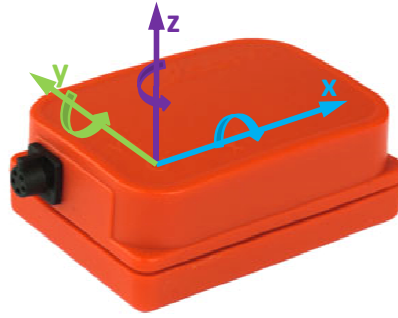


Figure 2.6: A Moven sensor and the original axes x , y and z , of the sensor. The curved arrows illustrates the rotation, which is measured by the 3D rate of turn sensors. Modified from [89].

considering the computational load in a detection algorithm. To decrease this number and thereby the computational load regarding the feature extraction, we used the length of the direction vector both for ACM and ANG instead of the three dimensional (3D) coordinates, x , y and z (e.g. for ACM):

$$ACM = \sqrt{ACM_x^2 + ACM_y^2 + ACM_z^2} \quad (2.1)$$

This process will induce some loss of information, but in order to decrease the computational load, we decided to apply this procedure instead of lowering the number of sensors (amount of placements on the body). Since we are more interested in the strength and frequency of the movements and not the orientation, the loss is not considered further. From this preprocessing of data we were left with 46 channels of data in total from these two modalities.

The signals are sampled with a frequency of 120 Hz, which was the highest possible, when we received the system in 2008. The maximum limits of the two modalities are specified to 21 rad/s for the rate of turn sensors, and 50 m/s² for the accelerometer. Since the system is made for human movements it is expected to be enough for both the physiological and the pathological activities of the patients.

The sensors are connected through wires and the signals are collected in two boxes, which are synchronized and sends the signals via blue-tooth to a computer. The data files are recorded and saved as .mvn-files by the appurtenant Moven program. These files can only be read by this specific program, but a conversion into an .mvnx-file is possible, using HTML code. This makes it possible to read it into MATLAB, which is the main programming tool used in this research project. Further information on the system may be found in the corresponding manuals or at the company's web-page [89].

The system only came with one suit (size: L), and only adult sizes were available. Thus we designed four extra suits (size: 3-6 years(y), 6-9 y, 9-16 y, and XL). Values for the normal height ranges for the different ages were found, and the placement of the pockets were calculated, with respect to the length of the suit, with help from anthropometric data [75]. We were forced to adjust some of the settings during

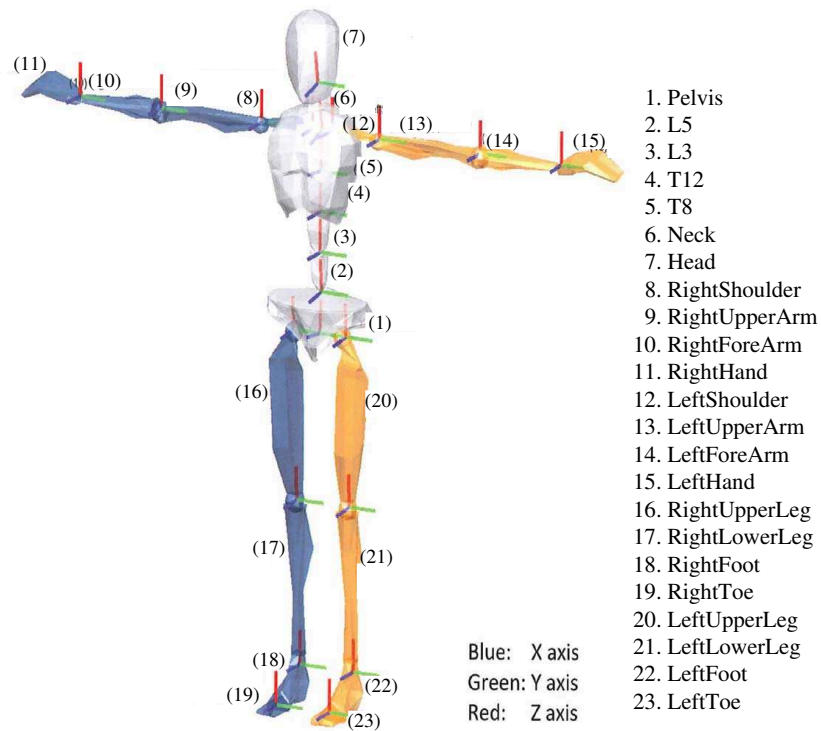


Figure 2.7: The placement of the sensor positions from the Moven system, see the Manual for Moven, revision D, June, 2008 [89].

the project, due to complications when using the suit on patients.

From the basis of manuals that came with the Moven system, we composed a manual (see appendix A), to instruct the user, when using the system in a hospital setting. With all the equipment achieved and the manual ready, we applied the Regional Ethics Committee (REC) for approval of recording with the Moven system on patients/control subjects along with the standard equipment in an EMU [14]. The approval was granted on April 15, 2009, enabling us to initiate our measurements in May, 2009.

2.3 Data acquisition

The recording of data is divided into two possibilities; multi-modal or uni-modal, where the terms only refer to the movement modalities. In all data acquisition the gold standard and ECG are recorded.

Multi-modal Acquisition

Where the patient was able to wear all our equipment, sEMG was measured from 14 placements on the body and furthermore the Moven system was mounted. In these measurement we were responsible for the mounting of all this equipment and furthermore for regular check up on the recording of these data. The collection of data was a major time-consumer within the project.

Uni-modal Acquisition

Besides from the multi-modal recordings, the staff at the Danish Epilepsy Center, mounted the patients in the EMU with sEMG electrodes (4-14 placements depending on the patient), where convulsive seizures were expected and the patient was able to cooperate to wear the electrodes.

DETECTION OF EPILEPTIC SEIZURES WITH MULTI-MODAL SIGNAL PROCESSING

Objective *Many different approaches have been followed to develop the optimal seizure detection algorithm for on-line use. It has turned out to be a challenging task. The reason for this is probably the high expectations associated with the results. For a detection algorithm to be useful it is essential that it achieves a sensitivity as close to 100% and at the same time as close to 0 false positives as possible. Thus many different attempts have been made to develop such an algorithm, where most have been based on a single modality, EEG, ECG or ACM, and only few have combined more modalities to strengthen the algorithm. This chapter is composed upon Paper I-III and serves to show the advantage of building a seizure detection algorithm on more than one modality.*

3.1 Background

The majority of previous studies has used single-modality detection [22, 23, 38, 40, 43, 45, 55, 58, 71]. To our knowledge only few other groups have combined more modalities in an attempt to detect seizures [7, 9, 47, 66] with respect to movement modalities. Though we did expect that a combination of more modalities would improve the results. The first goal was to show whether an algorithm would gain on including more modalities. To make this possible a second goal was to develop a database containing all modalities and with as many positions (channels) as possible. Thus it would be optimal if the motion sensors would be able to measure from the entire body. From such a large database it would then be possible to find the optimal combination of the three modalities and their placement on the body, in order to minimize the number of sensors needed.

Based on our first 3 control subjects recorded with all the equipment, we made a preliminary study (Paper I) based on a simple root mean square (RMS) feature [19]. This showed that the idea of gaining from the inclusion of more modalities seemed promising. To test this further we needed features to discriminate between seizure and non-seizure and a detection algorithm to classify based on this. In this setup the choice of feature is of highest importance [52], whereas one classifier might be as good as another, so we chose to work with the one being the most popular within biomedicine at the moment, Support Vector Machine (SVM) [78]. This was partly motivated by the fact that SVM had proven to perform better than e.g. artificial neural network (ANN) in other studies on biomedical signals [46, 64, 76]. The issue was then to identify the most promising features and furthermore the most appropriate classifier parameters to automatically differentiate between the two classes. Nijsen et al. [60] showed through a visual analysis that the continuous wavelet transformation (CWT) seemed to be a better feature than short time Fourier transformation (STFT) for ACM data. Seizure detection from sEMG signals was an even more unexplored field, but from a visual inspection of the data it seemed that both the amplitude and the frequencies of the signal during seizures were different from normal activities. The discrete wavelet transformation (DWT) seemed to be a good choice as a feature extraction method, since it provides a good frequency resolution at low frequencies and furthermore a good time resolution at high frequencies. Based on this we chose to focus our features around the wavelet theory, which is presented in Paper II-III [17, 18].

3.1.1 Research hypotheses

The main hypothesis is that a combination of modalities will have better performance than a uni-modal approach. To verify this we need multi-modal data and an appropriate algorithm for the detection of seizures.

Our hypotheses are:

- to be able to record multi-modal data from a full-body approach.
- to generate an algorithm able to discriminate seizures/simulated seizures from all other activities.
- to find a difference in the outcome, when including features from one or more modalities.

3.2 Recordings

For all recordings, EEG and video were recorded as the gold standard. This was required for the physicians to manually score the onsets and offsets of the epileptic seizures. Besides from the gold standard we also measured ECG, ACM, ANG and sEMG. The recruitment of patients for these measurements was quite difficult, since the patients had to be mentally well functioning and at the same time have many



Figure 3.1: A control subject mounted with EEG, sEMG and the Moven system equipment, simulating a GTC seizure at the Danish Epilepsy Center in Dianalund. The Moven program is running on the laptop, showing the 3D movements of the control subject.

seizures within few days. So, to get started on the signal processing we chose to simulate a normal measurement situation in the EMU on control subjects (healthy volunteers) including simulated seizures specified by a physician as well as normal activities, which are available to the patients during their admission. On Fig. 3.1 one of the control subjects is shown simulating a seizure, while mounted with all the equipment.

3.2.1 Multi-modal recordings on control subjects

Ten control subjects were monitored with all modalities and instructed to simulate seizures. During the recordings, a physician was present to check that the simulated seizures were visually similar to real ones. If they were not, the control subject was corrected and asked to simulate a new seizure. The recordings on control subjects were made at the Danish Epilepsy Center in Dianalund, Denmark. The control subjects had a median age of 25.5 years (range: 23-30), and included three females and seven males. It is assumed that there is no effect of gender. The measurements lasted 1.5-3 hours for each control subject, where all of the control subjects were asked to simulate three types of seizures and some normal activities. The control subjects were orally instructed about how to simulate the seizures and shown a video to give a visual illustration of an actual seizure. Prior to the recording the control subjects rehearsed the simulation of the seizures while assisted by a physician. The normal activities included were biking, use of a mobile phone, use of a computer, changing channels on a TV, eating and playing with dices. The last activity was chosen because of the similarity of the movement to clonic seizures or the clonic phase of GTC seizures. All were activities which the patients are allowed to perform during a normal admission in the EMU at the Danish Epilepsy center in Dianalund, Denmark. Each of the seizures was simulated five times for

each control subject. The times for the simulated seizures were annotated as during a normal admission. The three types of simulated seizures are as follows:

- **Myoclonic**, which is a very short lasting twitch in a single muscle. The control subject is asked to make a contraction of the right biceps brachii as short as possible, which will cause a very short lasting movement of the right lower arm.
- **Versive-asymmetric tonic seizure**, which is characterized by a turn of the head to an almost uncomfortable angle, where the control subject is looking upwards and to the side. This is followed by an isometric contraction in an asymmetric posture, where the arm, on the same side toward which the head is turned, will be placed above the head.
- **GTC seizure**, which starts as an isometric contraction of all the muscles. After a while it changes to rhythmically repetitive jerks made by alternating contraction and relaxation of the muscles.

Where the ACM and ANG data were sampled at a frequency of 120 Hz, the sEMG data were sampled at a frequency of 1024 Hz. The sEMG was applied using all 14 placements (see Fig. 2.4). Each of the surface electrodes were accompanied with its own reference electrode, placed on nearby bone or tendon, as described in section 2.2.1. The sEMG electrodes are connected to the EEG amplifier. The recordings were performed by starting all conventional measurements in the EMU (i.e. all modalities except for the Moven system). When this was up and running, the Moven system was started and the time in the sEMG sampling system was annotated by the neurophysiological assistant, as precisely as possible. All data types were then used from this point and on, whereby they were synchronized. Unfortunately, the sEMG data from the EMU at the Danish Epilepsy Center were filtered before exportation, so to avoid differences, we only analyzed the data with frequencies below 70 Hz.

3.2.2 Multi-modal recordings on patients

We started recruiting patients as soon as we had received the approval from the REC [14] in May 2009. However, the candidates admitted to the EMU in Dianalund generally proved not to be well enough functioning for our equipment or not to have the right type of seizures. In 2010 we moved the Moven system to Rigshospitalet (Copenhagen University Hospital) instead. There we succeeded in recording data from 14 epileptic patients in total, but unfortunately only one of them had seizures of the type with motor manifestations, which we focused on (myoclonic, tonic, GTC), during the recordings. As stipulated by the REC, all the epileptic patients were admitted to the EMU at Rigshospitalet for a diagnostic indication. The admissions lasted 1-3 days. The one patient with seizure, a 29 years old male, had only one seizure of the GTC seizure type. The onset and offset for the seizure was clinically annotated by the neurophysiology technicians and later checked by a physician. For this measurement the sEMG data were sampled at a frequency of 1000 Hz. The reason for the use of different sampling frequencies for the sEMG data is

that the two participating departments use different recording programs with different setup possibilities for the sampling frequencies. Furthermore, due to the use of caps for the EEG recordings on the patients at Rigshospitalet we were not able to use the head sensor (position 7 in Fig. 2.7), hence, due to the biomechanical calculations in the software, data are unfit for use for three positions (position 5, 6 and 7 in Fig. 2.7).

3.2.3 Uni-modal recordings on patients

At the Danish Epilepsy Center in Dianalund we measured sEMG data (along with the gold standard) from at least 4 sEMG electrodes (placement 2 and 7 on Fig. 2.4) on all the patients who were admitted with expectations on having epileptic seizures with motor manifestations. Five of these patients had seizures with motor manifestations and were included in this study, to verify the ability of the algorithm to detect actual seizures. The number and type of seizures along with the gender and age of the patients are listed in Table 3.1. Furthermore, the length of the signals for the testing phase of the classification is listed.

Table 3.1: The patients gender, age and the amount and type of seizures along with the length of the test file. Pt 2-5 are also presented in appendix C as: Pt2: TC9, Pt3: T1, Pt4: T5 and Pt5: T6.

	Gender	Age	# of Seizures	Seizure Type	Length of Test File [h]
Pt 1	F	2	13	Tonic, Myoclonic	12
Pt 2	F	30	4	GTC	27
Pt 3	M	6	14	Tonic, Spasm	31
Pt 4	M	48	10	Tonic	0.75
Pt 5	M	30	11	Tonic	8

3.3 Data presentation

To assess the reliability of using simulated seizure data from control subjects instead of epileptic patients, the raw data from the simulated seizures were compared visually to actual epileptic seizure data for all modalities. Since we only succeeded in recording seizure data from one patient (with motor manifestations), a statistical comparison of the quantitative data/parameters was not possible. A representative simulated GTC seizure was chosen for comparison with the real seizure.

Fig. 3.2 shows the time plots and spectrograms of a seizure/simulated seizure and the surrounding normal

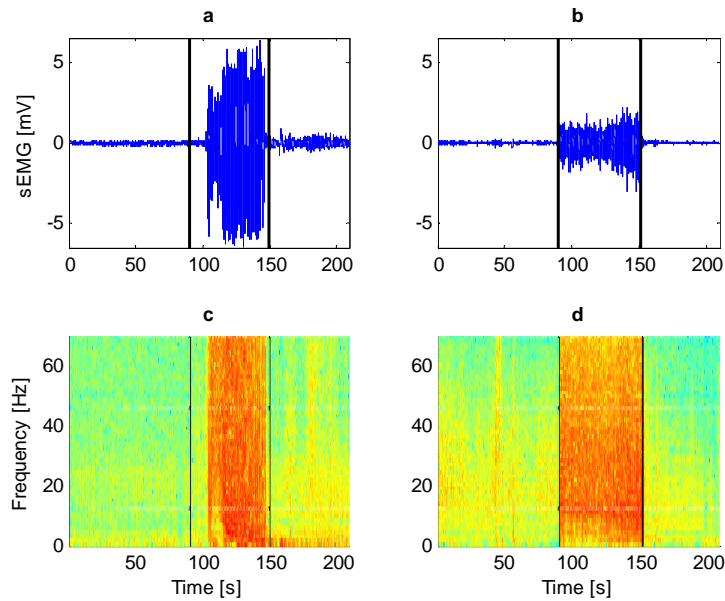


Figure 3.2: The sEMG data for a real seizure and a representative simulated seizure are shown in **a** and **b**, respectively. The matching spectrograms (for a normalization of the signals) are shown in **c** and **d**, where the red color means high power, blue color means low. The data is from the right biceps. The seizure and the simulated seizure are both surrounded by normal activity data. The black vertical lines represent onsets and offsets of seizures and simulated seizures.

activity for the patient and the control subject, respectively. The data is sEMG from the right biceps brachii, data from the other muscles recorded are shown in appendix B. The onset and offset of the seizure/simulated seizure are marked by the black vertical lines. For the patient it is seen that the seizure starts prior to the muscle activity, so the first signs of the seizure are only visible in the EEG or other muscles and not until a bit later was the GTC part of the seizure started in the biceps brachii. The starting point for the simulated seizure is defined as where the muscle activity starts. For some patients the start of a seizure might as well be when the muscle activities are started (visible in the sEMG), so this will not be seen as a difference. A clear difference is the amplitude of the signals, but it should be noted that this characteristic depends on the strength of the subject and the thickness of the skin/fat layer between electrode and muscle among others. The spectrograms are made based on normalized (with respect to the maximum value of the signal) signals to make sure the amplitude differences are not influencing our interpretation. From the spectrograms it is revealed that for both the seizure and the simulated seizure the power contained in the signal is increased for all frequencies through a longer period compared to the normal activities. It is clearly visible that the higher frequencies (above 70 Hz) are not unimportant, so in our later studies, we have made sure that no filtering is performed during the exportation of data. We cannot reject that besides the difference in amplitude there are other differences between the sEMG

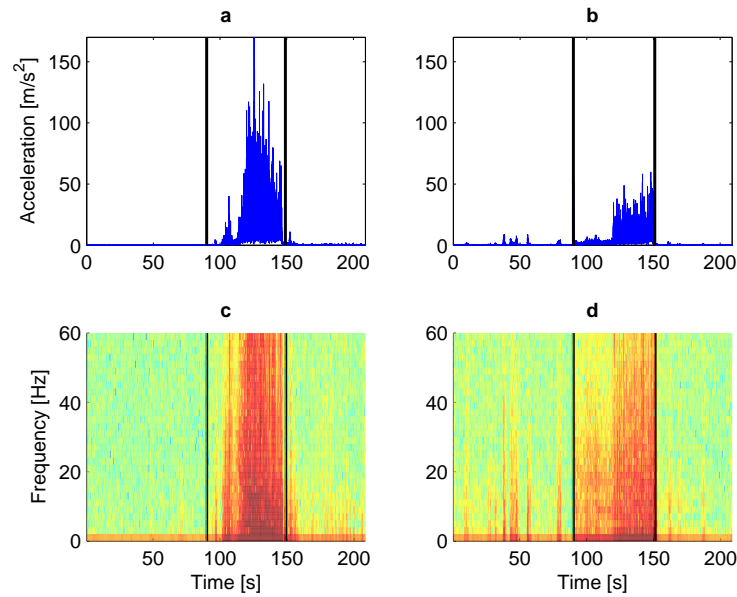


Figure 3.3: The ACM data for a real seizure and a representative simulated seizure are shown in **a** and **b**, respectively. The matching spectrograms (for a normalization of the signals) are shown in **c** and **d**, where the red color means high power, blue color means low. The data is from the sensor at the right lower arm. The seizure and the simulated seizure are both surrounded by normal activity data. The black vertical lines represent onsets and offsets of seizures and simulated seizures. In **b** and **d** the beginning of a second simulated seizure is seen in the right side of the plots.

signals from the epileptic seizure and the simulated seizures. Fig. 3.3 and 3.4, which show the ACM and ANG data, respectively, from the right forearm (all other places are shown in appendix B) for both the patient and a representative control subject, are visually similar. The amplitude, however, is also a problem for these modalities. The movements during the real seizure seem to have larger acceleration and angular velocity than during the simulated seizures and for both data types the movement seems to be more confounded for the real seizure, whereas most of the control subjects have lower accelerations and especially angular velocities.

There are also differences among patients with epilepsy and the patient we measured may have had faster movements than the average patient. We will have to trust that the acceleration of the simulated seizures is visually similar to real ones, when looking at the control subjects, since this is what the physician concluded during the simulations.

The spectrograms show that the real seizure has a larger power in the higher end of the frequencies, compared to the simulated seizures. The simulated seizures show a higher power in some frequencies (above 15 Hz) than the normal activities. These spectrograms are, as well as for the sEMG, generated based on normalized signals to avoid power differences based on the amplitude of the signals. There are smaller differences in the frequencies between ACM and ANG that seems to give some useful complementary

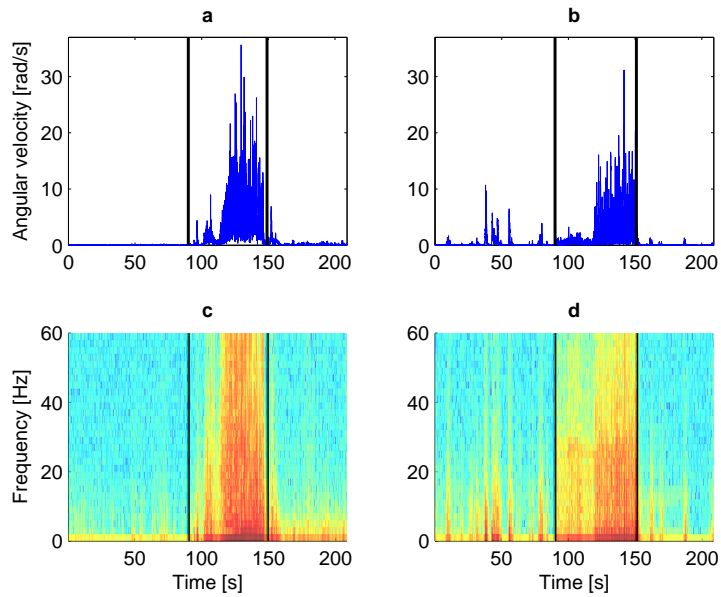


Figure 3.4: The ANG data for a real seizure and a representative simulated seizure are shown in **a** and **b**, respectively. The matching spectrograms (for a normalization of the signals) are shown in **c** and **d**, where the red color means high power, blue color means low and the color scale is the same. The data is from the sensor at the right lower arm. The seizure and the simulated seizure are both surrounded by normal activity data. The black vertical lines represent onsets and offsets of seizures and simulated seizures. In **b** and **d** the beginning of a second simulated seizure is seen in the right side of the plots.

features to our algorithm. Based on the visual inspection, the movements simulated by the control subjects closely resemble those occurring during the seizures, making it a reasonable assumption that the signals recorded by the motion sensors are similar to what we would have recorded from patients with epilepsy. This is also what we have observed when comparing the data from the simulated seizures to the real one, though with some differences in the strength of the seizures. However, these differences make the real seizure stand out even more from the normal background activity, suggesting that the algorithm might work even better on the real seizure data than on the simulated ones.

3.4 Methods

The description of the methods for detection of seizures based on uni- or multi-modal data is split into several steps as outlined in Fig. 3.5. The first step is to extract appropriate features and the second is to classify the data based on these features. Prior to these steps it is, however, necessary to take a look at the data and how it may be divided into training and test sets for the classification.

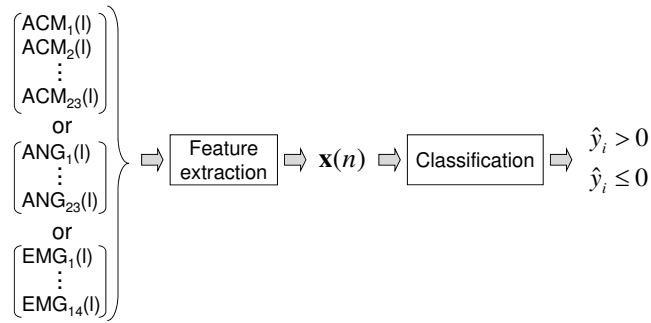


Figure 3.5: Method for detection of simulated seizures based on uni-/multi-modal data. Three types of data are used, from which features are extracted. The feature vector is sent through a classifier, which outputs y_i . A positive y_i classifies as a seizure/simulated seizure, whereas a negative y_i belongs to the normal activity class.

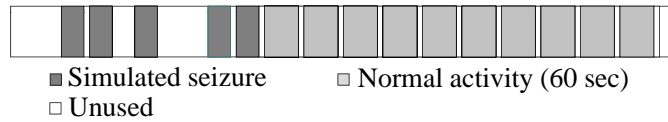


Figure 3.6: Diagram of the segmentation of the data strings from files containing simulated seizures. Between each segment a period of 5 s of data is left unused. Each normal activity segment lasts 1 min.

3.4.1 Data partitioning

Data were partitioned due to the fact that during the recordings, for practical reasons, all simulated seizures, were simulated within a short time with the control subjects practicing the simulations in between. It was therefore not possible to make a causal split of the data into training and test periods, where the first part would be used for training and the last part for test. For the classification, both a training set and a test set of data was needed. Therefore data was divided into smaller segments and split randomly into the training and test phases. By splitting data in smaller segments of seizures/simulated seizures and normal activity there were more segments to choose from, when randomizing the training and test phases related to the classification. This ensured that both the training and test phases contained segments from all the different activities performed. For each control subject several files were processed. A file containing simulated seizures was divided in subparts as shown in Fig. 3.6, where the data parts between the simulated seizures were left unused, since, as previously mentioned, the control subjects might have been practicing for the simulation of simulated seizures in between the actual simulations. The simulated seizures were split in separate segments containing each simulated seizure as a whole. The normal activity period after the simulated seizures was split into segments of 1 min. This length ensured that the movements within the segments made sense, and that a sufficient number of segments were obtained for training and test. Between each segment a sequence of 5 s was left unused to reduce the correlation between two successive periods as much as possible without too much loss of data. Files without simulated

seizures were treated in the same way as the period following the simulated seizures. The files were split into segments of 1 min, with 5 s sequences left unused between each. The sEMG data from the epileptic patients were handled in the same way, except that the data in between seizures were not discarded, but split in the same way as files without any seizure/simulated seizures.

3.4.2 Wavelet based feature extraction

In classification problems the choice of features is often more important than the choice of classifier [12, 52]. The features outline the details to discriminate between groups, whereas one classifier might provide a similar result as another based on the same set of features. The features for discriminating between seizures/simulated seizures and normal activities should therefore be chosen based on how well they distinguish between the two groups. Based on a visual inspection of data, Nijssen et al. [60] found that a wavelet decomposition with the fifth Daubechies as a mother wavelet was the most appropriate feature compared to the STFT for ACM data. Consequently, we have decided to use the fifth Daubechies as a mother wavelet for our data; ACM as well as sEMG and ANG. Compared to the STFT where a signal is split in sine functions with different frequencies, the continuous wavelet transformation divides the signal into shifted and scaled versions of a mother wavelet. The discrete wavelet decomposition is basically two filters that are applied sequentially to the input signal again and again (one time for each step). The filters are composed as low- (g) and high-pass (h) filters based on the mother wavelet. From each filtration an approximation (A) and a detail (D) signal is achieved. Each approximation signal can be further filtered into a new level with both an approximation and a detail signal, see Fig. 3.7. The black squares in the figure mark the division by the DWT, whereas the wavelet packet transform (WPT) is demonstrated by all squares, where also the detail signals are filtered. A mother wavelet is defined by a scaling function $\varphi(l)$ and a wavelet function $\psi(l)$ [49], described by the low-pass filter, g , and the high-pass filter, h [81]:

$$\varphi_{j,k}(l) = 2^{j/2} \cdot g_j(l - 2^j k) \quad (3.1)$$

$$\psi_{j,k}(l) = 2^{j/2} \cdot h_j(l - 2^j k) \quad (3.2)$$

where j is the resolution or scale parameter, k is the translation parameter and $2^{j/2}$ is a normalization factor for the inner product. The decomposition is then described as the discrete approximation, $A_j(k)$, and detail, $D_j(k)$, signals given by [81]:

$$A_j(k) = u(l) * \varphi_{j,k}(l) \quad (3.3)$$

$$D_j(k) = u(l) * \psi_{j,k}(l) \quad (3.4)$$

Each window of each channel (ACM, ANG or sEMG) was applied in the wavelet transformation as $u(l)$. By the extension of the DWT to further filtering on each detail signal as well, the WPT was

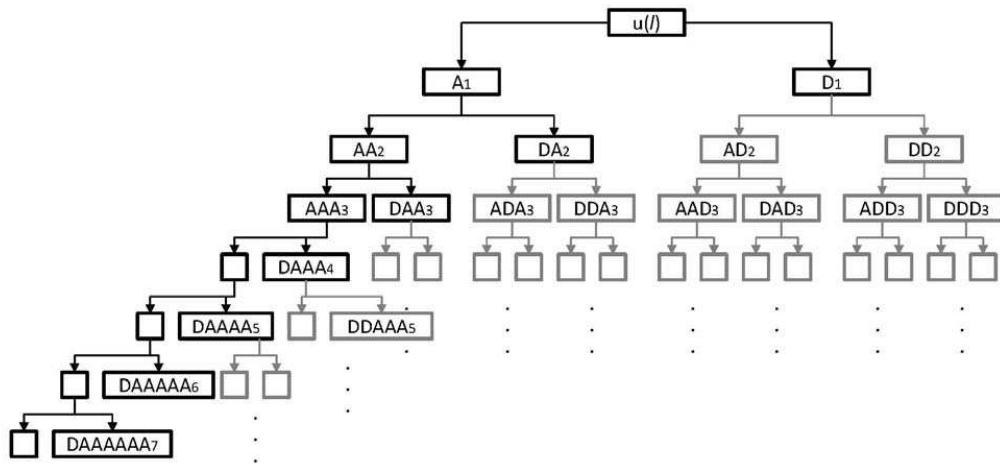


Figure 3.7: The signal, $u(l)$, is filtered and thereby split in approximation and detail signals. The scheme with the black boxes shows the decomposition with a normal wavelet, whereas the total scheme shows the decomposition with wavelet packets. The decomposition is in both cases made to level 7 (seven layers). According to this scheme the detail bands we use for the DWT would be named: DAAA₄, DAAAA₅, DAAAA₆ (and DAAAA₇ for sEMG signals). These names are long, which is why we use the short terms instead: D₄, D₅, D₆ (and D₇ sEMG signals).

obtained. Thereby the signal was split up in uniform frequency bands with equal frequency and time resolutions for all frequencies. This means that no matter which frequency band showed the largest difference between seizures/simulated seizures and normal activity in the movement data, an appropriate resolution was achieved for both time and frequency. So, a good time resolution was not compromised by a bad frequency resolution and, correspondingly, a good frequency resolution was not compromised by a bad time resolution. Each DWT and WPT was determined from a window of 0.75 and 1 s, respectively, both with an overlap of 50%. For the epileptic patients, only the DWT method was tested with a window of 1 s and 50% overlap. The windows should be short enough to capture the important details of the seizures and at the same time, long enough to keep a good frequency resolution. The window lengths were chosen based on the results of an evaluation of the optimal value for the two methods, DWT and WPT, respectively. Before the windows were divided in approximation and detailed signals, they were filtered by multiplying a Hann window of the same length as the signal window to smoothen the spectrum. All feature extractions were processed with the Wavelet Toolbox in MATLAB.

3.4.3 DWT feature extraction

The DWT can be made with an optional number of layers. We found that for the sEMG signals with a sampling frequency of 1024 Hz it was most efficient to use 7 layers, whereby the last bands had a

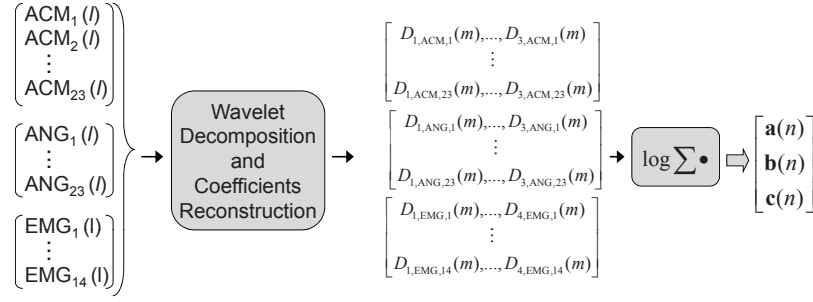


Figure 3.8: Flowchart of the feature extraction from Fig. 3.5. One window of data is analyzed at a time. l is the sample number. The chosen sub-bands are reconstructed, which for the DWT are D_4 , D_5 , D_6 and D_7 (only for sEMG signals). For the WPT the sub-bands used are DDA_3 and ADD_3 for the ACM and ANG signals, whereas $AAAA_5$ and $DDAAA_5$ are used for the sEMG signals (The names are given as illustrated in Fig. 3.7.). A "log-sum" measure is calculated from the used bands as input to the feature vector.

band-width of 4 Hz. For the ACM/ANG signals we found that 6 layers were to be used, whereby the last band had a band-width of 0.94 Hz. From a visual inspection of the features extracted from the different bands in the 7 (6) layers, the detail signals layer 4-6 (ACM/ANG signals) and 4-7 (sEMG signals) turned out to provide larger differences (for the log-sum/energy parameter introduced below), when comparing the simulated seizures to randomly chosen normal activities. For the ACM/ANG signals the frequencies extracted were 0.94-7.5 Hz and for the sEMG signals they were 4-64 Hz. To evaluate these signals and decrease the amount of data entering the feature vector we were interested in a measure for each signal indicating how much "energy" they contained. This was evaluated by calculating a "log-sum" measure of the signals as shown in Fig. 3.8 and given in 3.5:

$$x_{j-3} = \log\left(\sum_{k=1}^{\frac{L}{2^j}} |D_j(k)|\right), \quad (3.5)$$

where L is the number of samples in the signal $u(l)$, j is the level (4, 5, 6 for ACM/ANG and 4, 5, 6, 7 for sEMG) and $D_j(k)$ is the detail signal at level j . By applying the logarithm, it was ensured that the smaller differences between feature vectors from different classes were enhanced, while the larger differences between feature vectors were reduced. The influence on the system by possible outliers was thereby reduced. This means that the system was assumed to be less affected by outliers in the movement signals. The feature vector, \mathbf{x} , was then collected from the vectors \mathbf{a} , \mathbf{b} and \mathbf{c} , with three (ACM/ANG) or four (sEMG) "log-sum" measures for each data window for all channels in the different modalities:

$$\begin{aligned} \mathbf{a} &= [x_{1,ACM_1}, x_{2,ACM_1}, x_{3,ACM_1}, x_{1,ACM_2}, \dots, x_{1,ACM_{23}}, x_{2,ACM_{23}}, x_{3,ACM_{23}}] \\ \mathbf{b} &= [x_{1,ANG_1}, x_{2,ANG_1}, x_{3,ANG_1}, x_{1,ANG_2}, \dots, x_{1,ANG_{23}}, x_{2,ANG_{23}}, x_{3,ANG_{23}}] \\ \mathbf{c} &= [x_{1,EMG_1}, x_{2,EMG_1}, \dots, x_{4,EMG_1}, x_{1,EMG_2}, \dots, x_{3,EMG_{14}}, x_{4,EMG_{14}}] \\ \mathbf{x}_n &= [\mathbf{a}_n, \mathbf{b}_n, \mathbf{c}_n]^T, \end{aligned} \quad (3.6)$$

where ACM_1 means ACM channel 1 and so on and n is the time index. For convenience the time index, n , is omitted in the previous equations. The concatenation of the measures into a feature vector is shown as the last step in Fig. 3.8.

3.4.4 WPT feature extraction

As with the DWT, the WPT can be made with an optional number of layers. We used the same number of steps as for the DWT. This divides the sEMG signal into frequency bands with a bandwidth of 4 Hz. From a visual inspection of the reconstructed sEMG signals we found the reconstruction signals that contained the largest differences between simulated seizures and normal activities. It turned out to be the second and the fourth band in the fifth step, corresponding to frequency bands of 16-32 Hz and 48-64 Hz, respectively, making it unnecessary to decompose it into seven steps. For the ACM/ANG data, because of the lower sampling frequency, the decomposition was made in six layers as used for the DWT. This provided frequency bands for the reconstructed signals of 0.94 Hz. A visual inspection (as described above) was conducted with the result that the fourth (22.5-30 Hz) and seventh (45-52.5 Hz) band of the third step contained the larger differences between the simulated seizures and normal activities for both ACM and ANG.

As for the DWT, we calculate "log-sum" measures of the signals, as given in (3.7) (for sEMG data) and (3.8) (for ACM/ANG data):

$$x_p = \log\left(\sum_{k=1}^{2^{L/5}} |R(k)|\right), R = AAAAD_5(p=1), R = DDAAA_5(p=2) \quad (3.7)$$

$$x_p = \log\left(\sum_{k=1}^{2^{L/3}} |R(k)|\right), R = DDA_3(p=1), R = ADD_3(p=2) \quad (3.8)$$

where L is the number of samples in the signal $u(l)$ and $R(k)$ is the reconstructed signal for the given sub-band. As previously explained, the logarithm was applied to ensure that smaller differences between feature vectors from different classes were enhanced and the influence by possible outliers was assumed to be reduced. The feature vector, \mathbf{x} , was then collected from the vectors \mathbf{a} , \mathbf{b} and \mathbf{c} , with two "log-sum" measures for each data window for all channels in the three modalities:

$$\begin{aligned} \mathbf{a} &= [x_{1,ACM_1}, x_{2,ACM_1}, x_{1,ACM_2}, \dots, x_{1,ACM_{23}}, x_{2,ACM_{23}}] \\ \mathbf{b} &= [x_{1,ANG_1}, x_{2,ANG_1}, x_{1,ANG_2}, \dots, x_{1,ANG_{23}}, x_{2,ANG_{23}}] \\ \mathbf{c} &= [x_{1,EMG_1}, x_{2,EMG_1}, x_{1,EMG_2}, \dots, x_{1,EMG_{14}}, x_{2,EMG_{14}}] \\ \mathbf{x}_n &= [\mathbf{a}_n, \mathbf{b}_n, \mathbf{c}_n]^T, \end{aligned} \quad (3.9)$$

3.4.5 Final feature vector

All possible combinations ((**a**), (**b**), (**c**), (**a, b**), (**a, c**), (**b, c**) and (**a, b, c**)) of the three modalities were sent through the classifier, to explore which combination would be better for an alarm system. Eqs. (3.6) and (3.9) represent the combination where all data are used. The entering of the feature vector into the classifier is shown as the final step in the classification procedure (see Fig. 3.5).

3.4.6 Support vector machine based classification

We decided to see the classification problem as binary with the two classes *seizure* and *other activity*. Another choice could have been to classify the simulated seizures into different groups depending on the seizure type, but in this study we were interested in examining the possibility of making one classifier for all convulsive seizures. The class, *seizure*, contained different kinds of seizures/simulated seizures with motor manifestations, whereas the class *other activity* contained anything but the seizures/simulated seizures. The amount of data in the two classes was very different, since we had more *other activity* data than seizure/simulated seizure data, which made the SVM algorithm attractive compared to other algorithms, e.g. neural network classifiers [90]. When using the SVM, one is sure to find a global and unique solution to the classification problem (quadratic optimization problem, see equation 3.13), compared to neural network where there can be multiple local minima and thereby multiple solutions [11]. This means that one can be certain that an optimal solution is obtained using SVM. A third reason to choose SVM is that it is less disposed to overfitting, since it chooses a specific hyperplane (with the largest margins) to separate the two classes [21].

SVM belongs to the class of supervised learning algorithms. This means that the algorithm based on a training group of a dataset is able to fit the best decision boundary to separate classes and afterwards use this classifier for unknown test data. In our case we know which class our test data belongs to, which makes it possible to validate the classifier (best decision boundary).

The classification is the last part in the detection algorithm. Data was divided into two groups, training and test (Fig. 3.9), where the classifier was trained on the data from the training group. The data from the test group was then classified with the classifier trained for the purpose. The classifier returns a positive or negative value for each test vector, depending on whether it is classified as a seizure/simulated seizure or not. Since we had target values for each test point, we were able to validate the performance of the classifier. The division of the data into these groups (training and test) were made randomly, for both seizure/simulated seizure and all other activity data, ensuring close to equal amounts of each data type in each group. It was ensured that each seizure/simulated seizure type was represented in both phases (training and test).

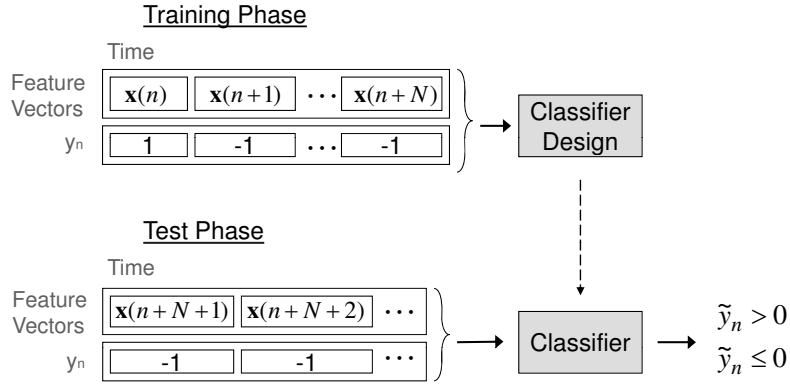


Figure 3.9: The classification part of the algorithm is split in two; the training and the testing phase. During the training phase the classifier is trained on feature vectors and their corresponding target (-1 (other activity) or 1 (seizure/simulated seizure)). In the test phase the "new" data is classified as *seizure/simulated seizure* or *other activity*. In the test phase y_n is unknown to the classifier, but used to validate the classifier.

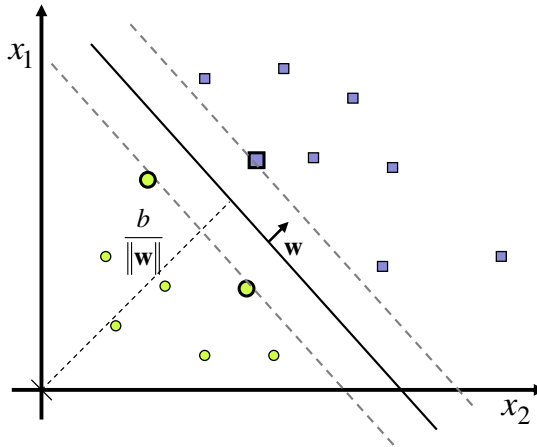


Figure 3.10: Two classes, green and purple, are linearly separable by the black hyperplane. Many other hyperplanes would separate the two classes, but this one maximizes the margin between the support vectors (the data points of most importance to the classifier (enlarged)) of the two classes.

For the training, data was labeled:

$$\{\mathbf{x}_n, y_n\}, n = 1, \dots, k, \quad y_n \in \{-1, 1\}, \mathbf{x}_n \in \mathbb{R}^d, \quad (3.10)$$

where k is the number of training examples, d is the dimension, \mathbf{x}_n is the feature vector (n is the time index) and y_n the matching target, indicating which of the classes the feature vectors belong to, 1 for seizures/simulated seizures and -1 for all other activities.

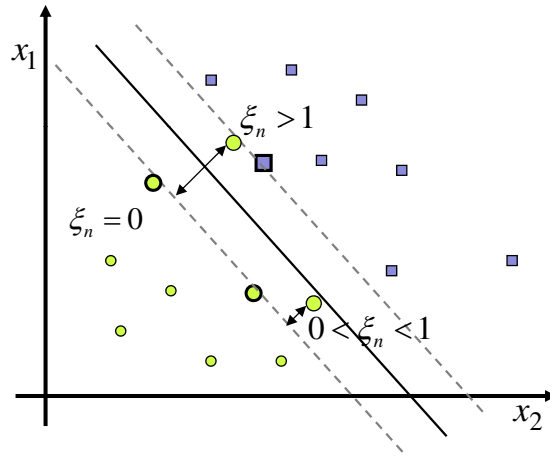


Figure 3.11: Two classes, as in Fig. 3.10, but now two points are shown to be on the wrong side of the margin, having slack variables different from 0. In such situations the hyperplane will be placed to maximize the margin and at the same time lower the errors. The trade-off between the two are decided by C in (3.13).

A two-class linearly separable data set can be classified by a hyperplane described by [72]:

$$f(\mathbf{x}_n) = \mathbf{w} \cdot \mathbf{x}_n + b = 0, \quad (3.11)$$

where \mathbf{w} is the normal to the hyperplane and b is a shifting constant. An example of the two datasets (in 2D) separated by (3.11) is shown in Fig. 3.10. The first SVM method described by Vapnik and Lerner [87] was the hard-margin linear SVM, which cannot take possible errors into account. Later Vapnik and Cortes [21] introduced a soft-margin version, which is the one we have used. It uses a slack variable, ξ_n , to handle errors (e.g. when two classes are not completely linearly separable). The hyperplane is computed based on support vectors. The classifier chooses the feature vectors of most importance (regarding separation of the two classes), and uses them as support vectors. These feature vectors from the two classes must satisfy [72]:

$$y_n \cdot (\mathbf{w} \cdot \mathbf{x}_n + b) \geq 1 - \xi_n, \quad \text{where } \xi_n \geq 0 \forall_n, \quad (3.12)$$

where the positive slack variable, ξ_n , is introduced to handle data, where the groups are not completely separable. Data points assigned to the wrong side of the margin (defined by (3.12)) thereby have a penalty that increases with the distance to the margin. This is illustrated in Fig. 3.11.

To separate the two classes, the problem of finding the optimal parameters, \mathbf{w} and b , can be reduced to

minimize the performance function [72]:

$$\min_{\mathbf{w}} \left(\frac{1}{2} \|\mathbf{w}\|^2 + C \sum_{n=1}^k \xi_n \right) \quad \text{subject to} \quad y_n \cdot (\mathbf{w} \cdot \mathbf{x}_n + b) \geq 1 - \xi_n, \quad (3.13)$$

where C is a factor setting the trade-off between the size of the margin and the penalty of the slack variable, ξ_n [72]. From tests we found that the most optimal value of C for our algorithm was 0.8, which was used for the results we present. For (3.13) to be minimized, each term should be minimized. Minimizing the first term means maximizing the margin between the support vectors of the two classes, which corresponds to maximizing the distance between the boundaries of the two classes. The second term, which encompasses the slack variable, is minimized by keeping the distance from incorrectly classified feature vectors to the margin as small as possible. When a feature vector is correctly classified ξ_n is set to 0, whereby the second term in (3.13) will be 0. For a feature vector correctly classified, but placed on the wrong side of the margin, ξ_n is between 0 and 1, whereas it is above 1, if the feature vector is wrongly classified. This is also illustrated in Fig. 3.11. In the two latter cases the margin is attempted placed as close to these incorrectly classified feature vectors as possible in order to minimize the second term in (3.13).

To solve (3.13) Lagrange multipliers are used and the equation is transformed from its primary form to the dual form, whereby it is possible to identify the parameters for the hyperplane which best separates the two classes. These steps are all performed in MATLAB by the *SVM^{light}* package specified in [39]. The package returns a classification model based on the given training set, which can then be used to classify a test set.

3.4.7 Test methodology

To evaluate how well the detection algorithms perform, certain measures may be calculated for each patient/control subject. The test measures used are:

- *Sensitivity* (SEN) - the fraction of seizures that are correctly classified.
- *Latency* (LAT) - the time from seizure start (clinical onset) to the detection time.
- *False Detection Rate* (FDR) - the number of falsely detected simulated seizure onsets per hour.

When the content of a window is classified as a simulated seizure an alarm will be generated. The latency is measured as the delay from simulated seizure start till the alarm is generated (first window with a positive outcast). Since this is sought to be implemented as an on-line algorithm, it means that the shortest possible latency will correspond to the length of the window (0.75 s and 1 s, respectively). Only the first window, in a row of successive detections, will generate an alarm. This means that when successive *other activity* windows are detected as a seizure/simulated seizure only the first one will generate

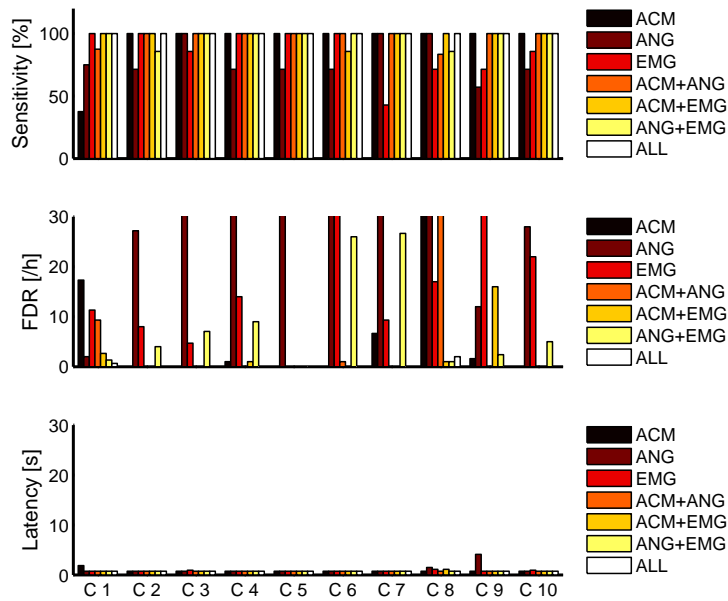


Figure 3.12: The results from the DWT feature extraction method. C means control.

a false alarm, and thereby it will only count for one false positive (FP). When evaluating the results of detecting seizures/simulated seizures on a large database, the FDR is a more ideal measure than the often used specificity, since it gives a better impression of the results. To obtain valuable results for FDR the measurements should contain several hours for testing. For practical reasons we only measured for 1.5–3 hours for the control subjects, which may influence our results.

3.5 Results

The results on the control subjects vary depending on the feature extraction method. The results for the DWT method are shown in Fig. 3.12, whereas the results for the WPT method are shown in Fig. 3.13. To compare the results of the different combinations of modalities, the median and 95% confidence level of all results are given in Table 3.2, for both methods.

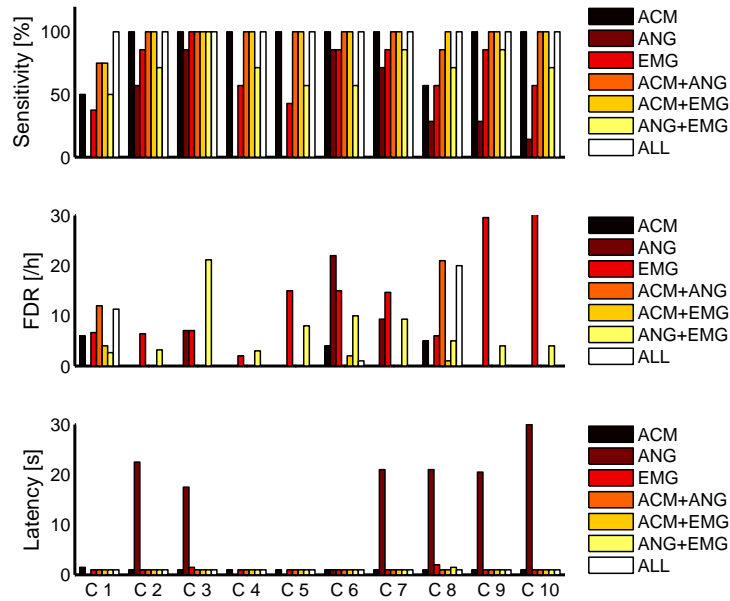


Figure 3.13: The results from the WPT feature extraction method. C means control.

3.5.1 DWT method

The DWT method (Fig. 3.12) shows an almost perfect result ($SEN = 100\%$, $FDR = 0$, $LAT = 0.75$ s), when combining all modalities, while the detection is less accurate when only one modality is used. For the first control subject (C) the worst performance is seen when only the ACM data is included, whereas the worst performance for control subject 2, 4, 5, 6, 9 and 10 are seen when only the ANG data is used. For the last three control subjects (3, 7 and 8) the worst performance is achieved when only the sEMG data is used. The latencies are short for all tests; the longest latency is seen for control subject 9, where only the ANG data is used. The FDR shows that for several tests the number of false detections per hour is remarkably high. For 7 of the 10 control subjects the highest FDR is observed when only the ANG data is used for the remaining three it is when only sEMG or ACM is used. When all modalities are used, the FDR is equal to 0 for 8 of the 10 control subjects, the last two (C1 and C8) have an FDR of 0.67 and 1.7, respectively. The results in Table 3.2 shows that the ANG modality alone has the worst performance and that clearly a combination of all modalities achieves the best performance.

Table 3.2: Median values (and in parentheses the 2.5% and 97.5% percentiles). 1: ACM, 2: ANG, 3: sEMG.

	Discrete wavelet transform						Wavelet packet transform					
	SEN [%]		FDR [/h]		LAT [s]		SEN [%]		FDR [/h]		LAT [s]	
1	100	(52-100)	0.5	(0-70)	0.75	(0.75-1.6)	100	(52-100)	0	(0-5.8)	1	(1-1.4)
2	71	(60-100)	49	(4.3-77)	0.75	(0.75-3.5)	29	(0-86)	0	(0-19)	19	(1-28)
3	93	(49-100)	13	(1.1-50)	0.75	(0.75-1.1)	71	(39-97)	11	(2.9-33)	1	(1-1.9)
1,2	100	(82-100)	0	(0-38)	0.75	(0.75-0.75)	100	(77-100)	0	(0-19)	1	(1-1)
1,3	100	(89-100)	0	(0-13)	0.75	(0.75-1.0)	100	(81-100)	0	(0-3.5)	1	(1-1)
2,3	100	(86-100)	4.5	(0.2-27)	0.75	(0.75-0.75)	71	(52-97)	4.5	(2.7-19)	1	(1-1.4)
All	100	(100-100)	0	(0-1.7)	0.75	(0.75-0.75)	100	(100-100)	0	(0-18)	1	(1-1)

3.5.2 WPT method

For all control subjects except for control subject 6, the accuracy is the lowest when only the ANG data is used, and for some the sensitivity is as low as 0%. For control subject 6 the performances are the worst when the ANG data is combined with the sEMG data. For all control subjects the best results are obtained, when all modalities are combined. The latency is seen to be short for all tests except for control subject 2, 3, 7, 8, 9 and 10, when only the ANG data is used. The FDR is as low as 0 for about half of the tests, for a few it is as high as 30, and for the rest the FDR is around 10. When all modalities are used for eight of the 10 control subjects it succeeded in keeping an FDR of 0, but for the remaining two (C1 and C8) the FDR is 11 and 18, respectively. Looking into Table 3.2 it is seen that the ANG modality alone performs the worst with a sensitivity that is too low and a median latency that is much too high. A combination of all modalities is shown to provide the best results.

3.5.3 Comparison of DWT and WPT

The results for the control subjects on multi-modal data (sEMG, ACM and ANG) show that the algorithm performs better when all three modalities are used (see Table 3.2). This is independent on whether the DWT or the WPT feature extraction method is applied. From Table 3.2 it is clearly seen that, when all modalities are used the two methods provide similar results, with the only exceptions being the latency, where the lower bound is depending on the window length, and the FDR which has a higher 97.5% percentile for the WPT method. This difference is caused by two controls (C1 and C8) who are seen to have much larger FDR in Fig. 3.13, than in Fig. 3.12, when all modalities are used. Besides from using all modalities it is difficult to say which method provides the best result. It depends on the individual control subject and whether the sensitivity or the FDR is considered the most important. The DWT gives the highest sensitivity for all, whereas the WPT provides a lower FDR.

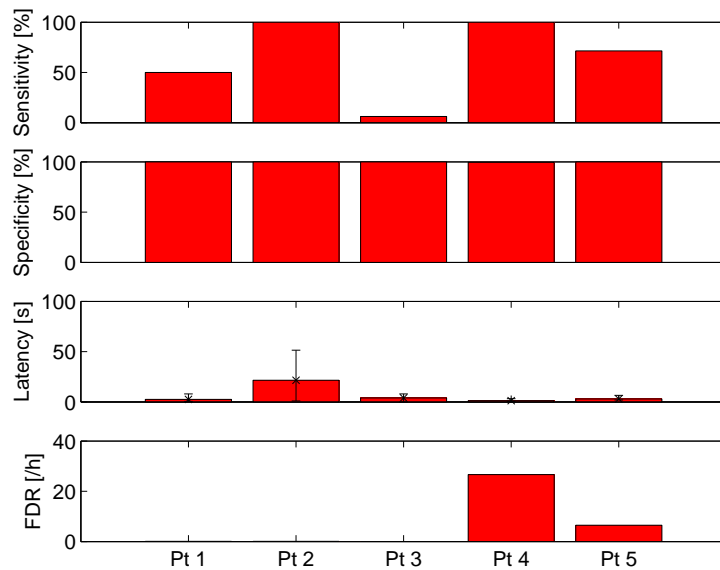


Figure 3.14: The sensitivity, specificity, latency and FDR are showed for the results on the EMG data from the five patients. The sensitivity, specificity and the FDR are shown as bars for each patient. For the latency the median is shown by the bars and the largest latency is indicated by the black line.

3.5.4 Results for epileptic patients

For the patients where only the sEMG data are provided, the results are shown in Fig. 3.14. In this case only the DWT method is tested. This shows that the algorithm detects only half of the seizures for patient 1. The reason is that the other half is myoclonus, which is very short lasting (< 0.5 seconds) and only happening in one muscle. This means that the muscles included in these seizures might not be the ones, which we have measured. It should be noticed that the seizures are detected at onset. Further it can be seen that there are only very few false positives (0.08/h). For patient 2 all seizures are detected, but most of them with a delay. There are very few false positives (0.07/h), which is important for an alarm system. For the third patient the algorithm is only able to detect one seizure, but at the same time it does not capture any false positives. It should be noticed that 50% of the seizures in the test data are spasms which the algorithm is not directly intended for. For the fourth patient all the seizures are detected at onset, but it has too many false alarms, the FDR, however, might be high due to the fact that we have less than an hour of data to test the algorithm on. For the last patient the algorithm is not able to detect all seizures, but those detected are detected at onset. No post-processing has yet been applied, which might have lowered the FDR for some patients. A change in the window size might be able to increase the sensitivity for patients with very short lasting seizures.

3.6 Discussion

The best results for the control subjects, for distinguishing between simulated seizures and other activities based on the two wavelet methods, are obtained when all three modalities are included. However, if the number of modalities or sensors/electrodes could be reduced, without worsening the results too much, it would be preferable considering the usability and comfort for the patients. The ANG modality alone is not useful, but the best results are obtained when it is combined with the ACM and the sEMG modalities. For both methods it would be the ANG modality that would be eliminated, if one wanted to base a system on only two modalities, since the combination of ACM and sEMG, show the next best performance for both methods. Based on the results it seems evident to combine all three modalities, but it does not allow us to determine which wavelet method is the best in this case.

3.6.1 Frequency bands

It should also be noted that DWT and WPT are based on different frequencies, so this might as well influence the results. During our briefly examination of which frequency bands provided the largest differences between simulated seizures and normal activities, it resulted in different frequency bands for the two methods. We could have used the exact same frequencies for the WPT as we used for the DWT, but our examination showed us to do otherwise. This has improved the results on some levels (overall lower FDR), while lowering it on other (lower overall sensitivity). This examination was made on a limited amount of data, and of course it would have been best if the examination had been expanded to include all data, and go through all possible combinations of the frequency bands. The results point to the fact, that the differences between seizure and other activity data are visible in more frequency bands and it seems evident that the result is improved by including more modalities independent of the chosen feature.

3.6.2 Epileptic seizures

Comparing the control subjects and the patients show equally well results using the algorithm based on the sEMG modality alone (SEN: C: 93%, Pt: 73%, FDR: C: 49/h, Pt: 0.08/h, LAT: C: 0.75 s, Pt: 0.75). The better results on the control subjects using more than one modality imply that better results might be achieved on patients when more modalities are applied. The movements simulated by the control subjects closely resembled those occurring during the seizures, therefore it is reasonable to assume that the signals recorded by the movement sensors are similar to what we would have recorded from patients with epilepsy. However the muscle signals depend on the recruitment of the motor nerve cells. In the case of control subjects the motor cells are physiologically activated, while in the case of "real" seizures the recruitment is pathological. Thus we cannot exclude that the sEMG signal recorded during the simulated

seizures have different characteristics than the epileptic ones.

3.6.3 Moven system issues

The prime limitation in getting the adequate patient data was the way the Moven sensors were attached to the patient. They were placed in pockets of a specially designed suit. Wearing this suit did not constitute a problem for the well functioning patients. However, these patients rarely have GTC seizures. The patients who frequently have this seizure type are typically mentally retarded, and they could not tolerate the suit. Thus for future studies fewer sensors should be used, and they should be applied without the dependence of a suit. Due to this lack of data from patients with the right type of seizures, it was not an option to find the optimal positioning of the different sensors, with respect to a seizure detection algorithm. It did reveal the advantage of using more modalities to obtain a more robust algorithm, based on data from the control subjects, and due to the similarities with the patient data it is assumed that it can be expected on real patients as well.

3.7 Conclusion

The first aim of this study was to record multi-modal data from a full body approach. We succeeded in this, but had to acknowledge that the suit used was not appropriate for the type of patients, which we were interested in.

The second aim of our study was to determine the outcome with a seizure detection algorithm when using one or more modalities and furthermore which combination of the modalities that would perform best. As our results on control subjects who could tolerate the suit are encouraging for using a combination of all three modalities, it is worthwhile to focus on further development of a sensor setup, which could be tolerated by the patients. Fewer and smaller sEMG electrodes and/or motion sensors attached to the patient, with wireless communication could solve this problem. To make such a change it would be helpful to investigate which places on the body that are more suited to wear these sensors and what number of sensors and/or electrodes is necessary to achieve an acceptable result.

The third aim was to develop an algorithm capable of discriminating seizures from all other activities based on uni- or multi-modal data. As mentioned earlier, we chose to look at the classification problem as binary, but when real seizures are collected it might improve the results if the seizures are split up in different groups, depending on the type. The results from the patient data, implied that it might be hard to make one detection algorithm which focuses on all seizure types with motor manifestations, due to the large inter-seizure differences.

From these observations, we changed our focus to only include two seizure types, which we were able

to detect with the presented algorithm; tonic and GTC seizures. Furthermore we looked more into a uni-modal approach, due to our trouble with collection of multi-modal data from patients.

INVESTIGATION OF GENERALIZED TONIC AND TONIC-CLONIC SEIZURES

Objective *Tonic muscle contraction constitutes the characteristic semiologic feature of several epileptic seizures. Tonic seizures are defined as sustained increase in muscle contraction lasting from seconds to minutes [31], whereas GTC seizures are defined as a sequence consisting of a tonic followed by a clonic phase [62]. Is a tonic seizure a fragment of a GTC seizure or fundamentally different? It is still unclear whether these seizure types share a final common pathway of MU activation, and it has not been elucidated whether the tonic muscle activation during the seizures is different from the physiologic one. If we can find differences between the physiologic and the pathologic tonic activation, this may provide features which can be used in a detection algorithm. This is the subject matter of Paper IV, which this chapter is composed upon.*

4.1 Background

Visual inspection of sEMG signals from polygraphic recordings has previously contributed to the identification of the pathomechanisms of several seizure-types: myoclonic, atonic, myoclonic-atonic, epileptic spasms, and startle-induced reflex seizures [56]. Recording sEMG signals during seizures proved to provide valuable diagnostic information in the clinical practice. Tassinari et al. [82] encouraged the use of off-line analysis of digital polygraphic recordings of epileptic seizures. Digital recording systems allow measuring precisely the time between the EEG and EMG signals, as well as the precise duration of the muscle activity [69, 83]. Although quantitative analysis of EMG signals was investigated extensively in several types of movement disorders [34], to the best of our knowledge myoclonus is the only seizure type in which this feature has been addressed [35, 65, 73].

Muscles are involved in the tonic and GTC seizures, at the end of the common final neural pathway, and

sEMG signals provide valuable information at a high temporal resolution.

The properties of the sEMG signals can be described by characteristics in the time domain and in the frequency domain. In the time domain, the amplitude characteristics of the signal are represented by the RMS. The frequency domain characteristics can be visualized using spectrograms and expressed by the median frequency (MF) and the relative power of the signal in the different frequency bands. The correlation between the muscle activation on the two sides can be reflected by the EMG-EMG coherence.

4.1.1 Research hypotheses

Epileptic seizures occur due to abnormal excessive or synchronous neuronal activity in the brain. We hypothesized that this will be reflected in the pathomechanism of the epileptic tonic muscle activation by a shift toward higher frequency domains, increase in coherence, and/or increase in the RMS feature. We hypothesized that some of the sEMG features would be promising for a seizure detection algorithm.

Our hypotheses are:

- to find differences between the pathologic and physiologic activation of the muscles during tonic activation.
- to find answers for how alike the two types of tonic activation (tonic seizure and tonic phase of GTC seizure) truly are.
- that some of our findings may be promising features in a seizure detection system.

4.2 Methods

The methodology of this research area both include information on the subjects, the recording and the seizures before it presents the different approaches used to outline the characteristics of the sEMG data during epileptic and simulated seizures.

4.2.1 Subjects

All patients included were admitted to the EMU at the Danish Epilepsy Center in Dianalund, Denmark, for diagnostic reasons. They all had a history of tonic or GTC seizures in the referral. In addition, we also included control subjects who simulated epileptic seizures.

Fifty-seven consecutive patients were included. Twenty-three patients did not have seizures during the monitoring, 20 patients had seizures with tonic muscle activation (10 patients had tonic (shown in Table

C.2 in appendix C), 10 patients had GTC seizures (see Table C.1 (TC1-TC10) in appendix C)), and 14 patients had epileptic seizures other than tonic and GTC. Twenty control subjects were recruited in total. In the group of the patients with epilepsy (seven females, 13 males) the average age was 24.8 years (range 6-58). The group of control subjects was age and gender matched: average age 25.4 years (range 6-54), eight were female and 12 were male (for the age: $p > 0.6$; for the gender: $p = 1$). The subgroup of patients with tonic seizures (four females, six males) had an average age of 20.4 years (range 6-58), whereas in the subgroup with GTC seizures (three females, seven males) the average age was 29.2 years (range 11-55). There was no significant difference among the two patient subgroups and the group of control subjects concerning the age ($p > 0.1$) or concerning the gender ($p > 0.7$).

4.2.2 Recordings

In addition to the standard EEG electrodes, sEMG electrodes were placed on the deltoid muscles (placement 2 in Fig. 2.4) as described in section 2.2.1.

The sEMG signals were sampled with a frequency of 1024 Hz, and an anti-aliasing filter of 512 Hz.

All sEMG signals were notch filtered (49-51 Hz) with a Butterworth infinite impulse response filter to remove noise from the power line and furthermore high-pass filtered (10 Hz) with an equiripple finite impulse response (FIR) filter, as the signal beneath 10 Hz may be obscured because of the movements of the electrodes against the skin [53]. For both filters, the group delay was assessed and found not to interfere with the investigated frequencies. Information on the filter is given in tables in appendix D.

4.2.3 Seizures

The long-term video-EEG recordings were reviewed by a clinical neurophysiologist and an epileptologist, who marked time epochs containing a tonic seizure or the tonic component of a GTC seizure, based on visual analysis. These epochs were marked only if they unequivocally corresponded to a seizure period.

In case of the secondarily generalized seizures the start of the bilateral symmetric tonic muscle contraction was marked as the onset.

We recorded 63 epileptic seizures with tonic muscle activation from the 20 patients, the number of seizures was in the range of one to ten (average 3.2 seizures/patient) during the recordings. The patients with tonic seizures had more seizures (average 4.5 seizures/patient; range 1-10) than the patients with GTC seizures (average 1.8 seizures/patient; range 1-4) ($p < 0.03$).

The control subjects were trained to perform the sustained, maximal muscle contraction in all limb muscles lying in a bed. The movements were described based on the detailed description by Gastaut [30] and the description in the definition of the GTC seizures by the international league against epilepsy (ILAE)

[62]. The control subjects watched video recordings with GTC seizures. The simulated seizures were recorded in the presence of the PhD student and a physician with experience in evaluating long-term video-EEG recordings. If necessary, the control subjects were asked to correct the way they activated the muscles. Each control subject simulated 5 GTC seizures, providing a total of 100 simulated seizures.

4.2.4 Data analysis

To characterize the sEMG signals during the epileptic and the simulated seizures, several quantitative parameters were calculated.

Time domain

The amplitude is fluctuating within broad ranges, and outliers have huge influence. To avoid this, instead of the raw amplitude, the classical RMS is used to characterize the amplitude:

$$\text{RMS}(u) = \sqrt{\frac{1}{L-1} \sum_{l=0}^L u(l)^2}, \quad (4.1)$$

where $u(l)$ is the sEMG signal and L is the window length. The RMS value was calculated in a 3 s long window and each window overlapped the preceding and following window with 2 s. As there seems to exist no established definition for the minimum duration of a tonic contraction to qualify as a tonic seizure, we used 3 s long successive time windows as proposed by Lüders et al. [48].

Frequency domain

The frequency features were visualized using plots of the magnitude of the fast Fourier transform (FFT) and spectrograms, and they were quantified by the MF and the relative power (100-500 Hz). f_{MF} is defined as the frequency that divides the magnitude spectrum in two parts of equal sizes (the area under the curve for the frequencies lower than f_{MF} equals the area under the curve for the frequencies higher than f_{MF}) [32, 88], and it is expressed as,

$$\sum_{f=0}^{f_{\text{MF}}} |U_m(f)| = \frac{1}{2} \sum_{f=0}^{f_s/2} |U_m(f)|, \quad m = 1, 2, 3, \dots, \quad (4.2)$$

where m is the window number, f_s is the sampling frequency, f_{MF} is the median frequency, and the U_m is the discrete frequency spectrum of the window m . $|\bullet|$ computes the absolute values of the discrete frequency spectrum. The MF values were calculated from time windows of 3 s duration, overlapping by 2 s. Spectrograms were calculated for each seizure. The power was calculated for a small window of

125 samples, and each window has 50% overlap to its neighboring windows. This offered a frequency and time resolution of 7.5 Hz and 0.125 s, respectively. In addition, we determined the relative power (RP) in the higher frequency domain. The band was chosen from a visual inspection of the spectrograms. In the frequency range 100-500 Hz the power was seen to be higher for the epileptic seizures compared to the simulated seizures (Fig. 4.3). The RP was calculated by dividing the power in the 100-500 Hz frequency range by the total power of the signal in the whole frequency domain, in each time-window of 3 s overlapping by 2 s:

$$\text{RP}(m) = \frac{\sum_{f=100}^{500} |U_m(f)|^2}{\sum_{f=0}^{f_s/2} |U_m(f)|^2}, \quad m = 1, 2, 3, \dots, \quad (4.3)$$

where $U_m(f)$ represents the N -point discrete frequency spectrum ($N = 4096$) of the m 'th window.

Coherence

Coherence is the correlation in the frequency domain between two oscillatory activities in spatially distinct systems [54]. This normalized measure of correlation has values between 0 and 1. A coherence value of 1 indicates a perfectly linear relationship, whereas 0 is when the two signals are completely independent. We calculated EMG-EMG coherence between the right and left sides, using the standard methods in this field [10, 26, 36, 41]. We opted for including the results from the analysis of the unrectified EMG signals because previous studies have suggested that rectification might impair the oscillatory input between two sEMG signals [57]. Furthermore, one of the previous studies showed that this analysis method is reliable also for unrectified data [10]. However, we also analyzed the rectified data, and the results were similar (see Table C.3 and C.4 in appendix C). Briefly, we used the following equation:

$$|S_{rl}(f)|^2 = \frac{|G_{rl}(f)|^2}{G_{rr}(f)G_{ll}(f)}, \quad (4.4)$$

where $|S_{rl}(f)|^2$ is the coherence between the signals, r (right) and l (left). The numerator features the cross-spectrum of the two signals, whereas the denominator is a product of the auto-spectra of the two signals. These are as given by Halliday et al. [36]. We added the approach used by Grosse et al. by including both the Fisher's transform and a 3-point moving average filter [35].

Fisher's transform is described by [27]:

$$z(f) = \frac{1}{2} \cdot \ln \frac{1 + |S_{rl}(f)|^2}{1 - |S_{rl}(f)|^2}, \quad (4.5)$$

and the moving average (MA) filter by [67]:

$$z_{\text{MA}}(f) = \frac{\sum z(f-1 : f+1)}{3}, \quad (4.6)$$

where z_{MA} is the final coherence spectra for a seizure. We plotted the coherence spectra for each seizure and furthermore calculated the coherence in the whole frequency band (10-512 Hz) as the mean of the coherence values in this domain.

For each subject we calculated the mean of the RMS, MF, RP, and coherence values of all time windows, during all seizures, and the mean of the values from the left and right deltoid muscles were used in the statistical analysis. Therefore, for each patient only one (mean) value was used in the statistical analysis, regardless of the number of seizures the patient had. This was done to avoid the bias toward the data from patients with more seizures. Because the sEMG parameters (calculated from the time windows of 3 s) were not constant within the seizures, we also calculated the 95th percentile (peak) values, for each patient for each quantitative sEMG parameter, besides determining the mean value of the different parameters for the whole seizure period (as described above). This make it possible to express the highest level of activation for a certain parameter, for each patient, without being biased by the outlier values, i.e. the upper 5th percentile.

Statistics

The normality of the data distribution was assessed using Kolmogorov-Smirnoff test. Depending on this we used either the Mann-Whitney test or t-test for the comparisons. To compare gender and the occurrence of the observed sEMG features between the two groups, Fisher's exact test was used.

4.3 Results

Examples of the sEMG signals from the different groups are shown in Fig. 4.1. The quantitative sEMG parameters are presented in Table 4.1 (whole seizure period).

Table 4.1: Median values of the whole seizure period for all patients (and in parentheses the 2.5% and 97.5% percentiles) for the different surface EMG parameters.

	Epileptic	Tonic	GTC	Simulated
RMS [mV]	0.636 (0.055-2.20)	0.251 (0.053-0.784)	1.16 (0.356-2.46)	0.440 (0.170-1.10)
MF [Hz]	76.8 (59.0-112)	86.2 (63.3-113)	73.6 (59.0-80.8)	63.9 (56.9-83.9)
RP (100-500 Hz) [Hz]	0.151 (0.047-0.395)	0.217 (0.114-0.401)	0.110 (0.041-0.176)	0.079 (0.039-0.207)
Coherence	0.120 (0.050-0.255)	0.117 (0.048-0.178)	0.120 (0.063-0.289)	0.071 (0.046-0.109)

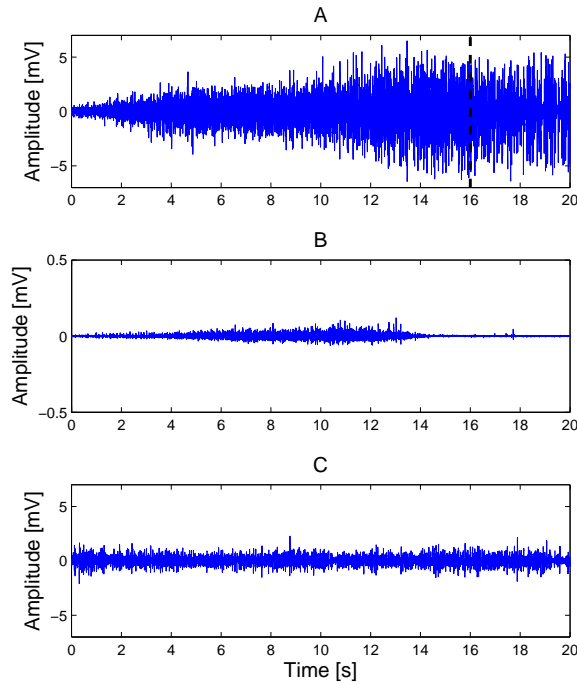


Figure 4.1: sEMG signals of representative seizures: (A) the tonic phase of a GTC seizure; (B) tonic seizure; (C) simulated seizure. The vertical, dotted line in figure A marks the end of the tonic phase/beginning of the clonic phase, as seen on the video-EEG recordings. The tonic phase starts at time = 0 s, and in figure B and C it ends at time = 20 s. The scale of the y-axis is different for subfigure B.

4.3.1 Amplitude characteristics

The visual inspection of the sEMG signals suggested that amplitudes were higher during the tonic phase of the GTC seizures as compared to the seizures from the other subjects (Fig. 4.1). The RMS (Table 4.1) for the group of epileptic seizures was not significantly different from that of the simulated seizures ($p > 0.4$). However, the subgroup analysis showed that the RMS during the tonic phase of the GTC seizures was significantly higher compared to the RMS of the simulated seizures ($p < 0.001$), and furthermore significantly higher than that of the tonic seizures ($p < 0.001$). The RMS during the tonic seizures were significantly lower than during the simulated seizures ($p < 0.05$).

4.3.2 Median frequency

The magnitude spectrum visualizes the distribution of the signal at the different frequency components (Fig. 4.2). During the epileptic seizures (especially the tonic ones) we observed a shift of the energy

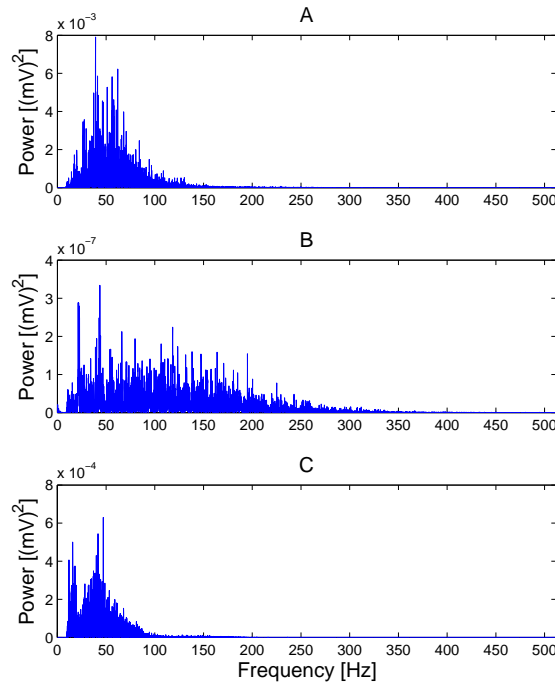


Figure 4.2: Power spectrums of representative seizures: (A) the tonic phase of a GTC seizure; (B) tonic seizure; (C) simulated seizure. The scale of the y-axis is different for the three seizures. For the simulated seizures most of the power is in the frequency band <100 Hz. During the epileptic seizures (especially the tonic seizure) one can observe a shift toward the higher frequencies.

toward higher frequencies. The power of the simulated seizures in the magnitude spectrum (Fig. 4.2C) are mostly below 100 Hz. The MF (Table 4.1) was significantly higher during the epileptic seizures compared to the simulated ones ($p < 0.005$). The subgroup analysis showed that MF was significantly higher during the tonic seizures than during the simulated seizures ($p < 0.001$), and furthermore significantly higher than during the tonic phase of the GTC seizures ($p < 0.05$). There was no significant difference between the MF during the tonic phase of the GTC seizures and the simulated ones ($p > 0.1$).

4.3.3 Relative power

Figure 4.3 shows spectrograms of the RP for the different frequencies. Inspection of the spectrograms suggested higher power for the frequency domains above 100 Hz during the epileptic seizures as compared to the simulated ones. To express this quantitatively we calculated the RP for the frequency range of 100-500 Hz. The RP (100-500 Hz) was significantly larger during the epileptic seizures compared to the simulated seizures ($p < 0.01$). RP (100-500 Hz) was higher during the tonic seizures than during the

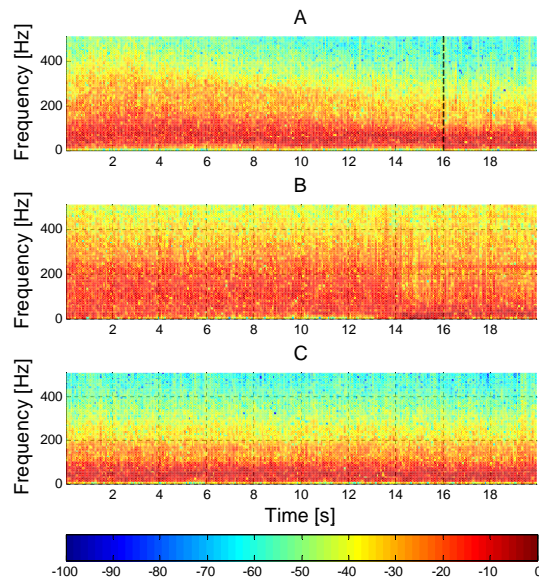


Figure 4.3: Spectrograms (time-frequency plots) of representative seizures: **(A)** the tonic phase of a GTC seizure; **(B)** tonic seizure; **(C)** simulated seizure. The vertical, dotted line in figure **A** marks the end of the tonic phase/beginning of the clonic phase, as seen on the video-EEG recordings. The color code represents the size of the logarithm of the relative power.

tonic phase of the GTC seizures ($p < 0.01$) and higher than during the simulated seizures ($p < 0.0005$). There was no significant difference between the RP (100-500 Hz) during the tonic phase of the GTC seizures and the simulated ones ($p > 0.3$).

4.3.4 Coherence

The visual inspection of the EMG signals showed bilateral-synchronous, sustained muscle activation during the analyzed seizure periods in all groups. The coherence spectra demonstrated that there were several frequencies with significant coherence for each patient (Fig. 4.4), and that these frequencies varied from subject to subject. In the absence of certain, dominating frequencies for the significant level of coherence, we opted to calculate the coherence for the whole frequency band and to compare this among the groups. The coherence was significantly higher during the epileptic seizures than during the simulated ones ($p < 0.0005$). There was not any significant difference in coherence between the two subgroups of epileptic seizures ($p > 0.3$), but in both epilepsy subgroups the coherence was higher than in the group with simulated seizures ($p < 0.01$).

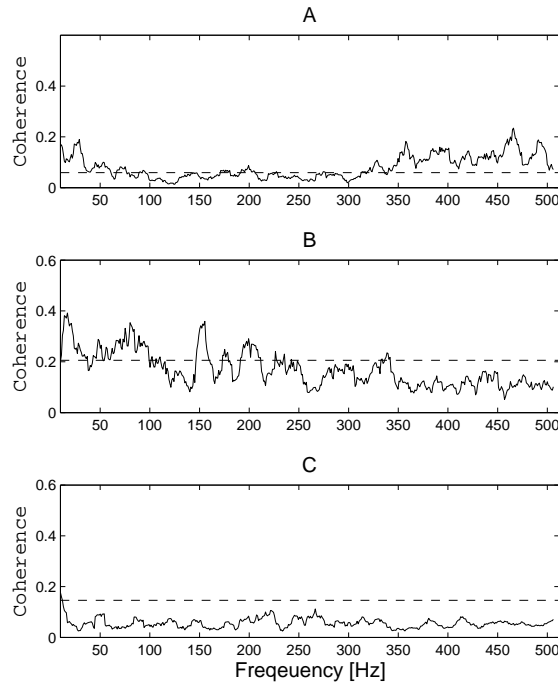


Figure 4.4: Coherence spectra (blue curve) for: (A) the tonic phase of a GTC seizure; (B) tonic seizure; (C) simulated tonic seizure. The black dotted line defines the significance level calculated as in the standard methods [26]. The coherence spectra were smoothed with a moving average filter [35].

4.3.5 Peak values

To reflect the highest level of activation achieved by each patient/control subject, in addition to mean values for the whole-seizure period (detailed above), we also calculated the 95th percentile of the parameters (peak values). The shift toward the higher frequencies during the tonic seizures, the increase in the RMS during the tonic phase of the GTC seizures, and the increase in the coherence in the epileptic seizures (both types) were even more pronounced when analyzing the peak values (Table 4.2).

Table 4.2: Median values of the peak values for all patients (and in parentheses 2.5% and 97.5% percentiles) for the different surface EMG parameters.

	Epileptic	Tonic	GTC	Simulated
RMS [mV]	1.09 (0.086-2.57)	0.666 (0.078-1.10)	2.00 (0.672-2.64)	0.665 (0.264-1.43)
MF [Hz]	92.5 (64.4-141)	101 (78.8-142)	87.9 (61.6-96.2)	73.6 (61.0-92.5)
RP (100-500 Hz) [Hz]	0.286 (0.072-0.583)	0.316 (0.265-0.602)	0.234 (0.052-0.297)	0.134 (0.052-0.273)
Coherence	0.135 (0.056-0.361)	0.219 (0.054-0.266)	0.123 (0.074-0.381)	0.081 (0.058-0.142)

4.3.6 The effect of duration

There was no statistically significant difference between the duration of the tonic seizures and the duration of the tonic phase of the GTC seizures in our patients (median: 14.66 and 15.95 s, respectively; $p > 0.6$). There was no significant correlation between the duration and the quantitative sEMG parameters that distinguished between the two seizure-types: RP (100-500 Hz), MF, RMS ($p > 0.12$). A multiple regression analysis for categorical (seizure-type: tonic vs. GTC) and continuous (duration) predictors showed that it was only the seizure type that predicted these quantitative sEMG parameters.

4.4 Discussion

We found a significant shift toward higher frequencies during tonic seizures. Patients with GTC seizures had a significantly increased RMS, whereas patients with tonic seizures had significantly lower RMS than the simulated seizures. The EMG-EMG coherence was significantly higher during the epileptic seizures in both subgroups.

The mechanism of muscle activation in the control subjects simulating the seizures is obviously a physiologic one. Although, based on visual assessment, the posturing and muscle contractions appeared similar during the simulated and the epileptic seizures, the mechanisms of muscle activation were different.

As the sEMG parameters were not constant within the seizures; in addition to determining the mean value of the different parameters for the whole seizure period, we also calculated the 95th percentile (peak) values. Our results were even more pronounced when analyzing the peak values than when analyzing the mean values of the whole seizure periods.

4.4.1 Tonic activation

Quantitative analysis of the sEMG demonstrated significant differences between the two subgroups of epileptic seizures in which the qualitative visual assessment showed "sustained muscle activation": tonic seizures are produced by a significant shift toward the higher frequency bands, whereas the tonic phase of the GTC seizures is produced by an increase in the amplitude characteristic. These differences between the tonic seizures and tonic phase of the GTC seizures are not merely a function of time, as there was no significant difference in duration between the two seizure types, and the quantitative EMG parameters that differentiated between them did not show a correlation with the duration of the tonic muscle activation.

As early as 1963, Gastaut, described that the tonic phase of the GTC seizures was "more intense" than the contraction of tonic seizures based on visual analysis of the sEMG in polygraphic recordings [31]. Our quantitative analysis demonstrating higher amplitude characteristic of the tonic phase of the GTC

seizures are consistent with these early observations. Our findings furthermore support that tonic seizures are not merely truncated manifestations or fragments of GTC seizures (i.e., minus the clonic phase), not even at the level of the final pathway (the MUs). We suggest that the "sustained tonic contraction" has to be defined differently for tonic and GTC seizures, emphasizing the increase in frequency in the case of the tonic seizures and the increase in amplitude for the GTC seizures.

4.4.2 Pathophysiological explanation

Although various quantitative sEMG parameters have been used to infer details about the CNS control mechanism of muscle activity, the technical limitations of the method should be emphasized, as the sEMG reflects both peripheral and central properties of the neuromuscular system [25]. However, the shift toward higher frequency domains during the muscle activation has been attributed to the recruitment of more motor neurons, including the ones with higher threshold [68, 88]. The shift toward higher frequencies during the tonic seizures can thus be explained by an increase in the recruitment of more, high threshold motor neurons. The increase in the RMS of the sEMG signal can be caused by synchronization of the MU activity or by lengthening of the muscular action potential [3]. This means that the two types of tonic seizures have different kinds of activation of the MUs, thus the signals from the CNS must be of different origin as well.

4.4.3 Control subjects

The control subjects were trained to activate the muscles on the two sides simultaneously and in synchronization. The visual analysis of the recordings showed that the "sustained" muscle activation during all analyzed seizures in all patients and control subjects were bilateral, symmetrical, and synchronous. However, the coherence was significantly higher during the epileptic seizures in both subgroups for the whole seizure period as compared with the simulated ones. This suggests that the neural networks on both sides are synchronously activated also in the efferent pathways. Grosse et al. [35] found markedly increased EMG-EMG mean coherence between the muscle pairs on the two sides in nine patients with high frequency rhythmic myoclonus. Our findings in patients with generalized tonic and GTC seizures are consistent with this.

4.5 Conclusion

The first aim of our study was to explore if there are any differences between the pathologic and physiologic activation of the muscles during tonic activation. We compared several quantitative sEMG parameters (median and "peak") for the entire seizure epoch and found that these can distinguish between

epileptic and non-epileptic muscle activation.

The second aim was to explore if the two types of tonic activation (tonic seizure and tonic phase of GTC seizure) are truly alike. Our results provide insight into the pathomechanism of the muscle activation during epileptic seizures, and we found significant differences between the 2 types of epileptic seizures: tonic and tonic phase of GTC. This advocates for a change in the corresponding ILAE definition.

The third aim was to validate if some of the parameters would be valuable as a feature for a seizure detection algorithm. Our results showed potentially diagnostic significance and the fact that several of the sEMG parameters are specific for epileptic muscle activation suggest that they potentially can constitute the substrate for automatic seizure detection algorithms. One specific sEMG feature that showed a significant difference between the epileptic and simulated seizures was the increase in frequency reflected by the MF and the RP.

Based on these observations, and our conclusions from the previous chapter we continuously focus on developing a detection algorithm based on sEMG alone, limiting it to investigate the higher frequencies. Thus, it will be possible to increase the number of modalities later if it is found to be necessary.

DETECTION OF GENERALIZED TONIC-CLONIC EPILEPTIC SEIZURES

Objective *Concerning seizure detection, the highest potential clinical relevance is for the GTC seizures, as these are associated with an increased risk of sudden unexpected death in epilepsy (SUDEP) in unsupervised patients. The advantage of an sEMG based seizure detection system is its feasibility as it only implies application of a small, portable device. To our knowledge, no other group have prior succeeded in designing an algorithm for seizure detection based on sEMG signals alone. This chapter serves to show the possibilities for a seizure detection algorithm based solely on sEMG data and, furthermore, to test it in a small wireless sEMG device. This is also presented in Paper V-VII, which this chapter is composed upon.*

5.1 Background

In chapter 3 we focused on using multi-modal data, including sEMG, accelerometers and gyroscopes for detection of epileptic seizures with motor manifestations. One other group has also tried to detect seizures based on a combination of accelerometers and sEMG [66]. Other authors have used EEG [2, 13, 77], video [23], ECG [38], EEG/ECG [84] or accelerometers [7, 22, 37, 43, 45, 58, 59] to develop seizure detection systems for GTC seizures. One group have even tried to discriminate GTC seizures from other seizures based on accelerometers [6, 7]. Both Kramer et al. and Lockman et al. achieved promising results on detecting GTC seizures based on accelerometer data. However, the seizures were detected rather late since the accelerometers were best at detecting the clonic phase of the seizures. Based on this and the promising results we obtained in the study described in Chapter 4 [20], we decided to focus on one modality, the sEMG.

A couple of the mentioned studies [43, 45] have their algorithm implemented and tested in small devices

based on accelerometers. Thus we will focus the design of an algorithm toward an implementation in a small sEMG device.

We suggest that better results will be obtained by designing a sensitive and specific algorithm that detects the seizures already in the tonic-phase, which precedes the clonic one. We chose sEMG as our modality, because there is an intensive activation of the muscles during the tonic phase. To make the system feasible (easy to wear by the patients) we aimed at using as few sensors as possible, i.e. only one or two channels [15, 16]. Furthermore, we focused on designing a simple detection algorithm in order to keep the algorithm computationally efficient and make an implementation of the algorithm in a portable device possible.

5.1.1 Research hypotheses

The main aim of the study is to propose the first algorithm based on only sEMG signals for detecting epileptic GTC seizures. Our hypothesis is that the information content of the sEMG is sufficient for early detection of GTC seizures.

Our hypotheses are:

- to develop a GTC seizure detection algorithm based on sEMG data (off-line study).
- to make it possible to implement the algorithm into a small wireless sEMG device (on-line study).

5.2 Recordings

This chapter consist of an off-line and an on-line implementation of the same algorithm. Thus, this section is divided into the off-line and the on-line study. The off-line study is performed based on normal sEMG data, used to design a GTC seizure detection algorithm. The on-line study is an evaluation of the algorithm implemented in a small wireless sEMG device.

5.2.1 Off-line study

This study was based on sixty consecutive patients admitted to the EMU at the Danish Epilepsy Center in Dianalund, Denmark for diagnostic reasons, with a history of GTC seizures in the referral. Eleven patients had GTC seizures. The rest of the patients had seizures other than GTC or did not have epileptic seizures at all during the monitoring period. The recordings included EEG, video, ECG and sEMG electrodes. The sEMG electrodes were mounted as described in section 2.2.1. For this study we have only analyzed the signals from the left deltoid and anterior tibial muscles. The admission lasted 1-4 days

depending on the patient. The sEMG was sampled with a frequency of 1024 Hz. The long-term video-EEG recordings were reviewed by a clinical neurophysiologist and an epileptologist, who marked the time-epochs containing a GTC seizure, based on visual analysis. The physician marked the start of the tonic phase, when this was unequivocal. In total we recorded 22 GTC seizures in 776 hours. The number of seizures and the demographic data are listed in Table C.1. The recording time for each patient is listed in Table 5.1.

Table 5.1: The length of the analyzed files.

Patient	File length [h]
TC1	15.9-25.3
TC2	92.5-95.2
TC3	89.4-93.4
TC4	46.6
TC5	89.9-95.5
TC6	90.9-95.2
TC7	91.5-94.3
TC8	12.4-16.2
TC9	37.2
TC10	89.0
TC11	88.1

During the long term monitoring, trained neurophysiology technicians monitored the recordings to make sure that data showed sEMG activity and not noise, which would imply a loose connection (high impedance). It happened that the sEMG electrodes were accidentally detached for some patients during the recordings. In these cases the technicians corrected this as soon as possible. The epochs with detached/loose electrodes were excluded from the analysis, but in total more than 96% of the data was used, making it reasonable to look at the algorithm working both at night and during the day. Since some periods were excluded, the time lengths were not exactly the same for the two muscles and thereby neither for the combination of them. Therefore different time lengths are provided for some patients in Table 5.1.

5.2.2 On-line study

Five consecutive patients were included from the Danish Epilepsy Center in Dianalund, Denmark, for diagnostic reasons. All included patients have a history of GTC seizures. The demographic data, the amount of GTC seizures during the recording, duration of the seizures and the recordings are all listed in

Table 5.2.

Table 5.2: The patients's gender, age, the amount of seizures, the length of the admission and the length of the GTC seizures.

Patient	Gender	Age	# GTC	Seizure duration [s]	File length [h]
D207	F	15	0		-
D208	M	34	3	88, 77, 52	68.4
D209	M	48	0		50.1
D210	M	38	0		53.3
D211	M	44	4	100, 105, 98, 102	126

The normal admission recordings included EEG, video, ECG and sEMG electrodes placed on several, clinically relevant muscles. Along with this a wireless sEMG device from the Danish company IctalCare A/S [5], with an implementation of our algorithm, was placed on a tibial muscle (left/right) as shown in Fig. 5.1. The choice of side for the placement of the device (left/right) was decided by the physician based on records on where each patient normally have their seizures expressed the most. The device only provides hidden alarms, which means that the staff at the hospital are unaware of the times of the alarms. The admission lasted 2-5 days depending on the patient, thus providing us with a huge amount of data for each patient. The sEMG was sampled with a frequency of 1024 Hz. Two of the patients had GTC seizures, while the others had other kinds of seizures or none at all. The times for the beginning and ending of the seizures were annotated by a physician based on the gold standard (video and EEG signals). For the first patient we had some recording problems, which meant that unfortunately no data was recorded from the wireless sEMG device placed on the tibial muscle, see table 5.2.

5.3 Methods

The methods section is divided into three sections; the feature extraction, the detection approach and the changes for the on-line implementation of the algorithm.

5.3.1 Feature extraction

In Chapter 4 we analyzed the similarities and differences between sEMG signals from real epileptic seizures and sEMG signals from simulated seizures. We showed that real seizures in contrast to normal activity had a large proportion of data in the frequency band above 100 Hz. In this study, a visual



Figure 5.1: The wireless sEMG device placed on the tibial muscle.

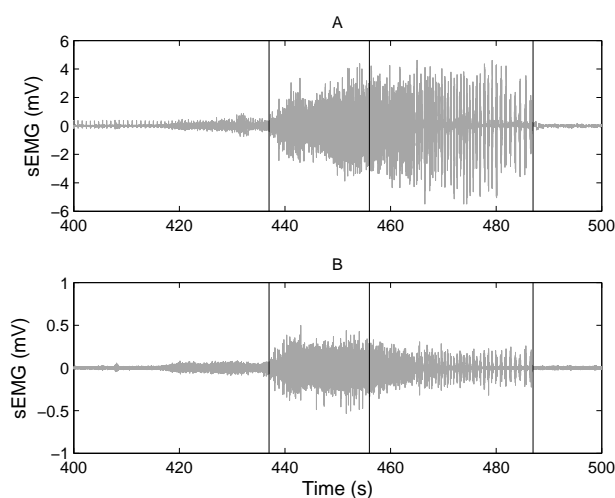


Figure 5.2: Figure 'A' shows the seizure (with surrounding activity) before filtering and figure 'B' the signal after filtering. The right and left black vertical lines denote the beginning and end of the GTC seizure, whereas the middle black vertical line denotes the start of the clonic phase, marked by the physician. The data is from the left deltoid.

evaluation of all seizures from the 11 off-line patients revealed that the differences between seizures and normal activities were even more pronounced when processed with a high-pass filter with a cut-off frequency of 150 Hz. The high-pass filtering ensures, that a larger amount of the artifacts will be removed. We have used a FIR hamming window filter, where the group delay is ensured to be linear in the frequency band of interest. A seizure from a representative patient is shown in Fig. 5.2 before and after filtering. The filter coefficients are given in Table D.3 in Appendix D.

Our results in Chapter 4 on the sEMG signals during real and simulated seizures showed that simple features are able to distinguish between the two groups. We therefore chose to focus this study on finding a simple and computationally efficient feature, that would be able to discriminate GTC seizures from normal activity. The final method is meant to be used in a seizure detection system and it is therefore important to capture the seizures soon after the onset. Since the seizures are started by a tonic phase, we searched for a feature to discriminate this part of the seizure from normal activities.

In Chapter 4 we found that the epileptic tonic activity contained a larger proportion of higher frequencies than the physiologic activities. We have therefore chosen to focus our feature choice on the frequency domain, since this might distinguish both types of seizures (tonic and GTC) from normal activities though we only focus on one type in this study. We chose a simple measure for the instantaneous frequency through the zero-crossing compared to the power spectrum (used in [20]), since it is more convenient for implementation in a portable detection device. Previously, other groups [86, 91] have used zero-crossing for prediction of epileptic seizures based on EEG. Since we wanted our algorithm to focus only on actual sEMG data, we decided to count only those zero-crossings, which extended above and below a hysteresis. This ensured that the actual zero-crossing count would not be affected by noise. We do not claim that this method will eliminate all noise and artifacts in a large scale trial of the detection system, and further noise and artifact reduction will probably be needed. From a quantitative inspection of data, we found background noise with a standard deviation (SD) as high as $15\mu\text{V}$, so to ensure that the zero-crossing only operates outside the noise region, we chose to include a hysteresis of $\pm 50\mu\text{V}$, corresponding to $3\text{-SD} \approx 50\mu\text{V}$. A zero-crossing is then only registered when the signal peaks preceding and following it exceeds $50\mu\text{V}$ and $-50\mu\text{V}$, respectively. So, if the signal starts by rising above $50\mu\text{V}$ one count is set when the signal goes below $-50\mu\text{V}$ and another count is set, when the signal again is above $50\mu\text{V}$ and so on. We found that when applying the zero-crossing method with a hysteresis of $\pm 50\mu\text{V}$ on the filtered data, the number of crossings was high throughout the entire tonic phase, see Fig. 5.3. The count of zero-crossings is seen to decrease at the end of the tonic phase and throughout the clonic phase. This decrease is however caused by the clonic phase consisting of alternating periods with high activity and no activity at all. We evaluated the count of zero-crossings with a smaller window size and found that the count is as high in the active clonic phases as in the tonic phase, so the reason for the decrease in the number of counts is that the window includes both the active periods and the periods with no activity in the clonic phase.

5.3.2 Detection approach

Although many more parameters could be considered to make the algorithm more advanced, in our search for the optimal method to classify the data into GTC seizures or normal activity, we chose to consider two parameters. The first one is the number of zero-crossings in a given window (called the threshold) and the second one is the number of succeeding windows, where the number of zero-crossings exceeds the threshold, needed to finally classify a seizure. As in Chapter 3, we chose to use a window of 1 s. In this

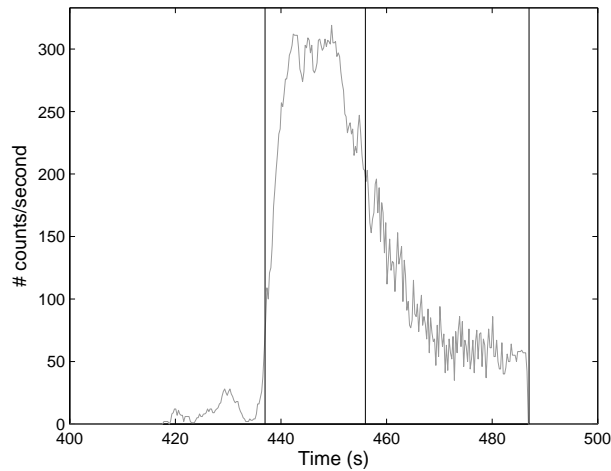


Figure 5.3: The number of zero-crossings in windows of 1 second as a function of the time for the filtered data in Fig. 5.2 (one seizure from a representative patient). It is clearly seen that the number of zero-crossings rises fast at the start of the tonic phase, stays high throughout the tonic phase and drops at the beginning of the clonic phase. The right and left black vertical lines denote the beginning and end of the GTC seizure, whereas the middle black vertical line denotes the beginning of the clonic phase.

study we opted for an overlap of 75% for the windows. These two values, length and overlap of windows, were chosen based on a visual inspection of the feature-plot (see example in Fig. 5.3) for all seizures. Furthermore, this inspection showed that the maximum number of zero-crossings during the tonic phase of the seizures was about 255 counts if all seizures were to be detected. We varied the threshold from 200 (180 for anterior tibial muscle) to 300, with an interval of 5 counts between (180) 200 and 240 and between 260 and 300, whereas we had an interval of one count from 241-259. When seeking to avoid too many false detections and at the same time ensuring a sufficiently short latency, the band of properly chosen numbers of windows to make a seizure detection is most likely narrow. We therefore varied the number of windows to make a seizure detection from 2 to 30, where two windows correspond to a minimum delay of 1.25 seconds and 30 to a minimum delay of 8.25 seconds, to ensure that all possible solutions are tested. The number of windows was varied with intervals of two between 2 and 10 and between 20 and 30, whereas it was varied with intervals of one between 11 and 19. The beginning of the GTC seizures were marked by a clinical neurophysiologist and an epileptologist by a visual evaluation of data, as this, so far, is more reliable than any automated method. However, the exact start-time was sometimes uncertain. In these cases we opted for marking the clinical time-point that unequivocally showed the onset of the tonic phase. Thus, in theory this marking might come a few seconds later than the real seizure-onset. We therefore added a condition in our interpretation of the results which changed the latency to the minimum (based on the number of windows included) if the estimated start-time turned out to be earlier than the clinical (actual) time-point (though within 100 seconds from it). For each pair of parameters the three measures from section 3.4.7 were calculated to evaluate the results.

In order to evaluate which parameters were optimal, we used a 4-fold cross validation method [80], where the 11 patients (pt) were randomly partitioned into four subgroups (1: pt 2,6,10; 2: pt 1,4,9; 3: pt 5,7,11; 4: pt 3,8). From the 4 subgroups, one was retained for validation of the parameters, whereas the other three subgroups were used for training the optimal choice of parameters. The validation group was then used to evaluate the trained choice of parameters. The cross-validation process was repeated four times, one time with each of the four subgroups as validation group. This method ensured that all patients were used (an equal number of times) for both training and validation. The optimal parameters for each training session were chosen from a 2D-plot, which express the relationship between the sensitivity and FDR (specificity), and the latency. The plot express the mean latency for all seizures in the training groups on the abscissa:

$$\text{abscissa} = \overline{\text{LAT}}, \quad (5.1)$$

and the sensitivity minus the false detection rate on the ordinate:

$$\text{ordinate} = \begin{cases} \text{SEN} - \text{FDR}, & \text{for } \text{SEN} - \text{FDR} \geq 0 \\ 0, & \text{for } \text{SEN} - \text{FDR} < 0 \end{cases}, \quad (5.2)$$

where SEN is the sensitivity (between 0 and 1) and FDR is the false detection rate given per hour (the FDR corresponds to the specificity). If none of the seizures for a patient are detected the latency is given the value of the maximum latency of the patients involved in the training session. The approach of plotting the sensitivity and the FDR on one axis, and the latency on the other makes it easier to search parameters that both ensures high sensitivity, low FDR (i.e. high specificity) and short latency. In Fig. 5.4 an example of the plot is shown for the training session of group 1-3. The encircled point on the curves in Fig. 5.4 is chosen as the best trade-off between the sensitivity and the FDR and the latency in our point of view. We have prioritized a sensitivity as close to 100% as possible, while keeping the FDR as low as possible, secondly we also tried to obtain a short latency. This is because we would rather have the detections delayed by a second, than not detecting them at all. In Fig. 5.4 the optimal point with respect to achieving both high sensitivity and specificity would be as close to one as possible on the y-axis. Secondly, we chose the point so as the latency would not be too large (the point being placed too far right on the x-axis). The optimal parameters are considered not to be outliers, so that small changes in the threshold or number of windows to finalize a detection does not change drastically (e.g. the amount of seizures detected). If so, another set of optimal parameters will be searched.

The optimal choice of parameters chosen based on a plot equal to the one shown in Fig. 5.4 for each of the four training sessions are given in Table 5.3 for the three training branches: deltoid muscle data alone, anterior tibial muscle data alone and the combination of data from both muscles. The parameters for the combination of the two muscles are achieved by requesting that the seizure should be visible through the

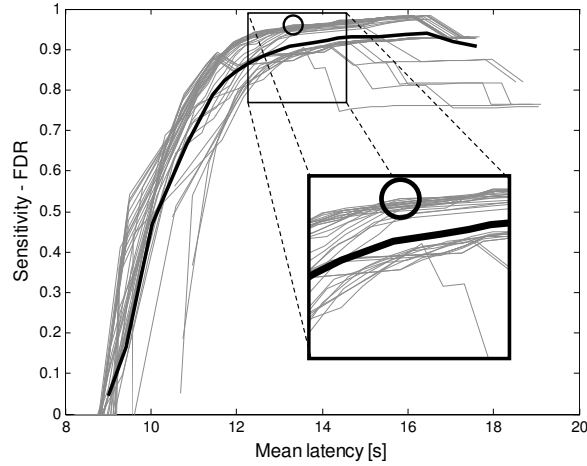


Figure 5.4: Each curve shows different threshold levels and for each curve the number of windows is varied. The black circle marks the chosen point on the curves. The thicker curve highlights the mean of the curves.

features in both muscles (channels) at the same time. This combination should reduce the number of false alarms, which are only visible in one muscle. Therefore lower values are expected for the two parameters, compared to the detection being based on just one muscle.

Table 5.3: The parameters chosen through the four training phases. # win=number of windows, th=threshold.

Training groups	Deltoid		Tibialis		Combined	
	# win	th	# win	th	# win	th
1,2,3	19	241	26	195	8	200
1,2,4	15	253	28	195	8	195
1,3,4	19	245	24	190	8	200
2,3,4	19	240	24	205	8	200

5.3.3 On-line implementation of the algorithm

For the on-line implementation of the algorithm the two parameters (*threshold* and *number of windows*) were trained for the data on which it was intended to be used (recorded with the wireless sEMG device). Even though we developed the algorithm with consideration to a later implementation in a small detection device, small changes had to be made to realize the implementation. The first thing changed was the filter, since the device could not encompass a filter of the size we used in the off-line version of the algorithm.

A new filter was designed, so as it resembled the old one as closely as possible, and at the same time with an order as low as 11 (the maximum number of coefficients allowed for the filter to follow the limitations regarding the capacity of the current version of the wireless sEMG device). The off-line implementation of the filter had an order of 21, meaning that both the summations and multiplications have been lowered with 10 in the algorithm. The filter characteristics of the off-line version is shown in blue in Fig. 5.5. The on-line filter was chosen as an FIR equiripple filter with order 11. This filter is shown in red in Fig. 5.5. The filter coefficients are given in Table D.3 in Appendix D.

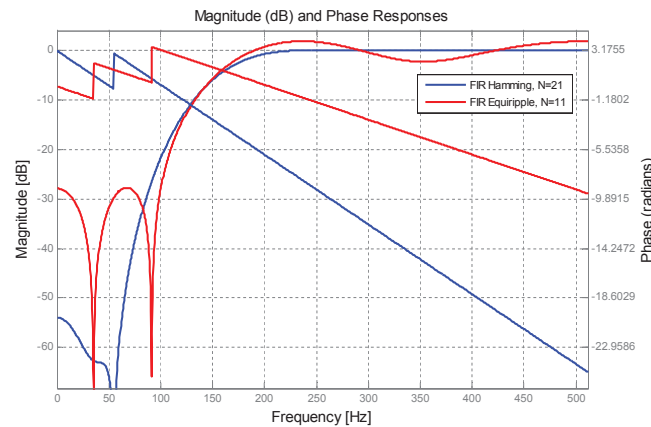


Figure 5.5: The filter characteristics for the off-line filter (blue) and the new on-line filter (red) implemented in the wireless sEMG device.

The frequencies of interest are all above 150 Hz, where the phase is seen to be linear for both filters. For the on-line filter the equiripples make small differences in the suppression of the signal above a frequency of 150 Hz, but these are considered insignificant. For the frequencies below 150 Hz, a larger difference is seen, but for both filters, this part of the signal is lowered tremendously. This means, that it will be insignificant, when continuing with the count of zero-crossings above and below the hysteresis of $\pm 50\mu\text{V}$. Since the algorithm is to be used on sEMG from the wireless sEMG device, the parameters must be fitted to this exact type of data. At the time of implementation, we only had data from two patients with GTC seizures. Normally we would record from both the biceps and the tibial muscle, but in the case of these two patients, unfortunately some technical problems had occurred with the device on the biceps, which meant that we only had sEMG data from the tibial muscle during the seizures. The parameters were trained as described in the previous section for the off-line version of the algorithm, from which we found the optimal parameters to be *number of windows* = 15 and *threshold* = 300 μV . Thus the number of windows is similar to the one obtained in the off-line version for the normal sEMG data, whereas the threshold in case of the wireless sEMG device data is a bit higher than for the normal sEMG data. The results of the on-line version of the algorithm is verified by comparing the hidden seizure alarms found by the algorithm to the times annotated by the neurophysiology technicians. The seizure times found by the algorithm is sent to a third party, before the true seizure times are received from the recording site.

This is to verify that it is a double-blind study.

5.4 Results

Since the off-line and on-line studies are conducted separately, this section is divided into two subsections each containing the results of one study.

5.4.1 Results for the off-line version

The test results for the two electrode placements (deltoid and anterior tibial) are presented in Table 5.4 together with the combined results where an alarm is generated if it is registered in both muscles at the same time. The overall results of the evaluation are very promising and suggest that it is possible to choose parameters such that the same algorithm (incl. parameters) may be used for all patients, providing a generic method for a detection system for epileptic patients with GTC seizures.

When using data only from the deltoid muscle all seizures are detected with an acceptable mean latency. The latency is different for the different patients, since it varies how abrupt the seizures start and how early the muscles are recruited into the seizure. A visual inspection of the sEMG data compared to the video shows that the seizures for patient 9, for whom the latency is very long, involve the deltoid muscle relatively late. Besides good sensitivity and latency, the results for the deltoid muscle alone also show a very low FDR. The mean FDR is 0.04, which corresponds to approximately 1 in 24-hours. Most of the false detections are in the daytime, and only three were during the night (12pm-8am) for the results on the deltoid muscle data, see Fig. 5.6. This is only approximately 10% of the false alarms, so if the algorithm was implemented in a system only to be used during the night, where a surveillance system is mostly needed, the FDR would be approximately one false alarm for every tenth day.

The results for the data from the anterior tibial muscle alone are not as good as for the deltoid muscle. For the anterior tibial the mean sensitivity is 77%. Only for 7 of the patients are all seizures detected, for two of the remaining three, none of the seizures are detected. This may be caused by the high number of windows. If it is too high the length of the period they cover might exceed the length of the tonic phase for some patients, and thereby cause detection to fail. The mean latency is longer for detections based only on the anterior tibial muscles compared to those based on the deltoid muscle. However, for some patients latency is lower than for the deltoid muscle and for some patients it is higher. For all those with a lower latency all seizures are detected. The same pattern is seen for the FDR, where the mean is much higher for the results on the anterior tibial muscle compared to the deltoid muscle, but for three patients it is actually lower.

Table 5.4: The results for validation of the trained parameters (see Table 5.3), based on a single muscle or the combination of two.

Patient	Deltoid			Anterior Tibial			Combined			
	SEN [%]	FDR [/h]	LAT [s]	SEN [%]	FDR [/h]	LAT [s]	SEN [%]	FDR [/h]	LAT [s]	
Group 1	2	100	0.03	8.38	0	0.01	-	100	0.01	4.88
	6	100	0.04	7.75	100	0.03	6.75	100	0.03	4.25
10	100	0.00	6.00	100	0.84	7.25	100	0.02	3.33	
Group 2	1	100	0.00	9.00	100	0.06	6.75	100	0.00	6.00
	4	100	0.09	11.25	100	0.09	19.25	100	0.00	14.75
9	100	0.03	34.44	100	0.00	27.44	100	0.00	26.31	
Group 3	5	100	0.04	7.13	50	0.05	11.75	100	0.19	5.75
	7	100	0.03	17.00	100	0.11	14.75	100	0.00	9.75
11	100	0.14	7.17	67	0.31	24.88	100	0.02	13.00	
Group 4	3	100	0.00	10.25	0	0.68	-	100	0.01	9.75
	8	100	0.00	12.33	100	0.32	11.08	100	0.16	7.33
Mean	100	0.04	13.66	77	0.20	14.11	100	0.04	9.85	

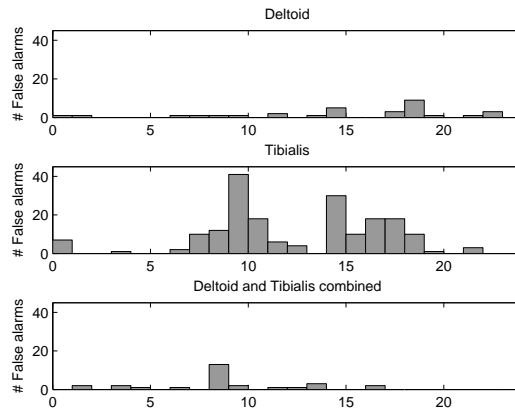


Figure 5.6: Histograms of the false alarms for all 11 patients. The abscissa shows the time of the day (24-hours).

If the two sets of data are combined, the results improve somewhat regarding latency, which was expected. Similarly to the results based on the deltoid muscle alone, all seizures are detected, the mean FDR is low, but the mean latency is even shorter for the detection based on both muscles. However for two patients (4 and 11) the latencies are increased for the combination of both muscles compared to the deltoid muscle alone. The explanation may be found in the fact that the latency is very high for these patients, when only the anterior tibial data are used, which implies that the seizures are seen later in this muscle than in the deltoid muscle.

5.4.2 Results for the on-line version

The data was collected from the recording site and visualized through the free-ware program EDFbrowser [85]. The data files contain one vector featuring the sEMG signal and one holding a notation vector, which contains the alarm times. An example of a GTC seizure and the matching hidden alarms are shown in Fig. 5.7. Several alarms are shown, but in a final product only the first one will set off an actual alarm. The time for each "first" alarm in a sequence is annotated as a seizure and compared to the true seizure times. The results for each patient are shown in Table 5.5. For patient D207 no data is recorded on the tibial muscle. Patient D209 and D210 had no seizures, but neither did we detect any false alarms. Patient D208 had three GTC seizures during the admission, while patient D211 had four. For patient D208 we were able to detect all three seizures, and at the same time we did not register any false alarms. For patient D211 we succeeded in detecting one of the four seizures, while the other three were missed. Furthermore, we registered one false alarm for this patient.

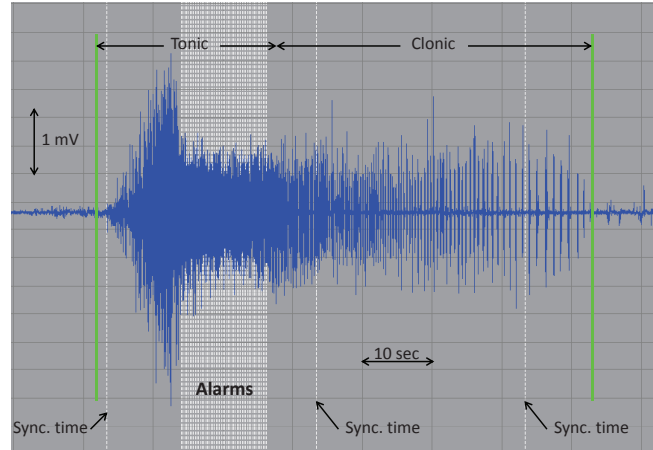


Figure 5.7: The sEMG during the second GTC seizure from patient D208. The period is divided into a tonic and a clonic phase. It is seen that all the consecutive alarms are set within the tonic phase. The two green vertical lines mark the beginning and end of the seizure. The three single white vertical lines are as stated synchronization time stamps, which are set by the wireless device to keep track of the time.

Table 5.5: The results for each of the on-line analyzed patients.

Patient	SEN [%]	LAT [s]	FDR [/h]
D207	-	-	-
D208	100	31; 18; 5	0.000
D209	-	-	0.000
D210	-	-	0.000
D211	25	46	0.008
Mean	57	25	0.003

5.5 Discussion

For the normal sEMG data (off-line system) the results for the two muscles and the combination of them are not only dependent on the chosen muscle, but also on the chosen parameters, see Table 5.3. For the combined method the number of windows for a detection is low, explaining the short latency. For the anterior tibial muscle the number of windows is large, which explains the long latencies. Looking at the parameters in Table 5.3, one will see that they are more alike for the combination of the two muscles, than for the deltoid muscle alone, where group three is tested with parameters somewhat different from the others. If group three had instead been tested with parameters similar to the other three groups (19 windows and a threshold of 241), the sensitivity would have stayed the same, but the latency would have been longer and the FDR smaller, which would bring the mean FDR to 0.03 and the mean latency to 13.9 for the deltoid muscle data alone. This suggests that a result corresponding to the one presented in Table 5.4 would be obtained by using the exact same parameters for all patients.

The on-line version of the algorithm proved to function intentionally for patient D208-D210 with a 100% sensitivity and no false alarms. Unfortunately, it did not perform as good for patient D211.

Comparing the mean results in Table 5.5 (SEN = 57%, LAT = 25s, FDR = 0.003/h) to the mean results on normal sEMG data on the tibial muscle in Table 5.4 (SEN = 77%, LAT = 14.1s, FDR = 0.2/h), the overall impression is an improvement, especially when taking into account that patient D211 is an outlier. The sensitivity was better for the algorithm on the normal sEMG data (though only when patient D211 is not excluded), but the false detection rate was significantly improved in the on-line algorithm.

5.5.1 Data quality

The normal electrodes used to collect the data are wired; the impedances are kept low by the health-care personal monitoring the signals and making sure that the background noise does not increase too much. For the wireless sEMG device used, there are no test of the impedances. For now, we have to rely on the quality of the data, but in the next version it will be designed to measure the impedance regularly.

Very few time periods were excluded from the evaluation of data, but in a real time situation it is important that all data is useful. The wireless sEMG device, which was used in the on-line test, was more adhesive, and were less likely to fall off. In periods where the electrode(s) or the wireless sEMG device are loose or have completely fallen off, the algorithm will not be able to detect any seizures.

The missing data for the first patient testing the wireless sEMG device imply that we have some recording problems, which need to be clarified. It should be noticed that the used wireless sEMG device is only a prototype and the next version is in preparation. Thus the complications are expected to be corrected.

5.5.2 Choice and number of muscles

Since combining the deltoid data with the anterior tibial data only improves the latency by 4 s on average, a detection system would more appropriately be based on the deltoid muscle alone, since the gain of adding data from an extra muscle is too small. If data should be combined from two muscles in a detection system one would probably choose two muscles closer together, than the deltoid and the tibial muscle.

Other muscles might be used as well. These two muscles were chosen since, in our experience, the deltoid muscle is always strongly involved in GTC seizures. The tibial muscle provides a less visible placement for a detection device, if it should be worn in daytime situations.

The wireless sEMG device was placed on biceps and the tibial muscle during the recordings, but for the first two included patients with seizures, only one third of the seizures had been recorded with the devices placed on biceps, which is the reason that we have not included this data. From the results on the conventional data we do believe that a better result of the on-line algorithm will be obtained, when it is applied on the biceps, instead of the tibial muscle. The reason for placing the wireless sEMG device on the biceps instead of the deltoid muscle is, that the biceps have tested to be a more comfortable place to wear this type of sensor.

5.5.3 Patient D211

For patient D211, where the on-line algorithm failed to detect three of the seizures, the seizures are quite different from the typical GTC seizures. These seizures consist of more interchanging tonic and clonic phases than the usual two. Furthermore each phase is shorter than during a classical GTC seizure. In Fig. 5.8 the count of zero-crossings during seizures are plotted for patient D200 (used for training of the parameters), D208 and D211. The feature (zero-crossing) for the seizures is very much alike within each patient. It is furthermore seen that the feature for the seizures for patient D208 is very similar to the ones for patient D200, whereas the ones for D211 is seen to be very different. The algorithm detects the peak, which is seen to be both shorter and lower for the seizures for patient D211. Thus the tonic phases for patient D211 may not be long and strong enough for the algorithm to capture them. The many alternating phases of tonic and clonic activity may explain the longer latency, since there is a clonic phase before the tonic phase, where the seizures are detected.

If the threshold was lowered to 250 (closer to the value for the normal sEMG data) six of the seven seizures were captured, but the amount of false positives would also increase to seven.

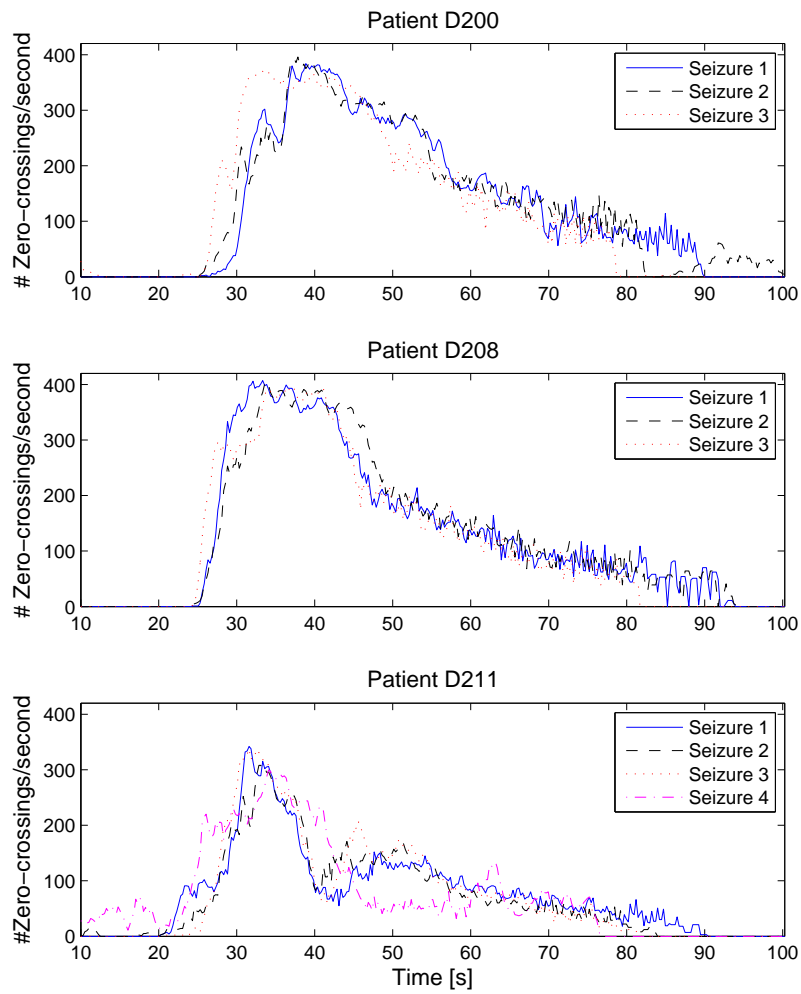


Figure 5.8: The zero-crossing counts for each seizure for patient D200, D208 and D211, respectively.

5.5.4 Comparison with seizure detection based on EEG

The sensitivity and specificity of seizure detection systems based on EEG signals vary widely: 70-100% (for sensitivity) and 0.5 -72 false detections / 24 hours (for specificity) [33, 40, 55, 63, 74]. The best performing ones are based on invasive recordings (intracranial electrodes) or many scalp electrodes (> 60) [55]. In the best performing studies they achieve the same sensitivity as our off-line approach, but a lower FDR and shorter latency. It should, however, be considered that their system would not be feasible for a long-term monitoring in the patients home or in the everyday life of a patient. In spite of using signals from a non-invasive recording (sEMG) and just one channel, we obtained a sensitivity of 100% and a specificity of 1 false-detection / 24 hours (deltoid muscle). This is compatible with the best performing EEG-based systems, but our system is easier to implement because it is non-invasive.

5.5.5 Comparison with seizure detection based on ACM

If we compare our deltoid results to other studies [43, 45] who have developed an algorithm to detect GTC seizures based on motion-data, our is more sensitive (SEN = 100% versus 88% [45] and 91% [43]). The study by Kramer et al. [43] includes 15 patients (22 seizures as in our study), whereas the results by Lockman et al. [45] is based on a very limited database (6 patients with 8 seizures). At the same time our algorithm captures seizures in the tonic-phase, whereas the other methods focus on the clonic-phase. Therefore our latencies are shorter than in these two studies with accelerometers. We are not able to compare the FDR to [45], since they have not listed how long their recordings were, but only that they captured 204 false alarms for the 8 patients. They do, however, state that they have a large false detection rate, so we would expect their system to have a larger FDR, than what we are able to provide. Kramer et al. [43] reports an FDR of 0.004/h (8 false alarms on 1692 hours), which is lower than what we have provided, but this should be held up against the lower sensitivity they achieved, which we find is more important to keep as close to 100% as possible.

If we compare our on-line results to Kramer et al. [43] our sensitivity is now lower, but our FDR (0.003/h) is slightly lower than theirs (0.004/h). Compared to Lockman et al. [45], at the same time our on-line results show a lower sensitivity as well, but also a much lower number of false alarms. Our on-line results do show a too low sensitivity compared to these studies, but if we exclude the outlier patient (D211), we would have shown a 100% sensitivity, which we expect to do for future patients with typical GTC seizures. Our FDR is the lowest of all the studies, which make our system the most reliable regarding false alarms. Since the other two methods are based on a detection in the clonic phase, as opposed to ours, which is based on the tonic phase, we expect to have a lower latency period.

5.5.6 Latency

Our latencies are longer, than for seizure detection algorithms based on EEG, but shorter than for seizure detection algorithms based on ACM. In general, the latency of our on-line algorithm could be improved. The used parameters are trained on a very narrow basis, and a modification of the algorithm toward a shorter detection time would be welcome in a future solution.

5.6 Conclusion

The first aim of this study was to develop a seizure detection algorithm based solely on the sEMG modality. We succeeded in doing this and to the best of our knowledge this is the first of its kind. The algorithm is a generic (the same algorithm/parameters are used for all patients) seizure detection system that is non-invasive (based on sEMG recordings), feasible (was applicable in all recruited patients), with high sensitivity (100%), low rate of false alarms (1 / 24 hours) and able to run in real-time. The algorithm was evaluated with a 4-fold cross-validation on one or two channels of sEMG from the deltoid or tibial muscle from 11 patients with GTC seizures. It is only addressed to GTC seizures. Nevertheless, it is the group of patients with this seizure type that has the highest risk for injuries following seizures and SUDEP [42]. If the algorithm would be used in nighttime only situations, it would provide an even lower median FDR of approximately one in ten days. Test on larger databases are needed to confirm the promising potentials of this algorithm in an on-line implementation.

The second aim was to implement the algorithm into a wireless sEMG device. We had to make some changes, but kept the algorithm as close to the original as possible. The implemented algorithm was tested through recordings with a wireless sEMG device and presented results which, when excluding the outlier, showed to be equally promising, with an even lower FDR. This makes our system preferable compared to the alarm devices used today that are based on accelerometers in a wristband or bed alarms.

CONCLUSION

The overall purpose of this Ph.D. project was to design a seizure detection algorithm for convulsive seizure based on movement signals registered with a uni- or multi-modality system. The dissertation objective is pursued through three research areas each with different purposes. In the first study, we tried to register subject movements with multiple modalities and to make an algorithm capable of discriminating convulsive epileptic seizures from normal activities. In the second study, the focus was to explore the differences and similarities between physiologic and pathologic activities, both tonic seizures and the tonic phase of GTC seizures. In the third study we focused on one modality and designed an algorithm able to discriminate GTC seizures from every other activity. Furthermore, the reliability of this algorithm was briefly tested in a wireless sEMG device.

The first research area provided us with valuable information regarding the use of one or more modalities in a detection algorithm. For the algorithm we presented, it was clear that the inclusion of more modalities provided a better result for the control subjects. We succeeded in measuring multi-modal data from 14 epileptic patients. Unfortunately, only one of the patients had a convulsive epileptic seizure during the recordings. We were, however, able to visually show that the simulated seizures are similar to real seizures. Thus, the results for the detection algorithm on patient recordings, when including more modalities are expected to show an improvement similar to the one seen for the control subjects. Besides from the multiple modalities multiple placements on the body were also used in this setup. This have probably been a valuable factor for the results as well.

The presented algorithm was made for all included convulsive seizures, but in the patient group we found that among the evaluated seizures, it was only appropriate for tonic and GTC seizures. This gave us a clear indication that better results could be achieved if we focused on a single seizure type instead of various seizure types.

For the second research area, we found several differences in the sEMG signal between the physiologic and the pathologic activity. These findings constitute the substrate for a seizure detection algorithm as feature input. Furthermore we detected clear differences between the tonic seizures and the tonic phase

of the GTC seizures, which advocate for a change in the ILAE definition of these seizures. The first part of a GTC seizure is defined as being equal to a tonic seizure, which our results clearly disprove.

The third research area aimed at developing a simple detection algorithm with low computational power based on sEMG signals alone and furthermore have it implemented into a wireless sEMG device for a double-blind test of the reliability. A novel detection algorithm was developed, which was able to detect GTC seizures with very few false detections. Compared to other methods/products such as the ones presented in Kramer et al. [43] and Lockman et al. [45] it presented a higher sensitivity, a lower or comparable FDR and a shorter detection latency, since our algorithm is able to detect the GTC seizure in the tonic phase compared to the other methods detecting the GTC seizures in the clonic phase (which succeeds the tonic phase).

The implementation of the algorithm into a wireless device was performed successfully with very few changes of the algorithm. The clinical test showed very promising results in 3 of 4 patients. The last patient had very atypical GTC seizures, and it is, thus, considered an outlier. This uni-modal approach showed very promising results, which might be further improved if an extra modality is added (e.g. ACM) as we saw in our first study.

6.1 Future perspectives

The area within detection of epileptic seizures is wide, and the possibilities are many. We suggest that some of the future studies to investigate further should be:

- to test the algorithm for GTC seizures implemented in the wireless sEMG device on more patients in order to achieve a more profound result for the reliability.
- to investigate the improvement on the reliability of adding an accelerometer into the wireless sEMG device.
- to investigate if the reliability is improved by adding more features or some kind of post-processing, to help lower the latency.
- to find a multi-modal system suitable for epileptic patients with convulsive seizures, and explore which positions on the body are the most appropriate for a seizure detection algorithm, in order to optimize the results, but furthermore with respect to user-friendliness.
- to investigate if the algorithm based on minor changes may be able to detect tonic seizures.
- to explore the possibilities of detecting other seizures with algorithms dedicated for the purpose, based on a multi-modal system as well as an uni-modal system.

BIBLIOGRAPHY

- [1] J. Alving, A. Sabers, and P. Uldall. *Basisbog i epilepsi*. Novartis Neuroscience, 1 edition, 2006.
- [2] M.R. Arab, A.A. Suratgar, and A.R. Ashtiani. Electroencephalogram signals processing for topographic brain mapping and epilepsies classification. *Computers in Biology and Medicine*, 40(9):733–739, 2010.
- [3] T.I. Arabadzhiev, V.G. Dimitrov, N.A. Dimitrova, and G.V. Dimitrov. Influence of motor unit synchronization on amplitude characteristics of surface and intramuscularly recorded emg signals. *European journal of applied physiology*, 108(2):227–237, 2010.
- [4] Ambu A/s. Baltorpbakken 13. 2750 ballerup. denmark, 2012. http://www.ambu-e-commerce.co.uk/product.php?id_product=802.
- [5] IctalCare A/s. Venlighedsvej 4. 2970 hørsholm. denmark, 2012. <http://www.ictalcare.dk>.
- [6] G. Becq, S. Bonnet, L. Minotti, M. Antonakios, R. Guillemaud, and P. Kahane. Collection and exploratory analysis of attitude sensor data in an epilepsy monitoring unit. In *Engineering in Medicine and Biology Society, 2007. EMBS 2007. 29th Annual International Conference of the IEEE*, pages 2775–2778. IEEE, 2007.
- [7] G. Becq, S. Bonnet, L. Minotti, M. Antonakios, R. Guillemaud, and P. Kahane. Classification of epileptic motor manifestations using inertial and magnetic sensors. *Computers in Biology and Medicine*, 41(1):46–55, 2011.
- [8] C. Bischoff, A. Fuglsang-Fredriksen, L. Vendelbo, and A. Sumner. In *Deuschl G., Eisen A. Recommendations for the practice of clinical neurophysiology: guidelines of the International Federation of Clinical Neurophysiology*. Amsterdam: Elsevier, chapter Standards of instrumentation of EMG, pages 199–211. Elsevier Science Health Science div, 1999.
- [9] S. Bonnet, P. Jallon, A. Bourgerette, M. Antonakios, R. Guillemaud, Y. Caritu, G. Becq, P. Kahane, P. Chapat, B. Thomas-Vialettes, et al. An ethernet motion-sensor based alarm system for epilepsy monitoring. *IRBM*, 32:155–157, 2011.

- [10] P. Brown, S.F. Farmer, D.M. Halliday, J. Marsden, and J.R. Rosenberg. Coherent cortical and muscle discharge in cortical myoclonus. *Brain*, 122(3):461–472, 1999.
- [11] C.J.C. Burges. A tutorial on support vector machines for pattern recognition. *Data mining and knowledge discovery*, 2(2):121–167, 1998.
- [12] A.F. Cabrera, D. Farina, and K. Dremstrup. Comparison of feature selection and classification methods for a brain-computer interface driven by non-motor imagery. *Medical and Biological Engineering and Computing*, 48:6123–6132, 2010.
- [13] E.C.P. Chua, K. Patel, M. Fitzsimons, and C.J. Bleakley. Improved patient specific seizure detection during pre-surgical evaluation. *Clinical Neurophysiology*, 122(4):672–679, 2011.
- [14] I. Conradsen, S. Beniczky, H. Hjalgrim, and P. Wolf. Experiment: Sj-115; overvågning og automatisk opdagelse af epileptiske anfald ved multi-modal signalanalyse, 2009.
- [15] I. Conradsen, S. Beniczky, K. Hoppe, P. Wolf, T. Sams, and H.B.D. Sorensen. Seizure Onset Detection Based on One sEMG Channel. In *Engineering in Medicine and Biology Society (EMBC), 2011 Annual International Conference of the IEEE*, pages 7715–7718. IEEE, 2011.
- [16] I. Conradsen, S. Beniczky, K. Hoppe, P. Wolf, and H. Sorensen. Automated algorithm for generalised tonic-clonic epileptic seizure onset detection based on semg zero-crossing rate. *Biomedical Engineering, IEEE Transactions on*, 59(2):579–585, 2012.
- [17] I. Conradsen, S. Beniczky, P. Wolf, J. Henriksen, T. Sams, and H.B.D. Sorensen. Seizure onset detection based on a Uni- or Multi-modal Intelligent Seizure Acquisition (UISA/MISA) system. In *Engineering in Medicine and Biology Society (EMBC), 2010 Annual International Conference of the IEEE*, pages 3269–3272. IEEE, 2010.
- [18] I. Conradsen, S. Beniczky, P. Wolf, T.W. Kjaer, T. Sams, and H.B.D. Sorensen. Automatic multi-modal intelligent seizure acquisition (misa) system for detection of motor seizures from electromyographic data and motion data. *Computer Methods and Programs in Biomedicine*, page Online, 2011.
- [19] I. Conradsen, S. Beniczky, P. Wolf, D. Terney, T. Sams, and H.B.D. Sorensen. Multi-modal intelligent seizure acquisition (MISA) system - a new approach towards seizure detection based on full body motion measures. In *Engineering in Medicine and Biology Society (EMBC), 2009 Annual International Conference of the IEEE*, pages 2591–2595. IEEE, 2009.
- [20] I. Conradsen, P. Wolf, T. Sams, H.B.D. Sorensen, and S. Beniczky. Patterns of muscle activation during generalized tonic and tonic-clonic epileptic seizures. *Epilepsia*, 52(11):2125–2132, 2011.
- [21] C. Cortes and V. Vapnik. Support-vector networks. *Machine learning*, 20(3):273–297, 1995.

- [22] K. Cuppens, L. Lagae, B. Ceulemans, S. Van Huffel, and B. Vanrumste. Detection of nocturnal frontal lobe seizures in pediatric patients by means of accelerometers: A first study. In *Conference proceedings: 31st Annual International Conference of the IEEE Engineering in Medicine and Biology Society.*, volume 1, pages 6608–6611, 2009.
- [23] K. Cuppens, L. Lagae, B. Ceulemans, S. Van Huffel, and B. Vanrumste. Automatic video detection of body movement during sleep based on optical flow in pediatric patients with epilepsy. *Medical and Biological Engineering and Computing*, 48(9):923–931, 2010.
- [24] J. Engel Jr, S. Wiebe, J. French, M. Sperling, P. Williamson, D. Spencer, R. Gumnit, C. Zahn, E. Westbrook, and B. Enos. Practice parameter: temporal lobe and localized neocortical resections for epilepsy. *Epilepsia*, 44(6):741–751, 2003.
- [25] D. Farina, R. Merletti, and R.M. Enoka. The extraction of neural strategies from the surface emg. *Journal of Applied Physiology*, 96(4):1486–1495, 2004.
- [26] S.F. Farmer, F.D. Bremner, D.M. Halliday, J.R. Rosenberg, and J.A. Stephens. The frequency content of common synaptic inputs to motoneurons studied during voluntary isometric contraction in man. *The Journal of physiology*, 470(1):127–155, 1993.
- [27] R.A. Fisher. On the” probable error” of a coefficient of correlation deduced from a small sample. *Metron*, 1(5):3–32, 1921.
- [28] R.S. Fisher, W.E. Boas, W. Blume, C. Elger, P. Genton, P. Lee, and J. Engel Jr. Epileptic seizures and epilepsy: definitions proposed by the International League Against Epilepsy (ILAE) and the International Bureau for Epilepsy (IBE). *Epilepsia*, 46(4):470–472, 2005.
- [29] J.A. French. Refractory epilepsy: one size does not fit all. *Epilepsy Currents*, 6(6):177–180, 2006.
- [30] H. Gastaut and R. Broughton. Epileptic seizures. *CC Thomas, Springfield, Illinois*, 1972.
- [31] H. Gastaut, J. Roger, S. Ocjahchi, M. Tmsit, and R. Broughton. An electro-clinical study of generalized epileptic seizures of tonic expression. *Epilepsia*, 4(1-4):15–44, 1963.
- [32] F. Gelli, F. Del Santo, T. Popa, R. Mazzocchio, and A. Rossi. Factors influencing the relation between corticospinal output and muscle force during voluntary contractions. *European Journal of Neuroscience*, 25(11):3469–3475, 2007.
- [33] J. Gotman. Automatic recognition of epileptic seizures in the eeg. *Electroencephalography and clinical Neurophysiology*, 54(5):530–540, 1982.
- [34] P. Grosse and P. Brown. In *Niedermeyer E., Da Silva F.H.L. Electroencephalography: basic principles, clinical applications, and related fields*, chapter Corticomuscular and intermuscular frequency analysis: physiological principles and applications in disorders of the motor system, pages 881–889. Lippincott Williams & Wilkins, 2005.

- [35] P. Grosse, R. Guerrini, L. Parmeggiani, P. Bonanni, A. Pogosyan, and P. Brown. Abnormal cortico-muscular and intermuscular coupling in high-frequency rhythmic myoclonus. *Brain*, 126(2):326–342, 2003.
- [36] D.M. Halliday, J.R. Rosenberg, A.M. Amjad, P. Breeze, B.A. Conway, S.F. Farmer, et al. A framework for the analysis of mixed time series/point process data—theory and application to the study of physiological tremor, single motor unit discharges and electromyograms. *Progress in Biophysics and molecular Biology*, 64(2-3):237–278, 1995.
- [37] P. Jallon. A bayesian approach for epileptic seizures detection with 3d accelerometers sensors. In *Engineering in Medicine and Biology Society (EMBC), 2010 Annual International Conference of the IEEE*, pages 6325–6328. IEEE, 2010.
- [38] J. Jeppesen, S. Beniczky, A. Fuglsang-Frederiksen, P. Sidenius, and Y. Jasemian. Detection of epileptic-seizures by means of power spectrum analysis of heart rate variability: A pilot study. *Technology and Health Care*, 18(6):417–426, 2010.
- [39] T. Joachims. Learning to classify text using support vector machines: Methods, theory, and algorithms. *Computational Linguistics*, 29(4):656–664, 2002.
- [40] Y.U. Khan and J. Gotman. Wavelet based automatic seizure detection in intracerebral electroencephalogram. *Clinical Neurophysiology*, 114(5):898–908, 2003.
- [41] J.M. Kilner, S.N. Baker, S. Salenius, V. Jousmäki, R. Hari, and R.N. Lemon. Task-dependent modulation of 15-30 hz coherence between rectified emgs from human hand and forearm muscles. *The Journal of physiology*, 516(2):559–570, 1999.
- [42] R. Kloster and T. Engelskjøn. Sudden unexpected death in epilepsy (sudep): a clinical perspective and a search for risk factors. *Journal of Neurology, Neurosurgery & Psychiatry*, 67(4):439–444, 1999.
- [43] U. Kramer, S. Kipervasser, A. Shlitner, and R. Kuzniecky. A novel portable seizure detection alarm system: Preliminary results. *Journal of Clinical Neurophysiology*, 28(1):36–38, 2011.
- [44] P. Kwan and M.J. Brodie. Early identification of refractory epilepsy. *New England Journal of Medicine*, 342(5):314–319, 2000.
- [45] J. Lockman, R.S. Fisher, and D.M. Olson. Detection of seizure-like movements using a wrist accelerometer. *Epilepsy & Behavior*, 20:638–641, 2011.
- [46] J. Lofhede, N. Lofgren, K. Lindcrantz, A. Flisberg, I. Kjellmer, and M. Thordstein. Comparison of three methods for classifying burst and suppression in the eeg of post asphyctic newborns. In *Engineering in Medicine and Biology Society, 2007. EMBS 2007. 29th Annual International Conference of the IEEE*, pages 5136–5139. IEEE, 2007.

- [47] K. Lorincz, B. Chen, G.W. Challen, A.R. Chowdhury, S. Patel, P. Bonato, M. Welsh, et al. Mercury: a wearable sensor network platform for high-fidelity motion analysis. In *Proceedings of the 7th ACM Conference on Embedded Networked Sensor Systems*, pages 183–196. ACM, 2009.
- [48] H. Lüders, J. Acharya, C. Baumgartner, S. Benbadis, A. Bleasel, R. Burgess, D.S Dinner, A. Ebner, N. Foldvary, E. Geller, et al. Semiological seizure classification. *Epilepsia*, 39(9):1006–1013, 1998.
- [49] S.G. Mallat. A theory for multiresolution signal decomposition: The wavelet representation. *IEEE Transactions on Pattern Analysis and Machine Intelligence*, 11(7):674–693, 1989.
- [50] E.N. Marieb. *Essentials of human Anatomy and Physiology*. CA: Benjamin/Cummings, 7 edition, 2003.
- [51] J.H. McAuley, T.C. Britton, J.C. Rothwell, L.J. Findley, and C.D. Marsden. The timing of primary orthostatic tremor bursts has a task-specific plasticity. *Brain*, 123(2):254–266, 2000.
- [52] M.F. McKinney and J. Breebaart. Features for audio and music classification. In *Proc. ISMIR*, volume 3, pages 151–158, 2003.
- [53] R. Merletti and P.A. Parker. *Electromyography: Physiology, engineering, and noninvasive applications*, volume 11. Wiley-IEEE Press, 2004.
- [54] T. Mima and M. Hallett. Corticomuscular coherence: a review. *Journal of clinical neurophysiology*, 16(6):501–511, 1999.
- [55] G.R. Minasyan, J.B. Chatten, M.J. Chatten, and R.N. Harner. Patient-specific early seizure detection from scalp eeg. *Journal of clinical neurophysiology*, 27(3):163–178, 2010.
- [56] I.W. Mothersill, P. Hilfiker, and G. Krämer. Twenty years of ictal eeg–emg. *Epilepsia*, 41:S19–S23, 2000.
- [57] O.P. Neto and E.A. Christou. Rectification of the emg signal impairs the identification of oscillatory input to the muscle. *Journal of neurophysiology*, 103(2):1093–1103, 2010.
- [58] T.M.E. Nijssen, R.M. Aarts, J.B.A.M. Arends, and P.J.M. Cluitmans. Automated detection of tonic seizures using 3-d accelerometry. In *4th European Conference of the International Federation for Medical and Biological Engineering*, pages 188–191. Springer, 2009.
- [59] T.M.E. Nijssen, J.B.A.M. Arends, P.A.M. Griep, and P.J.M. Cluitmans. The potential value of three-dimensional accelerometry for detection of motor seizures in severe epilepsy. *Epilepsy & Behavior*, 7(1):74–84, 2005.
- [60] T.M.E. Nijssen, P.J.M. Cluitmans, P.A.M. Griep, and R.M. Aarts. Short time Fourier and wavelet transform for accelerometric detection of myoclonic seizures. *IEEE/EMBS Benelux*, pages 7–8, 2006.

- [61] T.J. Nowak and A.G. Handford. *Pathophysiology - concepts and applications for health care professionals*, pages 632–651. McGraw Hill, 3 edition, 2004.
- [62] Commission on Classification and terminology of the ILAE. Proposal for revised clinical and electroencephalographic classification of epileptic seizures. *Epilepsia*, 22:489–501, 1981.
- [63] I. Osorio, M.G. Frei, J. Giftakis, T. Peters, J. Ingram, M. Turnbull, M. Herzog, M.T. Rise, S. Schaffner, R.A. Wennberg, et al. Performance reassessment of a real-time seizure-detection algorithm on long ecog series. *Epilepsia*, 43(12):1522–1535, 2002.
- [64] Y. Pan, S.S. Ge, F.R. Tang, and A. Al Mamun. Detection of epileptic spike-wave discharges using svm. In *Control Applications, 2007. CCA 2007. IEEE International Conference on*, pages 467–472. IEEE, 2007.
- [65] F. Panzica, L. Canafoglia, S. Franceschetti, S. Binelli, C. Ciano, E. Visani, and G. Avanzini. Movement-activated myoclonus in genetically defined progressive myoclonic epilepsies: Eeg-emg relationship estimated using autoregressive models. *Clinical neurophysiology*, 114(6):1041–1052, 2003.
- [66] S. Patel, C. Mancinelli, A. Dalton, B. Patriiti, T. Pang, S. Schachter, and P. Bonato. Detecting epileptic seizures using wearable sensors. In *Bioengineering Conference, 2009 IEEE 35th Annual Northeast*, pages 1–2. IEEE, 2009.
- [67] J.G. Proakis and D.G. Manolakis. *Digital Signal Processing - Principles, algorithms, and applications*. Pearson, Prentice Hall, 4 edition, 2007.
- [68] Z.A. Riley, M.E. Terry, A. Mendez-Villanueva, J.C. Litsey, and R.M. Enoka. Motor unit recruitment and bursts of activity in the surface electromyogram during a sustained contraction. *Muscle & nerve*, 37(6):745–753, 2008.
- [69] G. Rubboli and C.A. Tassinari. Negative myoclonus. an overview of its clinical features, pathophysiological mechanisms, and management. *Neurophysiologie Clinique/Clinical Neurophysiology*, 36(5-6):337–343, 2006.
- [70] L.A. Rudzinski and K.J. Meador. Epilepsy: Five new things. *Neurology*, 76, Suppl 2(7):S20–S25, 2011.
- [71] E. Schulc, I. Unterberger, S. Saboor, J. Hilbe, M. Ertl, E. Ammenwerth, E. Trinka, and C. Them. Measurement and quantification of generalized tonic-clonic seizures in epilepsy patients by means of accelerometry—an explorative study. *Epilepsy research*, pages 173–183, 2011.
- [72] J. Shawe-Taylor and N. Cristianini. *An introduction to support vector machines and other kernel-based learning methods*. Cambridge University Press, UK, 2000.
- [73] H. Shibasaki, Y. Yamashita, and Y. Kuroiwa. Electroencephalographic studies of myoclonus. *Brain*, 101(3):447–460, 1978.

- [74] A. Shoeb and J. Guttag. Application of machine learning to epileptic seizure detection. In *Proceedings of the 27th International Conference on Machine Learning (ICML 2010)*, pages 975–982, 2010.
- [75] E.B. Simonsen and L.K. Hansen. *Lærebog i biomekanik*, pages 42, 140–149. Munksgaard Danmark, 1 edition, 2007.
- [76] R. Singla, B. Chambayil, A. Khosla, and J. Santosh. Comparison of svm and ann for classification of eye events in eeg. *Journal of Biomedical Science*, 4:62–69, 2011.
- [77] T.L. Sorensen, U.L. Olsen, I. Conradsen, J. Henriksen, T.W. Kjaer, C.E. Thomsen, and H.B.D. Sorensen. Automatic epileptic seizure onset detection using matching pursuit: A case study. In *Engineering in Medicine and Biology Society (EMBC), 2010 Annual International Conference of the IEEE*, pages 3277–3280. IEEE, 2010.
- [78] A. Statnikov, C.F. Aliferis, and D.P. Hardin. *A Gentle Introduction to Support Vector Machines in Biomedicine: Volume 1: Theory and Methods*. World Scientific Pub Co Inc, 2011.
- [79] D. Staudenmann, K. Roeleveld, D.F. Stegeman, and J.H. van Dieën. Methodological aspects of semg recordings for force estimation—a tutorial and review. *Journal of Electromyography and Kinesiology*, 20(3):375–387, 2010.
- [80] M. Stone. Cross-validated choice and assessment of statistical predictions. *Journal of the Royal Statistical Society. Series B (Methodological)*, 36(2):111–147, 1974.
- [81] A. Subasi. Eeg signal classification using wavelet feature extraction and a mixture of expert model. *Expert Systems with Applications*, 32(4):1084–1093, 2007.
- [82] C.A. Tassinari, G. Cantalupo, and G. Rubboli. In *Panayiotopoulos CP, Benbadis SR., Beran RG. Atlas of epilepsies*, chapter Polygraphic recording of epileptic seizures, pages 723–740. Springer-Verlag, 2010.
- [83] C.A. Tassinari and G. Rubboli. In *Engel J.Jr., Pedley TA. Epilepsy. A comprehensive textbook*, chapter Polygraphic recordings, pages 873–894. Lippincott Williams & Wilkins, 2008.
- [84] M. Valderrama, C. Alvarado, S. Nikolopoulos, J. Martinerie, C. Adam, V. Navarro, and M. Le Van Quyen. Identifying an increased risk of epileptic seizures using a multi-feature eeg–eeg classification. *Biomedical Signal Processing and Control*, 2011.
- [85] T. van Beelen. Edfbrowser. www.teuniz.net/edfbrowser/.
- [86] M.J.A.M. van Putten, T. Kind, F. Visser, and V. Lagerburg. Detecting temporal lobe seizures from scalp eeg recordings: a comparison of various features. *Clinical neurophysiology*, 116(10):2480–2489, 2005.

- [87] V. Vapnik. Pattern recognition using generalized portrait method. *Automation and Remote Control*, 24:774–780, 1963.
- [88] J.M. Wakeling. Patterns of motor recruitment can be determined using surface emg. *Journal of Electromyography and Kinesiology*, 19(2):199–207, 2009.
- [89] Xsens. P.o. box 559. 7500 an enschede. the netherlands, 2012. <http://www.xsens.com>.
- [90] C.Y. Yang, J.S. Yang, and J.J. Wang. Margin calibration in svm class-imbalanced learning. *Neuro-computing*, 73(1-3):397–411, 2009.
- [91] S. Zandi, R. Tafreshi, M. Javidan, and G.A. Dumont. Predicting temporal lobe epileptic seizures based on zero-crossing interval analysis in scalp eeg. In *Engineering in Medicine and Biology Society (EMBC), 2010 Annual International Conference of the IEEE*, pages 5537–5540. IEEE, 2010.

APPENDIX

A

TUTORIAL

Tutorial

- for use of Moven.

By Isa Conradsen

Contents

1.1	Introduction	2
1.2	Orientation	2
1.3	Preparation of the suit	2
1.4	Application of the suit	5
1.5	Test of the placement of the sensors	8
1.6	Handling of visits to the lavatory	10
1.7	Data measurements	11
1.8	Limitations	12
1.9	Disconnection and removal of the suit	12
1.10	After the measurement	12
1.11	Charging batteries	15
1.11.1	AA batteries	15
1.11.2	Lithium batteries	15
1.12	Details for the test subjects (non-patients)	19
1.13	Electro magnetic disturbances in the EMU rooms	19
1.13.1	Room 1	19
1.13.2	Room 2	19
1.13.3	Room 3	19
1.13.4	Room 4	20
1.13.5	The common room	20

1.1 Introduction

The measurements involved in the project "Detection of Epileptic Seizures with Multimodal Signal Processing" are carried out at two places: the Danish Epilepsy Center in Dianalund and Rigshospitalet, the University hospital in Copenhagen. Both places contains an Epilepsy Monitoring Unit (EMU), where the measurements will take place, but the facilities are quite different for the two places. At Rigshospitalet the patients are bound to maintain in their bed during the entire admission, beside from visits to the bathroom. At the Danish Epilepsy Center in Dianalund the patients are free to move around in their own room, the common-room or outside (within a limited radius). The measurements are therefore dependent on where they take place. This manual will describe the preparation, the set-up and the performance in connection with the measurements.

1.2 Orientation

The patient is monitored with EEG electrodes as usual. The EMG electrodes are mounted as described by chief physician Sándor Beniczky in another document. At last the patient should be wearing a suit containing 16 sensors of the types shown at figure 1.1 and 1.2. The mounting of this suit and the measurements by it are described in this manual.

The entire guide should be read carefully before start.

It is very important that the sensors are handled with caution, since the wires do not sustain tearing. The sensors are to be separated by holding at the sockets and **not** at the wires! This is demonstrated at figure 1.3.

The suits are made of a very tensile fabric, which make them fit many persons of different heights and widths. The sizes are as stated in table 1.1. Even though the suits are tensile they should be treated carefully, since the fabric is very fine. Underneath the suit the patient may wear tight shorts and a t-shirt, besides from underwear. Other cloth should be worn on top of the suit. Since there are no wires or other physical connections to extern electronic equipment this will not be a problem. This means that only the device for collection of the EEG and EMG signals is to be mounted on top of the cloth.

1.3 Preparation of the suit

1. Based on the size of the person a suitable suit is chosen from table 1.1.

Table 1.1: Size of the suits.

Size	Body weighth [kg]	Heighth [cm]
3-6 years	14-21	94-115
6-9 years	20-29	115-134
9-16 years	29-61	134-173
L	60-88	170-190
XL	80-100	180-205



Figure 1.1: The sensor type used at the hands, feet, head and pelvis (lower back).



Figure 1.2: The sensor type used at the lower and upper arms, shoulders, lower legs and thighs.

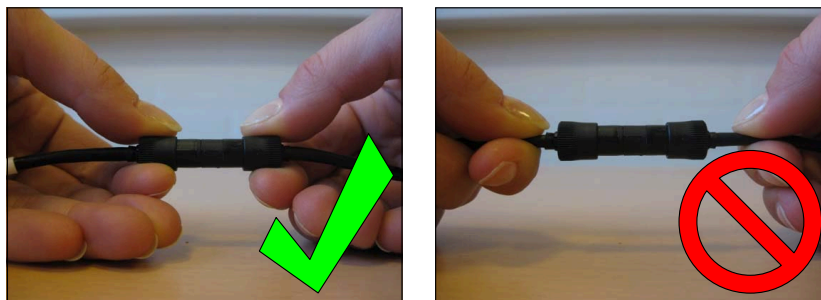


Figure 1.3: At the left it is shown how one should hold at the sockets, when the cords are to be separated. At the right it is shown what not to do.

2. All zippers in the suit should be opened.
3. The sensors are placed in the suit one by one so that the base side (the one where the screws are visible) is turned toward the skin of the person wearing the suit. The sensors should be connected as shown in figure 1.4. They are named by their placement in the suit around the body parts, see table 1.2. When the cords are placed in the cavities in the suit it is important that they are not broken, see figure 1.5. (If the wires are not long enough there are extension cords, which could be used.)
4. Start by placing the sensor at the right forearm (R fARM) in the suit so that the arrow points away from the wrist. The sensor is placed from the opening at the wrist with the cord first. It is placed in the white/orange pocket.
5. Afterward the sensor at the right upper arm (R uARM) is placed with the arrow pointing away from the previous sensor (R fARM). The sleeve is opened at the shoulder. The sensor is linked to the previous sensor and placed in the white/orange pocket with the cord first, so that the cord gets toward the shoulder.
6. The right shoulder sensor (R SHOU) is linked to the right upper arm sensor (R uARM) and placed in the white/orange pocket in the right shoulder of the suit. The cord is placed in the white/orange gap.
7. Repeat item 4-6 for left arm/shoulder (L fARM, L uARM, L SHOU).
8. Place right lower leg sensor (R ILEG) in the suit from the opening at the right ankle. The sensor should be placed in the white/orange pocket with the arrow pointing up along the leg. The cord from the other end of the sensor should be led into the gap in the white/orange fabric, so it end up at the ankle.
9. The sensor at the right thigh (R uLEG) is linked to the sensor at the right lower leg (R ILEG) through the leg opening at the hip. The sensor is placed in the white/orange pocket with the cord first and the arrow pointing away from the sensor at the lower leg (R ILEG). At the other end of the sensor the cord is connected with an extension cord marked *G*. This is further connected to one of the long gray cords and connected to Xbus Master #2.
10. Item 8 and 9 is repeated for the left lower leg and thigh (L uLEG, L ILEG). Only the long gray cord is here connected to Xbus Master #1.
11. The sensor for the lower back (PELV) is placed in the pocket at the lower back in the suit with the arrow pointing upwards toward the neck of the suit. The sensor is placed under the elastic band, so this is placed between the two sockets (entrance for the cords), see figure 1.6.
12. An extension cord marked *K* should be placed at the end of the cord at the left shoulder (L SHOU). The cord should then be pulled through the white/orange space in the back of the suit until it reaches the sensor in the lower back. The cord is linked to the sensor at the lower back (PELV). Another extension cord marked *E*

is linked to the other socket at the sensor at the lower back. This cord is pulled up through the white/orange space at the back of the suit. The cord is pulled through the hole at the top of the left pocket. This cord is connected to one of the long gray cords and further to Xbus Master #1.

13. An extension cord marked *K* should be linked to the sensor at the right shoulder (R SHOUL). The cord should be pulled through the white/orange space at the back of the suit and out at the hole at the neck of the suit and connected to the head sensor.
14. An extension cord marked *K* is pulled from the neck of the suit through the white/orange space at the back of the suit to the opening at the right pocket. The end of the cord with a hole should be placed at the neck and connected to the head sensor. The end with a pin should be placed through the pocket and connected to one of the long gray cords and further to Xbus Master #2.
15. The sensor for the right hand (R HAND) is placed in the glove for the right hand and the sensor for the left hand (L HAND) is placed in the glove for the left hand. The sensors for the feet (R FOOT / L FOOT) are placed in the covers for the shoes. Instead of the gloves and the shoe covers elastic bands might be used, since it might be more comfortable for the patient.

1.4 Application of the suit

1. If the patient wears shoes these should be removed. The patient undress until the parts that are suppose to be underneath the suit (tight shorts and a t-shirt). Jogging-trousers and a blouse with a zipper is recommended, for clothes to wear atop of the suit.
2. The two parts of the suit are separated by the cord from the pelvis sensor, which goes up through the upper part of the suit, to easier apply the suit.
3. The lower part of the suit is applied and pulled up to a comfortable place. Be careful not to step on any of the sensors.
4. The upper part of the suit is applied from below instead of pulling it from atop of the head. The arms are pulled through the sleeves; one at a time. The two cords linked to the headband should be hanging out from above at the neck. To avoid any displacement of the suit the patient should use the holes for the thumbs at the end of the sleeves. The cord separating the two parts of the suit in step 2 is connected.
5. Open the velcro in the covers for the shoes and pull them over the feet. It is important to check that the sensors are placed at the matching feet. Apply the patient his/her shoes, if he/she wants to wear shoes and pull down the covers and close them underneath the shoes/feet with the velcro. Elastic bands might be used instead of the covers for the shoes. Link the sensors for the feet to the cords from

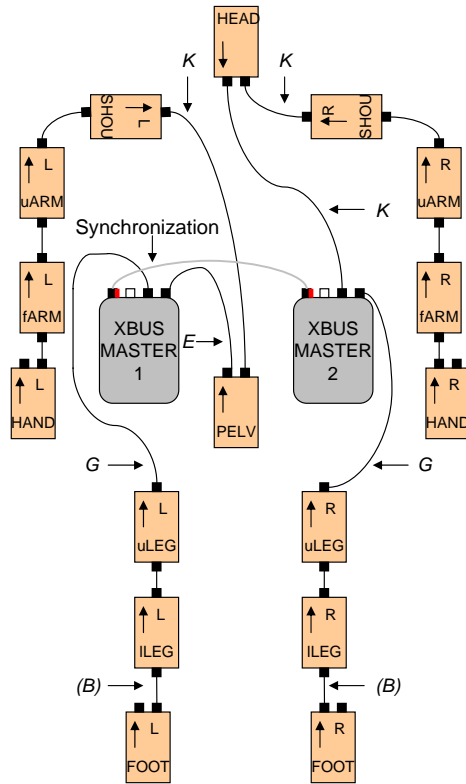


Figure 1.4: The connections of the sensors. This shows the set-up for which way they should be turned and which sensors should be linked together.

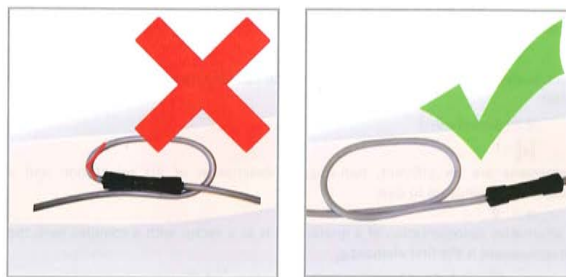


Figure 1.5: The placement of the cords. Be carefull not to bend the wires.

Table 1.2: Placement of the sensors

Text on the sensors	Placement
PELV	Pelvis
L SHOUL	Left shoulder
L uARM	Left upper arm
L fARM	Left forearm
L HAND	Left hand
L uLEG	Left thigh
L ILEG	Left lower leg
L FOOT	Left foot
HEAD	Head
R SHOUL	Right shoulder
R uARM	Right upper arm
R fARM	Right forearm
R HAND	Right hand
R uLEG	Right thigh
R ILEG	Right lower leg
R FOOT	Right foot



Figure 1.6: The placement of the sensor at the lower back (PELV). The elastic band is placed between the to sockets for the cords.

the sensors at the lower legs. If the cords are too short the extension cords marked *B* may be used.

6. Close all zippers. The headband should be placed in one of the front pockets or be taped to the suit on the front of the patient.
7. Apply the gloves with the sensors or mount the sensors underneath the elastic bands and link the sensors in the gloves to the cords from the sensors at the lower arms.
8. The two Xbus Masters are placed in a bag together with the batteries. The cords from the batteries are connected to the Xbus Masters at the middle, see figure 1.7.
9. The two Xbus Masters are connected with the cord with a red mark, through the sockets marked with red.

1.5 Test of the placement of the sensors

1. The Xbus Masters are started by a push on the clear/white button, see figure 1.7. The little diode at the Xbus Masters next to the on/off button will now flash with a light. When there is a connection it will be blue. If it has a different color the explanation can be found in figure 1.8.
2. The program **Moven Studio 2.5** is started by double clicking at the icon at the desktop of the computer. The window shown in figure 1.9 will appear.
3. The test should take place without electro magnetic disturbances. These are shown by yellow/red circles instead of green in the Xsens MVN program.
4. The patient's height and length of feet should be typed in under the flag *Actor Dims* in the left side. Afterward the flag *Calibrations* is chosen, see figure 1.10. Different posing types can be chosen for the calibration of the system. Choose an N-pose, which is the natural pose, and also the easiest for the patient to perform.
5. Push N-pose, so that it is marked. Then push the *calibrate* button and figure 1.11 appears. It is important that the patient is standing exactly as shown with the legs placed with the width of the hips and the arms down by the side with the palm toward the body. Push *next* and wait until the time has run out (4 sec). (The same is done, when the suit needs to be calibrated during a recording, only the measurement has to be stopped at first).
6. The system is now calibrated and Moven Studio gives a validation of how well it is done. If the calibration is *good* or *acceptable* push *accept* to continue otherwise a new calibration is performed by pressing *restart*. Once again the patient should be asked to stand correctly and totally still. Push *next* and await 4 sec.



Figure 1.7: At the bottom it is shown where to connect the battery packages. At the top the on/off button is shown. The Xbus masters are turned on with one push and are turned off by three fast pushes. Both when the Xbus Master are turned on and when they are shut down a short beep sound will be heard.

7. The movements stated in table 1.3 are performed. For the sensors to be rightfully placed every movement should reveal the movement on the screen that the patient is performing. If the patient is not capable of performing the movements himself the personnel may be helpful.
8. If the tests do not show the expected some of the sensors may be placed wrong. It is possible to start by checking whether the sensor(s) showing something wrong is(are) rightfully placed.
9. If it is not possible to find the sensor that makes the mistake, the patient may undress the suit and all the sensors should be checked for placement and direction. This occasion should though be rare.
10. When the sensors are back in the suit it is applied to the patient once again.
11. The test of the placement of the sensors should be performed.
12. The patient and the program is now ready for the measurements, see under **Data measurements** how to perform these.

1.6 Handling of visits to the lavatory

When the patient needs to go to the lavatory, he/she needs to partly undress. This is done by the items described underneath. The patient or nurse should be instructed in this procedure.

1. It is mentioned to the personnel that the patient has to go to the toilet, so that this can be annotated with the storage of data.
2. If necessary the EMG and EEG cords are disconnected.
3. The bag containing the Xbox Masters and the batteries is carried along with the patient to the bathroom.
4. The pants are carefully pulled down, and the cords between the upper and lower parts of the suit are held aside for the patient to be able to sit on the toilet.
5. After the visit to the lavatory the pants are pulled up again like normal pants.
6. The measurement may stop as the patient enters the lavatory, but it will automatically resume, when the patient arrives back to the main room.

Table 1.3: Test of the placement of the sensors.

Number	Movement
1	Hold the arms stretched as in a T-pose. Bend in the elbows, so that the hands gets in front of the face.
2	Hold the arms stretched as in a T-pose. Bend in the elbows (so the hands approaches the face) until the joint has an angle of 45 degrees. Turn 45 degrees in the shoulder joint, so the hands get into the air.
3	Kick right leg forward (stretch).
4	Kick right leg to the right (stretch).
5	Kick left leg forward (stretch).
6	Kick left leg to the left (stretch).
7	Lift the right leg by bending in the knee joint and turning the leg to the right.
8	Lift the left leg by bending in the knee joint and turning the leg to the left.
9	Tip right hand up and down and from side to side.
10	Tip left hand up and down and from side to side.
11	Tip right foot up and down and from side to side.
12	Tip left foot up and down and from side to side.

1.7 Data measurements

1. In the EMU at the Danish Epilepsy Center the patient should, due to problems with electro magnetic disturbances, be placed in room 2. See last in the document for further explanations. In the EMU at Rigshospitalet, the University hospital in Copenhagen, both beds available may be used.
2. Under *File* in **Moven Studio 2.5** *New Recording Session* is chosen. A box will appear where the patients number or initials should be written under *Session name* and under *Folder C:\Documents and Settings\All Users\Moven_data* should be written. Afterward push "Ok". The session is now ready. The window seen in figure 1.9 will now appear.
3. The system is ready for the measurements to start. The EEG and EMG measurements are started through Nervus or Harmony as usual. The Moven measurement is started by pushing the red button, see Fig. 1.12. The time in the EEG recording program (Nervus or Harmony) is annotated at the point where the Moven program is started. This time is used to synchronize the two measurements later on.
4. If the Moven system loses contact and ends the session (this is seen by the figure disappearing and the frame counting stopping) the previous item should be repeated.
5. The batteries holds for about 8 hours. When the batteries are almost flat they should be exchanged with the other set. The flat batteries should be charged, see **Charging batteries**. To make sure that the system do not run out of power the batterier should be charged every 7.5 hour.
6. After the measurement is finished the Xbus Masters should both be turned off by pushing fast three times at the white button as shown in figure 1.7.

1.8 Limitations

In the EMU at the Danish Epilepsy Center if the patients wants to go outside, a new calibration is needed and the computer should be placed outside with the patient. See last in the document for more details.

In Rigshospitalet the measurement will most likely stop each time a patient goes to the bathroom, but the system will start a new recording when the patient return to the main room.

1.9 Disconnection and removal of the suit

1. Hand and feet sensors are disconnected from the rest of the system.
2. The gloves with sensors are removed.
3. The shoe covers are opened. The shoes (if the patient wears any) are removed and afterward the covers with sensors.
4. All zippers are opened. The long gray wires as well as the wires between the upper and lower parts of the suit are disconnected. The upper part of the suit is carefully removed from the arms and pulled down to be fully removed.
5. The lower part is pulled down and removed without dropping any of the sensors on the floor.

1.10 After the measurement

1. The battery packages are charged.

LED color	Xbus Master active mode
Off	Power down
● Green	Serial mode
● Blue	Wireless mode - connected
●/○ Blue flashing	Wireless mode – sending data
● Blue Purple switch	Trying to connect
● Purple	Wireless mode – host not found
● Yellow	Low battery mode
● Red	Fault mode

Figure 1.8: The table defines the colors of the diode at the Xbus Masters and the meaning of them.

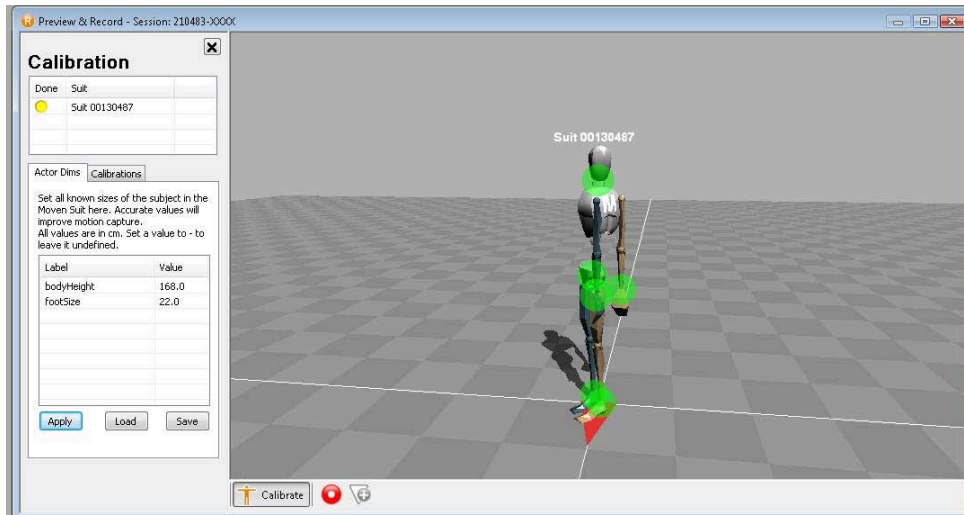


Figure 1.9: The patients height and length of feet are typed in under “bodyHeight” and “footSize”.

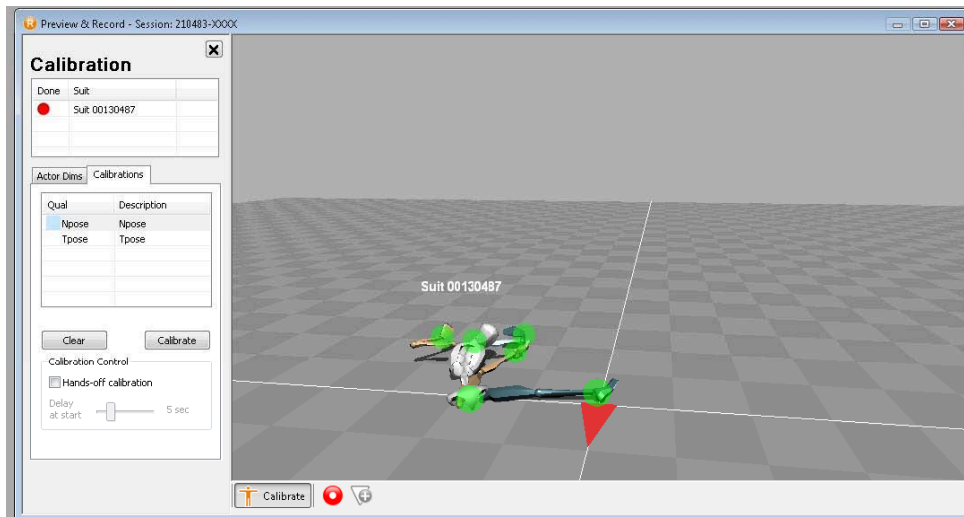


Figure 1.10: The window in Moven Studio before calibration.

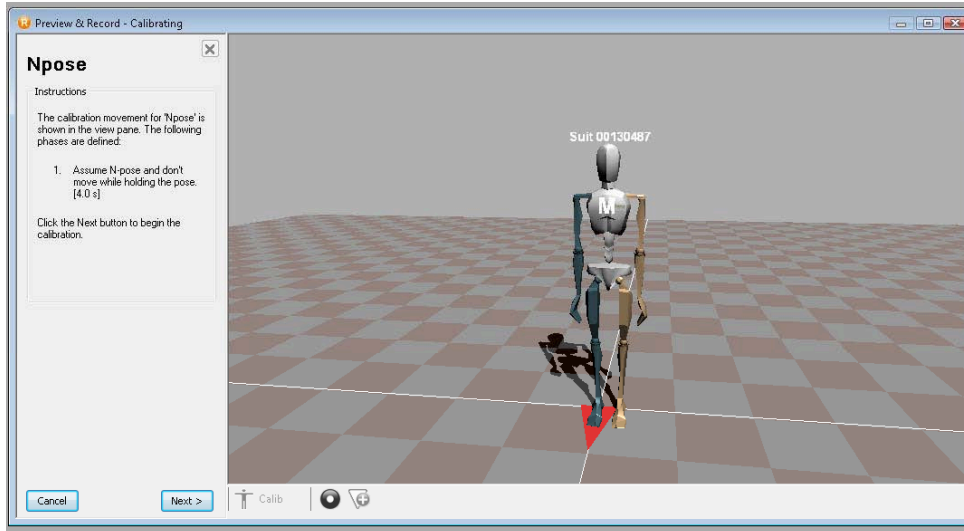


Figure 1.11: The window in Moven Studio during calibration.

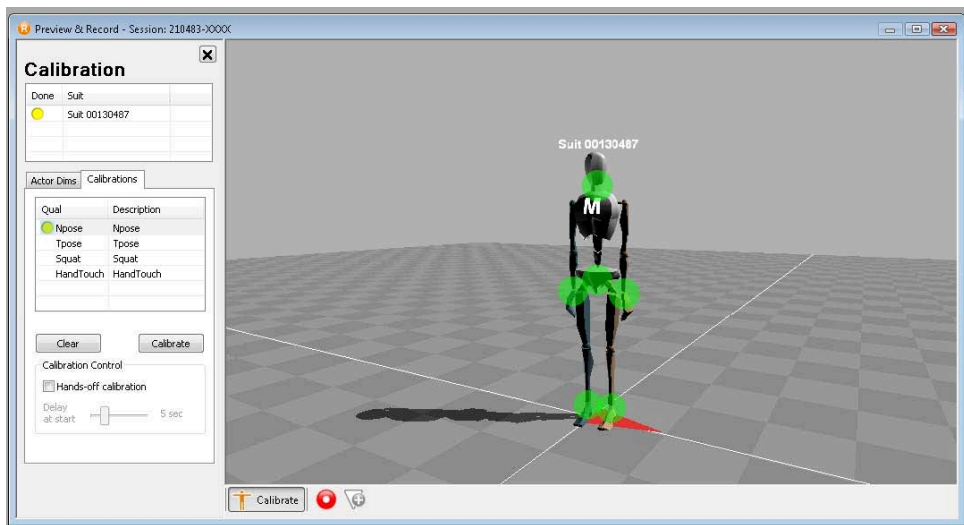


Figure 1.12: The window in Moven Studio after calibration. The measurement is started by pushing the red button. At the bottom of the window the *Frame* number will then be increasing.

2. The AA batteries in the Xbus Masters are removed and charged. The other set of batteries are put into the Xbus Masters.
3. All sensors are removed from the suit and placed in the suitcase.
4. The suit is washed with a disinfectant at maximum 30 degrees and it is dried by hanging. The gloves, the shoe covers and the headband are washed with disinfectant in cold water by hands.
5. (Only for the person responsible for the measurements: The MVN files are opened and saved as MVNX files under the same names (File -> Save as). The MVN files are saved at the server network and the mvnx files are transferred to a transportable harddisc. Nervus/Harmony data is saved as EDF+ files. These are as well saved on the extern/transportable hard disc.)

1.11 Charging batteries

1.11.1 AA batteries

The batteries are placed in the Xbus Masters as shown at figure 1.14. When they need to be charged they should be removed and replaced by another set. The charging is performed by placing the first battery at the left in the charger, see figure 1.13. Then pressing the button “Soft” until “Soft charging” is written at the display in the upper right corner. The rest of the batteries may be placed in the charger one by one from the left. After a while small batteries charging is seen above each battery. The batteries are charged when it writes *done* instead of showing the little battery pictures.

1.11.2 Lithium batteries

The lithium batteries are charged by the system shown in figure 1.15. When the batteries are to be charged these are connected to the charger while it is turned off. First the balance plug is connected as shown in figure 1.16. Afterward the charger cord is used to connect the battery to the charger as shown in figure 1.17. The battery is now ready to be charged. The power supply is turned on and there will be light in the display of the charger. In the display “[MEMORY No. 0] A123 9.9V 4600“ or “[MEMORY No. 0] C: 4.6A 50°C“ is shown. **It is very important not to press any button but the ones stated to be pushed.** The “Enter” button is held down until one hears two beeps. The display now shows “CHARGE START SOLO MODE”. Once again the “Enter” button is pushed and the charger will check the number of cells in the battery. Afterward the charging is started and the display shows “A123 SOLO/CHG 00.00 (time) 0.00A () 00.00V (power)”. The device will beep when the charging is finished. There is a charge limit of 45 min, so after that the charger will also beep. When the beep is heard it is important to immediately stop the charging. It is stopped by holding down the “Enter” button. After charging the power supply should be turned off. The battery may then be disconnected.

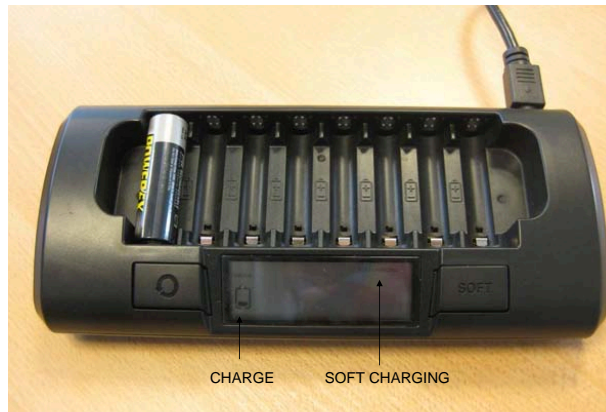


Figure 1.13: The placement of the batteries in the Charger for the AA batteries.



Figure 1.14: The placement of the batteries in the Xbus Masters are on the back.

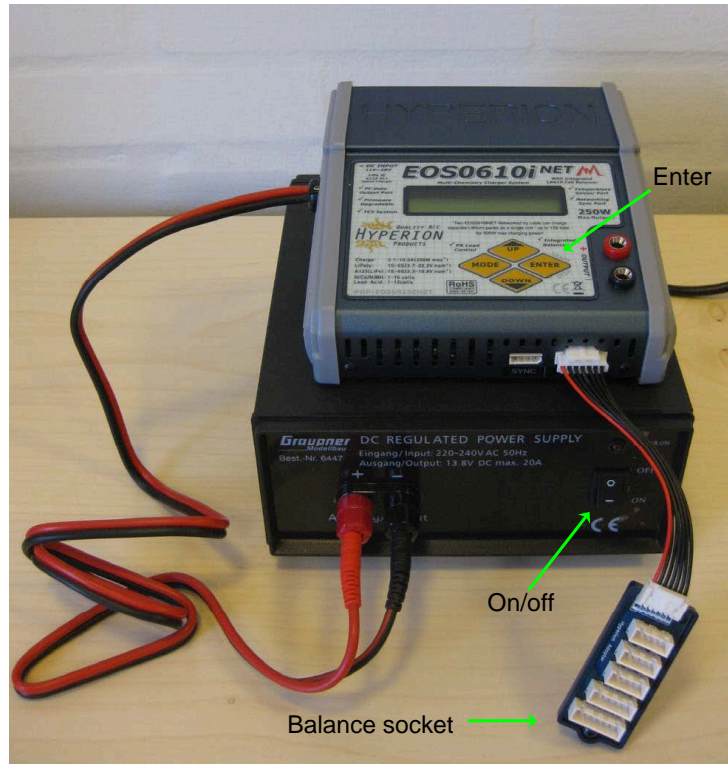


Figure 1.15: The charger for the lithium batteries.

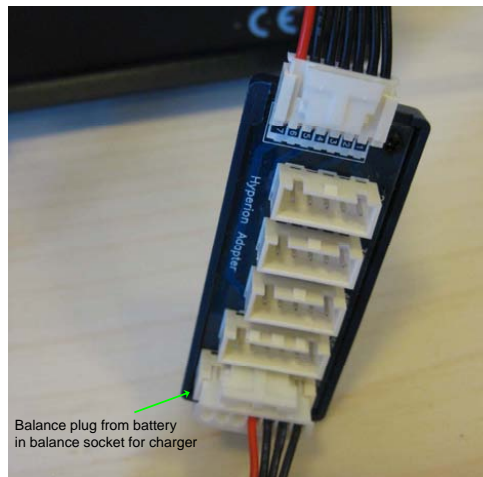


Figure 1.16: Connection of the balance plug.



Figure 1.17: Charging of a lithium battery.

1.12 Details for the test subjects (non-patients)

The measurements take between 2-4 hours. The subjects are asked to perform some predefined activities. These include: scanning through the TV channels with the remote controller, use of a cell phone, use of a computer, training on an exercise bike, gambling with dices (inducing a non-seizure shaking movement to the measurements) and eating. Furthermore the subjects are asked to simulate three different types of seizures - five of each. They have videos shown of the seizures and are further instructed by a physician.

Tonic-Clonic

This type of seizure is generated with the test subject lying on a bed. The tonic phase is made as an isometric contraction in all muscles at once (limbs extended). This is followed by the clonic phase which consists of rhythmically repetitive jerks made by alternation of contracting and relaxing the muscles.

Versive - asymmetric tonic seizure

The versive seizures are characterized by a forced turn of the head to an almost uncomfortable angle, where the subject looks to the right side and upwards. This should be followed by an isometric muscle contraction in an asymmetric posturing with the right arm raised above the head.

Myoclonic

A myoclonia is a very short lasting jerk (less than a second), where just a single muscle contracts. To simulate this, the right biceps should be contracted for as short a time as possible.

1.13 Electro magnetic disturbances in the EMU rooms

1.13.1 Room 1

Everything but the bed seems fine. When the person is in contact with the bed (e.g. sits on the bed) the sensors close to the bed show magnetic disturbances. Afterward the body on the computer screen is no longer normal as it is after the calibration.

1.13.2 Room 2

A small electro magnetic disturbance when approaching the bed from the side closest to the window. Otherwise no problems with this room.

1.13.3 Room 3

This room has the same problem as room 1. When the person wearing the suit has been in the bed the graphic illustration of the body on the computer screen is screwed up.

1.13.4 Room 4

The worst room. There are both problems with electro magnetic disturbances at the wall (towards the bathroom), the changing table and the bed.

1.13.5 The common room

No problems. But when the patient heads outside, the body is screwed up on the screen (from passing through the door) and a new calibration is needed. When the patient is outside, the computer should be placed outside as well for the patient to have a freedom as large as possible to move around.

MULTI-MODAL PATIENT DATA

The multi-modal data from the patient, who had a GTC seizure, while monitored with all modalities, ACM, ANG and EMG. From the sEMG data in Fig. B.1 it seems that the seizure sets off almost at the same time in all muscles shown. Unfortunately it is also seen that the signals have been cut due to their amplitude being too large compared to the voltage, which the amplifier is able to deliver. This makes it hard to compare the strength of the signals between the muscles. The next figure (Fig. B.2) shows the spectrograms of the sEMG signals. This verifies that the pattern described in Chapter 3, of all the frequencies being represented during the seizure compared to the surrounding activity, is strongly presented here. Fig. B.3 and B.5 shows that acceleration and angular velocity data respectively, for the same seizure as seen in Fig. B.1. It is clear that the power is very different for the sensors, placed all around the body. Both the acceleration and the angular velocity are larger when a sensor is placed at a more agile limb, e.g. placement 9, 10, 13, 14, the upper and lower arm positions. In Fig. B.4 and B.6 the spectrograms for the data in Fig. B.3 and B.5 are presented, these as well show the pattern described in Chapter 3, where the higher frequencies only are pronounced during the seizure.

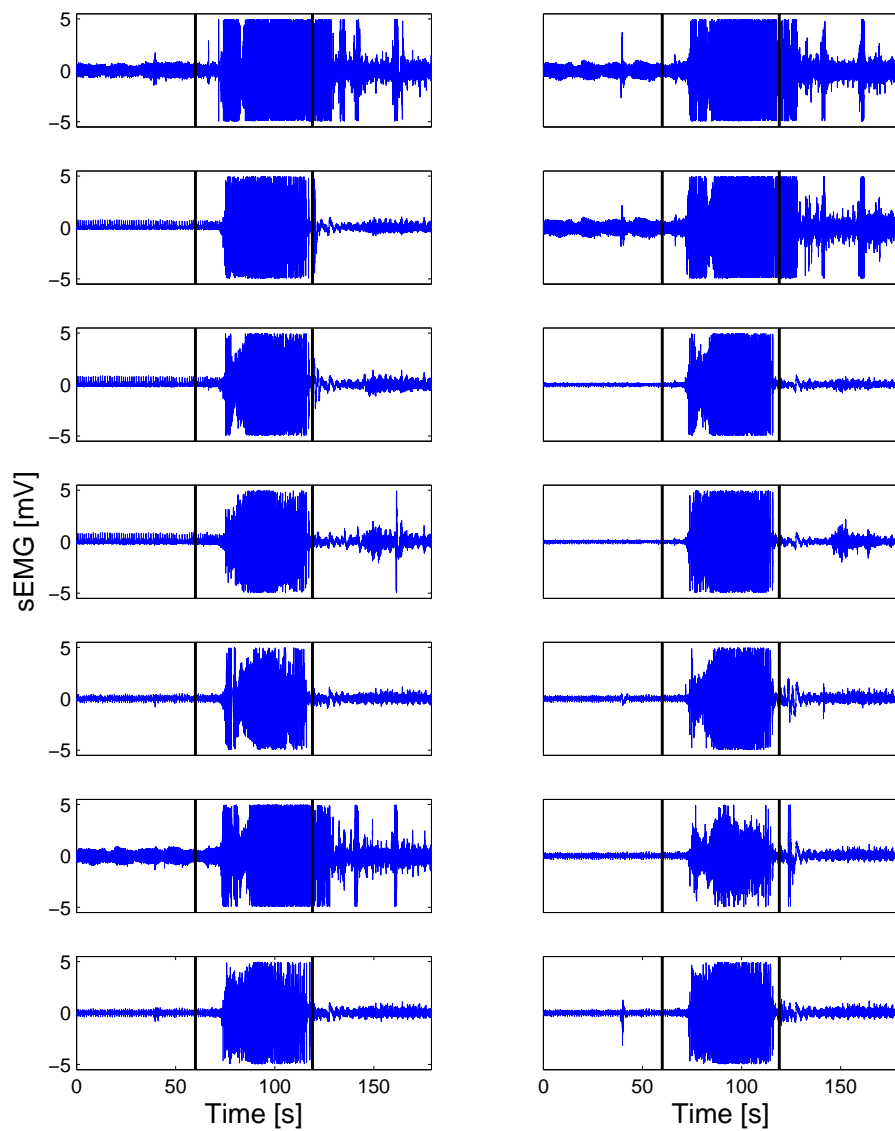


Figure B.1: The sEMG signal during a real seizure. The muscles shown are (from the top and down) sternocleidomastoid, deltoid, biceps brachii, triceps brachii, biceps femoris, quadriceps femoris, and tibialis anterior, at the left are the muscle on the left side of the body and at the right are the muscles on the right side.

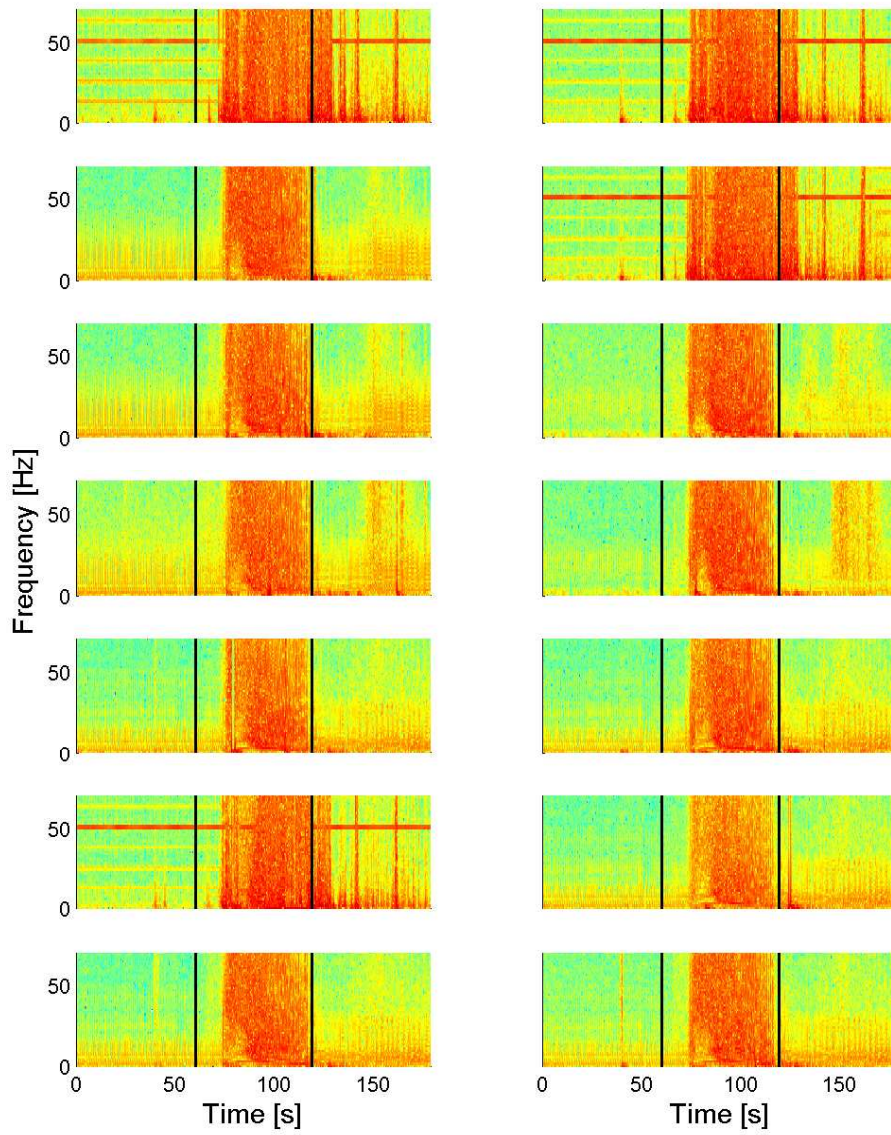


Figure B.2: The spectrograms of the sEMG signal shown in Fig. B.1. The signals are presented in the same order as in Fig. B.1.

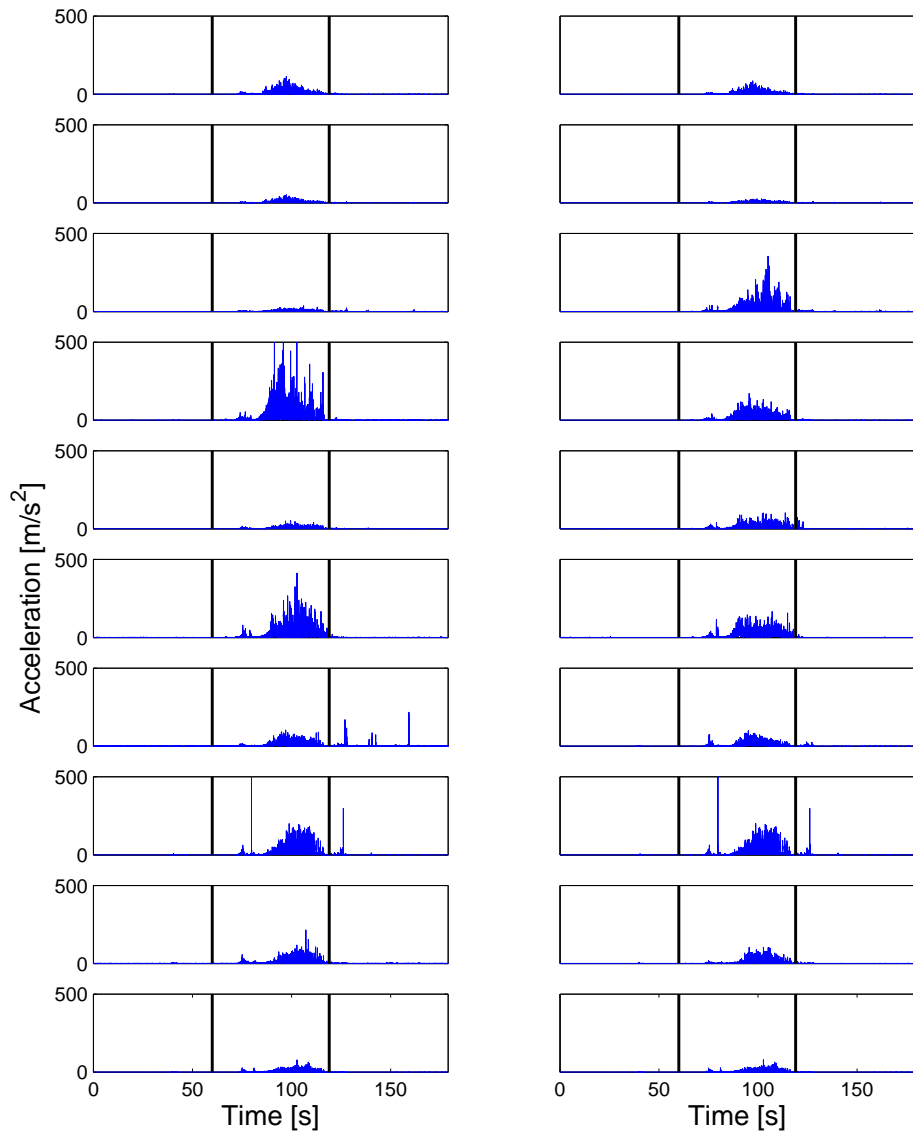


Figure B.3: The ACM signal during a real seizure (the same as seen in Fig. B.1). The positions shown are (from the top (left then right) and down) 1, 2, 3, 4, 8, 9, 10, 11, 12, 13, 14, 15, 16, 17, 18, 19, 20, 21, 22, 23.

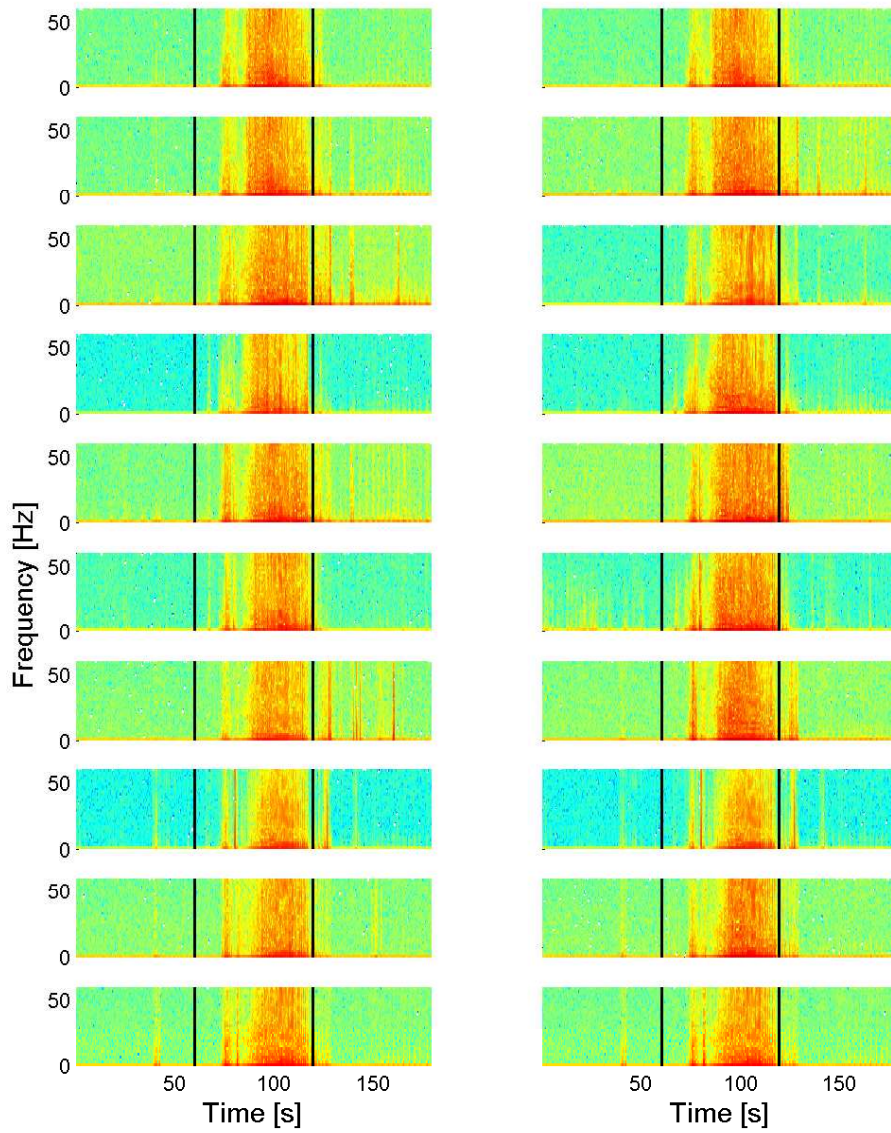


Figure B.4: The spectrograms of the ACM signal shown in Fig. B.3. The signals are presented in the same order as in Fig. B.3.

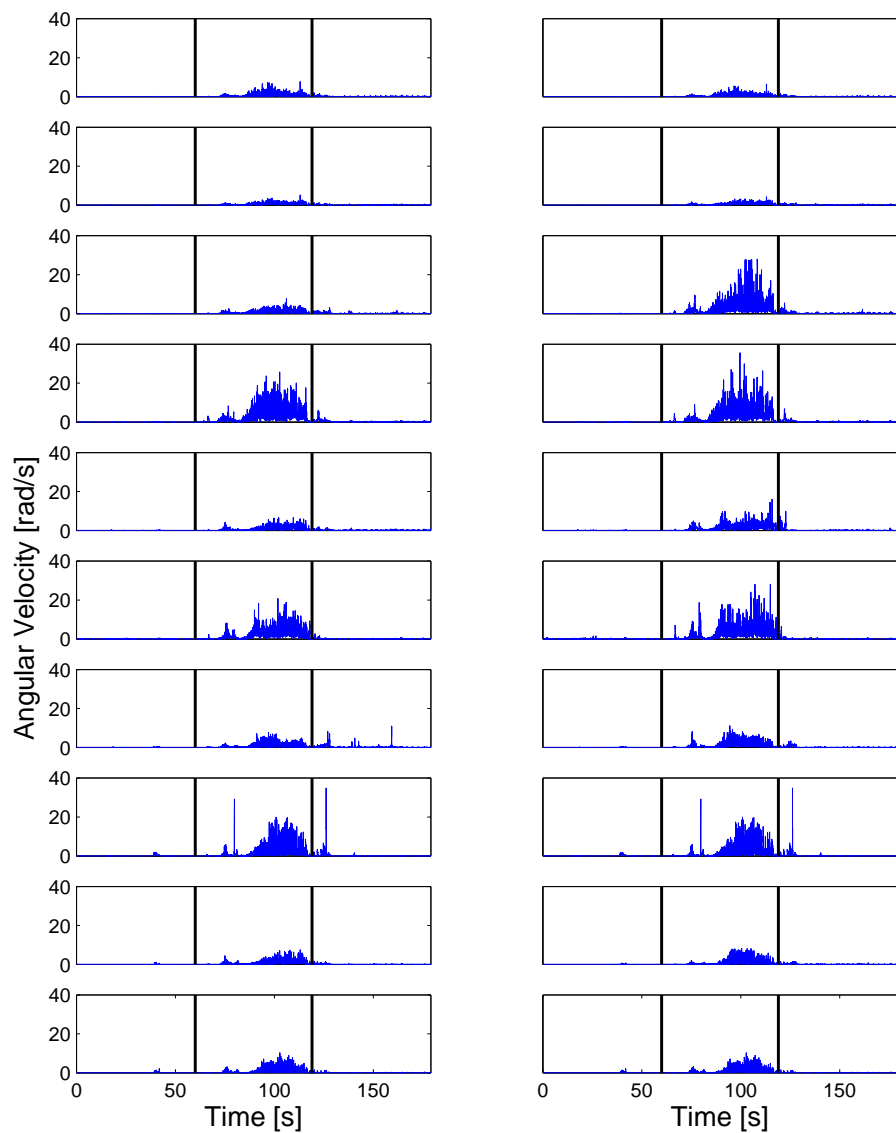


Figure B.5: The ANG signal during a real seizure (the same as seen in Fig. B.1). The signals are presented in the same order as in Fig. B.3.

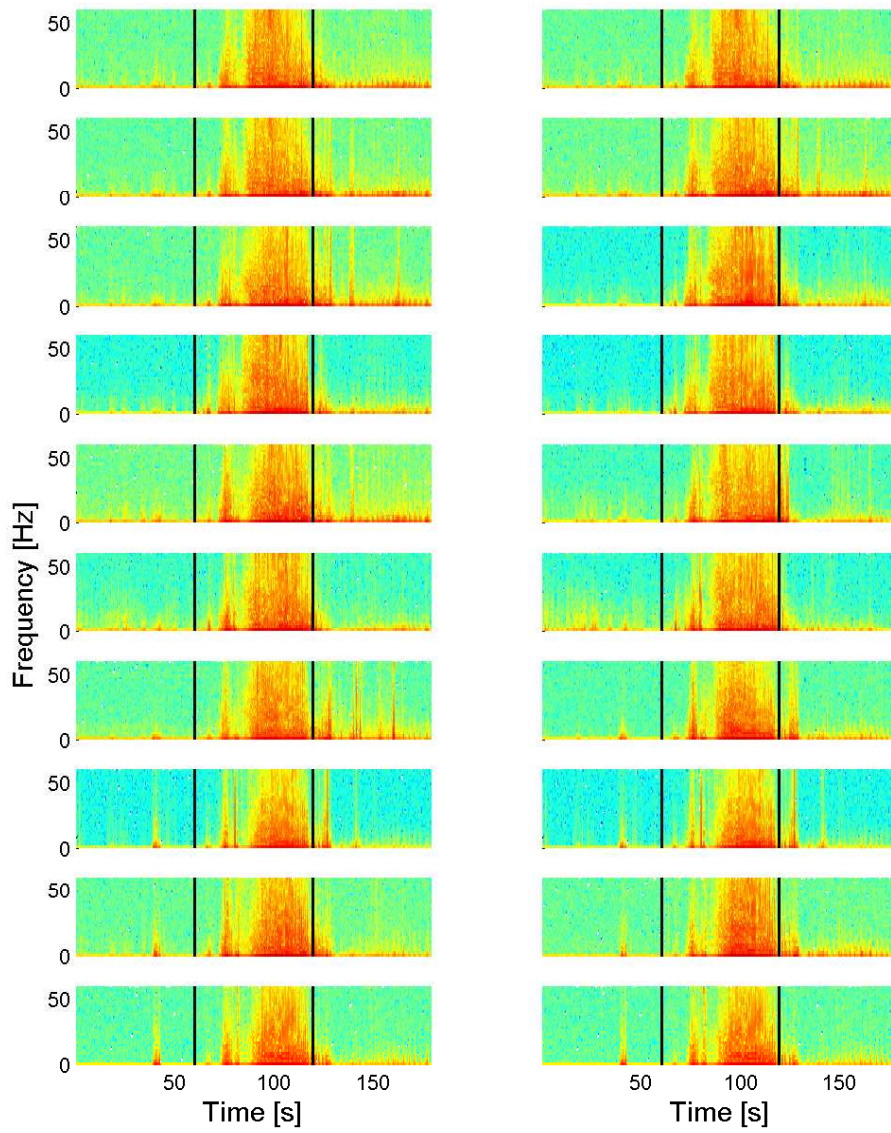


Figure B.6: The spectrograms of the ANG signal shown in Fig. B.5. The signals are presented in the same order as in Fig. B.3.

SEMG PATIENT DATA

In Table C.1 the number of seizures and the demographic data are listed for all patients with GTC seizures.

In Table C.2 the number of seizures and the demographic data are listed for all patients with tonic seizures.

In Table C.3 the parameter values are given for the coherence of the rectified sEMG.

In Table C.4 the statistical results for the coherence are given both for the rectified and the unrectified sEMG.

Table C.1: Demographic data and number of seizures for patients with GTC seizures.

Patient	Age	Gender	Epilepsy diagnosis	Antiepileptic medication at the time of recording	MRI	# GTC seizures	# hours recorded
TC1	23	F	Symptomatic Focal Epilepsy	Clobazam, lamotrigine	Cortical dysplasia (right frontal lobe)	1	97
TC2	26	F	Symptomatic Focal Epilepsy	Withdrawn before the recording session	Mesial Temporal Sclerosis (left)	2	97
TC3	39	M	Symptomatic Focal Epilepsy	Withdrawn before the recording session	Dysembryoplastic neuroepithelial tumor	1	96
TC4	25	M	Symptomatic Focal Epilepsy	Withdrawn before the recording session	Mesial Temporal Sclerosis (left)	1	49
TC5	62	M	Symptomatic Focal Epilepsy	Withdrawn before the recording session	Cortical dysplasia (right frontal lobe)	2	96
TC6	38	M	Symptomatic Focal Epilepsy	None	Atrophy of the right temporal lobe	1	97
TC7	19	M	Symptomatic Focal Epilepsy	Zonisamide, lamotrigine	Cortical dysplasia (right frontal lobe)	1	97
TC8	55	M	Symptomatic Focal Epilepsy	Withdrawn before the recording session	Normal	3	20
TC9	30	F	Juvenile Myoclonic Epilepsy	topiramate, lamotrigine	Normal	4	74
TC10	26	M	Symptomatic Focal Epilepsy	Withdrawn before the recording session	Cortical dysplasia (left frontal and temporal lobe)	3	96
TC11	11	M	Symptomatic Multifocal Epilepsy	Clobazam, pregabalin, lamotrigine	Small multifocal lesions hyperintense on T2 and FLAIR (history of meningoenkephalitis)	3	70

Table C.2: Demographic data and number of seizures for patients with tonic seizures.

Patient	Age	Gender	Epilepsy diagnosis at the time of recording	MRI	# Tonic seizures
T1	6	M	Symptomatic Focal Epilepsy	Cortical dysplasia (right frontal lobe)	7
T2	58	M	Symptomatic Focal Epilepsy	Mesial Temporal Sclerosis (bilateral)	4
T3	14	M	Symptomatic Focal Epilepsy	Cortical and subcortical atrophy and gliosis (due to perinatal asphyxia)	3
T4	17	M	Cryptogenic Focal Epilepsy	Normal	3
T5	48	M	Symptomatic Focal Epilepsy	Cortical and subcortical atrophy and gliosis (due to perinatal asphyxia)	8
T6	30	M	Symptomatic Focal Epilepsy	Cortical dysplasia (band heterotopia)	10
T7	6	F	Symptomatic Focal Epilepsy	Cortical dysplasia (left frontal lobe)	2
T8	9	F	Symptomatic Focal Epilepsy	Cortical dysplasia (left frontal lobe) Mesial Temporal Sclerosis (bilateral)	5
T9	10	F	Symptomatic Focal Epilepsy	Cortical and subcortical atrophy and gliosis (due to perinatal asphyxia)	1
T10	6	F	Symptomatic Multifocal Epilepsy	Small multifocal lesions hyperintense on T2 and FLAIR (history of meningoencephalitis)	1

Table C.3: Median values of the whole seizure period for all patients (and in parentheses the 2.5% and 97.5% percentiles) for the coherence of the rectified and the unrectified surface EMG data.

	Epileptic	Tonic	GTC	Simulated
Unrectified	0.120 (0.050-0.255)	0.117 (0.048-0.178)	0.120 (0.063-0.289)	0.071 (0.046-0.109)
Rectified	0.113 (0.043-0.320)	0.115 (0.041-0.202)	0.091 (0.056-0.357)	0.068 (0.037-0.109)

Table C.4: P-values for the coherence of rectified and unrectified EMG data, respectively.

	Unrectified	Rectified
Epileptic vs. Simulated	0.0005	0.0024
Tonic vs. Simulated	0.068	0.0046
GTC vs. Simulated	0.0034	0.0386
Tonic vs. GTC	1	0.3447

FILTER SPECIFICATIONS

For the filters introduced in section 4.2.2 the data are given in Table D.1 and D.2, respectively. For the filters introduced in section 5.3 the filter coefficients are given in Table D.3.

Table D.1: The filter constants for the equiripple high-pass filter introduced in section 4.2.2.

Stopband frequency (Hz)	9
Passband frequency (Hz)	10
Stopband Attenuation	0.1
Passband Ripple	0.0575
Density Factor	20

Table D.2: The filter constants for the Butterworth notch filter introduced in section 4.2.2.

First Passband Frequency (Hz)	49
First Stopband Frequency (Hz)	49.8
Second Stopband Frequency (Hz)	50.2
Second Passband Frequency (Hz)	51
Stopband Attenuation (dB)	0.458
Passband Ripple (dB)	23.0

Table D.3: The filter coefficients for the filters introduced in section 5.3.

Off-line	On-line
-0.000558	0.049484
-0.003295	0.092877
-0.005887	-0.099066
-0.001947	-0.139826
0.014547	-0.248322
0.034152	0.729993
0.027894	-0.248322
-0.031912	-0.139826
-0.139848	-0.099066
-0.247502	0.092877
0.706695	0.049484
-0.247502	
-0.139848	
-0.031912	
0.027894	
0.034152	
0.014547	
-0.001947	
-0.005887	
-0.003295	
-0.000558	

PAPER I

TITLE Multi-modal Intelligent Seizure Acquisition (MISA) system - a new approach towards seizure detection based on full body motion measures

AUTHORS Isa Conradsen, Sándor Beniczky, Peter Wolf, Daniella Terney, Thomas Sams, and Helge B.D. Sorensen

JOURNAL Engineering in Medicine and Biology Society (EMBC), 2009 Annual International Conference of the IEEE

PUBLICATION HISTORY Submission date: 04-04-2009, Acceptance date: 02-06-2009

Multi-modal Intelligent Seizure Acquisition (MISA) system - A new approach towards seizure detection based on full body motion measures

Isa Conradsen^{†*}, Sándor Beniczky^{*}, Peter Wolf^{*}, Daniella Terney^{*}, Thomas Sams[†] and Helge B.D. Sorensen[†]

[†]Department of Electrical Engineering, Technical University of Denmark, Kgs. Lyngby, Denmark

^{*}Danish Epilepsy Center, Dianalund, Denmark

Abstract—Many epilepsy patients cannot call for help during a seizure, because they are unconscious or because of the affection of their motor system or speech function. This can lead to injuries, medical complications and at worst death. An alarm system setting off at seizure onset could help to avoid hazards. Today no reliable alarm systems are available. A Multi-modal Intelligent Seizure Acquisition (MISA) system based on full body motion data seems as a good approach towards detection of epileptic seizures. The system is the first to provide a full body description for epilepsy applications. Three test subjects were used for this pilot project. Each subject simulated 15 seizures and in addition performed some predefined normal activities, during a 4-hour monitoring with electromyography (EMG), accelerometer, magnetometer and gyroscope (AMG), electrocardiography (ECG), electroencephalography (EEG) and audio and video recording. The results showed that a non-subject specific MISA system developed on data from the modalities: accelerometer (ACM), gyroscope and EMG is able to detect 98% of the simulated seizures and at the same time mistakes only 4 of the normal movements for seizures. If the system is individualized (subject specific) it is able to detect all simulated seizures with a maximum of 1 false positive. Based on the results from the simulated seizures and normal movements the MISA system seems to be a promising approach to seizure detection.

I. INTRODUCTION

Epilepsy is a neurological disorder: the propensity of the brain to generate epileptic seizures. Approximately one third of the patients continue to have seizures in spite of adequate medication. Many of these start suddenly and unpredictably, make the patient lose consciousness and may carry risks of severe trauma and even death. If the patient is alone the seizures may pass unnoticed, especially during sleep. This makes it desirable to detect them, if it is not possible to prevent them. When the seizures are detected an alarm can warn staff at the hospital or relatives at home of the seizures. Today such alarm systems exist, but they are not reliable. A study on the sensitivity of epilepsy bed alarms and pulse oxymeters [9] showed that in the case of tonic-clonic seizures the sensitivity was 30-35% and for other seizures it was even less. A new device for warning about seizures is therefore needed. Several groups have worked on detecting seizures based on ACM data [1], [6], [7]. Nijsen et al. [1]

I. Conradsen, Electrical Engineering, Technical University of Denmark, 2800 Kgs. Lyngby, Denmark ic@elektro.dtu.dk

H.B.D Sorensen, Electrical Engineering, Technical University of Denmark, 2800 Kgs. Lyngby, Denmark hbs@elektro.dtu.dk

S. Beniczky, Neurophysiological Department, Danish Epilepsy Center, 9340 Dianalund, Denmark sbz@filadelfia.dk

have shown that in a test on 18 patients it was possible to detect the seizures of 10 patients based on visual inspection of ACM data. From these results an alarm system based on ACM data seems as a good approach. Other modalities which might improve the functioning of ACM data for detection of epileptic seizures are EMG, gyroscopes and magnetometers. The current paper therefore proposes a new approach to seizure detection denoted Multi-modal Intelligent Seizure Acquisition (MISA) system containing all of the four above mentioned modalities. This system is the first to provide a full body description for epilepsy applications. For this graphical description of the subject the magnetometers help the positioning in space. Nijsen et al. [2] state that to capture the majority of the seizures (especially the myoclonic seizures) focus should be on the lower arm which is the body part mostly involved in myoclonic seizures. Based on this result the current paper initially is centered on the movements of the lower arm. We analyzed signals from the movement sensor on the lower arm and the EMG from the biceps. As a first step in developing the MISA system the current paper will examine whether the different modalities of the system provide complementary information with respect to the detection of seizures.

II. METHODOLOGY

A. Subjects and Data Collection

The data was collected in the Epilepsy Monitoring Unit (EMU) at the Danish Epilepsy Center in Dianalund. The subjects were monitored for about 4 hours and EEG, AMG, EMG, ECG, audio and video recordings were stored. The AMG sensor system used is Xsens MVN, which is developed by Xsens Technologies [10]. Xsens MVN contains 16 sensors placed in a suit worn by the test subject. Each sensor contains both a 3D accelerometer, 3D magnetometer and 3D gyroscope. Data from the AMGs are sent via a bluetooth connection to a server where it is stored. The subject wore 28 surface EMG electrodes resulting in 14 bipolar EMG channels placed on 14 muscles. The active EMG electrode is placed on the belly of the muscle, while the reference electrode is placed on nearby bone or tendon. The EMG signals are collected at a sampling frequency of 1 kHz (bandpass filter: 1 Hz - 500 Hz). The digital signals were synchronized with the signals from the other modalities recorded during monitoring. In the future all modalities will be wireless, whereby the MISA system will be completely

wireless, making it easier for the patients to get around and be more free of equipment.

For this pilot project three test subjects were enrolled, two males and one female, though gender has no theoretical influence. Due to ethical considerations we only included adults, whereas children will also be included in the more detailed follow-up investigation. The recordings contain normal activity such as eating, biking, use of computer and cellular phone and gambling with dices. Furthermore the subjects were instructed by physicians to simulate 15 seizure events of three seizure types (five events of each). The seizures simulated are tonic-clonic, versive-asymmetric tonic and myoclonic. The times when seizures occurred have been clinically annotated.

B. The seizures

1) *Tonic-Clonic*: This type of seizure is generated with the test subject lying on a bed. The tonic phase is made as an isometric contraction in all muscles at once (limbs extended). This is followed by the clonic phase which consists of rhythmically repetitive jerks made by alternation of contracting and relaxing the muscles.

2) *Versive - asymmetric tonic seizure*: The versive seizures are characterized by a forced turn of the head to an almost uncomfortable angle, where the subject looks to a side and upwards. This is followed by an isometric muscle contraction in an asymmetric posturing with an arm raised above the head.

3) *Myoclonic*: A myoclonia is a very short lasting jerk (less than a second), where just a single muscle contracts. To simulate this, one biceps has been contracted for as short a time as possible.

C. Multi-modal Motion Data Presentation

In MATLAB a program is designed to visualize the simulated seizures and the normal physiological movements. The program is able to display acceleration and angular velocity in three dimensions, in addition to the electrical signals from the muscle (EMG).

From a visual inspection of the data, it can be seen that for all modalities each seizure type is stereotypical. Two figures each showing the acceleration and angular velocity in the lower arm together with the EMG signal from the biceps are presented.

In Fig. 1 a simulated tonic-clonic seizure is presented. For this simulated seizure the tonic phase lasts about 8 seconds followed by the clonic phase lasting about 14 seconds, where the rhythmic repetitive jerks are easily seen. The tonic phase starts with a high acceleration and angular velocity of the lower arm, but through the tonic phase these values are close to zero, because the arm is not moving, the muscles are isometrically contracted, as indicated by the EMG signal. Later in the clonic phase the acceleration and angular velocity are again large, seen as rhythmic jerks caused by alternating activation-deactivation of the muscles. The absolute maximum amplitudes of the acceleration and angular velocity are about 100 m/s^2 and 10 rad , respectively.

The absolute maximum amplitude of the EMG signal is about 3 mV .

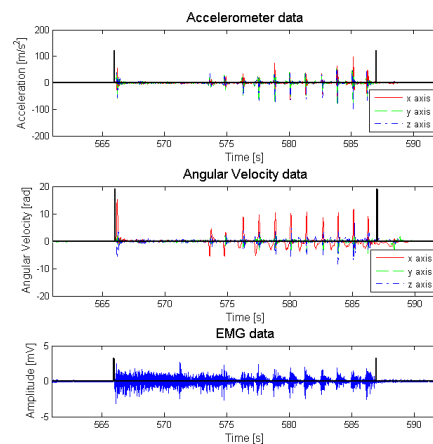


Fig. 1. A tonic-clonic simulated seizure framed by the black vertical lines placed by physicians. On top of the figure the acceleration is shown, in the middle is the angular velocity and at the bottom the muscle activity. The acceleration and angular velocity are from the AMG sensor at the lower arm, whereas the EMG data is from the biceps.

In Fig. 2 the data from a versive - asymmetric tonic seizure is shown. As it can be seen in the first part where the head is turning the lower arm is not involved, but when the raised arm becomes part of the seizure (asymmetric tonic seizure) the amplitude of the acceleration and angular velocity increases to about 30 m/s^2 and 12 rad , respectively. At the same time the EMG signal has an absolute maximum amplitude of about 2.5 mV .

The data from the myoclonic seizure is not shown, but the duration is found to be about half a second. Real myoclonia are even shorter in duration. The acceleration, angular velocity and EMG signal have absolute maximum amplitudes of 35 m/s^2 , 7 rad and 3.5 mV , respectively.

D. Processing Motion Data

Based on the seizures having stereotypical patterns, theoretically it should be possible to distinguish the seizures from the normal activities by a biomedical signal processing algorithm. A simple approach towards such an algorithm could be the Root-Mean-Square (RMS) value, $\text{RMS}(\mathbf{x}) = \sqrt{\frac{1}{N} \sum_{n=1}^N \mathbf{x}(n)^2}$, which is often used in connection with physiological data [4]. This is calculated for a window of half a second of the data and the windows are overlapping by 50%. The size of the window is chosen based on the fact that the myoclonic seizures are shorter than half a second, so to enhance the amplitude of these seizures a short window is needed. On the other hand the window should not be too short, which would induce a poor frequency resolution. Normally a window of 1 second is used when working with physiological data [3].

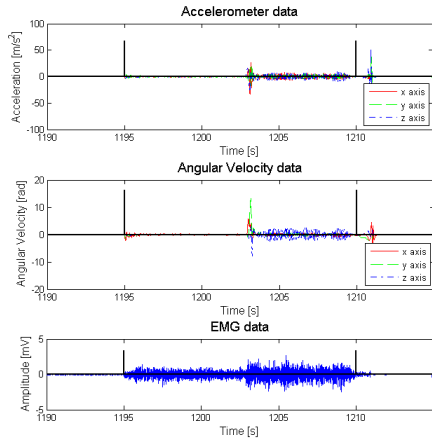


Fig. 2. A versive - asymmetric tonic simulated seizure framed by the black vertical lines placed by physicians. On top of the figure the acceleration is shown, in the middle is the angular velocity and at the bottom the muscle activity. The acceleration and angular velocity are from the AMG sensor at the lower arm, whereas the EMG data is from the biceps.

The RMS value of a window is calculated for all three modalities: acceleration, angular velocity and muscle activity. For the acceleration and the angular velocity it is proposed that the mean of the RMS values are calculated across the three dimensions, $RMS_{total} = (RMS_x + RMS_y + RMS_z)/3$. This is seen similar in other research projects [8]. This is done for all the time epochs analyzed (i.e. the periods containing the seizures and the periods containing different normal activities performed by the subjects). The periods of the normal activities are identified visually by inspection of the videos. From the RMS values the largest value is found for each modality for each period analyzed. These results can be plotted in a feature scatter plot showing the possibility of distinguishing seizures from normal activity.

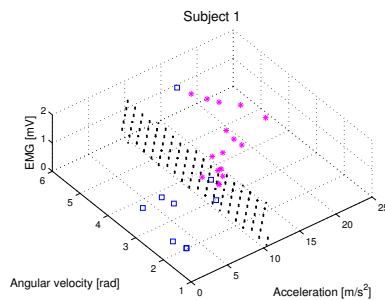


Fig. 3. The absolute maximal RMS values for simulated seizures and normal activities for the first subject. The * denote the seizures, whereas the squares denote the normal activities. The · marks the Bayes classifier discriminating between seizures and normal activity.

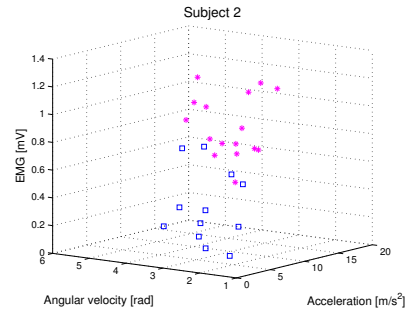


Fig. 4. The absolute maximal RMS values for simulated seizures and normal activities for the second subject. The * denote the seizures, whereas the squares denote the normal activities.

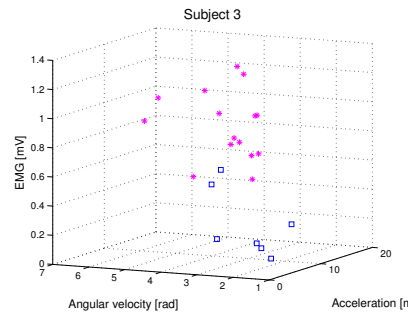


Fig. 5. The absolute maximal RMS values for simulated seizures and normal activities for the third subject. The * denote the seizures, whereas the squares denote the normal activities.

III. RESULTS AND DISCUSSION

From the feature scatter plots for the two subjects shown in Fig. 3, 4 and 5, it can be seen that the different modalities provide complementary information, meaning that the group of seizure-events cannot be differentiated from the group of normal activities based on just one modality. It is seen that the seizures are actually grouped in the 3D plot whereas most of the normal activities are grouped at another place in the feature space. Only few of the normal activities are placed closer to the group of seizure data than the one with normal activity data. Those that are placed closer to the group of seizure data are still not surrounded by seizure data, but are only placed in the outer sphere of the seizure-group. This means that by using all modalities it becomes possible to distinguish between seizures and normal activities. The distribution functions of the data are assumed to be gaussian, which makes the Bayes classifier optimal. In Fig. 3 a Bayes classifier decision boundary is added, based on the decision function [5]:

TABLE I
DETECTION OF SEIZURES BASED ON DATA FROM THE LOWER ARM SENSOR AND THE BICEPS. (AV: ANGULAR VELOCITY)

Modalities			1. subject		2. subject		3. subject		All	
ACM	AV	EMG	Sen [%]	FP	Sen [%]	FP	Sen [%]	FP	Sen [%]	FP
x			100	2	53	1	67	3	87	8
	x		53	1	73	6	67	0	52	6
		x	100	1	100	2	100	3	96	4
x	x		100	3	93	2	100	2	89	8
x		x	100	1	100	2	100	0	96	3
	x	x	100	0	100	2	100	0	98	4
x	x	x	100	0	100	1	100	0	98	4

TABLE II
DETECTION OF SEIZURES BASED ON DATA FROM THE THIGH SENSOR AND THE QUADRICEPS. (AV: ANGULAR VELOCITY)

Modalities			1. subject		2. subject		3. subject		All	
ACM	AV	EMG	Sen [%]	FP	Sen [%]	FP	Sen [%]	FP	Sen [%]	FP
x			67	6	100	9	33	0	33	7
	x		67	3	67	0	67	3	78	12
		x	100	6	67	2	100	3	100	15
x	x		80	2	100	0	93	2	91	6
x		x	100	4	100	3	100	2	98	11
	x	x	100	4	100	4	100	2	89	7
x	x	x	100	4	100	0	100	2	98	8

$$d_i(\mathbf{x}) = \ln P(C_i) - \frac{1}{2} \ln |\mathbf{C}_i| - \frac{1}{2} [(\mathbf{x} - \mathbf{m}_i)^T \mathbf{C}_i^{-1} (\mathbf{x} - \mathbf{m}_i)] \quad (1)$$

where $i = 1, 2$ and \mathbf{m}_i and \mathbf{C}_i are the mean and covariance matrix for class i , respectively. These measures are given by:

$$\mathbf{m}_i = E_i[\mathbf{x}] \quad (2)$$

$$\mathbf{C}_i = E_i[(\mathbf{x} - \mathbf{m}_i)(\mathbf{x} - \mathbf{m}_i)^T]. \quad (3)$$

Since no a priori probability is known and data are to be split in two classes, $P(C_i)$ is set to 1/2. The use of a classifier indicate the possibility of classifying multi-modal motion signals as seizure or non-seizure. In Table I the sensitivity (sen) (percentage of the seizures that are detected) and false positives (FP) (the number of normal activities that are detected as seizures during the 4-hour recording session) are given for each subject, for the three modalities separately and for a combinations of them. It is clearly seen that the best results, i.e. the highest sensitivity and the lowest number of false positives, are achieved when all three modalities are used. The table both shows the result of a subject specific MISA system for each of the subjects and of the non-subject specific MISA system. The non-subject specific system is able to detect 98% of the simulated seizures and at the same time it captures only 4 false positives. On the other hand the subject specific systems are able to register all simulated seizures and only captures 0-1 false positive. The movements that are detected as seizures for the non-subject specific system constitute one period of gambling with dices from

the first and the second subject, respectively, and furthermore one period of biking from the second and the third subject, respectively. The periods of gambling with dices might be registered as a seizure due to the relatively high muscle force and the rhythmic/alternating feature of the movements while shaking the dice cup. This could be mistaken for a clonic movement. There are no physiological explanation to why the biking periods are detected as seizures based on the data from the arm, since it is mostly the legs that are used on an exercise bike.

Furthermore the same study is made for the sensor at the thigh and the EMG electrode at the quadriceps. The results seen in Table II show that it is not just a MISA system based on data from the arm that makes it possible to distinguish between simulated seizures and normal activities. Even a MISA system based on the leg is able to partly detect the simulated seizures without detecting too many false positives. This is explained by the fact that the legs are also involved in some of the seizures as it is difficult to keep them entirely still when contracting other muscles during the seizures where the legs are not involved.

IV. CONCLUSION

A fairly simple first version of the MISA system in a non-subject specific version is shown to be able to achieve a sensitivity of 98% and at the same time only capture 4 false positives. This means that it is actually able to distinguish between the simulated seizures and the normal activity from the test subjects in this study. Looking at the subject specific MISA system even better results are seen with a sensitivity of 100% and only 0-1 false positive. Based on these results and the knowledge of real seizures having an even larger force than one can produce voluntarily, it seems possible

to distinguish between real seizures and normal activity based on biomedical signal processing algorithms dedicated for a MISA system. Furthermore it has been shown that the use of all the modalities of the MISA system provide complementary information which ensures a higher classification accuracy. Real seizures might not be as similar as the simulated ones. This means that in a future perspective more advanced features should be extracted and possibly a non-linear classification algorithm should be used to distinguish between seizures and normal activities. A second generation fully automatic MISA system is under development based on data from epileptic patients.

REFERENCES

- [1] T.M.E. Nijsen, J.B.A.M. Arends, P.A.M. Griep and P.J.M. Cluitmans, "The potential value of three-dimensional accelerometry for detection of motor seizures in severe epilepsy", *Epilepsy & Behavior*, 2005, vol. 7, pp. 74-84.
- [2] T.M.E. Nijsen, R.M. Aarts, J.B.A. Arends, and P.J.M. Cluitmans, "Model for arm movements during myoclonic seizures", *Engineering in Medicine and Biology Society, 29th Annual International Conference of the IEEE*, 2007, pp. 1582-1585.
- [3] D.A. Gabriel and G. Kamen, "Experimental and modeling investigation of spectral compression of biceps brachii sEMG activity with increasing force level", *Journal of Electromyography and Kinesiology*, 2008.
- [4] H. Linderhed, "Methods for Analysis and Evaluation of Surface EMG", *Linkpings universitet*, 1 edition, 1996.
- [5] R.M. Rangayyan, "Biomedical Signal Analysis - a case-study approach", *Wiley-interscience*, 2002, pp. 460-461.
- [6] G. Becq, S. Bonnet, L. Minotti, M. Antonakios, R. Guillaud, and P. Kahane, "Collection and exploratory analysis of attitude sensor data in an epilepsy monitoring unit", *Proceedings of the 29th annual international conference of IEEE EMBS*, France, 2007, pp. 2775-2778.
- [7] K. Cuppens, S. Omloop, P. Coleman, B. Ceulemans, and B. Vanrumste, "Detection of nocturnal epileptic seizures of pediatric patients using accelerometers. *Belgian Day on Biomedical Engineering*, 2007.
- [8] T.R. Burchfield and S. Venkatesan, "Accelerometer-based human abnormal movement detection in wireless sensor networks", *Proceedings of the 1st ACM SIGMOBILE international workshop on Systems and networking support for healthcare and assisted living environments*, ACM New York, NY, USA, 2007, pp. 67-69.
- [9] R.M. Mathiasen and C.P. Hansen, "Sensitivity of Epilepsy Bed Alarms and Pulse Oxymeters in the Danish Epilepsy Centre, Dianalund", *Epilepsia*, 2005, vol. 46 (Suppl. 6), pp. 50.
- [10] Xsens Technologies B.V., Website: <http://www.xsens.com/en/home.php/> (2008), January 16, 2009

PAPER II

TITLE Seizure Onset Detection based on a Uni- or Multi-modal Intelligent Seizure Acquisition (UISA/MISA) system

AUTHORS Isa Conradsen, Sándor Beniczky, Peter Wolf, Jonas Henriksen, Thomas Sams, and Helge B.D. Sorensen

JOURNAL Engineering in Medicine and Biology Society (EMBC), 2010 Annual International Conference of the IEEE

PUBLICATION HISTORY Submission date: 29-03-2010, Acceptance date: 10-06-2010

Seizure Onset Detection based on a Uni- or Multi-modal Intelligent Seizure Acquisition (UISA/MISA) System

Isa Conradsen^{†*}, Sándor Beniczky^{*}, Peter Wolf^{*}, Jonas Henriksen[†], Thomas Sams[†] and Helge B.D. Sorensen[†]

Abstract—An automatic Uni- or Multi-modal Intelligent Seizure Acquisition (UISA/MISA) system is highly applicable for onset detection of epileptic seizures based on motion data. The modalities used are surface electromyography (sEMG), acceleration (ACC) and angular velocity (ANG). The new proposed automatic algorithm on motion data is extracting features as “log-sum” measures of discrete wavelet components. Classification into the two groups “seizure” versus “non-seizure” is made based on the support vector machine (SVM) algorithm.

The algorithm performs with a sensitivity of 91-100%, a median latency of 1 second and a specificity of 100% on multi-modal data from five healthy subjects simulating seizures. The uni-modal algorithm based on sEMG data from the subjects and patients performs satisfactorily in some cases. As expected, our results clearly show superiority of the multi-modal approach, as compared with the uni-modal one.

I. INTRODUCTION

More than 50 million people around the world suffer from epilepsy and about 25% of them cannot become seizure free. Patients dreading the next seizure onset has potential to become socially isolated. Severe and sometimes fatal injuries can occur during seizures. An alarm system, capable of detecting seizures, could alert relatives and caretakers and ensure help for the patient. Several groups [1], [2] have already tried to develop such a system based on motion data, but none of them is performing well enough to reach clinical use. We therefore propose a new automatic detection algorithm capable of capturing the seizures with motor manifestations, without too many false alarms. It was decided in our previous study [3] to work further with movement sensors and surface electromyography (sEMG) registrations, as these provided promising results. Our new approach on these multi-modal motion data encompasses feature extraction with a discrete wavelet decomposition and an automatic classification with support vector machines (SVM). The MISA method including motion and sEMG data, was tested on 5 healthy subjects simulating seizures. However, due to impediments with the recruitment of patients, at present time it was only possible to test a uni-modal method on sEMG data alone, from 5 patients suffering from epilepsy.

Corresponding authors: Isa Conradsen, isaconradsen@gmail.com, Helge BD Sorensen, hbs@elektro.dtu.dk

[†]DTU Electrical Engineering, Ørstedes Plads, building 349, DK-2800 Kgs. Lyngby

^{*}Danish Epilepsy Center, Kolonivej 1, DK-4293 Dianalund

II. METHODOLOGY

A. Data Collection

Data were recorded at the Danish Epilepsy Center in Dianalund, Denmark. The 5 healthy subjects were measured with 16 movement sensors, containing 3D accelerometers, 3D gyroscopes and 3D magnetometers, and 14 bipolar sEMG channels for 2-4 hours using our setup described in [3]. Each subject simulated 15 seizures in total, divided in the three types, myoclonic, tonic-clonic and versive. These are defined by epileptologists and described in details in [3]. The healthy volunteers carefully watched a video-recording with the movement pattern they had to imitate. An epileptologist explained them the typical aspects of the seizures, and the participants practised the movements before the recording. It was difficult to find patients with enough seizures with motor manifestations who could cooperate to wear all the equipment, so for this study the patients have only been measured with 4 sEMG channels with a sampling frequency of 1024Hz. The sEMG electrodes were placed on deltoid and tibialis anterior muscles on both sides of the body (active electrode on the muscle bulk, reference electrode on the tendon adjacent to it). The number and type of seizures along with the sex and age of the patients are listed in Table I. Furthermore the length of the signals for the testing phase of the classification is listed.

TABLE I

THE PATIENTS GENDER, AGE AND THE AMOUNT AND TYPE OF SEIZURES ALONG WITH THE LENGTH OF THE TEST FILE.

	Gender	Age	# of seizures	Seizure Type	Length of Test File [h]
Pt 1	F	2	13	Tonic, Myoclonic	12
Pt 2	F	29	4	Tonic-clonic	27
Pt 3	M	5	14	Tonic, Spasm	31
Pt 4	M	48	10	Tonic	0.75
Pt 5	M	30	11	Tonic	8

B. Data Processing

The processing of data is split into three parts. The first part is the data partitioning, followed by the feature extraction and the last part is the classification into seizure and non-seizure events.

1) *Data Partitioning*: Data are split in smaller parts of seizure and non-seizure data to have more parts to choose from for the different iterations in the training and testing phases related to the classification. This provides a more

reliable result. The data are partitioned based on which subject is measured: healthy subject or patient, respectively. For each subject several files are processed. A patient file containing seizures is divided in subparts as shown in Fig. 1, where each data part between the seizures is split into periods of 1 minute. This is long enough to ensure that the movements within the period make sense, and short enough to ensure that sufficiently many periods for training and testing are obtained. Between each period a sequence of 5 seconds is left unused to avoid correlation between two successive periods. In the files containing simulated seizures, the periods between these are left unused, since the healthy subjects were practicing for the seizure simulations in between seizure periods. A file without seizures is treated equally, regardless of whether it is from a healthy subject or a patient. The file is split into periods of 1 minute, with 5 seconds sequences left unused between each - just as explained above for the patient file containing seizures.

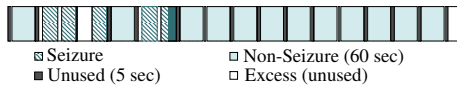


Fig. 1. The segmentation of a patient file containing five seizures. Between the seizures data are split into periods of 1 minute, with a sequence of 5 seconds left unused between successive periods.

2) *Feature Extraction*: Nijssen et al [1] showed that the wavelet decomposition would be a better choice for a feature than the short time Fourier transformation. The inherent properties of the wavelet transformation compared to the short time Fourier transformation gives a better time-frequency (time-scale) representation of normal movements versus seizures. As in [1] we have chosen to use the fifth Daubechies as the mother wavelet. The features are extracted from the discrete wavelet decomposition of windows of 1 second. The windows overlap by 50% and are filtered prior to the wavelet decomposition using a Hann filter of the same size as the window. This is done to smoothen the spectrum of the signal before processing it. The wavelet decomposition is performed through filtration with a high- and a low-pass filter as given by [4]:

$$A = v_{\text{low}}[m] = \sum_{l=0}^{L-1} u[l]g[2m-l] \quad (1)$$

$$D = v_{\text{high}}[m] = \sum_{l=0}^{L-1} u[l]h[2m+1-l] \quad (2)$$

where 2 is the downsampling factor, m and l are the sample number in the signal, L is the number of samples in the window and g and h are low- and high-pass filters, respectively. For each filtration the signal is then divided in an Approximation- (A) and a Detail- (D) signal. y_{low} is the approximation signal, whereas y_{high} is the detail signal. From each approximation signal a new step with filtrations is made by splitting as shown in Fig. 2. Each channel (ACC, ANG or EMG) is applied in the wavelet decomposition as $u(l)$.

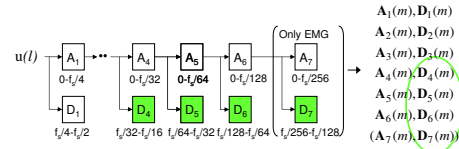


Fig. 2. The signal, $u(l)$, is filtered and thereby split in approximation and detail signals, each approximation signal is further filtered. This is done six (seven) times. For the feature vector we only use the detail signals from the fourth to the sixth (seventh) sub-band ($f_i = 1\text{kHz}$). The frequencies beneath the squares state the bounds for the sub-band.

From a visual inspection based on a comparison of the spectral content for seizure and non-seizure events, respectively, the frequencies of interest were found to be in the lower range. Based on this conclusion, only the detail signals layer 4-6 (7) are further used for the feature extraction.

To decrease the amount of data entering the feature vector, a “log-sum” measure is calculated for each sub-band used.

$$x_{j-3} = \log\left(\sum_{m=1}^M |D_j(m)|\right), \text{ where } j = 4, 5, 6(, 7) \quad (3)$$

where M is the number of samples in the signal $u(l)$, j is the sub-band number (4,5,6(,7)) and $D(m)$ is the detail signal. For our data $M = 120$ for ACC/ANG and $M = 1024$ for EMG data. By applying the logarithm it is ensured that the smaller and more essential details are enhanced, while the larger and insignificant ones are reduced.

The feature vector, \mathbf{x} , is then collected as:

$$\begin{aligned} \mathbf{a} &= [x_{1,ACC_1}, \dots, x_{3,ACC_1}, D_{1,ACC_2}, \dots, x_{2,ACC_{69}}, x_{3,ACC_{69}}] \\ \mathbf{b} &= [x_{1,ANG_1}, \dots, x_{3,ANG_1}, D_{1,ANG_2}, \dots, x_{2,ANG_{69}}, x_{3,ANG_{69}}] \\ \mathbf{c} &= [x_{1,EMG_1}, \dots, x_{4,EMG_1}, D_{1,EMG_2}, \dots, x_{4,EMG_{14}}] \\ \mathbf{x}_n &= [\mathbf{a}_n, \mathbf{b}_n, \mathbf{c}_n]^T, \end{aligned} \quad (4)$$

where ACC_1 means ACC channel 1 and so on and n is the time index. For convenience the time index, n , is omitted in the previous equations.

For the ACC/ANG data, six steps of filtration are made, but only the detail signals from sub-band four to six are used further on. The sEMG data are filtered in seven steps and the detail signals from sub-band four to seven are used further on. These are also the sub-bands outlined in Fig. 2. These numbers of filtrations mean that we only use the frequencies 0.94-7.5 Hz for the ACC/ANG data and the frequencies from 4-64 Hz of the sEMG signals. The frequencies are chosen based on a visual inspection of the spectra of the signals.

The feature vector is now complete and can be submitted to a classifier.

3) *Classification*: The problem is to solve a binary classification problem with the classes *Seizure* and *Non-seizure*. The class *Seizure* contains all the seizures in the measurements, whereas the class *Non-seizure* contains everything else. This means that the class *Non-seizure* contains much

more data than the class *Seizure*. As a classifier SVM is used, since it has proven to be better (than other complex algorithms such as artificial neural network) at handling data with very dissimilar amounts of data in the classes [5]. Data are divided into two groups, “train” and “test”, whereas the classifier is trained on data from the “train” group. The data from the “test” group can then be classified with the classifier trained for the purpose. The classifier will return a positive or negative value for each “test” vector, dependent on whether it is estimated as belonging to a seizure period or not. The divisions into these groups of the healthy subject data are made randomly, for both seizure and non-seizure data, ensuring close to equal amounts of each data type in each group. For the patients, the first couple of seizures along with non-seizure data are used for training and the rest of the seizures with non-seizure data for testing. The division is made in this way to keep it causal and thereby imitate a real-time situation.

For the training, data is labeled:

$$\{\mathbf{x}_n, y_n\}, n = 1, \dots, l, y_n \in \{-1, 1\}, \mathbf{x}_n \in \mathfrak{R}^d, \quad (5)$$

where l is the number of training examples, \mathbf{x}_n is the feature vector (n is the time index) and y_n the matching target, indicating which of the classes the feature vectors belong to, -1 for non-seizure and 1 for seizure.

A two-class linearly separable data set (where $d > 2$) can be separated by a hyperplane described by:

$$f(\mathbf{x}_n) = \mathbf{w} \cdot \mathbf{x}_n + b = 0, \quad (6)$$

where \mathbf{w} is the normal to the hyperplane and b is a shifting constant. The hyperplane is computed based on support vectors, which are the feature vectors that are placed closest to the hyperplane separating the two classes. These feature vectors from the two classes must satisfy:

$$y_n \cdot (\mathbf{w} \cdot \mathbf{x}_n + b) \geq 1 - \xi_n, \quad \text{where } \xi_n \geq 0 \forall n, \quad (7)$$

where ξ_n , a positive slack variable, is introduced to handle data, due that most classification problems are not completely separable. Data points assigned to the wrong side of the margin (defined by (7)) thereby have a penalty that increases with the distance to the margin.

To separate the two classes the problem of finding the optimal parameters, \mathbf{w} and b , can be reduced to minimizing the performance function (8):

$$\frac{1}{2} \|\mathbf{w}\|^2 + C \sum_{n=1}^l \xi_n \quad \text{subject to} \quad y_n \cdot (\mathbf{w} \cdot \mathbf{x}_n + b) \geq 1 - \xi_n, \quad (8)$$

where C is a factor which sets the trade-off between the size of the margin and the penalty of the slack variable, ξ_n [6].

For (8) to be minimized, each term should be minimized. Minimizing the first term means maximizing the margin between the support vectors of the two classes. The second term which encompass the slack variable is minimized by keeping the distance from incorrectly classified feature vectors to the margin as small as possible. When a feature vector is

correctly classified ξ_n is set to 0, whereby the second term in (8) will be 0. For a feature vector correctly classified, but placed on the wrong side of the margin, ξ_n is between 0 and 1. Whereas it is above 1, if the feature vector is wrongly classified. In the two latter cases the margin is attempted placed as close to these incorrectly classified feature vectors as possible to minimize the second term in (8).

To solve (8) Lagrange multipliers are multiplied and the equation is transformed from its primary form to the dual form, whereby it is possible to identify the parameters for the hyperplane which best separates the two classes. These steps are all performed in MATLAB by the SVM^{light} package specified in [7]. The package returns a classification-model based on the given training set, which can then be used to classify a test set.

III. RESULTS AND DISCUSSION

The results are presented as sensitivity (the amount of the seizures that are detected), specificity (the amount of non-seizures that are not detected) and latency (the time it takes to detect the seizures after seizure onset). The specificity might not be the best measure for the number of false alarms, but for the healthy subjects the measurements were very compact and every movement was planned beforehand, so no other measure would provide a more reliable value. On the other hand, we have further chosen to calculate the false detection rate (FDR) for the epilepsy patients, which is the amount of false detections per hour. An optimal result has 100% sensitivity and specificity, a latency of 1 second (due to the window length) and an FDR of 0.

The results for the healthy subjects on multi-modal data are shown in Fig. 3. The mean sensitivity and specificity are calculated for 30 iterations, whereas for the latencies the median is provided. It is clearly seen that for subject 1-4 the system has the highest sensitivity when all modalities are used. For the fifth subject the algorithm performs better with respect to sensitivity, if the EMG data is left out. Almost the same is seen concerning the specificity. The algorithm performs best for most subjects when all modalities are used, with exception of subject 2 where it is better if the EMG data is left out. With respect to the latency of the detections of the simulated seizures the result is also dependent on the subject, but most subjects have the best - or at least a very acceptable result when all modalities are used. There are a few outliers, but one should remember that it is the maximum latency that is depicted.

For the patients where only the sEMG data are provided, the results are shown in Fig. 4. This shows that the algorithm detects only half of the seizures for patient 1. The reason is that the other half is myoclonus, which is very short lasting (< 0.5 seconds) and only happening in one muscle. This means that the muscles included in these seizures might not be the ones, which we have measured. It should be noticed that the seizures are detected at onset. Further it can be seen that there are only very few false positives (0.08/h). For patient 2 all seizures are detected, but most of them with a delay. The false positives are very few (0.07/h), which

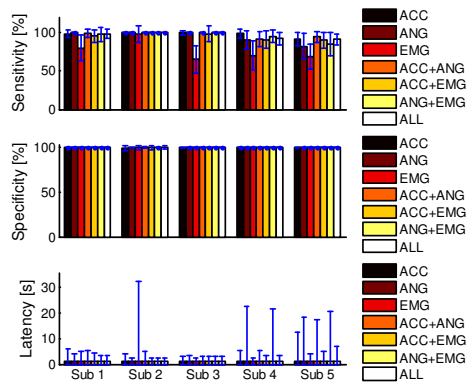


Fig. 3. The sensitivity, specificity and latency is showed for the results on the data from the five healthy subjects. For each subject the result is given for each modality alone and combinations of them. For the sensitivity and specificity the mean for 30 iterations (bars) and the standard deviation (blue lines) are shown. For the latency the median is shown by the bars (a bit difficult to see) and the blue line indicate maximum latency.

is important for an alarm system. For the third patient the algorithm is only able to detect one seizure, but neither does it capture any false positives. Notice that 50% of the seizures in the test data are spasms which the algorithm is not directly intended for. For the fourth patient all the seizures are detected at onset, but it has too many false alarms, the FDR might however be high due to the fact that we have less than an hour of data to test the algorithm on. For the last patient the algorithm is not able to detect all seizures, but those detected are however detected at onset. No post-processing has yet been applied, which might lower the FDR for some patients. A change in the window size might be able to increase the sensitivity for patients with very short lasting seizures. Comparing the healthy subjects and the patients show equally well results using the UISA system on sEMG data. The better results on the healthy subjects using the MISA algorithm imply that better results might be achieved on patients using our multi-modal approach, which is the focus for our future experiments. The movements simulated by the healthy volunteers closely resembled those occurring during the seizures, therefore it is reasonable to assume that the signals recorded by the movement sensors are similar to what we would have recorded from patients with epilepsy. However the muscle-signals depend on the recruitment of the motor nerve cells. In the case of volunteers the motor cells are physiologically activated, while in the case of "real" seizures the recruitment is a pathological one. Thus we cannot exclude that the EMG signal recorded during the simulated seizures have different characteristics than the epileptic ones.

IV. CONCLUSION

The automatic MISA system implemented is a new approach for motion data with feature extraction from discrete

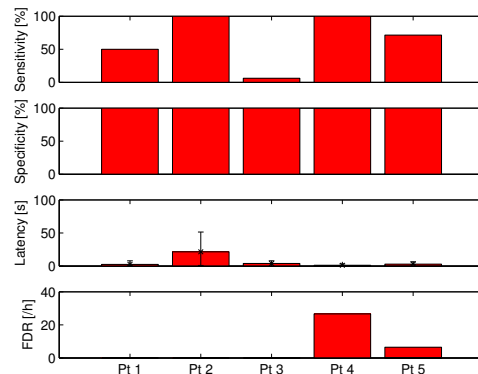


Fig. 4. The sensitivity, specificity, latency and false detection rate (FDR) are showed for the results on the EMG data from the five patients. The sensitivity, specificity and the FDR are shown as bars for each patient. For the latency the median is shown by the bars and the largest latency is indicated by the black line.

wavelet components. Data are classified with an SVM algorithm into the classes *seizure* and *non-seizure*. On the multi-modal data from the healthy subjects the algorithm performs as intended, with a sensitivity of 91-100%, a median latency of 1 second and a specificity of 100%. Analysis of the sEMG data performed satisfactorily for both some of the patients and some of the healthy subjects imitating seizures. Our data on healthy subjects show the superiority of the multi-modal approach as compared to the unimodal one. At the moment, the device is a prototype for research use only. We have experienced that some patients feel uncomfortable wearing the suit containing the sensors. As a consequence suit and device setup is being modified for future experiments.

REFERENCES

- [1] T. Nijssen, P. Cluitmans, P. Griep, and R. Aarts, "Short time Fourier and wavelet transform for accelerometric detection of myoclonic seizures," *IEEE/EMBS Benelux*, pp. 7-8, 2006.
- [2] K. Cuppens, L. Lagae, B. Ceulemans, S. Van Huffel, and B. Vanrumste, "Detection of nocturnal frontal lobe seizures in pediatric patients by means of accelerometers: A first study," in *Conference proceedings:31st Annual International Conference of the IEEE Engineering in Medicine and Biology Society*, vol. 1, pp. 6608-6611, 2009.
- [3] I. Conradsen, S. Beniczky, P. Wolf, D. Terney, T. Sams, and H. Sorensen, "Multi-modal intelligent seizure acquisition (MISA) system-A new approach towards seizure detection based on full body motion measures," in *Conference proceedings:31st Annual International Conference of the IEEE Engineering in Medicine and Biology Society*, vol. 1, pp. 2591-2595, 2009.
- [4] J. Proakis and D. Manolakis, *Digital signal processing: principles, algorithms, and applications*. Macmillan Publishing Co., Inc. Indianapolis, IN, USA, 1992.
- [5] C. Yang, J. Yang, and J. Wang, "Margin calibration in SVM class-imbalanced learning," *Neurocomputing*, 2009.
- [6] N. Cristianini and J. Shawe-Taylor, *An introduction to support Vector Machines: and other kernel-based learning methods*. Cambridge Univ Pr, 2000.
- [7] T. Joachims, "Learning to classify text using support vector machines: Methods, theory, and algorithms," *Computational Linguistics*, vol. 29, no. 4, pp. 656-664, 2002.

PAPER III

TITLE Automatic multi-modal intelligent seizure acquisition (MISA) system for detection of motor seizures from electromyographic data and motion data

AUTHORS Isa Conradsen, Sándor Beniczky, Peter Wolf, Troels W. Kjaer, Thomas Sams, and Helge B.D. Sorensen

JOURNAL Computer Methods and Programs in Biomedicine

PUBLICATION HISTORY Submission date: 10-08-2010, Acceptance date: 08-06-2011



ELSEVIER

journal homepage: www.intl.elsevierhealth.com/journals/cmpb

Automatic multi-modal intelligent seizure acquisition (MISA) system for detection of motor seizures from electromyographic data and motion data

Isa Conradsen^{a,b,*}, Sándor Beniczky^{b,c}, Peter Wolf^b, Troels W. Kjaer^d, Thomas Sams^a, Helge B.D. Sorensen^{a,**}

^a Technical University of Denmark, Department of Electrical Engineering, Ørstedes plads bygn. 349, 2800 Kgs. Lyngby, Denmark

^b Danish Epilepsy Centre, Department of Neurophysiology, Kolonivej 1, 4293 Dianalund, Denmark

^c University of Southern Denmark, Institute of Regional Health Services Research, Winsløwparken 19, 3, DK-5000 Odense C, Denmark

^d Rigshospitalet University Hospital, Department of Clinical Neurophysiology, 2100 Copenhagen, Denmark

ARTICLE INFO

Article history:

Received 10 August 2010

Received in revised form

20 May 2011

Accepted 8 June 2011

Keywords:

Epilepsy

Movement sensors

Seizure detection

Surface EMG sensors

Support vector machine learning

Wavelet packet

ABSTRACT

The objective is to develop a non-invasive automatic method for detection of epileptic seizures with motor manifestations. Ten healthy subjects who simulated seizures and one patient participated in the study. Surface electromyography (sEMG) and motion sensor features were extracted as energy measures of reconstructed sub-bands from the discrete wavelet transformation (DWT) and the wavelet packet transformation (WPT). Based on the extracted features all data segments were classified using a support vector machine (SVM) algorithm as simulated seizure or normal activity. A case study of the seizure from the patient showed that the simulated seizures were visually similar to the epileptic one. The multi-modal intelligent seizure acquisition (MISA) system showed high sensitivity, short detection latency and low false detection rate. The results showed superiority of the multi-modal detection system compared to the uni-modal one. The presented system has a promising potential for seizure detection based on multi-modal data.

© 2011 Elsevier Ireland Ltd. All rights reserved.

1. Introduction

Epilepsy is a functional disorder of the brain caused by excessive discharges of groups of neurons clinically characterized by repeated unprovoked seizures lasting from seconds to minutes. About 1% of the world's population has epilepsy. Seizure manifestations can be motor (tonic, clonic, tonic-clonic, etc.), sensory, psychic or vegetative, and consciousness may be retained or altered, sometimes with automatic behavior. In spite of much progress with pharmacological, surgical and

other treatments, about 25% of epilepsy patients continue to have seizures. For many of these patients, seizure onset is unpredictable, impairing independent living and increasing the risk of injuries, e.g. by falls or burns. Therapy resistant patients with generalized tonic-clonic seizures have an increased risk of dying as a consequence of a seizure, especially when they live alone and the seizures occur during sleep [1,2]. An automatic seizure detection system that alerts relatives or other helpers of an on-going seizure would alleviate several of these problems. The earlier a seizure is detected,

* Corresponding author at: Ørstedes plads bygn. 349, 2800 Kgs. Lyngby, Denmark. Tel.: +45 45253704; fax: +45 45880117.

** Corresponding author.

E-mail addresses: ic@elektro.dtu.dk, isacnradnsen@gmail.com (I. Conradsen), hbs@elektro.dtu.dk (H.B.D. Sorensen).

0169-2607/\$ – see front matter © 2011 Elsevier Ireland Ltd. All rights reserved.

doi:10.1016/j.cmpb.2011.06.005

the more useful the system would be. It could also be beneficial in determining therapeutic success or failure in patients who live alone and cannot reliably report whether they still have seizures. A clinically feasible detection system needs to be both reliable and comfortable.

Today the diagnostic gold standard in epilepsy is electroencephalography (EEG) with simultaneous video surveillance. EEG is known to be reliable for detection of seizures [3–5]. EEG-recordings require, however, either an invasive recording (intracranial electrodes) or the placement of several scalp-electrodes, which is less stable over time. The patient might also be uncomfortable wearing electrodes on the scalp, which are very noticeable for others, and thereby stigmatizing the patient further. Despite the EEG method being the gold standard, it does not necessarily seem to be the best option for a seizure alarm outside the hospital. It has been attempted to use video recordings for seizure detection [6], but they had too many restrictions and limitations (obstacle-free area of movement covered by light and camera).

Nijssen et al. [7] used accelerometers (ACM) for seizure detection. The visual analysis of the movement data recorded with these sensors showed promising results (91% of the seizures with motor phenomena were detected), and was considered feasible for detection of seizures. Others [8,9] have tried to detect seizures based on ACM data, but an ideal method has not yet been presented.

Earlier studies [7–9] on detecting seizures from ACM data did not report on aspects concerning the time between seizure onset and the detection, but only on detection versus no detection. It is highly desirable to achieve an early detection of seizures (i.e. with only a few seconds of delay) to make possible an intervention to stop the seizures and/or prevent injuries during the seizures. To make such a system reliable for detection of seizures we decided to work with multi-modal data, so we extended the system from using only ACM to combine it with sEMG and gyroscopes (angular velocity (ANG) data). Gyroscopes provide information on the rotation of each joint, so this data covers e.g. movements where the limbs are accelerated less, but still rotated. In a preliminary study [10] we found that the three modalities sEMG, ACM and ANG provided complementary information with potential improvement of classification accuracy. The next issue was to identify the most promising features to distinguish between seizures and normal activities and furthermore identify the most appropriate classifier to automatically differentiate between the two classes based on the feature vectors. Nijssen et al. [11] showed through a visual analysis that the continuous wavelet transformation (CWT) seems to be a better feature than short time Fourier transformation (STFT) for ACM data. Seizure detection from sEMG signals is a rather unexplored field, but from a visual inspection of the data it seems that both the amplitude and the frequencies of the signal during seizures are different from normal activities. The discrete wavelet transformation (DWT) seems to be a good choice as a feature extraction method, since it provides a good frequency resolution at low frequencies and furthermore a good time resolution at the high frequencies. Based on this we used DWT for feature extraction and support vector machines (SVM) as a classifier in a pilot study [12], including both sEMG, ACM and ANG data, with very promising results

on distinguishing between seizures/simulated seizures and normal activities.

In this paper we search for the best feature extraction method based on the wavelet transformation to separate simulated seizures from normal activity. The wavelet transformation is good at describing both the morphology and the spatial distribution in the movement signals. Compared to the DWT, the wavelet packet transformation (WPT) provides equal time and frequency resolution for all frequencies. Besides DWT we have therefore also tested the WPT as a method for extracting features for all modalities in this automatic multi-modal intelligent seizure acquisition (MISA) system. To classify our data into the two groups, seizures and normal activities, we used SVM [13] (as in our pilot study [12]) as a binary classifier trained on feature vectors from both classes, since it is well known to function better than other classifiers when the data classes are of unequal sizes. We used data from healthy subjects who simulated seizures (as instructed by a physician) to develop our algorithm upon. To assess the similarity between the simulated seizures and a real one, we have visually compared the raw data from the simulated seizures with a real seizure from a patient for all modalities.

This paper is organized as follows: the recordings are presented in Section 2; data presentation is given in Section 3; the method in details in Section 4 and the results in Section 5. At last Sections 6 and 7 encompass the discussion and the conclusion, respectively.

2. Recordings

The goal of the project was to detect simulated seizures from multi-modal signals based on movement data (sEMG, ACM and ANG). To be able to statistically explore whether the automatic detection algorithm is functioning, the number of simulated seizures for each healthy subject had to be more than five. The reason for initially using healthy subjects (who simulated seizures) instead of epileptic patients was the difficulty in the patient recruitment. Most patients with more than five seizures with motor manifestations within a few days are mentally retarded and therefore have difficulties in cooperating, when wearing the suit containing the movement sensors. Therefore it has yet only been possible to collect seizure data from one patient and we only succeeded in obtaining one seizure from this patient. Ten healthy subjects who were instructed to simulate seizures are therefore monitored with all modalities and used for the project.

The project had been approved by the ethics committee of Region Zealand, Denmark. All subjects involved received information on the project and gave their written consent to participate in the study.

The recordings on healthy subjects were made at the Danish Epilepsy Centre in Dianalund, Denmark. Ten healthy subjects aged 23–30, both male and female, were included. It is assumed that there is no effect of gender. The measurements lasted 1.5–3 h for each healthy subject. All of the healthy subjects were asked to simulate three types of seizures and some normal activities. They were given a description of the seizures, and they watched seizures on a video. Before the recording the healthy subjects trained simulating the seizures

Table 1 – Information about the healthy controls.

Subjects	Gender	Age	Test file length [h]
1	F	26	1.5
2	M	30	1.25
3	M	26	0.85
4	F	24	1
5	F	26	1
6	M	24	1
7	M	27	0.75
8	M	25	1
9	M	24	1.25
10	M	23	1

while assisted by a physician. During the recordings a physician was present to check that the simulated seizures were visually similar to real ones, when looking at the patients. If they were not, the subject was corrected and asked to simulate a new one. The normal activities were biking, use of mobile phone, computer and TV, eating and gambling with dices. The last activity was chosen because of the movement's similarity to clonic seizures or the clonic phase of the tonic-clonic seizures, whereas the rest were activities which the patients as well as gambling have access to during a normal admission in the epilepsy monitoring unit (EMU). Each of the seizures was simulated five times for each healthy subject. The times for the simulated seizures were annotated like during a normal admission. The three types of simulated seizures and their descriptions are as follows:

Myoclonic is a very short lasting twitch in a single muscle. The healthy subject is asked to make as short a contraction of the right biceps brachii as possible, which will cause a very short lasting movement of the right lower arm.

Versive-asymmetric tonic seizure is characterized by a turn of the head to an almost uncomfortable angle, where the healthy subject is looking upwards and to the side. This is followed by an isometric contraction in an asymmetric posturing, where the arm, on the same side towards which the head is turned, will be placed above the head.

Tonic-clonic starts as an isometric contraction of all the muscles. After a while it changes to rhythmically repetitive jerks made by alternating contraction and relaxation of the muscles.

The gender and age of the healthy subjects are listed in Table 1, as well as the length of the signals for the testing phase of the classification. The sEMG data were sampled at frequency of 1024 Hz, whereas ACM and ANG were sampled at frequency of 120 Hz.

The epileptic patient was admitted to the EMU at Rigshospitalet (Copenhagen University Hospital) for a diagnostic indication, as stipulated by the ethics committee. The admission lasted 3 days, where the patient, a 29 years old male had one seizure (of the generalized tonic-clonic seizure type). The time for the seizure has been clinically annotated by the neurophysiology technicians and later checked by a physician. The sEMG data were sampled at frequency of 1000 Hz, whereas the ACM and ANG were sampled at a frequency of 120 Hz as for the healthy subjects. The reason for the use of different sampling frequencies for the sEMG data is that the two participating departments use different recording programs with

different setup possibilities for the sampling frequencies. Furthermore the sEMG data from the EMU at the Danish Epilepsy Centre were filtered before exportation, so to equalize the frequency bands of the sEMG signals for the different subjects all data was filtered with a low-pass filter with a cut-off at 70 Hz.

The recordings all included both EEG, video, sEMG, electrocardiography (ECG) and motion sensors (ACM and ANG), but for this study only sEMG data and the data from the motion sensors were used. The motion sensors used are the system by Xsens [14] called Xsens MVN, which is a wireless system consisting of a suit with 16 sensors. Each of these sensors includes 3D ACM, 3D gyroscopes and 3D magnetometers. Based on the recordings, the Xsens MVN software system performs necessary biomechanical calculations, which provide data from 7 extra positions on the body (shown as position 2, 3, 4, 5, 6, 19 and 23 in Fig. 1). The output therefore is 3D ACM and 3D ANG from 23 different locations on the body, see Fig. 1. With these 23 placements on the body a full body system able to outline practically all movements of the body parts during seizures is obtained. For each of these two modalities we have 69 channels. For the recording on the patient we were not able to use the head sensor (position 7 in Fig. 1), hence, due to the biomechanical calculations in the software, data are useless for three positions (position 5, 6 and 7 in Fig. 1). The third modality, sEMG, is applied as 14 surface electrodes, each accompanied with its own reference electrode, placed on nearby bone or tendon. The sEMG electrodes are placed on the center of the belly of the muscle and symmetrically on the body on the following muscles: sternocleidomastoid, deltoid, biceps brachii, triceps brachii, biceps femoris, quadriceps femoris, and tibialis anterior. The muscles are chosen by a physician based on the knowledge on which parts of the body are most active during seizures, and to ensure full body coverage.

The recordings were performed by starting all conventional measurements in the EMU (i.e. all modalities except for the motion sensor system). When this was up and running, the motion sensor system was started and the time in the sEMG sampling system was annotated by the neurophysiological assistant, as precisely as possible. All data types were then used from this point and on, whereby they were synchronized.

The sEMG electrodes are connected to the EEG amplifier, which, in this case, is not wireless. It is the plan to implement the system as fully wireless in the future, allowing for the patients to move around more freely, while wearing the alarm and monitoring device. The hope is to identify which sensor positions are better at distinguishing seizures from normal activities and thereby being able to lower the number of sensors.

3. Data presentation

To assess the reliability of using simulated seizure data from healthy subjects instead of epileptic patients, the raw data from the simulated seizures were compared visually to an epileptic one for all modalities. Since we only could record one patient with epilepsy, a statistical comparison of the quantitative data/parameters was not possible. A representative simulated tonic-clonic seizure is shown in this paper for comparison with the real seizure. Fig. 2 shows the time

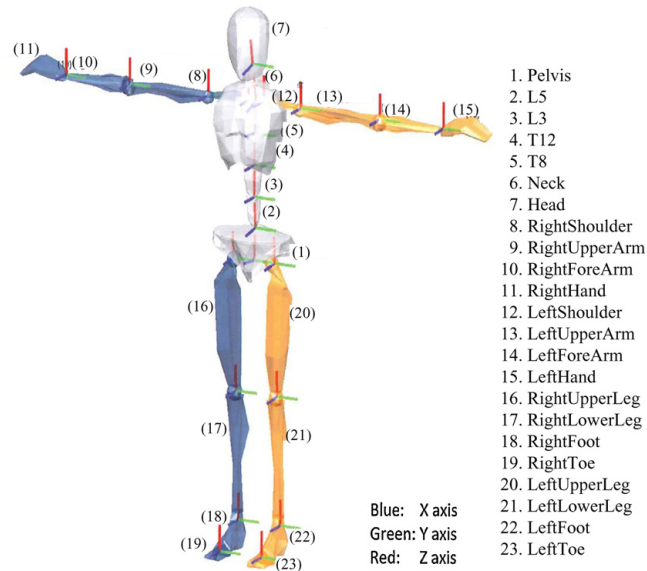


Fig. 1 – The placement of the sensor positions from the Xsens MVN system, see the Manual for Xsens MVN, revision D, June, 2008 [14].

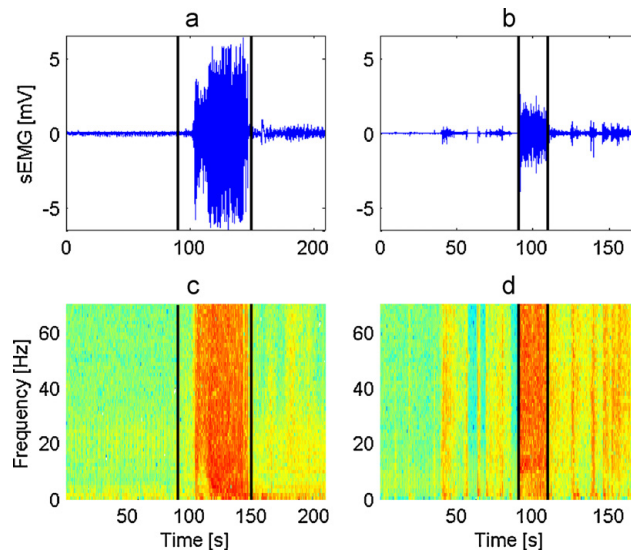


Fig. 2 – The sEMG data for a real seizure and a representative simulated seizure are shown in a and b, respectively. The matching spectrograms (for a normalization of the signals) are shown in c and d, respectively, where the red color means high power, blue color means low. The data is from the right biceps. The seizure and the simulated seizure are both surrounded by normal activity data, 1.5 min prior and 1 min later. The black vertical lines represent onsets and offsets of seizures and simulated seizures. (For interpretation of the references to color in this figure legend, the reader is referred to the web version of the article.)

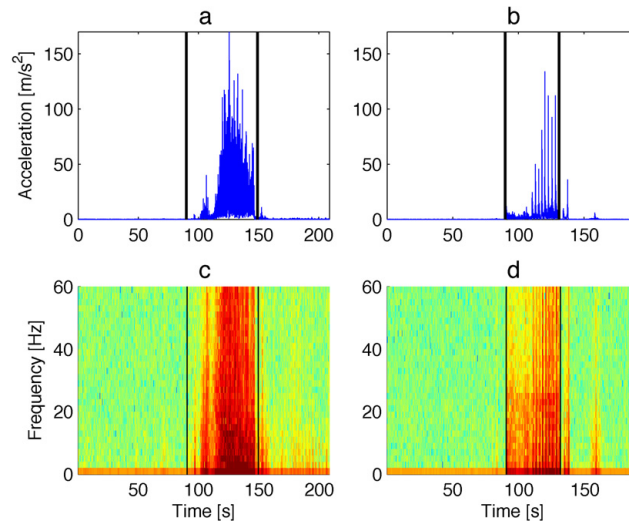


Fig. 3 – The ACM data for a real seizure and a representative simulated seizure are shown in a and b, respectively. The matching spectrograms (for a normalization of the signals) are shown in c and d, respectively, where the red color means high power, blue color means low. The data is from the right lower arm. The seizure and the simulated seizure are both surrounded by normal activity data, 1.5 min prior and 1 min later. The black vertical lines represent onsets and offsets of seizures and simulated seizures. (For interpretation of the references to color in this figure legend, the reader is referred to the web version of the article.)

plots and spectrograms of a seizure/simulated seizure and the surrounding normal activity for the patient and the healthy subject, respectively. The data is sEMG from the right biceps brachii. The start and end of the seizure/simulated seizure is marked by the black vertical lines. For the patient it can be seen that the seizure starts prior to the muscle activity, so the first signs of the seizure were only visible in the EEG or other muscles and first a bit later did the tonic-clonic part start in the biceps brachii. The starting point for the simulated seizure is defined as where the muscle activity starts. For some patients the seizure might as well be when the muscle activities are started, so this will not be seen as a difference. A clear difference is the amplitude of the signals, but it should be noted that this characteristic depends among other on the strength of the subject and the thickness of the skin/fat layer between electrode and muscle. The spectrograms are made based on normalized signals (to make sure the amplitude differences will not influence our interpretation) and plotted with the same color bar. From the spectrograms it is revealed that for both the seizure and the simulated seizure the power contained in the signal is increased for all frequencies through a longer period compared to the normal activities. In a future study we might examine the higher frequencies (above 70 Hz), since the signals do not seem to be unimportant above this limit. We cannot exclude that besides the difference in amplitude there are other differences too between the sEMG signals from the seizure and the simulated seizures.

Figs. 3 and 4, which show the raw ACM and ANG data from the right forearm, respectively, for both the patient and a representative healthy subject, are visually similar.

The amplitude, however, is also a problem for these modalities. The movements during the real seizure seem to have larger acceleration and angular velocity and furthermore both movements seem to be more confounded in the real seizure, whereas most of the healthy subjects have lower accelerations and angular velocities especially. There are though also differences among patients with epilepsy and the one we recorded from may have had faster movements than the average patient. We will have to trust that the acceleration of the simulated seizures were similar to real ones seen visually, when looking at the healthy subjects, since this was what the physician concluded during the simulations. The spectrograms show that the real seizure has a larger power in the higher end of the frequencies, than the simulated seizure, but the simulated seizures do though show a higher power in some frequencies (above 15 Hz for the ANG signal and above 1 Hz for the ACM signal) than the normal activities. These spectrograms are as well as for the sEMG generated based on the normalized signals to avoid power differences based on the amplitude of the signal. There are smaller differences in the frequencies between ACM and ANG that seems to give some useful complementary features to our algorithm.

The movements simulated by the healthy subjects visually (when looking at the healthy subject) closely resembled those occurring during the seizures, therefore it is reasonable to assume that the signals recorded by the motion sensors are similar to what we would have recorded from patients with epilepsy. This is also what we observed when we compared the data from the simulated seizures to the real one, though with some differences in the strength of the seizures. How-

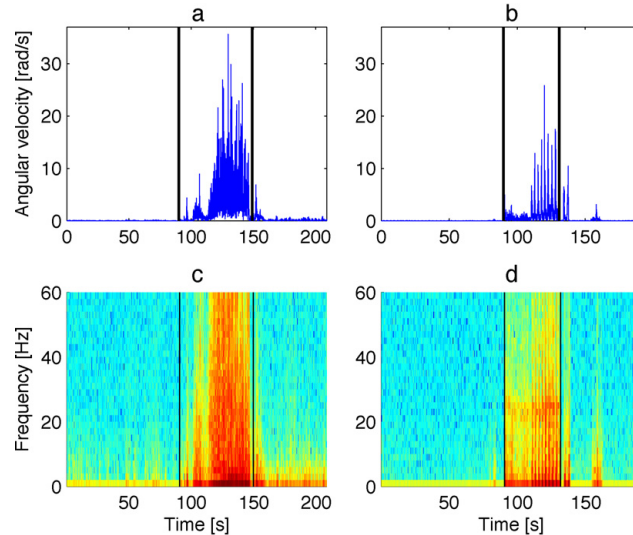


Fig. 4 – The ANG data for a real seizure and a representative simulated seizure are shown in a and b, respectively. The matching spectrograms (for a normalization of the signals) are shown in c and d, respectively, where the red color means high power, blue color means low. The data is from the right lower arm. The seizure and the simulated seizure are both surrounded by normal activity data, 1.5 min prior and 1 min later. The black vertical lines represent onsets and offsets of seizures and simulated seizures. (For interpretation of the references to color in this figure legend, the reader is referred to the web version of the article.)

ever, these differences make the real seizure stand out even more from the normal background activity, suggesting that the algorithm might work even better on the real seizure data than on the simulated ones.

4. Method

The method for detection of seizures based on multi-modal data is split in several steps as outlined in Fig. 5. The first step is to extract appropriate features and the second is to classify the data based on these features. Prior to these steps it is, however, necessary to take a look at the data and how it may

be divided into training and test sets for the classification. All of the signal processing is performed in MATLAB 7.6.

4.1. Data partitioning

Data are partitioned due to the fact that during the recordings, for practical reasons, all simulated seizures, were simulated within a short time with the healthy subjects practicing the simulations in between. It is therefore not possible to make a causal split of the data into training and test periods, where the first part would be used for training and the last part for test.

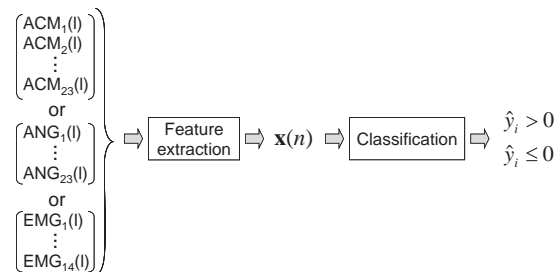


Fig. 5 – Method for detection of simulated seizures based on multi modal data. Three types of data are used, from which features are extracted. The feature vector is sent through to a classifier, which outputs y_i . A positive y_i classifies as a simulated seizure, whereas a negative y_i belongs to the normal activity class.



Fig. 6 – Diagram of the segmentation of the data strings from files containing simulated seizures. Between each segment a period of 5 s of data is left unused. Each normal activity segment lasts 1 min.

For the classification, both a training set and a test set of data is needed. Therefore data is divided into smaller segments and split randomly into the training and test phases. By splitting data in smaller segments of simulated seizures and normal activity data there are more segments to choose from, when randomizing the training and test phases related to the classification. This ensures that both the training and test phases contain segments from all the different activities performed. For each healthy subject several files are processed. A file containing seizures is divided in subparts as shown in Fig. 6, where the data parts between the simulated seizures are left unused, since, as earlier mentioned, the healthy subjects might have been practicing for the simulation of simulated seizures in between the actual simulations. The simulated seizures are split in separate segments as to contain each simulated seizure as a whole. The data period after the simulated seizures is split into segments of 1 min. This length ensures that the movements within the segments make sense, and that a sufficient number of segments are obtained for training and test. Between each segment a sequence of 5 s is left unused to reduce the correlation between two successive periods as much as possible without too much loss of data. A file without simulated seizures is treated in the same way as the period following the simulated seizures. The file is split into segments of 1 min, with 5 s sequences left unused between each—just as explained above.

4.2. Preprocessing

With 14 sEMG channels and 69 channels of ACM and ANG, respectively, we have 152 channels in total. In order to decrease this number and thereby the computational load regarding the feature extraction, for ACM and ANG we used the length of the direction vector instead of the three dimensional (3D) coordinates, x , y and z (e.g. for ACM):

$$ACM = \sqrt{ACM_x^2 + ACM_y^2 + ACM_z^2} \quad (1)$$

Naturally since we only have one signal for each sEMG electrode, the raw sEMG data will be used.

This preprocessing of data leaves us with 60 channels (preliminary features) of data in total.

4.3. Feature extraction

In classification problems the choice of features is often more important than the choice of classifier [15], since the features outline the details to discriminate between two groups,

whereas one classifier might provide a similar result as another, based on the same set of features.

The features for discriminating between *simulated seizures* and *normal activities* should therefore be chosen based on how well they distinguish between the two groups. Based on a visual inspection of data Nijsen et al. [11] found that a wavelet decomposition with the fifth Daubechies as a mother wavelet was the most appropriate feature compared to the STFT for ACM data. Consequently, we have decided to use the fifth Daubechies as a mother wavelet for our data; ACM as well as sEMG and ANG. Compared to the STFT where a signal is split in sine functions with different frequencies, the wavelet transformation divides the signal into shifted and scaled versions of a mother wavelet. The discrete wavelet decomposition is basically two filters that are applied sequentially to the input signal again and again (one time for each step), the filters are composed as low- (g) and high-pass (h) filters based on the mother wavelet. From each filtration an approximation (A) and a detail (D) signal is achieved. Each approximation signal can be further filtered into a new level with both an approximation and a detail signal, see Fig. 7. The black squares mark the division by the DWT, whereas the WPT is demonstrated by all squares, where also the detail signals are filtered. A mother wavelet is defined by a scaling function $\phi(x)$ and a wavelet function $\psi(x)$ [16], described by the low-pass filter, g , and the high-pass filter, h [17]:

$$\phi_{j,m}(l) = 2^{j/2} \cdot g_j(l - 2^j m) \quad (2)$$

$$\psi_{j,m}(l) = 2^{j/2} \cdot h_j(l - 2^j m), \quad (3)$$

where j is the resolution or scale parameter, m is the translation parameter and the inner product normalization is described by $2^{j/2}$. The decomposition is then described as the discrete approximation, $A_j(m)$, and detail, $D_j(m)$, signals given by [17]:

$$A_j(m) = u(l) * \phi_{j,m}(l) \quad (4)$$

$$D_j(m) = u(l) * \psi_{j,m}(l), \quad (5)$$

Each window of each channel (ACM, ANG or sEMG) is applied in the wavelet transformation as $u(l)$. By the extension of the DWT to further filtering on each detail signal as well, the WPT is, as stated above, obtained. Thereby the signal is split up in uniform frequency bands with equal frequency and time resolutions for all frequencies. This means that no matter which frequency band shows the largest difference between simulated seizures and normal activity in the movement data, an appropriate resolution is achieved for both time and frequency. So a good time resolution is not compromised by a bad frequency resolution and correspondingly a good frequency resolution is not compromised by a bad time resolution.

Each DWT and WPT is determined from a window of 0.75 and 1 s, respectively, both with an overlap of 50%. The windows should be short enough to capture the important details of the seizures and at the same time, long enough to keep a good frequency resolution. The window lengths are chosen based on the results of our assessment of the optimal value for the two methods (DWT and WPT), respectively. Before the

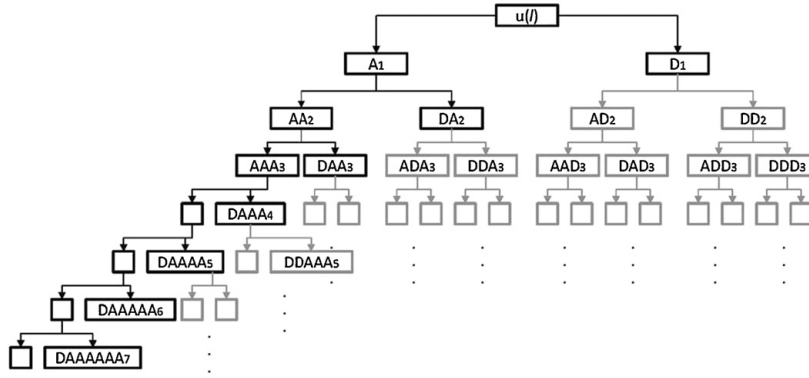


Fig. 7 – The signal, $u(l)$, is filtered and thereby split in approximation and detail signals. The scheme with the black boxes shows the decomposition with a normal wavelet, whereas the total scheme shows the decomposition with wavelet packets. The decomposition is in both cases made to level 7 (seven layers). According to this scheme the detail bands we use for the DWT would be named: DAAA₄, DAAA₅, DAAAA₆ (and DAAAA₇ for sEMG signals). These names are long, which is why we use the short terms instead: D₄, D₅, D₆ (and D₇ sEMG signals).

windows are divided in approximation and detailed signals, they are filtered by multiplying a Hann window of the same length as the signal window to smoothen the spectrum. All feature extractions are processed in MATLAB with the Wavelet Toolbox.

4.4. DWT feature extraction

The DWT can be made with an optional number of layers. We found that for the sEMG signals with a sampling frequency of 1024 Hz it would be most efficient to use 7 layers, whereby the last bands had a resolution of 4 Hz. For the ACM/ANG signals we found that 6 layers were to be used, whereby the last band had a resolution of ~1 Hz. From a visual inspection of the features extracted from the different bands in the 7 (6) layers, the detail signals layer 4–6 (ACM/ANG signals) and 4–7 (sEMG signals) turned out to provide larger differences (for the log-sum/energy parameter introduced below), when comparing the simulated seizures to randomly chosen normal activi-

ties. For the ACM/ANG signals the frequencies extracted are 0.94–7.5 Hz and for the sEMG signals they are 4–64 Hz.

To evaluate these signals and decrease the amount of data entering the feature vector we are interested in a measure for each signal indicating how much “energy” they contain. This can be evaluated by calculating a “log-sum” measure of the signals as shown in Fig. 8 and given in (6):

$$x_{j-3} = \log \left(\sum_{m=1}^{L/2^j} |D_j(m)| \right), \quad (6)$$

where L is the number of samples in the signal $u(l)$, j is the resolution (4, 5, 6 for ACM/ANG and 4, 5, 6, 7 for sEMG) and $D_j(m)$ is the detail signal. By applying the logarithm, it is ensured that the smaller differences between feature vectors from different classes are enhanced, while the larger differences between feature vectors are reduced. The influence on the system by possible outliers is thereby reduced. This means that the sys-

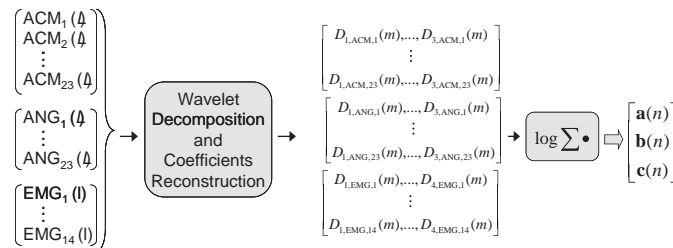


Fig. 8 – Flowchart of the feature extraction from Fig. 5. One window of data is analyzed at a time. l is the sample number. The chosen sub-bands are reconstructed, which for the DWT are D₄, D₅, D₆ and D₇ (only for sEMG signals). For the WPT the sub-bands used are DDA₃ and ADD₃ for the ACM and ANG signals, whereas AAAA₅ and DDA₅ are used for the sEMG signals (The names are given as illustrated in Fig. 7). A “log-sum” measure is calculated from the used bands as input to the feature vector.

tem is assumed to be less affected by outliers in the movement signals.

The feature vector, \mathbf{x} , is then collected from the vectors \mathbf{a} , \mathbf{b} and \mathbf{c} , with three (ACM/ANG) or four (sEMG) "log-sum" measures for each data window for all channels in the different modalities:

$$\begin{aligned} \mathbf{a} &= [x_{1,ACM_1}, x_{2,ACM_1}, x_{3,ACM_1}, x_{1,ACM_2}, \dots, x_{1,ACM_{2B}}, x_{2,ACM_{2B}}, x_{3,ACM_{2B}}] \\ \mathbf{b} &= [x_{1,ANG_1}, x_{2,ANG_1}, x_{3,ANG_1}, x_{1,ANG_2}, \dots, x_{1,ANG_{2B}}, x_{2,ANG_{2B}}, x_{3,ANG_{2B}}] \\ \mathbf{c} &= [x_{1,EMG_1}, x_{2,EMG_1}, x_{3,EMG_1}, x_{4,EMG_2}, x_{1,EMG_2}, \dots, x_{1,EMG_{14}}, x_{2,EMG_{14}}, x_{3,EMG_{14}}, x_{4,EMG_{14}}] \\ \mathbf{x}_n &= [\mathbf{a}_n, \mathbf{b}_n, \mathbf{c}_n]^T \end{aligned} \quad (7)$$

where ACM_1 means ACM channel 1 and so on and n is the time index. For convenience the time index, n , is omitted in the previous equations. The concatenation of the measures into a feature vector is shown as the last step in Fig. 8.

4.5. WPT feature extraction

As with the DWT, the WPT can be made with an optional number of layers. We used the same number of steps as for the DWT. This divides the signal into frequency bands of 4 Hz. From a visual inspection of the reconstructed sEMG signals we found the reconstruction signals that contained the largest differences between simulated seizures and normal activities. It turned out to be the second and the fourth band in the fifth step, corresponding to frequency bands of 16–32 Hz and 48–64 Hz, respectively. So it showed unnecessary to decompose it into seven steps. For the ACM/ANG data, because of the lower sampling frequency, the decomposition was made in six layers as used for the DWT. This gave frequency bands for the reconstructed signals of 0.94 Hz. A visual inspection as described above was conducted with the result that the fourth (22.5–30 Hz) and seventh (45–52.5 Hz) band of the third step contained the larger differences between the simulated seizures and normal activities for both ACM and ANG.

As for the DWT, we calculate "log-sum" measure of the signals, as given in (8) (for sEMG data) and (9) (for ACM/ANG data):

$$\begin{aligned} x_k &= \log \left(\sum_{m=1}^{2^{L/5}} |R(m)| \right), \text{ where } R = AAAAD_5(k=1), \\ R &= DDAAA_5(k=2) \end{aligned} \quad (8)$$

$$\begin{aligned} x_k &= \log \left(\sum_{m=1}^{2^{L/3}} |R(m)| \right), \text{ where } R = DDA_3(k=1), \\ R &= ADD_3(k=2) \end{aligned} \quad (9)$$

where L is the number of samples in the signal $u(l)$ and $R(m)$ is the reconstructed signal for the given sub-band. As earlier explained, the logarithm is applied to ensure that smaller differences between feature vectors from different classes are

enhanced and the influence by possible outliers is assumed to be reduced.

The feature vector, \mathbf{x} , is then collected from the vectors \mathbf{a} , \mathbf{b} and \mathbf{c} , with two "log-sum" measures for each data window for all channels in the three modalities:

$$\begin{aligned} \mathbf{a} &= [x_{1,ACM_1}, x_{2,ACM_1}, x_{1,ACM_2}, \dots, x_{1,ACM_{2B}}, x_{2,ACM_{2B}}] \\ \mathbf{b} &= [x_{1,ANG_1}, x_{2,ANG_1}, x_{1,ANG_2}, \dots, x_{1,ANG_{2B}}, x_{2,ANG_{2B}}] \\ \mathbf{c} &= [x_{1,EMG_1}, x_{2,EMG_1}, x_{1,EMG_2}, \dots, x_{1,EMG_{14}}, x_{2,EMG_{14}}] \\ \mathbf{x}_n &= [\mathbf{a}_n, \mathbf{b}_n, \mathbf{c}_n]^T \end{aligned} \quad (10)$$

where ACM_1 means ACM channel 1 and so on and n is the time index as described above. As earlier noted the time index, n , is omitted in the previous equations for convenience.

4.6. Final feature vectors

All possible combinations (\mathbf{a} , \mathbf{b} , \mathbf{c} , \mathbf{a} and \mathbf{b} , \mathbf{a} and \mathbf{c} , \mathbf{b} and \mathbf{c} and \mathbf{a} , \mathbf{b} and \mathbf{c}) of the three modalities are sent through the classifier, to explore which combination would be better for an alarm system. Eqs. (7) and (10) represent the combination where all data are used. The entering of the feature vector into the classifier is shown as the final step in the classification procedure (see Fig. 5).

4.7. Classification

We decided to see the problem as a binary classification problem with the classes *Seizure* and *Normal* activity. One could also have chosen to classify the simulated seizures into different groups, but in this study we wanted to examine the possibility of making one classifier for all motor seizures. The class, *Seizure*, contains different kinds of simulated seizures with motor manifestations, whereas the class *Normal* activity contains anything but the simulated seizures. The amount of data in the two classes is very different, since we have more normal activity data than simulated seizure data, which makes the SVM algorithm attractive compared to, e.g. neural network classifiers [18]. When using the SVM one can also be sure to find a global and unique solution to the classification problem (quadratic problem), compared to neural network where there are multiple local minima and thereby multiple solutions [19]. This means that one can be sure that an optimal solution is obtained using SVM. A third reason to choose SVM is that it is less disposed to overfitting, since it chooses a specific hyperplane (with the largest margins) to separate the two classes [20].

The classification is the last part in the detection algorithm. Data are divided into two groups, *training* and *test*, see Fig. 9, where the classifier is trained on the data from the *training* group. The data from the *test* group can then be classified with

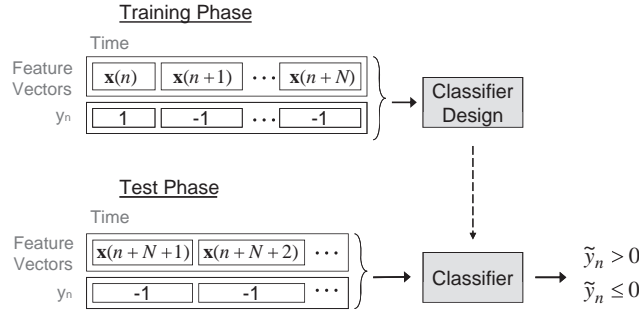


Fig. 9 – The classification part of the algorithm is split in two; the training and the testing phase. During the training phase the classifier is trained on feature vectors and their corresponding target (–1 (normal activity) or 1 (simulated seizure)). In the testing phase the “new” data is classified as simulated seizure or normal activity.

the classifier trained for the purpose. The classifier will return a positive or negative value for each test vector, dependent on whether it is classified as a simulated seizure or not.

The divisions of the data into these groups are made randomly, for both simulated seizure and normal activity data, ensuring close to equal amounts of each data type in each group. It is ensured that each simulated seizure type is represented in both phases (training and test).

For the training, data is labeled:

$$\{\mathbf{x}_n, y_n\}, \quad n = 1, \dots, k, \quad y_n \in \{-1, 1\}, \quad \mathbf{x}_n \in \mathbb{R}^d, \quad (11)$$

where k is the number of training examples, d is the dimension, \mathbf{x}_n is the feature vector (n is the time index) and y_n the matching target, indicating which of the classes the feature vectors belong to, -1 for normal activity and 1 for simulated seizure.

A two-class linearly separable data set (where $d > 2$) can be classified by a hyperplane described by:

$$f(\mathbf{x}_n) = \mathbf{w} \cdot \mathbf{x}_n + b = 0, \quad (12)$$

where \mathbf{w} is the normal to the hyperplane and b is a shifting constant.

The hyperplane is computed based on support vectors, which are the feature vectors placed closest to the hyperplane separating the two classes. These feature vectors from the two classes must satisfy:

$$y_n \cdot (\mathbf{w} \cdot \mathbf{x}_n + b) \geq 1 - \xi_n, \quad \text{where } \xi_n \geq 0 \forall n, \quad (13)$$

where ξ_n , a positive slack variable, is introduced to handle data, due to the fact that most classification problems are not completely separable. Data points assigned to the wrong side of the margin (defined by (13)) thereby have a penalty that increases with the distance to the margin.

To separate the two classes, the problem of finding the optimal parameters, \mathbf{w} and b , can be reduced to minimizing the performance function [13]:

$$\frac{1}{2} \|\mathbf{w}\|^2 + C \sum_{n=1}^l \xi_n \quad \text{subjected to } y_n \cdot (\mathbf{w} \cdot \mathbf{x}_n + b) \geq 1 - \xi_n, \quad (14)$$

where C is a factor which sets the trade-off between the size of the margin and the penalty of the slack variable, ξ_n [13]. From tests we found that the most optimal value of C for our algorithm is 0.8 , which is used for the results presented later in this paper.

For (14) to be minimized, each term should be minimized. Minimizing the first term means maximizing the margin between the support vectors of the two classes. The second term, which encompasses the slack variable, is minimized by keeping the distance from incorrectly classified feature vectors to the margin as small as possible. When a feature vector is correctly classified ξ_n is set to 0 , whereby the second term in (14) will be 0 . For a feature vector correctly classified, but placed on the wrong side of the margin, ξ_n is between 0 and 1 , whereas it is above 1 , if the feature vector is wrongly classified. In the two latter cases the margin is attempted placed as close to these incorrectly classified feature vectors as possible in order to minimize the second term in (14).

To solve (14) Lagrange multipliers are applied and we obtain [13]:

$$L(\mathbf{w}, b, \xi, \alpha, \mathbf{r}) = \frac{1}{2} (\mathbf{w} \cdot \mathbf{w}) + C \sum_{n=1}^l \xi_n - \sum_{n=1}^l \alpha_n [y_n (\mathbf{x}_n \cdot \mathbf{w}) + b - 1 + \xi_n] - \sum_{n=1}^l r_n \xi_n, \quad (15)$$

where $\alpha_n \geq 0$ and $r_n \geq 0$. Eq. (15) is then transformed from its primary form to the dual form by differentiating it with respect

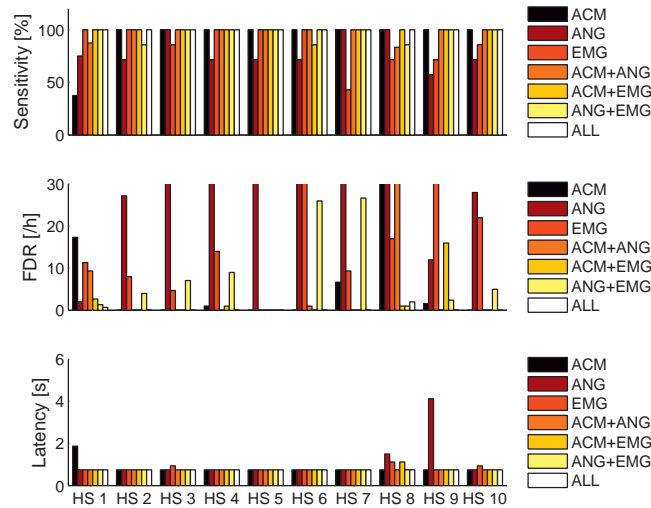


Fig. 10 – The results from the DWT feature extraction method. HS means healthy subject.

to \mathbf{w} , ξ_n and b and substitute the obtained relations into the primal form to obtain [13]:

$$L(\mathbf{w}, b, \xi, \alpha, \mathbf{r}) = \sum_{n=1}^l \alpha_n - \frac{1}{2} \sum_{n,j=1}^l y_n y_j \alpha_n \alpha_j \langle \mathbf{x}_n \cdot \mathbf{x}_j \rangle \quad (16)$$

The hyperplane which separates the two classes the best could then be found by maximizing (16) with respect to $\sum_{n=1}^l y_n \alpha_n = 0$, $C \geq \alpha_n \geq 0$, $n = 1, \dots, l$.

In (15) $\langle \mathbf{x}_n \cdot \mathbf{x}_j \rangle$ may also be written as $K(\mathbf{x}_n, \mathbf{x}_j)$, where K is a kernel. If the two classes are not linearly separable a non-linear kernel may be applied. A kernel is a function which transforms a signal from one space (input space) into another space of a higher dimension, called the feature space. Thereby a linear hyperplane, separating the two classes may be found in the new feature space. In our case, we have been able to separate the classes linearly, so a non-linear kernel has been considered unnecessary.

The steps explained above are all performed in Matlab by the SVM^{light} package from Joachims [21]. The package returns a classification-model based on the given training set, which can then be used to classify a test set.

4.8. Test methodology

To evaluate how well the detection algorithms function, certain measures may be calculated for each healthy subject. The test measures used in this article are:

- Sensitivity (SEN) is the fraction of seizures that are correctly classified.
- Latency (LAT) is the time from seizure start to the detection.
- False detection rate (FDR) is the number of falsely detected simulated seizure onsets per hour.

When the content of a window is classified as a simulated seizure an alarm will be generated. The latency is measured as the delay from simulated seizure start till the alarm is generated (first window with a positive outcast). This means that the shortest possible latency will correspond to the length of the window (0.75 s for the DWT method and 1 s for the WPT method, respectively). Only the first window, in a row of successive detections, will generate an alarm. This means that when successive *normal activity* windows are detected as a *simulated seizure* only the first one will generate a false alarm, and thereby it will only count for one FP.

The FDR is a better measure than the often used specificity, when evaluating results on seizure/simulated seizure detection. To obtain valuable results for FDR the measurements should contain several hours for testing. For practical reasons we only measured for 1.5–3 h for the healthy subjects, which may influence our results.

5. Results

The results vary depending on the feature extraction method. The results for the DWT method are shown in Fig. 10, whereas the results for the WPT method are shown in Fig. 11. To compare the results of the different combinations of modalities, the median and 95% confidence level of all results (both methods) are given in Table 2.

5.1. DWT method

The DWT method (Fig. 10) shows an almost perfect result, when combining all modalities, while the detection is less accurate when only one modality is used. For the first healthy subject (HS) the worst result is seen, when only the ACM data is included, whereas the worst result for healthy subject 2, 4,

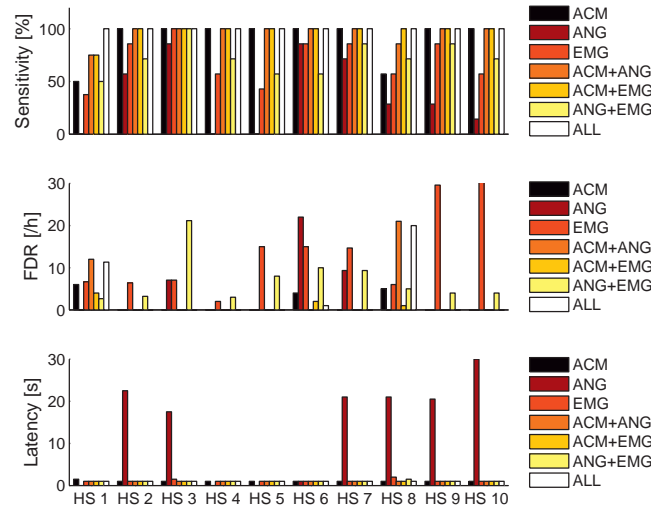


Fig. 11 – The results from the WPT feature extraction method. HS means healthy subject.

5, 6, 9 and 10 are seen when only the ANG data is used. For the last three healthy subjects (3, 7 and 8) the worst result is achieved when only the sEMG data is used. The latencies are short for all tests; the longest latency is seen for the ninth healthy subject, where only the ANG data is used. The FDR shows that for several tests the number of false detections per hour is truly high. For 7 of the 10 healthy subjects the highest FDR is observed when only the ANG data is used for the remaining three it is when only sEMG or ACM is used. When all modalities are used, the FDR is though equal to 0 for 8 of the 10 healthy subjects, the last two (HS 1 and 8) have an FDR of 0.67 and 1.7, respectively. In Table the results are presented to easy compare the different combinations of modalities. This shows that the ANG modality alone performs the worst and that clearly a combination of all modalities performs the best.

6 the results are the worst when the ANG data is combined with the sEMG data. For all healthy subjects the best results are obtained, when all modalities are combined. The latency is seen to be short for all tests except for healthy subject 2, 3, 7, 8, 9 and 10, when only the ANG data is used. The FDR is as low as 0 for about half of the tests, for a few it is as high as 30, and for the rest the FDR is around 10. When all modalities are used for eight of the 10 healthy subjects it succeeded in keeping an FDR of 0, but for the remaining two (HS 1 and 8) the FDR is 11 and 18, respectively. Looking into Table 2 it is seen that the ANG modality alone performs the worst with a too low sensitivity and much too high median latency. A combination of all modalities is shown to provide the best results.

5.2. WPT method

For all healthy subjects except for healthy subject 6, the accuracy is the lowest when only the ANG data is used, and for some the sensitivity is as low as 0%. For the healthy subject

5.3. Comparison

The results for the healthy subjects on multi-modal data (sEMG, ACM and ANG) clearly show that the algorithm performs better when all three modalities are used (see Table 2). This is independent on whether the DWT or the WPT feature extraction method is applied. From Table 2 it is clearly seen

Table 2 – Median values (and in parentheses the 95 confidence level). SEN: sensitivity; FDR: false detection rate; LAT: latency.

	Discrete wavelet transform			Wavelet packet transform		
	SEN [%]	FDR	LAT [s]	SEN [%]	FDR	LAT [s]
ACC	100 (52–100)	0.5 (0–70)	0.75 (0.75–1.6)	100 (52–100)	0 (0–5.8)	1 (1–1.4)
ANG	71 (60–100)	49 (4.3–77)	0.75 (0.75–3.5)	29 (0–86)	0 (0–19)	19 (1–28)
sEMG	93 (49–100)	13 (1.1–50)	0.75 (0.75–1.1)	71 (39–97)	11 (2.9–33)	1 (1–1.9)
ACC, ANG	100 (82–100)	0 (0–38)	0.75 (0.75–0.75)	100 (77–100)	0 (0–19)	1 (1–1)
ACC, sEMG	100 (89–100)	0 (0–13)	0.75 (0.75–1.0)	100 (81–100)	0 (0–3.5)	1 (1–1)
ANG, sEMG	100 (86–100)	4.5 (0.2–27)	0.75 (0.75–0.75)	71 (52–97)	4.5 (2.7–19)	1 (1–1.4)
All	100 (100–100)	0 (0–1.7)	0.75 (0.75–0.75)	100 (100–100)	0 (0–18)	1 (1–1)

Please cite this article in press as: I. Conradsen, et al., Automatic multi-modal intelligent seizure acquisition (MISA) system for detection of motor seizures from electromyographic data and motion data, Comput. Methods Programs Biomed. (2011), doi:10.1016/j.cmpb.2011.06.005

that, when all modalities are used the two methods provide similar results, with the only exceptions of the latency, where the lower bound is dependent on the window length, and the FDR which has a wider 95% confidence range for the WPT method. This difference is caused by two healthy subjects (1 and 8) who are seen to have much larger FDR in Fig. 11, than in Fig. 10, when all modalities are used. Besides from using all modalities it is difficult to say which method provides the best result. It depends on the individual subject and whether the sensitivity or the FDR is the most important. The DWT gives the highest sensitivity for all, whereas the WPT provides a lower FDR.

6. Discussion

The best results, for distinguishing between simulated seizures and normal activities based on the two wavelet methods, are clearly obtained when all three modalities are included. However, if the number of modalities or sensors/electrodes could be reduced, without worsening the results too much, it would be preferable considering the usability for the patients.

The ANG modality alone is not useful, but the best results are obtained when it is combined with the ACM and the sEMG modalities. For both methods it would though be the ANG modality that would be eliminated, if one wanted to base a system on only two modalities, since the combination of ACM and sEMG, show the next best result for both methods.

Based on the results it seems evident to combine all three modalities, but it does not allow us to determine which wavelet method is the best. Beside the different approaches, DWT and WPT, it should also be noted that the two are based on different frequencies, so this might as well influence the results. When we examined which frequency bands gave the largest differences between simulated seizures and normal activities, it resulted in different bands for the two methods. Based on that examination we ended up investigating different frequencies for the two methods. We expect that future tests on patient data will reveal which wavelet method is preferable for a final detection system. Also, as mentioned earlier, we chose to look at the classification problem as binary, but when real seizures are collected it might improve the results further if the seizures are split up in different groups, dependent on the type. Furthermore we will focus on using more patient-friendly measuring equipment, suitable for long term monitoring.

The prime limitation in getting the adequate patient data was the way the motion sensors were attached to the patient. They were placed in pockets of a specially designed suit. Wearing this suit did not constitute a problem for the well functioning patients. However, these patients rarely have generalized tonic-clonic seizures. The patients who frequently have this seizure type are typically mentally retarded, and they could not tolerate the suit.

The aim of our study was to determine whether an algorithm for seizure detection based on multimodal data can be developed and further which combination of the modalities that would perform the best. As our results on healthy subjects who could tolerate the suit are encouraging for using a

combination of all three modalities, it is worthwhile to focus on further development of a sensor setup, which could be tolerated by the patients. Fewer and smaller sEMG electrodes and/or motion sensors, attached to the patient, with wireless communication could solve this problem. To make such a change it would be helpful to investigate which places on the body that are more suited to wear these sensors and with how few sensors and/or electrodes is it possible to achieve an acceptable result.

7. Conclusion

The automatic MISA system implemented offers a new approach for use of movement data with feature extraction from discrete wavelet components or wavelet packet components combined with an advanced classifier, to detect epileptic seizures. Based on the present studies both feature extraction methods provided equally promising results, and for both the best result was obtained for all healthy subjects, when combining all modalities. Future studies are needed to reveal which feature extraction method is the best choice for patient data.

Our data show the superiority of the multi-modal approach as compared to a uni-modal approach, especially compared to the ANG modality alone. At the moment, the device is a prototype for research use only. We have experienced that some patients feel uncomfortable wearing the suit containing the sensors. The superiority of the multi-modal results encourage us to develop a more patient-friendly multi-modal equipment containing the sensors, suitable for long term monitoring of the patients with epilepsy. It is convenient to base this new equipment on knowledge of which sensor/electrode placements alone or combined can provide acceptable results, with the presented algorithm. The next step is therefore to test the algorithm on a feature vector containing fewer sensor/electrode places. It is furthermore important to research on improving the biomedical signal processing for either a patient specific or a patient generic system using our multi-modal seizure onset detection approach.

Conflict of interest statement

The authors declare that they do not have any conflict of interests.

Acknowledgements

We would like to thank the staff at the EMU at the Danish Epilepsy Centre and at the EMU at Rigshospitalet Copenhagen University Hospital for their great co-operation and assistance.

This work has received financial support from the Peter & Jytte Wolf Foundation for Epilepsy, the Danish Epilepsy Centre, the Danish Agency of Science Technology and Innovation, and the Technical University of Denmark. Aside from co-author P. Wolf, who is a board member of the Peter & Jytte Wolf Foundation for Epilepsy, the sponsors for this study had no other

involvement, than the sponsorship. The financial support is greatly appreciated.

REFERENCES

- [1] L. Nashef, P. Ryvlin, Sudden unexpected death in epilepsy (SUDEP): update and reflections, *Neurologic Clinics* 27 (4) (2009) 1063–1074.
- [2] J.R. Hughes, A review of sudden unexpected death in epilepsy: prediction of patients at risk, *Epilepsy and Behavior* 14 (2) (2009) 280–287.
- [3] K.M. Kelly, D.S. Shiau, R.T. Kern, J.H. Chien, M.C.K. Yang, K.A. Yandora, J.P. Valeriano, J.J. Halford, J.C. Sackellares, Assessment of a scalp EEG-based automated seizure detection system, *Clinical Neurophysiology* 121 (11) (2010) 1832–1843.
- [4] A. Schad, K. Schindler, B. Schelter, T. Maiwald, A. Brandt, J. Timmer, A. Schulze-Bonhage, Application of a multivariate seizure detection and prediction method to non-invasive and intracranial long-term EEG recordings, *Clinical Neurophysiology* 119 (1) (2008) 197–211.
- [5] A.M. Chan, F.T. Sun, E.H. Boto, B.M. Wingeier, Automated seizure onset detection for accurate onset time determination in intracranial EEG, *Clinical Neurophysiology* 119 (12) (2008) 2687–2696.
- [6] Z. Li, A.M. da Silva, J.P.S. Cunha, Movement quantification in epileptic seizures: a new approach to video-EEG analysis, *IEEE Transactions on Biomedical Engineering* 49 (6) (2002) 565–573.
- [7] T.M.E. Nijssen, J.B.A.M. Arends, P.A.M. Griep, P.J.M. Cluitmans, The potential value of three-dimensional accelerometry for detection of motor seizures in severe epilepsy, *Epilepsy and Behavior* 7 (1) (2005) 74–84.
- [8] G. Becq, S. Bonnet, L. Minotti, M. Antonakios, R. Guillemaud, P. Kahane, Collection and exploratory analysis of attitude sensor data in an epilepsy monitoring unit, in: 29th Annual International Conference of the IEEE Engineering in Medicine and Biology Society, 2007, pp. 2775–2778.
- [9] K. Cuppens, L. Lagae, B. Ceulemans, S. Van Huffel, B. Vanrumste, Detection of nocturnal frontal lobe seizures in pediatric patients by means of accelerometers: a first study, in: 31st Annual International Conference of the IEEE Engineering in Medicine and Biology Society, 2009, pp. 6608–6611.
- [10] I. Conradsen, S. Beniczki, P. Wolf, D. Terney, T. Sams, H.B.D. Sorensen, Multi-modal intelligent seizure acquisition (MISA) system—a new approach towards seizure detection based on full body motion measures, in: 31st Annual International Conference of the IEEE Engineering in Medicine and Biology Society, 2009, pp. 2591–2595.
- [11] T.M.E. Nijssen, P.J.M. Cluitmans, P.A.M. Griep, R.M. Aarts, Short time Fourier and wavelet transform for accelerometric detection of myoclonic seizures, in: Engineering in Medicine and Biology Society, EMBS Benelux Symposium, 2006, pp. 155–158.
- [12] I. Conradsen, S. Beniczki, P. Wolf, J. Henriksen, T. Sams, H.B.D. Sorensen, Seizure onset detection based on a uni- or multi-modal seizure acquisition (UISA/MISA) system, in: 32nd Annual International Conference of the IEEE Engineering in Medicine and Biology Society, 2010, pp. 3269–3272.
- [13] N. Cristianini, J. Shawe-Taylor, An Introduction to Support Vector Machines: And Other Kernel-Based Learning Methods, 1st ed., Cambridge University Press, 2000.
- [14] Xsens, P.O. Box 559, 7500 An Enschede, The Netherlands, <http://www.xsens.com>.
- [15] M.F. McKinney, J. Breebaart, Features for audio and music classification, *Proceedings of the ISMIR* (2003) 151–158.
- [16] S.G. Mallat, A theory for multiresolution signal decomposition: the wavelet representation, *IEEE Transactions on Pattern Analysis and Machine Intelligence* 11 (7) (1989) 674–693.
- [17] A. Subasi, EEG signal classification using wavelet feature extraction and a mixture of expert model, *Expert Systems with Applications* 32 (2007) 1084–1093.
- [18] C.Y. Yang, S. Yang Jr., J.J. Wang, Margin calibration in SVM class-imbalanced learning, *Neurocomputing* 73 (1–3) (2009) 397–411.
- [19] C.J.C. Burges, A tutorial on support vector machines for pattern recognition, *Data Mining and Knowledge Discovery* 2 (2) (1998) 121–167.
- [20] C. Cortes, V. Vapnik, Support-vector networks, *Machine Learning* 20 (3) (1995) 273–297.
- [21] T. Joachims, Learning to classify text using support vector machines: methods, theory, and algorithms, *Computational Linguistics* 29 (4) (2002) 656–664.

PAPER IV

TITLE Patterns of muscle activation during generalized tonic and tonic–clonic epileptic seizures

AUTHORS Isa Conradsen, Peter Wolf, Thomas Sams, Helge B.D. Sorensen, and Sándor Beniczky

JOURNAL Epilepsia

PUBLICATION HISTORY Submission date: 13-04-2011, Acceptance date: 24-08-2011

FULL-LENGTH ORIGINAL RESEARCH

Patterns of muscle activation during generalized tonic and tonic–clonic epileptic seizures

*†Isa Conradsen, *Peter Wolf, †Thomas Sams, †Helge B. D. Sorensen, and *‡Sándor Beniczky

*Danish Epilepsy Centre, Department of Neurophysiology, Dianalund, Denmark; †Department of Electrical Engineering, Technical University of Denmark, Lyngby, Denmark; and ‡Aarhus University Hospital, Department of Clinical Neurophysiology, Århus C, Denmark

SUMMARY

Purpose: Tonic seizures and the tonic phase of tonic–clonic epileptic seizures are defined as “sustained tonic” muscle contraction lasting a few seconds to minutes. Visual inspection of the surface electromyogram (EMG) during seizures contributed considerably to a better understanding and accurate diagnosis of several seizure types. However, quantitative analysis of the surface EMG during the epileptic seizures has received surprisingly little attention until now. The aim of our study was to elucidate the pathomechanism of the tonic muscle activation during epileptic seizures.

Methods: Surface EMG was recorded from the deltoid muscles, on both sides, during 63 seizures from 20 patients with epilepsy (10 with generalized tonic and 10 with tonic–clonic seizures). Twenty age- and gender-matched normal controls simulated 100 generalized tonic seizures. To characterize the signal properties we calculated the root mean square (RMS) of the amplitudes, the median frequency (MF), and the coherence. Based on the spectrograms of both epileptic and simulated seizures, we chose to determine the relative

spectral power (RP) in the higher (100–500 Hz) frequency domain.

Key Findings: During the tonic seizures there was a significant shift toward higher frequencies, expressed by an increase in the MF and the RP (100–500 Hz). The amplitude characteristic of the signal (RMS) was significantly higher during the tonic phase of the tonic–clonic seizures as compared to the simulated ones, whereas the RMS of the tonic seizures was significantly lower than the simulated ones. The EMG–EMG coherence was significantly higher during the epileptic seizures (both types) as compared to the simulated ones.

Significance: Our results indicate that the mechanism of muscle activation during epileptic seizures is different from the physiologic one. Furthermore the sustained muscle activation during the tonic phase of tonic–clonic seizures is different from that during tonic seizures: The tonic phase of tonic–clonic seizures is characterized by increased amplitude of the signal, whereas tonic seizures are produced by a significant increase in the frequency of the signal.

KEY WORDS: EMG, Epilepsy, Signal analysis, Tonic–clonic seizures, Tonic seizures.

Tonic muscle contraction constitutes the characteristic semiologic feature of several epileptic seizures. Tonic seizures are defined as sustained increase in muscle contraction lasting from seconds to minutes (Gastaut et al., 1963), whereas tonic–clonic seizures are defined as a sequence consisting of a tonic followed by a clonic phase (Commission on Classification and terminology of the ILAE, 1981). Clinically, it is not always easy to distinguish between pure tonic and tonic–clonic seizures. Is a tonic seizure a fragment of a tonic–clonic seizure or fundamentally different? It is still unclear whether these seizure types share a final com-

mon pathway of motor unit (MU) activation, leading to the characteristic, sustained tonic muscle activation, and it has not been elucidated whether the tonic muscle activation during the seizures is different from the physiologic one. The electroencephalography (EEG) during these seizure types is usually obscured by artifacts.

Visual inspection of surface electromyography (EMG) signals from polygraphic recordings contributed to identifying the pathomechanisms of several seizure-types: myoclonic (including negative myoclonus), atonic, myoclonic–atonic, epileptic spasms, and startle-induced reflex seizures (Mothersill et al., 2000). Recording surface EMG signals during seizures proved to provide valuable diagnostic information in the clinical practice: Tassinari et al., (2010) encouraged the use of off-line analysis of digital polygraphic recordings of epileptic seizures. Digital recording systems allow measuring precisely the time between the

Accepted August 24, 2011; Early View publication October 5, 2011.
Address correspondence to Isa Conradsen, Oerstedts Plads Bygn. 349, 2800 Kgs. Lyngby, Denmark. E-mail: isaconradsen@gmail.com

Wiley Periodicals, Inc.
© 2011 International League Against Epilepsy

EEG and EMG signals, as well as the precise duration of the muscle activity (Rubboli & Tassinari, 2006; Tassinari & Rubboli, 2008).

Although quantitative analysis of EMG signals was investigated extensively in several types of movement disorders (Grosse & Brown, 2005), to the best of our knowledge myoclonus is the only seizure type in which this feature was addressed (Grosse et al., 2003; Panzica et al., 2003; Shibasaki et al., 1978).

The properties of the surface EMG signals can be described by characteristics in the time domain (variation in time of the amplitude) and in the frequency domain. The amplitude characteristics of the signal are reflected by the root mean square (RMS). The frequency domain characteristics can be visualized using spectrograms and they can be expressed by the median frequency (MF) and the relative power of the signal in the different frequency bands. The correlation between the muscle activation on the two sides can be reflected by the EMG–EMG coherence.

These quantitative parameters reflect different features of the MU activation and recruitment. To elucidate the pathomechanism of tonic muscle activation during seizures, we recorded surface EMG during tonic and tonic–clonic epileptic seizures, as well as seizures simulated by healthy volunteers. We calculated the RMS, MF, and coherence between the muscles on the left and right sides. Based on the changes observed in the spectrogram, we calculated the relative power of the signal in the frequency domain 100–500 Hz.

Epileptic seizures occur due to abnormal excessive or synchronous neuronal activity in the brain. We hypothesized that this will be reflected in the pathomechanism of the epileptic tonic muscle activation by a shift toward higher frequency domains, increase in coherence, and/or increase in the amplitude feature.

METHODS

Subjects

Fifty-seven consecutive patients admitted to our Epilepsy Monitoring Unit for diagnostic reasons and who had a history of tonic or tonic–clonic seizures in the referral were included. Twenty-three patients did not have seizures during the monitoring, 20 patients had seizures with tonic muscle activation (10 patients had tonic, and 10 patients had tonic–clonic seizures), and 14 patients had epileptic seizures other than tonic and tonic–clonic. In addition, 20 healthy controls who simulated epileptic seizures had been recruited. The project had been approved by the local ethics committee and all subjects received information on the project and gave their written consent.

In the group of the patients with epilepsy (7 female, 13 male) the mean age was 24.8 years (range 6–58). The group of healthy controls was age and gender matched: mean age 25.4 years (range 6–54), eight were female and

12 male (for the age: $p = 0.64$; for the gender: $p = 1$). The subgroup of patients with tonic seizures (four female, six male) had a mean age of 20.4 years (range 6–58), whereas in the subgroup with tonic–clonic seizures (three female, seven male) the mean age was 29.2 years (range 11–55). There was no significant difference among the two patient subgroups and the group of healthy controls concerning the age ($p > 0.1$) or concerning the gender ($p > 0.7$).

One patient with tonic–clonic seizures had idiopathic generalized epilepsy (juvenile myoclonic epilepsy); the other nine patients in this group had symptomatic focal epilepsy, with secondarily generalized seizures. In the group with generalized tonic seizures, one patient had cryptogenic epilepsy; all others had symptomatic focal or multifocal epilepsy. Seven patients in this group had symptomatic Lennox-Gastaut syndrome (Data S1).

Recordings

In addition to the standard EEG electrodes, surface EMG electrodes (silver/silver chloride 9-mm surface electrodes) were placed on the deltoid muscles on both sides in a monopolar setting (the active electrode was placed on the midpoint of the muscle belly, whereas the reference electrode was placed on the acromioclavicular joint, just proximal to the insertion of the muscle). We opted for this setting to circumvent the effects of phase-cancellation that occur in the bipolar setting, when both electrodes are placed on the muscle (Bischoff et al., 1999; McAuley et al., 2000; Staudenmann et al., 2010).

The surface EMG signals were sampled with a frequency of 1,024 Hz, and an anti-aliasing filter of 512 Hz. All EMG signals were notch (49–51 Hz) filtered with an infinite impulse response filter to remove noise from the power line and furthermore high pass (10 Hz) filtered with a finite impulse response filter, as the signal beneath 10 Hz is obscured because of the movements of the electrodes against the skin (Merletti & Parker, 2004). For both filters, the group delay was assessed and found not to interfere with the investigated frequencies.

Seizures

The long-term video–electroencephalography (EEG) recordings were reviewed by a clinical neurophysiologist and an epileptologist, who marked the time epochs containing a tonic seizure or the tonic component of a tonic–clonic seizure, based on visual analysis. These epochs were marked only if they unequivocally corresponded to a seizure-period. In case of the secondarily generalized seizures, the start of the bilateral symmetric phase was marked as the onset.

We recorded 63 epileptic seizures with tonic muscle activation from the 20 patients (mean 3.2 seizures/patient; range 1–10). The patients with tonic seizures had more seizures (mean 4.5 seizures/patient; range 1–10) than the patients

with tonic-clonic seizures (mean 1.8 seizures/patient; range 1–4) ($p = 0.027$). To avoid an excessive influence on the group-data from the patients with more seizures, the mean of the seizures was calculated for each patient.

The healthy controls were trained to perform the sustained, maximal muscle contraction in all upper limb muscles in a position imitating the one during the epileptic seizures, as instructed and as shown on the video. The recording was done in the presence of two of the authors (including a physician with experience in evaluating long-term video-EEG recordings), and the healthy controls were asked to correct the way they activated the muscles if that was necessary. Each healthy control subject simulated five seizures, which gives in total 100 simulated seizures.

Data analysis

To characterize the surface EMG signals during the epileptic and the simulated seizures, several quantitative parameters were calculated. All data analysis was done using MATLAB 7.6 software (Mathworks, Natick, MA, U.S.A.).

Time domain

The amplitude is fluctuating within broad ranges, and outliers have huge influence. To avoid this, instead of the raw amplitude, an expression of the mean value of a short time window is used to characterize the amplitude (Arabdzhiiev et al., 2010). An arithmetic mean of the raw signal would provide a value close to zero; therefore, the signal is squared before calculation of the mean and then to even out the square effect, the root is applied. This is called the root mean square (RMS) and is characterized using the RMS value:

$$\text{RMS}(x) = \sqrt{\frac{1}{N} \sum_{n=0}^{N-1} x(n)^2},$$

where $x(n)$ is the EMG signal and N is the window length. The RMS value was calculated for a window of a length of 3 s and each window overlapped the previous and the next one with 2 s. As there seems to exist no established definition for the minimum duration of a tonic contraction to qualify as a tonic seizure, we used for the successive time windows a duration of 3 s as proposed by Lüders et al., (1998).

Frequency domain

The frequency features were visualized using plots of the magnitude of the fast Fourier transform (FFT) and spectrograms, and they were quantified by the MF and the relative power (100–500 Hz).

MF is defined as the frequency that divides the magnitude spectrum in two parts of equal sizes (the area under the curve for the frequencies lower than MF equals the area under the curve for the frequencies higher than MF) (Gelli

et al., 2007; Wakeling, 2009), and it is expressed according to the formula:

$$\sum_{f=0}^{f_{\text{MF}}} |\text{FFT}_m(f)| = 0.5 \sum_{f=0}^{f_s/2} |\text{FFT}_m(f)|, m = 1, 2, 3, \dots,$$

where m is the window number, f_s is the sampling frequency, f_{MF} is the MF, and the FFT_m is the discrete frequency spectrum of the window m . $|\cdot|$ computed the absolute values of the discrete frequency spectrum. The MF values were calculated from time windows of 3 s duration, overlapping by 2 s.

Spectrograms (diagrams visualizing the power of the signal in the different frequency components across the time) were calculated for each seizure. The power was calculated for a small window of 125 samples, and each window was overlapping the previous and the next by 50%. This offered a frequency and time resolution of 7.5 Hz and 0.125 s, respectively. The frequency was represented on the y-axis, and the successive time windows on the x-axis. For each time window the power was visualized for all frequencies in a color-code (the size of the logarithm of the relative power for the particular time window and frequency band).

In addition, we determined the relative power (RP) in the higher frequency domain. Based on the visual inspection of the spectrograms we chose the frequency range 100–500 Hz. The RP was calculated by dividing the power in the 100–500 Hz frequency range by the total power of the signal in the whole frequency domain, in each time-window, of 3 s overlapping as for the other features by 2 s:

$$\text{relP}(m) = \frac{\sum_{f=100}^{500} |X_m(f)|^2}{\sum_{f=0}^{f_s/2} |X_m(f)|^2}, m = 1, 2, 3, \dots,$$

where $X_m(f)$ is the N -point discrete frequency spectrum ($N = 4,096$) of the m 'th window.

Coherence

Coherence is the correlation in the frequency domain between two oscillatory activities in spatially distinct systems (Mima & Hallett, 1999). This normalized measure of correlation has values between 0 and 1. A coherence value of 1 indicates a perfectly linear relationship, whereas 0 is when the two signals are completely independent.

We calculated EMG–EMG coherence between the right and left sides, using the standard methods in this field (Brown et al., 1999; Farmer et al., 1993b; Halliday et al., 1995; Kilner et al., 1999). We opted for including in this article results from the analysis of the unrectified EMG signals because previous studies have suggested that rectification might impair the oscillatory input between two EMG signals (Neto & Christou, 2010). Furthermore, one of the previous studies showed that this analysis method is reliable

also for unrectified data (Brown et al., 1999). However, we also analyzed the rectified data, and the results were similar (Data S2). We plotted the coherence spectra for each subject and furthermore calculated the coherence in the whole frequency band (10–512 Hz) as the mean of the coherence values in this domain.

For each subject we calculated the mean of the RMS, MF, RP, and coherence values of all time windows, during all seizures, and the mean of the values from the left and right deltoid muscles were entered into the statistical analysis. Therefore, for each patient only one (mean) value was entered into the statistical analysis, regardless of the number of seizures the patient had. We did this to avoid the bias toward the data from patients with more seizures.

Because the surface EMG parameters (calculated from the time windows of 3 s) were not constant within the seizures, besides determining the mean value of the different parameters for the whole seizure period (as described above), we also calculated the 95th percentile (peak) values, for each patient and for each quantitative EMG parameter. This way we can express the highest level of activation for a certain parameter, for each patient, without being biased by the outlier values (upper 5th percentile).

Statistics

The normality of the data distribution was assessed using Kolmogorov-Smirnov test. Because the data were not normally distributed we compared the quantitative EMG parameters among the subject groups using Wilcoxon test. To assess the matching of the gender between the two groups and further between the subgroups, Fisher's exact test was used.

RESULTS

Examples of the EMG signals from the different groups are shown in Fig. 1. The quantitative EMG parameters are presented in Table 1.

Median frequency

The magnitude spectrum visualizes the distribution of the signal at the different frequency components (Fig. 2). During the epileptic seizures (especially the tonic ones) we observed a shift to the right (toward the higher frequencies). The FFT of the simulated seizures (Fig. 2C) are mostly below 100 Hz.

The MF (Table 1) was significantly higher during the epileptic seizures as compared with the simulated ones ($p = 0.005$).

The subgroup analysis showed that MF was significantly higher during the tonic seizures than during the simulated seizures ($p = 0.001$), and furthermore significantly higher than during the tonic phase of the tonic-clonic seizures ($p = 0.03$). There was no significant difference between the

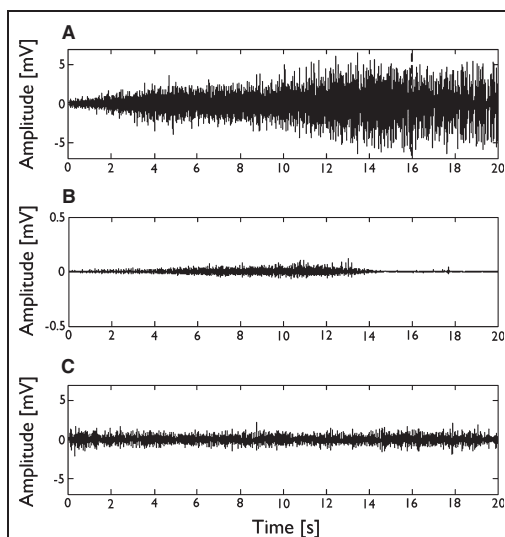


Figure 1. EMG signals of representative seizures: (A) the tonic phase of a tonic-clonic seizure; (B) tonic seizure; (C) simulated seizure. The vertical, dotted line in figure A marks the end of the tonic phase/beginning of the clonic phase, as seen on the video-EEG recordings. The scale of the y-axis is different for the three seizures. *Epilepsia* © ILAE

MF during the tonic phase of the tonic-clonic seizures and the simulated ones ($p = 0.18$).

Relative power

Figure 3 shows spectrograms of the RP for the different frequencies. Inspection of the spectrograms suggested higher power for the frequency domains above 100 Hz during the epileptic seizures as compared with the simulated ones. To express this quantitatively we calculated the RP for the frequency range of 100–500 Hz.

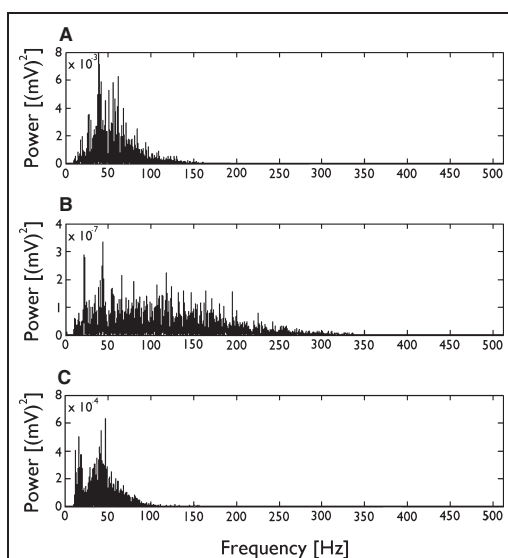
The RP (100–500 Hz) was significantly larger during the epileptic seizures as compared with the simulated ones ($p = 0.006$). RP (100–500 Hz) was higher during the tonic seizures than during the tonic phase of the tonic-clonic seizures ($p = 0.009$) and higher than during the simulated seizures ($p = 0.0004$). There was no significant difference between the RP (100–500 Hz) during the tonic phase of the tonic-clonic seizures and the simulated ones ($p = 0.37$).

Amplitude characteristics

The visual inspection of the EMG signals suggested that amplitudes were higher during the tonic phase of the tonic-clonic seizures as compared to the seizures from the other subjects (Fig. 1).

Table 1. Median values of the whole seizure period for all patients (and in parentheses 95% confidence intervals) for the different surface EMG parameters

	Epileptic	Tonic	Tonic-clonic	Simulated
MF (Hz)	76.8 (59.0–112)	86.2 (63.3–113)	73.6 (59.0–80.8)	63.9 (56.9–83.9)
RP (100–500 Hz)	0.151 (0.047–0.395)	0.217 (0.114–0.401)	0.110 (0.041–0.176)	0.079 (0.039–0.207)
RMS (mV)	0.636 (0.055–2.20)	0.251 (0.053–0.784)	1.16 (0.356–2.46)	0.440 (0.170–1.10)
Coherence	0.120 (0.050–0.255)	0.117 (0.048–0.178)	0.120 (0.063–0.289)	0.071 (0.046–0.109)

**Figure 2.**

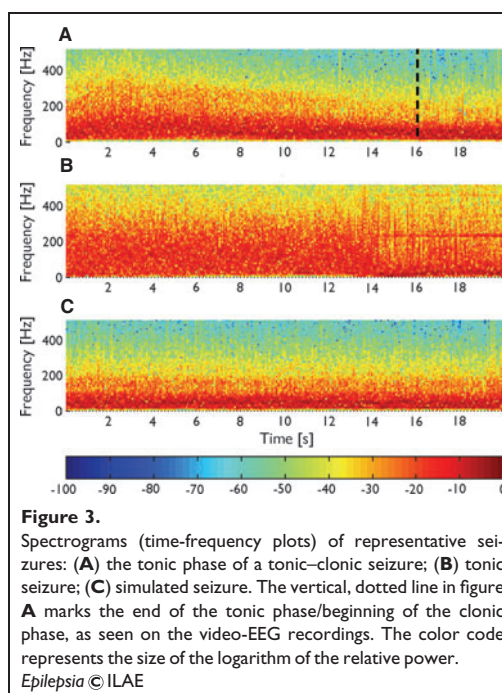
Power spectrums of representative seizures: (A) the tonic phase of a tonic-clonic seizure; (B) tonic seizure; (C) simulated seizure. The scale of the y-axis is different for the three seizures. For the simulated seizures most of the power is in the frequency band <100 Hz. During the epileptic seizures (especially the tonic seizure) one can observe a shift toward the higher frequencies.

Epilepsia © ILAE

The RMS (Table 1) for the group of epileptic seizures was not significantly different from that for the simulated seizures ($p = 0.47$). However the subgroup analysis showed that the RMS during the tonic phase of the tonic-clonic seizures was significantly higher than during the simulated seizures ($p = 0.001$), and furthermore significantly higher than during the tonic seizures ($p = 0.0008$). The RMS during the tonic seizures were significantly smaller than during the simulated seizures ($p = 0.045$).

Coherence

The visual inspection of the EMG signals showed bilateral-synchronous, sustained muscle activation during the analyzed seizure periods in all groups. The coherence

**Figure 3.**

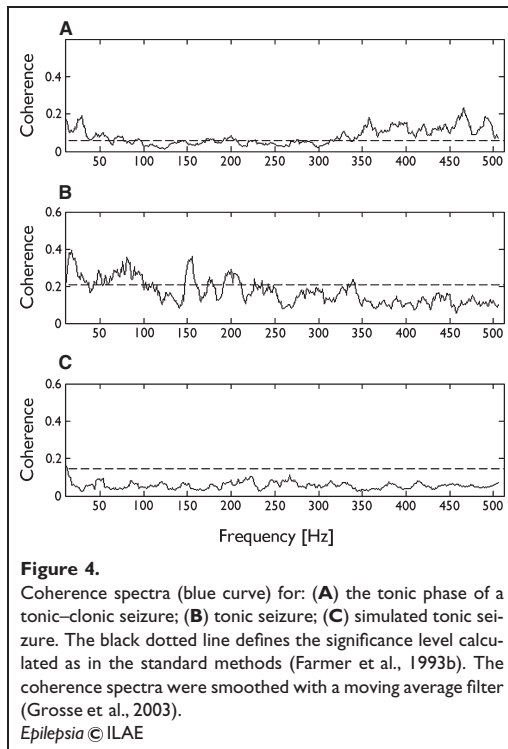
Spectrograms (time-frequency plots) of representative seizures: (A) the tonic phase of a tonic-clonic seizure; (B) tonic seizure; (C) simulated seizure. The vertical, dotted line in figure A marks the end of the tonic phase/beginning of the clonic phase, as seen on the video-EEG recordings. The color code represents the size of the logarithm of the relative power.

Epilepsia © ILAE

spectra demonstrated that there were several frequencies with significant coherence for each patient (Fig. 4), and that these frequencies varied from subject to subject. In the absence of certain, dominating frequencies for the significant level of coherence, we opted to calculate the coherence for the whole frequency band and to compare this among the groups. The coherence was significantly higher during the epileptic seizures than during the simulated ones ($p = 0.0005$). There was not any significant difference in coherence between the two subgroups of epileptic seizures ($p > 0.3$), but in both epilepsy subgroups the coherence was higher than in the group with simulated seizures ($p \leq 0.007$).

Peak values

To reflect the highest level of activation achieved by each patient/subject, in addition to mean values for the whole-seizure period (detailed above), we also calculated the 95th



percentile of the parameters (peak values). The shift toward the higher frequencies during the tonic seizures, the increase in the amplitude characteristic (RMS) during the tonic phase of the tonic-clonic seizures, and the increase in the coherence in the epileptic seizures (both types) were even more pronounced when analyzing the peak values (Data S3).

The effect of duration

There was no statistically significant difference between the duration of the tonic seizures and the duration of the tonic phase of the tonic-clonic seizures in our patients (median: 14.66 and 15.95 s, respectively; $p = 0.6$). There was no significant correlation between the duration and the quantitative EMG parameters that distinguished between the two seizure-types: RP 100–500 Hz, MF, RMS ($p > 0.12$). A multiple regression analysis for categorical (seizure-type: tonic vs. tonic-clonic) and continuous (duration) predictors showed that it was only the seizure type that predicted these quantitative EMG parameters.

DISCUSSION

We found a significant shift toward higher frequencies during tonic seizures. Patients with tonic-clonic seizures

had significantly increased amplitude characteristic (RMS), whereas patients with tonic seizures had significantly lower RMS than the simulated seizures. The EMG–EMG coherence was significantly higher during the epileptic seizures (in both subgroups).

The mechanism of muscle activation in the healthy volunteers simulating the seizures is obviously a physiologic one. Although, based on visual assessment, the posturing and muscle contractions appeared similar during the simulated and the epileptic seizures, the mechanisms of muscle activation were different.

As the surface, EMG parameters were not constant within the seizures; in addition to determining the mean value of the different parameters for the whole seizure period, we also calculated the 95th percentile (peak) values. Our results were even more pronounced when analyzing the peak values than when analyzing the mean values of the whole seizure periods.

Quantitative analysis of the surface EMG demonstrated significant differences between the two subgroups of epileptic seizures in which the qualitative (visual) assessment showed “sustained muscle activation”: tonic seizures are produced by a significant shift toward the higher frequency bands, whereas the tonic phase of the tonic-clonic seizures is produced by an increase in the amplitude characteristic. These differences between the tonic seizures and tonic phase of the tonic-clonic seizures are not merely a function of time, as there was no significant difference in duration between the two seizure types, and the quantitative EMG parameters that differentiated between them did not show a correlation with the duration of the tonic muscle activation.

Except for one patient with idiopathic generalized epilepsy (JME) all patients (in both epileptic subgroups) had symptomatic or unknown etiology. When excluding the JME patient from the tonic-clonic group we obtained similar results for all analyses. However, it is interesting to point out that the patient with JME was an outlier: The increase in the RMS and coherence was even more pronounced than in the other patients.

Although various quantitative surface EMG parameters have been used to infer details about the central nervous system (CNS) control mechanism of muscle activity, the technical limitations of the method should be emphasized, as the surface EMG reflects both peripheral and central properties of the neuromuscular system (Farina et al., 2004). However, the shift toward higher frequency domains during the muscle activation has been attributed to the recruitment of more motor neurons, including the ones with higher threshold (Wakeling, 2009; Riley et al., 2008). The increase in the amplitude characteristic (RMS) of the surface EMG signal can be caused by synchronization of the MU activity or by lengthening of the muscular action potential (Arabadzhev et al., 2010).

The shift toward higher frequencies during the tonic seizures can thus be explained by an increase in the

recruitment of more, high threshold motor neurons. Patients with Parkinson's disease have an altered pattern of MU recruitment: There is a preferential activation of the low-threshold MUs suggesting that the extrapyramidal system is involved in coordinating the recruitment of the high threshold MUs (Glendinning & Enoka, 1994). Based on this, we hypothesize that the observed shift toward the higher frequencies during tonic seizures is due to excessive activation of the extrapyramidal system. In the early electroclinical studies of the tonic seizures, Gastaut opined that these seizures result from an activation of the subcortical/extrapyramidal structures (Gastaut et al., 1963). This is consistent with our findings and the recently published ictal single photon emission computed tomography (SPECT) data showing hyperperfusion in the basal ganglia during focal tonic seizures (Wong et al., 2010).

The increase in the amplitude characteristics of the EMG signal during the tonic phase of the tonic-clonic seizures can be explained by an increased synchronization in the recruited motor neuron pool. Studies of patients with lesions of the corticospinal tract demonstrated the importance of these pathways in the presynaptic synchronization of the spinal motor neurons (Farmer et al., 1993a; Smith et al., 1999). This suggests that the increase in the amplitude during the tonic phase of the tonic-clonic seizure could be attributed to an excessive activation of the corticospinal pathways, as opposed to the possible extrapyramidal dominance during the tonic seizures.

As early as 1963, Gastaut, based on visual analysis of the surface EMG in polygraphic recordings described that the tonic phase of the tonic-clonic seizures was "more intense" than the contraction of tonic seizures (Gastaut et al., 1963). Our quantitative analysis demonstrating higher amplitude characteristic of the tonic phase of the tonic-clonic seizures are consistent with these early observations. Our findings further support that tonic seizures are not merely truncated manifestations or fragments of tonic-clonic seizures (i.e., minus the clonic phase), not even at the level of the final pathway (the MUs). We suggest that the "sustained tonic contraction" has to be defined differently for tonic and tonic-clonic seizures, emphasizing the increase in frequency in the case of the tonic seizures and the increase in amplitude for the tonic-clonic seizures. A different aspect that we did not include in our study is the transition in tonic-clonic seizures from the tonic to the clonic phase with its cycles of inhibition interrupted by reappearance of the tonic contraction, producing atonia alternating with violent flexor spasms (Zifkin & Dravet, 2008).

The healthy controls were trained to activate simultaneously and synchronously the muscles on the two sides. The visual analysis of the recordings showed that the "sustained" muscle activation during all analyzed seizures in all patients and subjects were bilateral, symmetrical, and synchronous. However, the coherence was significantly higher

during the epileptic seizures (in both subgroups for the whole seizure period) as compared with the simulated ones. This suggests that the neural networks on both sides are synchronously activated also in the efferent pathways. Grosse et al., (2003) found markedly increased EMG-EMG mean coherence between the muscle pairs on the two sides in nine patients with high frequency rhythmic myoclonus. Our findings in patients with generalized tonic and tonic-clonic seizures are consistent with this.

In conclusion we demonstrated distinct patterns of muscle activation during tonic seizures and the tonic phase of tonic-clonic seizures. Our results provide further insight into the pathomechanism of the muscle activation during epileptic seizures. In addition, our results have potential diagnostic significance. A combination of these parameters could provide supplementary information in selected, difficult cases where the differentiation between epileptic and nonepileptic seizures is difficult only based on video-EEG data. A combination of these distinct EMG features could also be used to design algorithms for automatic seizure detection based on surface EMG data.

To the best of our knowledge this is the first publication addressing the quantitative analysis of the surface EMG signals during tonic and tonic-clonic epileptic seizures.

ACKNOWLEDGMENTS

We wish to thank all sponsors for the PhD project of the author I. Conradsen. The supporters are the Danish Agency of Science Technology and Innovation, the Danish Epilepsy Centre, the Peter & Jytte Wolf Foundation for Epilepsy [grant PJWS 02-07 to I.C.], and the Technical University of Denmark. Two authors S.B. and H.B.D.S. contributed equally to the work done on this article.

DISCLOSURE

None of the authors has any conflict of interest to disclose. We confirm that we have read the Journal's position on issues involved in ethical publication and affirm that this report is consistent with those guidelines.

REFERENCES

- Arabadzhiev TI, Dimitrov VG, Dimitrova NA, Dimitrov GV. (2010) Influence of motor unit synchronization on amplitude characteristics of surface and intramuscularly recorded EMG signals. *Eur J Appl Physiol* 108:227-237.
- Bischoff C, Fuglsang-Frederiksen A, Vendelbo L, Sumner A (1999) Standards of instrumentation of EMG. In Deuschl G, Eisen A (Eds) *Recommendations for the practice of clinical neurophysiology: guidelines of the International Federation of Clinical Neurophysiology*. 2nd revised and enlarged ed. Elsevier, Amsterdam; *Electroencephalogr Clin Neurophysiol Suppl* 52:199-211.
- Brown P, Farmer SF, Halliday DM, Marsden J, Rosenberg JR. (1999) Coherent cortical and muscle discharge in cortical myoclonus. *Brain* 122:461-472.
- Commission on Classification and terminology of the ILAE. (1981) Proposal for revised clinical and electroencephalographic classification of epileptic seizures. *Epilepsia* 22:489-501.
- Farina D, Merletti R, Enoka RM. (2004) The extraction of neural strategies from the surface EMG. *J Appl Physiol* 96:1486-1495.

- Farmer SF, Swash M, Ingram DA, Stephens JA. (1993a) Changes in motor unit synchronization following central nervous lesions in man. *J Physiol* 463:83–105.
- Farmer SF, Bremner FD, Halliday DM, Rosenberg JR, Stephens JA. (1993b) The frequency content of common synaptic inputs to motoneurons studied during voluntary isometric contraction in man. *J Physiol* 470:127–155.
- Gastaut H, Roger J, Ouahchi S, Timsit M, Broughton R. (1963) An electroclinical study of generalized epileptic seizures of tonic expression. *Epilepsia* 4:15–44.
- Gelli F, Del Santo F, Popa T, Mazzocchio R, Rossi A. (2007) Factors influencing the relation between corticospinal output and muscle force during voluntary contractions. *Eur J Neurosci* 25:3469–3475.
- Glendinning DS, Enoka RM. (1994) Motor unit behavior in Parkinson's disease. *Phys Ther* 74:61–70.
- Grosse P, Brown P (2005) Corticomuscular and intermuscular frequency analysis: physiological principles and applications in disorders of the motor system. In Niedermeyer E, Lopes da Silva F (Eds) *Electroencephalography. Basic principles, clinical applications and related fields*. 5th ed. Lippincott, Williams and Wilkins, Philadelphia, pp. 881–889.
- Grosse P, Guerrini R, Parmeggiani L, Bonanni P, Pogossyan A, Brown P. (2003) Abnormal corticomuscular and intermuscular coupling in high-frequency rhythmic myoclonus. *Brain* 126:326–342.
- Halliday DM, Rosenberg JR, Amjad AM, Breeze P, Conway BA, Farmer SF. (1995) A framework for the analysis of mixed time series/point process data – theory and application to the study of physiological tremor, single motor unit discharges and electromyograms. *Prog Biophys Mol Biol* 64:237–278.
- Kilner JM, Baker SN, Salenius S, Jousmäki V, Hari R, Lemon RN. (1999) Task-dependent modulation of 15–30 Hz coherence between rectified EMGs from human hand and forearm muscles. *J Physiol* 516:559–570.
- Lüders H, Acharya J, Baumgartner C, Benbadis S, Bleasel A, Burgess R, Dinner DS, Ebner A, Foldvary N, Geller E, Hamer H, Holthausen H, Kotagal P, Morris H, Meencke HJ, Noachtar S, Rosenow F, Sakamoto A, Steinhoff BJ, Tuxhorn I, Wullie E. (1998) Semiological seizure classification. *Epilepsia* 39:1006–1013.
- McAuley JH, Britton TC, Rothwell JC, Findley LJ, Marsden CD. (2000) The timing of primary orthostatic tremor bursts has a task-specific plasticity. *Brain* 123:254–266.
- Merletti R, Parker PA (2004) *Electromyography (physiology, engineering and noninvasive applications)*. 1st ed. IEEE press series in Biomedical Engineering, John Wiley & Sons Inc., Hoboken, New Jersey, pp. 120–121.
- Mima T, Hallett M. (1999) Corticomuscular coherence: a review. *J Clin Neurophysiol* 16:501–511.
- Mothersill IW, Hilfiker P, Krämer G. (2000) Twenty years of ictal EEG-EMG. *Epilepsia* 41(Suppl. 3):19–23.
- Neto OP, Christou EA. (2010) Rectification of the EMG signal impairs the identification of oscillatory input to the muscle. *J Neurophysiol* 103:1093–1103.
- Panzica F, Canafoglia L, Franceschetti S, Binelli S, Ciano C, Visani E, Avanzini G. (2003) Movement-activated myoclonus in genetically defined progressive myoclonic epilepsies: EEG-EMG relationship estimated using autoregressive models. *Clin Neurophysiol* 114:1041–1052.
- Riley ZA, Terry ME, Mendez-Villanueva A, Litsey JC, Enoka RM. (2008) Motor unit recruitment and bursts of activity in the surface electromyogram during a sustained contraction. *Muscle Nerve* 37:745–753.
- Rubboli G, Tassinari CA. (2006) Negative myoclonus. An overview of its clinical features, pathophysiological mechanisms, and management. *Neurophysiol Clin* 36:337–343.
- Shibasaki H, Yamashita Y, Kuroiwa Y. (1978) Electroencephalographic studies myoclonus. *Brain* 101:447–460.
- Smith HC, Davey NJ, Savic G, Maskill DW, Ellaway PH, Frankel HL. (1999) Motor unit discharge characteristics during voluntary contraction in patients with incomplete spinal cord injury. *Exp Physiol* 84:1151–1160.
- Staudenmann D, Roelvelde K, Stegeman DF, van Dieën JH. (2010) Methodological aspects of SEMG recordings for force estimation – a tutorial and review. *J Electromyogr Kinesiol* 20:375–387.
- Tassinari CA, Rubboli G (2008) Polygraphic recordings. In Engel J Jr, Pedley TA (Eds) *Epilepsy. A comprehensive textbook*. 2nd ed. Lippincott Williams and Wilkins, Philadelphia, pp. 873–894.
- Tassinari CA, Cantalupo G, Rubboli G (2010) Polygraphic recording of epileptic seizures. In Panayiotopoulos CP, Benbadis SR, Beran RG (Eds) *Atlas of epilepsies*. Springer-Verlag, London, pp. 723–740.
- Wakeling JM. (2009) Patterns of motor recruitment can be determined using surface EMG. *J Electromyogr Kinesiol* 19:199–207.
- Wong CH, Mohamed A, Larcos G, McCreddie R, Somerville E, Bleasel A. (2010) Brain activation patterns of versive, hypermotor, and bilateral asymmetric tonic seizures. *Epilepsia* 51:2131–2139.
- Zifkin BG, Dravet C (2008) Generalized tonic-clonic seizures. In Engel J Jr, Pedley TA (Eds) *Epilepsy. A comprehensive textbook*. 2nd ed. Lippincott, Williams and Wilkins, Philadelphia, vol 1, pp. 553–562.

SUPPORTING INFORMATION

Additional Supporting Information may be found in the online version of this article:

Data S1. Clinical data of the 20 patients with epilepsy (T, tonic seizures; TC, tonic-clonic seizures).

Data S2. p-Values for the coherence of rectified and unrectified EMG data, respectively. Median values of the whole seizure period for all patients (and in parentheses 95% confidence intervals) for the coherence of the rectified and the unrectified surface EMG data.

Data S3. Median values of the peak values for all patients (and in parentheses 95% confidence intervals) for the different surface EMG parameters.

Please note: Wiley-Blackwell is not responsible for the content or functionality of any supporting information supplied by the authors. Any queries (other than missing material) should be directed to the corresponding author for the article.

PAPER V

TITLE Seizure Onset Detection based on one sEMG channel

AUTHORS Isa Conradsen, Sándor Beniczky, Karsten Hoppe, Peter Wolf, Thomas Sams, and Helge B.D. Sorensen

JOURNAL Engineering in Medicine and Biology Society (EMBC), 2011 Annual International Conference of the IEEE

PUBLICATION HISTORY Submission date: 24-03-2011, Acceptance date: 09-06-2011

Seizure Onset Detection based on one sEMG channel

Isa Conradsen^{abd}, Sándor Beniczky^{bc}, Karsten Hoppe^d, Peter Wolf^b, Thomas Sams^a and Helge B.D. Sorensen^a

Abstract—We present a new method to detect seizure onsets of tonic-clonic epileptic seizures based on surface electromyography (sEMG) data. The proposed method is generic and based on a single channel making it ideal for a small detection or monitoring device. The sEMG signal is high-pass filtered with a Butterworth filter with a cut-off frequency of 150 Hz. The number of zero-crossings with a hysteresis of $\pm 50\mu\text{V}$ is the only feature extracted. The number of counts in a window of 1 second and the number of windows to make a detection is tested with a leave-one-out method. On 6 patients the method performs with a sensitivity of 100%, a median latency of 7.6 seconds and a median false detection rate of 0.04/h.

I. INTRODUCTION

Epilepsy is a neurological disorder that causes seizures due to an abnormal excessive or synchronous neural activity in the brain [1]. About 1% of the world's population suffers from this condition. If patients are medicated appropriately most become seizure free, but about 25% do not. Most of these patients experience seizures with predominantly motor symptoms such as tonic-clonic seizures. Their fear of having seizures in public may result in social isolation, and an objective risk of severe and sometimes fatal injuries during seizures increases their perceptions of insecurity. During the seizures the patients are not able to call for help. A simple alarm system, capable of detecting seizures, could help the patients by alerting relatives and caretakers, whenever a seizure sets in. We propose a single channel method, which is reliable and may be implemented in a small monitoring or detection device.

Attempts have been made [2], [3], [4], [5] to develop such a system based on motion data, but none of them is performing well enough to reach clinical use. Earlier we have focused on using several modalities and channels [2], [3], but have now found that a better algorithm may be developed with just one channel from a single modality. We propose a new method capable of capturing the tonic-clonic seizures, with a relatively short latency and without too many false alarms. Our approach is generic and based on a single channel of sEMG from the deltoid muscle and encompasses feature extraction by counting zero-crossings. The method is evaluated on 6 patients with tonic-clonic seizures.

Corresponding author: Isa Conradsen, isaconradsen@gmail.com
Contact information: SB: sbz@filadelphia.dk,
HBDS: hbs@elektro.dtu.dk, KH: kh@delta.dk

^aDTU Electrical Engineering, Ørsted's Plads, building 349, DK-2800 Kgs. Lyngby

^bDanish Epilepsy Center, Kolonivej 1, DK-4293 Dianalund

^cUniversity of Southern Denmark, Institute of Regional Health Services Research, Winsløwparken 19, 3, DK-5000 Odense C

^dDELTA/Ictalcare, Venlighedsvej 4, DK-2970 Hørsholm

II. METHODOLOGY

A. Data Collection

The 6 patients were admitted to the Danish Epilepsy Center in Dianalund, Denmark for diagnostic reasons. The recordings included electroencephalography (EEG), video, electrocardiography (ECG) and sEMG electrodes placed on several, clinically relevant muscles. We analysed signals from the left deltoid muscle, as this placement seemed to be the most stable one. The active electrode was placed on the center of the muscle, whereas the reference was placed on the acromioclavicular joint. The admission lasted 2-4 days depending on the patient. The sEMG was sampled with a frequency of 1024Hz. All patients had tonic-clonic seizures. The number of seizures, sex and age of the patients are listed in Table I together with the lengths of the signals. The times for the beginning and ending of the seizures was annotated by a physician based on video and EEG signals.

TABLE I
THE PATIENTS GENDER, AGE, THE AMOUNT OF SEIZURES AND THE LENGTH OF THE ADMISSION.

Patient	Gender	Age	# seizures	File length [h]
1	M	39	1	93.4
2	M	25	1	46.6
3	F	23	1	25.3
4	F	26	2	95.2
5	M	38	1	96.5
6	M	62	2	95.5

B. Data Processing

The processing of data is split into two parts. The first part is the feature extraction and the last part is the detection approach.

1) *Feature Extraction*: In a previous study we analyzed the similarities and differences between sEMG signals from real epileptic seizures and sEMG signals from simulated seizures [6]. We showed, that real seizures had a large proportion of data in the frequency band above 100 Hz, in contrast to normal activity. For this study we furthermore made a visual evaluation of all the seizures for the 6 patients and found that the seizures still contained a large proportion of the signal, when preprocessed with a high-pass filter with a cut-off frequency of 150 Hz. This furthermore ensures that a large amount of the artifacts will be removed. We have chosen a Butterworth filter with an order of 20. The group delay of this filter is linear in the frequency band of interest. The seizure of the first patient including prior and posterior normal activity, is shown in Fig. 1 before and after filtering.

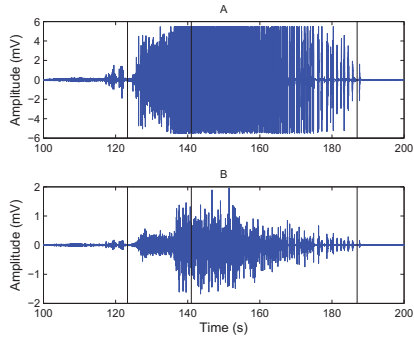


Fig. 1. The upper figure shows the seizure (with surrounding activity) before filtering and the lower shows the signal after filtering. The vertical black dotted lines shows the beginning and ending of the seizure.

In our previous study on the sEMG signals during real and simulated seizures we showed that simple features are able to distinguish between the two groups [6]. Therefore we chose to focus this study on finding a simple feature, which is able to discriminate tonic-clonic seizures from normal activity. Since the final method is meant to be used in a seizure detection system it is important to capture the seizures at onset. We therefore searched for a feature to discriminate the tonic part of the seizure from normal activities, since the clonic part almost always starts late in these tonic-clonic seizures. We found that with a simple zero-crossing method counting the zero-crossings with a hysteresis of $\pm 50\mu\text{V}$, the number of crossings was high throughout the entire tonic phase, see Fig. 2. This hysteresis also ensures that low-amplitude artifacts, remaining even after the filtration, are eliminated from a possible detection as a seizure.

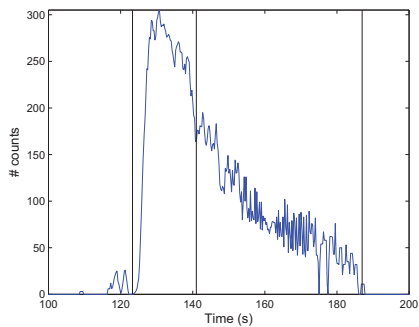


Fig. 2. The number of zero-crossings in windows of 1 second as a function of the time. It is clearly seen that the number of zero-crossings rises fast at seizure beginning, stays high throughout the tonic phase and is then lowered at the start of the clonic phase. The black vertical lines denote the beginning and end of the seizure.

2) *Detection Approach:* For our method we have chosen to vary two parameters, when searching for the optimal classification of the data into the two options; tonic-clonic seizure and normal activity. The first one is the number of zero-crossings in a given window, called the threshold, and the second one is the number of windows with a count above the threshold needed to classify a seizure. As in one of our previous studies, we have chosen to use a window of 1 second [3]. In this case we have chosen an overlap of 75% for the windows. We chose these values for the two parameters, based on a visual inspection of the feature-plot (see example in Fig. 2 for all seizures). Furthermore this inspection showed that the maximum number of zero-crossings during the tonic phase of the seizures is about 255 counts if all seizures are to be detected. We have though varied the number of counts from 180 to 340. In order to avoid too many false detections while ensuring a sufficiently short latency, the band of well chosen number of windows to make a seizure detection is probably narrow. To ensure that all possible solutions are tested, we have thus varied the number of windows to make a seizure detection from 1 to 40.

We have evaluated the results of the variation of the two parameters by a leave-one-out method, where the values of the parameters are chosen from the best combination based on 5 of the patients, when looking at all combinations in a color-plot. The best combination of parameters is then tested on the last patient. This means that all patients are used five times for training and one time for testing the parameters. An example of the color-plots is shown for the training on patient 1-5 in Fig. 3-5. The green color represents the good choice, yellow is in between and red is a bad choice. The parameters are first of all chosen to ensure that the sensitivity is 100%, which means that only a point in the darker green area of Fig. 3 may be chosen. On Fig. 4 and 5 we then searched for the point that both was closest to a green color within the darker green area from Fig. 3. This will provide the best solution to the combination of a low amount of false positives and at the same time a short latency. A higher threshold and/or a higher number of windows implies a lower number of FP, whereas the latency is lowered by lowering the number of windows and/or lowering the threshold. The green and yellow area for higher number of windows in Fig. 4 is caused by less seizures being detected or even non seizures being detected, see Fig. 3. The choice of parameters for each of the five training sessions are given in Table II.

TABLE II
THE CHOSEN PARAMETERS DURING THE TRAINING PHASE.

Training patients	counts	windows
2,3,4,5,6	254	18
1,3,4,5,6	254	16
1,2,4,5,6	250	18
1,2,3,5,6	250	18
1,2,3,4,6	250	18
1,2,3,4,5	250	18

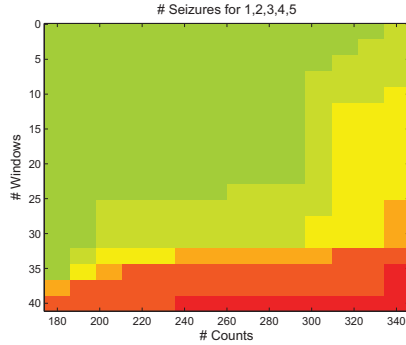


Fig. 3. The sensitivity, where green symbolises 100% and red symbolises 0%.

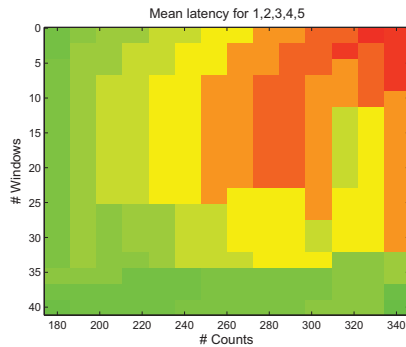


Fig. 4. The mean latency of the seizure detection, where green equals low latency and red equals high latency.

III. RESULTS AND DISCUSSION

Based on the leave-one-out method the results for each of the patients obtained with the parameters from Table II is given in Table III. The results for the different patients are very similar; all with a sensitivity of 100%. The false detection rate (FDR) is found to be between 0 and 0.1885, which compared to other studies are very promising values. The latencies are between 7 and 10.5 seconds. This is fine for a monitoring system and would as well be acceptable in a detection device. The latency may be shortened by a change of the parameters, but this will of course induce more false positives as well. To improve the system even more it could be implemented with an adaptive update on the threshold, so every time a seizure is detected the threshold would be fitted to suit the number of counts during the seizures even better. The deltoid muscle was selected for sampling because it is easily accessible, and always involved in generalized tonic-clonic seizures. If a patients seizures have a tonic motor onset in a different location, the method can probably be adapted accordingly whereas different seizure types starting

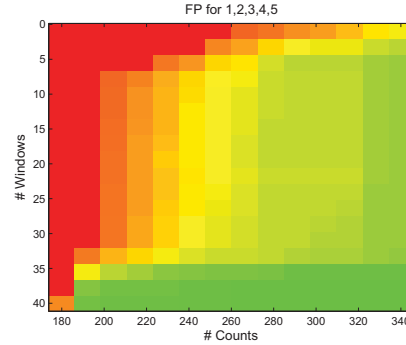


Fig. 5. The number of false positives (FP), where green equals few FP and red equals many FP.

e.g. with myoclonia, automatisms or sensory symptoms will need different approaches. In future studies we will include more patients and seizures to confirm the promising results in this paper.

TABLE III
THE RESULTS FOR EACH OF THE PATIENTS BASED ON THE PARAMETERS FROM TABLE II.

Patient	Sensitivity [%]	Latency [s]	FDR [/h]
1	100	9.5	0.0529
2	100	10.5	0.1075
3	100	8.25	0
4	100	8; 7.25	0.0310
5	100	7	0.0207
6	100	7; 7.25	0.1885

IV. CONCLUSION

The generic method we present is the first towards detection of tonic-clonic seizures based on a single sEMG channel. The data were classified as tonic-clonic seizure or normal activity based on a leave-one-out method. Our method performed as intended with a sensitivity of 100%, a median latency of 7.6 seconds and a median FDR of 0.04/h. We used no kind of adaption to the individual patients and the method is therefore easy to implement in a simple system for seizure monitoring or detection.

V. ACKNOWLEDGEMENTS

This work was supported by the Peter Jytte Wolf Foundation for Epilepsy, the Danish Epilepsy Centre, the Danish Agency of Science Technology and Innovation, the Technical University of Denmark, and the Danish National Advanced Technology foundation.

REFERENCES

- [1] R. Fisher, W. Boas, W. Blume, C. Elger, P. Genton, P. Lee, and J. Engel Jr, "Epileptic seizures and epilepsy: definitions proposed by the International League Against Epilepsy (ILAE) and the International Bureau for Epilepsy (IBE)," *Epilepsia*, vol. 46, no. 4, pp. 470-472, 2005.

- [2] I. Conradsen, S. Beniczky, P. Wolf, D. Terney, T. Sams, and H. Sorensen, "Multi-modal intelligent seizure acquisition (MISA) system: A new approach towards seizure detection based on full body motion measures," in *Engineering in Medicine and Biology Society, 2009. EMBC 2009. Annual International Conference of the IEEE*, pp. 2591–2595, IEEE, 2009.
- [3] I. Conradsen, S. Beniczky, P. Wolf, J. Henriksen, T. Sams, and H. Sorensen, "Seizure onset detection based on a Uni-or Multi-modal Intelligent Seizure Acquisition (UISA/MISA) system," in *Engineering in Medicine and Biology Society (EMBC), 2010 Annual International Conference of the IEEE*, pp. 3269–3272, IEEE, 2010.
- [4] T. Nijsen, P. Cluitmans, P. Griep, and R. Aarts, "Short time Fourier and wavelet transform for accelerometric detection of myoclonic seizures," *IEEE/EMBS Benelux*, pp. 7–8, 2006.
- [5] K. Cuppens, L. Lagae, B. Ceulemans, S. Van Huffel, and B. Vanrumste, "Detection of nocturnal frontal lobe seizures in pediatric patients by means of accelerometers: A first study," in *Conference proceedings: 31st Annual International Conference of the IEEE Engineering in Medicine and Biology Society*, vol. 1, pp. 6608–6611, 2009.
- [6] I. Conradsen, P. Wolf, T. Sams, H. Sorensen, and S. Beniczky, "Patterns of muscle activation during generalised tonic and tonic-clonic epileptic seizures." In review.

PAPER VI

TITLE Automated Algorithm for Generalised Tonic-Clonic Epileptic Seizure Onset Detection Based on sEMG Zero-Crossing Rate

AUTHORS Isa Conradsen, Sándor Beniczky, Karsten Hoppe, Peter Wolf, and Helge B.D. Sorensen

JOURNAL IEEE TRANSACTIONS ON BIOMEDICAL ENGINEERING

PUBLICATION HISTORY Submission date: 15-06-2011, Acceptance date: 20-11-2011

Automated Algorithm for Generalized Tonic–Clonic Epileptic Seizure Onset Detection Based on sEMG Zero-Crossing Rate

Isa Conradsen*, *Student Member, IEEE*, Sándor Beniczky, Karsten Hoppe, Peter Wolf, and Helge B. D. Sorensen, *Member, IEEE*

Abstract—Patients are not able to call for help during a generalized tonic–clonic epileptic seizure. Our objective was to develop a robust generic algorithm for automatic detection of tonic–clonic seizures, based on surface electromyography (sEMG) signals suitable for a portable device. Twenty-two seizures were analyzed from 11 consecutive patients. Our method is based on a high-pass filtering with a cutoff at 150 Hz, and monitoring a count of zero crossings with a hysteresis of $\pm 50 \mu\text{V}$. Based on data from one sEMG electrode (on the deltoid muscle), we achieved a sensitivity of 100% with a mean detection latency of 13.7 s, while the rate of false detection was limited to 1 false alarm per 24 h. The overall performance of the presented generic algorithm is adequate for clinical implementation.

Index Terms—Epilepsy, seizure detection, surface electromyography (sEMG), tonic–clonic.

I. INTRODUCTION

EPILEPSY is a neurological disorder that causes seizures due to an abnormal excessive or synchronous neural activity in the brain [1]. About 0.5–1% of the world's population suffers from this condition [2]. In spite of much progress with pharmacological, surgical, and alternative treatments (ketogenic diet and vagal nerve stimulation), about 30–40% of epilepsy patients continue to have seizures [2]. For many of these patients, seizure onset is unpredictable, impairing independent living and increasing the risk of injuries, e.g., by falls or burns. As patients do not remember the seizures, many of these episodes will be

Manuscript received June 15, 2011; revised August 22, 2011 and November 10, 2011; accepted November 20, 2011. Date of publication December 5, 2011; date of current version January 20, 2012. This work was supported by the Peter and Jytte Wolf Foundation for Epilepsy, the Danish Epilepsy Centre, the Danish Agency of Science Technology and Innovation, the Technical University of Denmark, and the Danish National Advanced Technology foundation. *Asterisk indicates corresponding author.*

*I. Conradsen is with the Biomedical Department of Electrical Engineering, Technical University of Denmark, 2800 Kgs. Lyngby, Denmark, and also with the Danish Epilepsy Centre, 4293 Dianalund, Denmark (e-mail: isaconradsen@gmail.com).

S. Beniczky is with the Danish Epilepsy Centre, 4293 Dianalund, Denmark, and also with the Department of Clinical Neurophysiology, Aarhus University Hospital, 8000 Aarhus, Denmark (e-mail: sbz@filadelfia.dk).

K. Hoppe is with DELTA, 2970 Hørsholm, Denmark (e-mail: kh@delta.dk).

P. Wolf is with the Danish Epilepsy Centre, 4293 Dianalund, Denmark (e-mail: pwl@filadelfia.dk).

H. B. D. Sorensen is with the Biomedical Department of Electrical Engineering, Technical University of Denmark, 2800 Kgs. Lyngby, Denmark (e-mail: hbs@elektro.dtu.dk).

Digital Object Identifier 10.1109/TBME.2011.2178094

unrecorded (if not observed by someone else). The lack of precise data on the frequency of seizure occurrence precludes the optimal adjustment of the treatment. Therapy resistant patients with generalized tonic–clonic seizures have an increased risk of dying in connection with a seizure, especially when they live alone and the seizures occur during sleep [3], [4]. An alarm system, capable of detecting these seizures, could help the patients by alerting relatives and caretakers, whenever a seizure occurs.

Previously, we have focused on using multimodal data, including surface electromyography (sEMG) and accelerometers for detection of epileptic seizures with motor manifestations [5], [6]. One other group has also tried to detect seizures based on a combination of accelerometers and sEMG [7]. Other authors have used electroencephalography (EEG) [8]–[10], electrocardiography (ECG) [11] or accelerometers [12]–[16] to develop a seizure detection system for tonic–clonic seizures. One group has even tried to discriminate tonic–clonic seizures from other seizures based on accelerometers [17], [18]. Both Kramer *et al.* and Lockman *et al.* achieved promising results on detecting tonic–clonic seizures based on accelerometer data. However, the seizures were detected rather late since the accelerometers were best at detecting the clonic phase of the seizures. Our aim was to obtain better results by developing a sensitive and specific algorithm that detects the seizures already in the tonic phase (that precedes the clonic one). We chose sEMG as our modality (signals) because there is an intensive activation of the muscles during the tonic phase. To make the system feasible (easy to wear by the patients), we aimed at using as few sensors as possible (only two channels). Furthermore, we focused on keeping the algorithm computationally efficient to make an implementation of the algorithm in a portable device possible. The main aim of the study is to propose the first algorithm based on only sEMG signals for detecting epileptic generalized tonic–clonic seizures. Our hypothesis is that the information content of the sEMG is sufficient for the early detection of tonic–clonic seizures. A preliminary version of this work has been reported [19].

II. RECORDINGS

Sixty consecutive patients admitted to the Epilepsy Monitoring Unit at the Danish Epilepsy Center in Dianalund, Denmark, for diagnostic reasons, who had a history of tonic–clonic seizures in the referral were included. Eleven patients had tonic–clonic seizures. The rest of the patients had seizures other than

TABLE I
PATIENTS GENDER, AGE, THE AMOUNT OF SEIZURES, AND THE LENGTH OF THE FILES

Patient	Gender	Age	# seizures	File length [h]
1	F	23	1	15.9-25.3
2	F	26	2	92.5-95.2
3	M	39	1	89.4-93.4
4	M	25	1	46.6
5	M	62	2	89.9-95.5
6	M	38	1	90.9-95.2
7	M	19	1	91.5-94.3
8	M	55	3	12.4-16.2
9	F	30	4	37.2
10	M	11	3	88.1
11	M	26	3	89.0

tonic-clonic or did not have epileptic seizures at all during the monitoring period. The study was approved by the regional ethics committee, and it was conducted according to the declaration of Helsinki. The recordings included EEG, video, ECG, and sEMG electrodes. We used 9-mm silver/silver chloride sEMG electrodes placed on the deltoid and anterior tibial muscles on both sides in a monopolar setting (the active electrode was placed on the midpoint of the muscle belly, while the reference electrode was placed on the acromioclavicular joint, just proximal to the insertion of the muscle). For this study, we have only analyzed the signals from the left deltoid and anterior tibial muscles. The admission lasted 1–4 days depending on the patient. The sEMG was sampled with a frequency of 1024 Hz. The long-term video-EEG recordings were reviewed by a clinical neurophysiologist and an epileptologist, who marked the time epochs containing a tonic-clonic seizure, based on visual analysis. The physician marked the start of the tonic phase, when this was unequivocal. In total, we recorded 22 tonic-clonic seizures in 776 h. The number of seizures, the demographic data, and the recording time for each patient are listed in Table I.

During the long-term monitoring, trained neurophysiology technicians monitored the recordings to make sure that data showed EMG activity and not noise, which would imply a loose connection (high impedance). It happened that the sEMG electrodes were accidentally detached in some patients. In these cases, the technicians corrected this as soon as possible. The epochs with detached/loose electrodes were excluded from the analysis, but in total more than 96% of the data was used, making it reasonable to look at the algorithm working both at night and during the day. Since some periods were excluded, the time lengths were not exactly the same for the two muscles; therefore, different time lengths are given in Table I.

III. METHODS

The methods section is divided into two sections: the feature extraction and the detection approach, respectively.

A. Feature Extraction

In a previous study, we analyzed the similarities and differences between sEMG signals from real epileptic seizures and from simulated seizures [20]. We showed that real seizures in contrast to normal activity had a large proportion of data in the

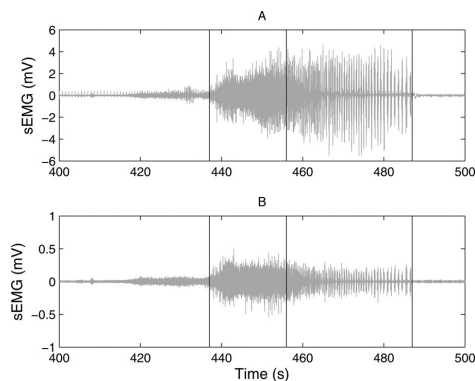


Fig. 1. (A) Seizure (with surrounding activity) before filtering. (B) Signal after filtering. The right and left black vertical lines denote the beginning and end of the generalized tonic-clonic seizure, whereas the middle black vertical line denotes the start of the clonic phase, marked by the physician. The data are from the left deltoid.

frequency band above 100 Hz. In this study, a visual evaluation of all seizures from the 11 patients revealed that the differences between seizures and normal activities were even more pronounced, when processed with a high-pass filter with a cut-off frequency at 150 Hz. The high-pass filtering furthermore ensures that a larger amount of the artifacts will be removed. We have used a Butterworth filter with an order of 20 for the filtering, where the group delay is ensured to be linear in the frequency band of interest. A seizure from a representative patient is shown in Fig. 1, before and after filtering.

Our previous study [20] on the sEMG signals during real and simulated seizures showed that simple features are able to distinguish between the two groups. Therefore, in this study, we chose to focus on finding a simple and computationally efficient feature that would be able to discriminate tonic-clonic seizures from normal activities. The final method is meant to be used in a seizure detection system and it is, therefore, important to capture the seizures soon after the onset. Since the seizures are started by a tonic phase, we searched for a feature to discriminate this part of the seizure from normal activities. In our previous study [20], we found that the epileptic (generalized tonic and the tonic phase of the generalized tonic-clonic) seizures contained a larger proportion of higher frequencies than normal activities. We have, therefore, chosen to focus our feature choice on the frequency domain, since this might distinguish both types of seizures from normal activities (though we only focus on one type in this study). The authors of [12] and [13], who have used accelerometer data, found algorithms to distinguish the clonic part from normal activities. These methods seem to perform well, but have longer latencies, because the clonic phase only comes after the tonic phase of the seizure. We chose a simple measure for the instantaneous frequency through the zero crossing compared to the power spectrum (used in [20]), since it is more convenient for implementation in a portable detection device. Previously, other groups [21], [22] have used zero crossing for the prediction of epileptic seizures based on EEG. Since we wanted our

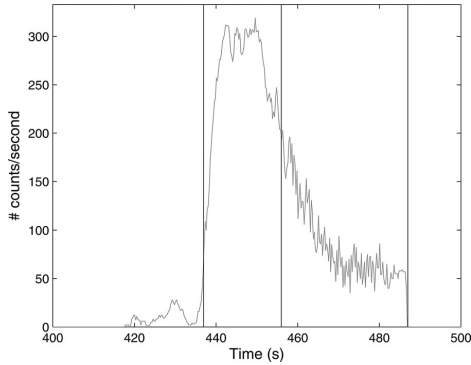


Fig. 2. Number of zero crossings in windows of 1 s as a function of the time for the filtered data in Fig. 1 (one seizure from a representative patient). It is clearly seen that the number of zero crossings rises fast at the start of the tonic phase, stays high throughout the tonic phase and drops at the beginning of the clonic phase. The right and left black vertical lines denote the beginning and end of the generalized tonic-clonic seizure, whereas the middle black vertical line denotes the beginning of the clonic phase.

algorithm to focus only on actual sEMG data, we decided to count only those zero crossing, which extended above and below a hysteresis. This ensured that the actual zero-crossing count would not be affected by noise. From a quantitative inspection of our data, we found background noise with a standard deviation (SD) as high as $15 \mu\text{V}$, so to ensure that the zero crossing only operates outside the noise region, we chose to include a hysteresis of $\pm 50 \mu\text{V}$, corresponding to $3\text{SD} \approx 50 \mu\text{V}$. A zero crossing is counted only when the signal peaks preceding and following it exceed $50 \mu\text{V}$ and $-50 \mu\text{V}$, respectively. So if the signal starts by rising above $50 \mu\text{V}$, one count is set when the signal goes below $-50 \mu\text{V}$, and another count is set when the signal again is above $50 \mu\text{V}$ and so on. We found that when applying the zero-crossing method with a hysteresis of $\pm 50 \mu\text{V}$ on the filtered data, the number of crossings was high throughout the entire tonic phase, see Fig. 2. The count of zero crossings is seen to decrease at the end of the tonic phase and throughout the clonic phase. This decrease is, however, caused by the clonic phase consisting of alternating periods with high activity and no activity at all. We evaluated the count of zero crossings with a smaller window size and found that the count is as high in the active clonic phases as in the tonic phases, so the reason for the decrease in the number of counts is that the window includes both the active periods and the periods with no activity in the clonic phase.

B. Detection Approach

Although many more parameters could be varied to make the algorithm more advanced, in our search for the optimal method to classify the data into tonic-clonic seizures or normal activity, we chose to vary two parameters. The first one is the number of zero crossings in a given window (called the threshold) and the second one is the number of succeeding windows, where the number of zero crossings exceeds the threshold, needed to finally

classify a seizure. As in one of our previous studies, we chose to use a window of 1 s [6]. In this study, we opted for an overlap of 75% for the windows. These two values, length and overlap of windows, were chosen based on a visual inspection of the feature plot (see example in Fig. 2) for all seizures. Furthermore, this inspection showed that the maximum number of zero crossings during the tonic phase of the seizures was about 255 counts if all seizures were to be detected. We varied the threshold from 200 (180 for anterior tibial muscle) to 300, with an interval of five counts between (180) 200 and 240, and between 260 and 300, whereas we had an interval of one count from 241 to 259. When seeking to avoid too many false detections and at the same time ensuring a sufficiently short latency, the band of properly chosen numbers of windows to make a seizure detection is most likely narrow. We, therefore, varied the number of windows to make a seizure detection from 2 to 30, where two windows correspond to a minimum delay of 1.25 s and 30 windows to a minimum delay of 8.25 s, to ensure that all possible solutions are tested. The number of windows was varied with intervals of two between 2 and 10 and between 20 and 30, whereas it was varied with intervals of one between 11 and 19. The beginning of the tonic-clonic seizures were marked by a clinical neurophysiologist and epileptologist by a visual evaluation of data, as this is more reliable than any automated method, thus far. However, the exact start time was sometimes uncertain. In these cases, we opted for marking the clinical time point that unequivocally showed the onset of the tonic phase. Thus, in theory, this marking might come a few seconds later than the real seizure onset. We therefore added an equation in our interpretation of the results which changed the latency to the minimum (based on the number of windows included) if the estimated start time turned out to be earlier than the clinical (actual) time point (though within 100 s from it). For each pair of parameters, three measures were calculated to evaluate the results.

- 1) The sensitivity (SEN): the percentage of the seizures, which were classified by the algorithm.
- 2) The false detection rate (FDR): the amount of false detections (normal activity classified as a seizure) per hour. This is a measure of the specificity.
- 3) The latency (LAT): the time from the beginning of a seizure to the detection of that seizure.

We used a fourfold cross-validation method [23], where the 11 patients (pt) were randomly partitioned into four subgroups (1: pt 2,6,11; 2: pt 1,4,9; 3: pt 5,7,10; 4: pt 3,8), to evaluate which parameters were optimal. From the four subgroups one was retained for validation of the parameters, whereas the other three subgroups were used for training the optimal choice of parameters. The validation group was then used to evaluate the trained choice of parameters. The cross-validation process was repeated four times, one time with each of the four subgroups as validation group. This method ensured that all patients were used (an equal number of times) for both training and validation. The optimal parameters for each training session were chosen from a 2-D plot, which express the relationship between the sensitivity and FDR (specificity), and the latency. The plot expresses the mean latency (for all seizures in the training groups) on the

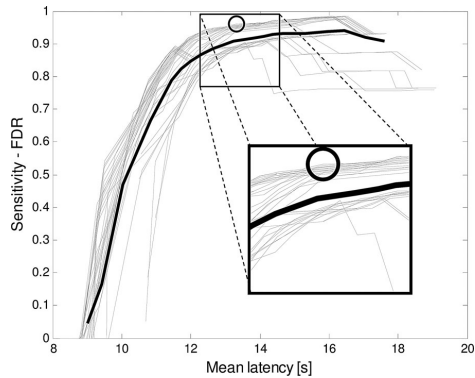


Fig. 3. Each curve shows different threshold levels, and for each curve the number of windows is varied. The black circle marks the chosen point on the curves. The thicker curve highlights the mean of the curves.

abscissa:

$$\text{abscissa} = \overline{\text{LAT}} \quad (1)$$

and the sensitivity minus the FDR on the ordinate:

$$\text{ordinate} = \begin{cases} \text{SEN} - \text{FDR}, & \text{for } \text{SEN} - \text{FDR} \geq 0 \\ 0, & \text{for } \text{SEN} - \text{FDR} < 0 \end{cases} \quad (2)$$

where SEN is the sensitivity (between 0 and 1), and FDR is the false detection rate given per hour (the FDR corresponds to the specificity). If none of the seizures for a patient are detected, the latency is given the value of the maximum latency of the patients involved in the training session. The approach of plotting the sensitivity and the FDR on one axis and the latency on the other makes it easier to search parameters that both ensure high sensitivity, low FDR (i.e., high specificity), and short latency. In Fig. 3, an example of the plot is shown for the training session of groups 1–3. The point on the curves in Fig. 3 is chosen as the best tradeoff between the sensitivity and the FDR and the latency in our point of view. We have prioritized a sensitivity as close to 100% as possible and at the same time as low an FDR as possible; second, we also tried to obtain a short latency. This is because we would rather have the detections delayed by a second, than not detecting them at all. In Fig. 3, the optimal point with respect to achieving both high sensitivity and specificity would be as close to 1 as possible on the y-axis. Second, we chose the point so as the latency would not be too large (the point being placed too far right on the x-axis). The optimal parameters are considered not to be outliers, so that small changes in the threshold or number of windows to finalize a detection does not change drastically (e.g., the amount of seizures detected). If so another set of optimal parameters will be searched.

The optimal choice of parameters (chosen based on a plot equal to the one shown in Fig. 3) for each of the four training sessions is given in Table II for the three training branches: deltoid muscle data alone, anterior tibial muscle data alone, and the combination of data from both muscles. The parameters for the combination of the two muscles are achieved by requesting

TABLE II
PARAMETERS CHOSEN THROUGH THE FOUR TRAINING PHASES

Training groups	Deltoid		Tibialis		Combined	
	# win	th	# win	th	# win	th
1,2,3	19	241	26	195	8	200
1,2,4	15	253	28	195	8	195
1,3,4	19	245	24	190	8	200
2,3,4	19	240	24	205	8	200

#win=number of windows, th=threshold.

that the seizure should be visible through the features in both muscles (channels) at the same time. This combination should reduce the number of false alarms, which are only visible in one muscle. Therefore, lower values are expected for the two parameters, compared to the detection being based on just one muscle.

IV. RESULTS

The test results for the two electrode placements (deltoid and anterior tibial) are presented in Table III together with the combined results, where an alarm is generated if it is registered in both muscles at the same time. The overall results of the evaluation are very promising and suggest that it is possible to choose parameters such that the same algorithm (including parameters) may be used for all patients, providing a generic method for a detection system for epileptic patients with generalized tonic-clonic seizures.

When using data only from the deltoid muscle, all seizures are detected with an acceptable mean latency. The latency is different, however, for the different patients, since not all patients have seizures which start equally abruptly, and furthermore how early the muscles are recruited into the seizure varies. A visual inspection of the sEMG data compared to the video shows that the seizures for patient 9, for whom the latency is very long, involve the deltoid muscle relatively late. Besides good sensitivity and latency, the results for the deltoid muscle alone also show a very low FDR. The mean FDR is 0.04, which corresponds to approximately 1 in 24 h. Most of the false detections were in the daytime, and only three were during the night (12 P.M.–8 A.M.); for the results on the deltoid muscle data, see Fig. 4. This is only approximately 10% of the false alarms, so if the algorithm was implemented in a system only to be used during the night, where a surveillance system is mostly needed, the FDR would be approximately one false alarm for every tenth day.

The results for the data from the anterior tibial muscle alone are not as good as for the deltoid muscle. For the anterior tibial, the mean sensitivity is 77%. Only for seven patients, all seizures are detected; for two of the remaining three, none of the seizures are detected. This may be caused by the high number of windows. If the number of windows is too high, the length of the period they cover might exceed the length of the tonic phase for some patients, and thereby cause detection to fail. The mean latency is longer for detections based only on the anterior tibial muscles compared to those based on the deltoid muscle. However, for some patients the latency is lower for the tibial muscle than for the deltoid muscle, and for some patients it is higher. For all those with a lower latency, all seizures are detected. The

TABLE III
RESULTS FOR VALIDATION OF THE TRAINED PARAMETERS (SEE TABLE II), BASED ON A SINGLE MUSCLE OR THE COMBINATION OF TWO

Patient	Deltoid			Anterior Tibial			Combined			
	SEN [%]	FDR [/h]	LAT [s]	SEN [%]	FDR [/h]	LAT [s]	SEN [%]	FDR [/h]	LAT [s]	
Group 1	2	100	0.03	8.38	0	0.01	-	100	0.01	4.88
	6	100	0.04	7.75	100	0.03	6.75	100	0.03	4.25
	11	100	0.00	6.00	100	0.84	7.25	100	0.02	3.33
Group 2	1	100	0.00	9.00	100	0.06	6.75	100	0.00	6.00
	4	100	0.09	11.25	100	0.09	19.25	100	0.00	14.75
	9	100	0.03	34.44	100	0.00	27.44	100	0.00	26.31
Group 3	5	100	0.04	7.13	50	0.05	11.75	100	0.19	5.75
	7	100	0.03	17.00	100	0.11	14.75	100	0.00	9.75
	10	100	0.14	7.17	67	0.31	24.88	100	0.02	13.00
Group 4	3	100	0.00	10.25	0	0.68	-	100	0.01	9.75
	8	100	0.00	12.33	100	0.32	11.08	100	0.16	7.33
Mean	100	0.04	13.66	77	0.20	14.11	100	0.04	9.85	

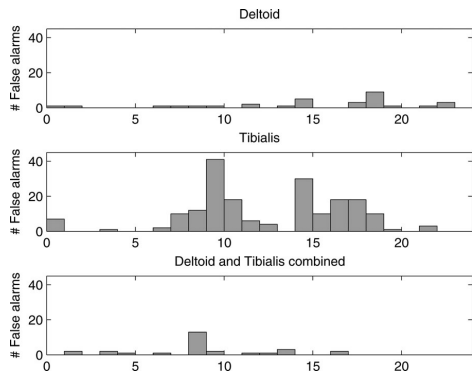


Fig. 4. Histograms of the false alarms for all 11 patients. The abscissa shows the time of the day (24 h).

same pattern is seen for the FDR, where the mean is much higher for the results on the anterior tibial muscle compared to that of the deltoid muscle, but for three patients it is actually lower.

If the two sets of data are combined, the results improve somewhat regarding latency, as expected. Similar to the results based on the deltoid muscle alone, all seizures are detected; the mean FDR is low, but the mean latency is even shorter for the detection based on both muscles. However, for two patients (4 and 10) the latencies are increased for the combination of both muscles as compared to the deltoid muscle alone. The explanation may be found in the fact that the latency is very high for these patients, when only the anterior tibial data are used, which implies that the seizures are seen later in this muscle than in the deltoid muscle.

V. DISCUSSION

The different results for the two muscles and the combination of both are not only dependent on the chosen muscle, but also

on the chosen parameters (see Table II). Thus, for the combined method the number of windows for a detection is less, which explains the short latency and for the anterior tibial muscle the number of windows is greater, which gives long latencies. Looking at the parameters in Table II, one will see that they are more alike for the combination of the two muscles, than for the deltoid muscle alone, where group 3 is tested with parameters somewhat different from the others. If group 3 had instead been tested with parameters more alike to the other three groups (19 windows and a threshold of 241), the sensitivity would have stayed the same, but the latency would have been longer and the FDR smaller, which would bring the mean FDR to 0.03 and the mean latency to 13.9 for the deltoid muscle data alone. This suggests that an equivalent well result as presented in Table III would be obtained by using the exact same parameters for all patients.

Since combining the deltoid data with the anterior tibial data only improves the latency (by 4s on average), a detection system would more appropriately be based on the deltoid muscle alone, since the gain of adding data from an extra muscle is too small. If data were combined from two muscles in a detection system, one would probably choose two muscles closer together than the two we have used in this study.

The sensitivity and specificity of seizure detection systems based on EEG signals vary widely: 70–100% (for sensitivity) and 0.5–72 false detections per 24 h (for specificity) [24]–[27]. The best-performing ones are based on invasive recordings (intracranial electrodes) or many scalp electrodes (>60) [27]. In the best of these studies, they achieve the same sensitivity as our approach, but a lower FDR and shorter latency. It should, however, be considered that their system would not be feasible for a long-term monitoring in the patients home or in the everyday life of a patient. In spite of using signals from a noninvasive recording (sEMG) and just one channel, we obtained a sensitivity of 100% and a specificity of 1 false detection per 24 h. This is compatible with the best-performing EEG-based systems, but our system is easily implemented, because it is noninvasive.

If we compare our deltoid results to other studies [12], [13] who have developed an algorithm to detect tonic-clonic seizures based on motion data, ours are more sensitive (SEN = 100% versus 88% [12] and 91% [13]). The study by Kramer *et al.* [13] includes 15 patients (22 seizures as in our study), whereas the results by Lockman *et al.* [12] are based on a very limited database (six patients with eight seizures). At the same time, our algorithm captures seizures in the tonic phase, whereas the other methods focus on the clonic phase. Therefore, our latencies are shorter than in these two studies with accelerometers. We are not able to compare the FDR to [12], since they have not listed how long their recordings were, but only that they captured 204 false alarms for the eight patients. They do, however, state that they have a large FDR, so we would expect their system to have a larger FDR, than what we are able to provide. Kramer *et al.* [13] report an FDR of 0.004 (eight false alarms in 1692 h), which is lower than what we have provided, but this should be held up against the lower sensitivity they achieved, which we find is more important to keep as close to 100% as possible.

Very few time periods were excluded from the evaluation of data, but in a real time situation it is important that all data are useful. That means that in real time the electrode(s) collecting the data for the algorithm must be extra adhesive, so as they will not become loose. In periods where the electrode(s) are loose or have completely fallen off, the algorithm will not be able to detect any seizures.

The electrodes used to collect the data are wired; the impedances are kept low by the healthcare personal monitoring the signals and making sure that the background noise does not increase too highly. More than 96% of the data are used. In a home situation, wireless electrodes, firmly attached by a plaster specifically designed for this purpose (Ictalcare A/S, Denmark), would be used. The next step in our process is to implement the algorithm into the hardware of a device with such a wireless electrode.

Other muscles might be used as well. These two muscles were chosen since, in our experience, the deltoid muscle is always strongly involved in generalized tonic-clonic seizures. Anterior tibial muscle provides a less visible placement for a detection device, if it should be worn in daytime situations.

To the best of our knowledge, this is the first seizure detection algorithm based solely on the sEMG modality. We have developed a generic (the same algorithm/parameters are used for all patients) seizure detection system that is noninvasive (based on sEMG recordings), feasible (was applicable in all recruited patients), with high sensitivity (100%), low rate of false alarms (1/24 h) and able to run in real time. The algorithm was evaluated with a fourfold cross validation on one or two channels of sEMG from the deltoid or anterior tibial muscle from 11 patients with tonic-clonic seizures. It can only detect one seizure type: the tonic-clonic ones. Nevertheless, it is the group of patients with this seizure type that has the highest risk for injuries following seizures and sudden unexpected death in epilepsy patients [28]. Implemented in a portable device, the algorithm presented provides advantages over the alarm devices used today, based on accelerometers in a wristband or a bed alarm.

VI. CONCLUSION

We have developed a generic seizure detection algorithm, which is the first of its kind to be based on sEMG data alone. The algorithm focuses on detection of tonic-clonic seizures as compared to normal activity. Our algorithm was validated with a fourfold cross validation and we found that it is highly sensitive, with low false detection rate and short detection latency. For one muscle alone (deltoid), our method performed with a sensitivity of 100%, a median latency of 13.7 s, and a median FDR of 0.04/h corresponding to one false alarm in 24 h. The algorithm performs well enough to be implemented in clinical practice. A first implementation in a nighttime only device would provide a median FDR of approximately 1 in ten days.

ACKNOWLEDGMENT

The authors are grateful to Prof. D. Farina for the fruitful discussions on this topic and for his comments and suggestions.

REFERENCES

- [1] R. Fisher, W. Boas, W. Blume, C. Elger, P. Genton, P. Lee, and J. Engel Jr., "Epileptic seizures and epilepsy: Definitions proposed by the International League Against Epilepsy (ILAE) and the International Bureau for Epilepsy (IBE)," *Epilepsia*, vol. 46, no. 4, pp. 470–472, 2005.
- [2] J. Engel, Jr., S. Wiebe, J. French, M. Sperling, P. Williamson, D. Spencer, R. Gumnit, C. Zahn, E. Westbrook, and B. Enos, "Practice parameter: Temporal lobe and localized neocortical resections for epilepsy," *Epilepsia*, vol. 44, no. 6, pp. 741–751, 2003.
- [3] L. Nashef and P. Ryvlin, "Sudden unexpected death in epilepsy (SUDEP): Update and reflections," *Neurol. Clin.*, vol. 27, no. 4, pp. 1063–1074, 2009.
- [4] J. Hughes, "A review of sudden unexpected death in epilepsy: Prediction of patients at risk," *Epilepsy Behav.*, vol. 14, no. 2, pp. 280–287, 2009.
- [5] I. Conradsen, S. Beniczky, P. Wolf, D. Terney, T. Sams, and H. Sorensen, "Multi-modal intelligent seizure acquisition (MISA) system—A new approach towards seizure detection based on full body motion measures," in *Proc. IEEE Annu. Int. Conf. Eng. Med. Biol. Soc.*, 2009, pp. 2591–2595.
- [6] I. Conradsen, S. Beniczky, P. Wolf, J. Henriksen, T. Sams, and H. Sorensen, "Seizure onset detection based on a Uni- or Multi-modal Intelligent Seizure Acquisition (UISA/MISA) system," in *Proc. IEEE Annu. Int. Conf. Eng. Med. Biol. Soc.*, 2010, pp. 3269–3272.
- [7] S. Patel, C. Mancinelli, A. Dalton, B. Patritti, T. Pang, S. Schachter, and P. Bonato, "Detecting epileptic seizures using wearable sensors," in *Proc. IEEE 35th Annu. Northeast Bioeng. Conf.*, 2009, pp. 1–2.
- [8] T. Sorensen, U. Olsen, I. Conradsen, J. Henriksen, T. Kjaer, C. Thomsen, and H. Sorensen, "Automatic epileptic seizure onset detection using matching pursuit: A case study," in *Proc. IEEE Annu. Int. Conf. Eng. Med. Biol. Soc.*, 2010, pp. 3277–3280.
- [9] E. Chua, K. Patel, M. Fitzsimons, and C. Bleakley, "Improved patient specific seizure detection during pre-surgical evaluation," *Clin. Neurophysiol.*, vol. 122, no. 4, pp. 672–679, 2011.
- [10] M. Arab, A. Suratgar, and A. Ashtiani, "Electroencephalogram signals processing for topographic brain mapping and epilepsies classification," *Comput. Biol. Med.*, vol. 40, no. 9, pp. 733–739, 2010.
- [11] J. Jeppesen, S. Beniczky, A. Fuglsang-Frederiksen, P. Sidenius, and Y. Jasemian, "Detection of epileptic-seizures by means of power spectrum analysis of heart rate variability: A pilot study," *Technol. Health Care*, vol. 18, no. 6, pp. 417–426, 2010.
- [12] J. Lockman, R. Fisher, and D. Olson, "Detection of seizure-like movements using a wrist accelerometer," *Epilepsy Behav.*, vol. 20, no. 4, pp. 638–641, 2011.
- [13] U. Kramer, S. Kipervasser, A. Shlitner, and R. Kuzniecky, "A novel portable seizure detection alarm system: Preliminary results," *J. Clin. Neurophysiol.*, vol. 28, no. 1, pp. 36–38, 2011.
- [14] T. Nijssen, J. Arends, P. Griep, and P. Cluitmans, "The potential value of three-dimensional accelerometry for detection of motor seizures in severe epilepsy," *Epilepsy Behav.*, vol. 7, no. 1, pp. 74–84, 2005.

- [15] T. Nijssen, R. Aarts, J. Arends, and P. Cluitmans, "Automated detection of tonic seizures using 3-D accelerometry," in *Proc. 4th Eur. Conf. Int. Federat. Med. Biol. Eng.*, 2009, pp. 188–191.
- [16] K. Cuppens, L. Lagae, B. Ceulemans, S. Van Huffel, and B. Vanrumste, "Detection of nocturnal frontal lobe seizures in pediatric patients by means of accelerometers: A first study," in *Proc. IEEE 31st Annu. Int. Conf. Eng. Med. Biol. Soc.*, 2009, vol. 1, pp. 6608–6611.
- [17] G. Becq, S. Bonnet, L. Minotti, M. Antonakios, R. Guillemaud, and P. Kahane, "Collection and exploratory analysis of attitude sensor data in an epilepsy monitoring unit," in *Proc. IEEE 29th Annu. Int. Conf. Eng. Med. Biol. Soc.*, 2007, pp. 2775–2778.
- [18] G. Becq, S. Bonnet, L. Minotti, M. Antonakios, R. Guillemaud, and P. Kahane, "Classification of epileptic motor manifestations using inertial and magnetic sensors," *Comput. Biol. Med.*, vol. 41, pp. 46–55, 2010.
- [19] I. Conradsen, S. Beniczky, K. Hoppe, P. Wolf, T. Sams, and H. Sorensen, "Seizure onset detection based on one sEMG channel," in *Proc. IEEE Annu. Int. Conf. Eng. Med. Biol. Soc.*, 2011, pp. 7715–7718.
- [20] I. Conradsen, P. Wolf, T. Sams, H. Sorensen, and S. Beniczky, "Patterns of muscle activation during generalized tonic and tonic-clonic epileptic seizures," *Epilepsia*, vol. 52, no. 11, pp. 2125–2132, 2011.
- [21] M. van Putten, T. Kind, F. Visser, and V. Lagerburg, "Detecting temporal lobe seizures from scalp eeg recordings: A comparison of various features," *Clin. Neurophysiol.*, vol. 116, no. 10, pp. 2480–2489, 2005.
- [22] S. Zandi, R. Tafreshi, M. Javidan, and G. Dumont, "Predicting temporal lobe epileptic seizures based on zero-crossing interval analysis in scalp EEG," in *Proc. IEEE Annu. Int. Conf. Eng. Med. Biol. Soc.*, 2010, pp. 5537–5540.
- [23] M. Stone, "Cross-validators choice and assessment of statistical predictions," *J. R. Statist. Soc. Ser. B (Methodol.)*, vol. 36, no. 2, pp. 111–147, 1974.
- [24] J. Gotman, "Automatic recognition of epileptic seizures in the EEG," *Electroencephalograph. Clin. Neurophysiol.*, vol. 54, no. 5, pp. 530–540, 1982.
- [25] I. Osorio, M. Frei, J. Giftakis, T. Peters, J. Ingram, M. Turnbull, M. Herzog, M. Rise, S. Schaffner, R. Wennberg, T. Walczak, M. Risinger, and C. Ajmone-Marsan, "Performance reassessment of a real-time seizure-detection algorithm on long ECoG series," *Epilepsia*, vol. 43, no. 12, pp. 1522–1535, 2002.
- [26] Y. Khan and J. Gotman, "Wavelet based automatic seizure detection in intracerebral electroencephalogram," *Clin. Neurophysiol.*, vol. 114, no. 5, pp. 898–908, 2003.
- [27] G. Minasyan, J. Chatten, M. Chatten, and R. Harner, "Patient-specific early seizure detection from scalp EEG," *J. Clin. Neurophysiol.: Official Publ. Amer. Electroencephalograph. Soc.*, vol. 27, no. 3, p. 163, 2010.
- [28] R. Kloster and T. Engelskjøn, "Sudden unexpected death in epilepsy (SUDEP): A clinical perspective and a search for risk factors," *J. Neurol., Neurosurg. Psychiatry*, vol. 67, no. 4, pp. 439–444, 1999.



recognition.

Isa Conradsen (S'11) received the M.Sc. degrees in biomedical engineering from the Technical University of Denmark, Lyngby, Denmark, and the University of Copenhagen, Copenhagen, Denmark, in 2008. She is currently working toward the Ph.D. degree in the Department of Electrical Engineering, Technical University of Denmark. Her Ph.D. project is carried out in close collaboration with the Danish Epilepsy Centre, Dianalund, Denmark.

Her research interests include biomedical signal processing, epilepsy, classification, and pattern



and epilepsy.

Sándor Beniczky received the MD degree from the medical school, in 1997, and the Ph.D. degree in neuroscience, in 2004, from the University of Szeged, Szeged, Hungary.

He is a Board Certified Neurologist and Clinical Neurophysiologist (both in Hungary and in Denmark). He is currently with the Danish Epilepsy Centre, Dianalund, Denmark, and the Department of Clinical Neurophysiology, Aarhus University Hospital, Aarhus, Denmark. His main research interests include evoked potentials, source localization, EEG,



Karsten Hoppe received the M.Sc. degree in electrical engineering from the Technical University of Denmark, Lyngby, Denmark, in 1995.

He is currently working as an Application Specialist in the ePatch group at DELTA, Hørsholm, Denmark. His main interest includes ePatch-based medical device design.



Peter Wolf received the MD degree from Heidelberg University in 1968, and the Ph.D. degree in neurology from Berlin, Germany, in 1977. He is a retired Professor of Neurology affiliated to the Danish Epilepsy Center, Dianalund, Denmark.

He is involved in various international education programs and has held numerous honorary positions in the field of epilepsy. He is the Immediate Past President of the International League against Epilepsy. His research has addressed many aspects of clinical epileptology and is at present focused on reflex epilepsies, epilepsy partialis continua, and the cultural history of epilepsy.



Helge B. D. Sorensen (M'90) received the M.Sc. and Ph.D. degrees from the Institute of Electronic Systems, Aalborg University, Aalborg, Denmark, in 1985, and 1992, respectively, both in electrical engineering.

He was initially a Research Assistant at the Institute of Electronic Systems, Aalborg University, where he was also an Assistant Professor from 1989 to 1993. From 1993 to 1995, he was an Associate Professor at Engineering Academy, Denmark. Since 1995, he has been an Associate Professor and the Head of the Biomedical Signal Processing research group at the Department of Electrical Engineering, Technical University of Denmark, Lyngby, Denmark.

PAPER VII

TITLE Evaluation of novel algorithm embedded in a wearable sEMG device for seizure detection

AUTHORS Isa Conradsen, Sándor Beniczky, Peter Wolf, Poul Jennum and Helge B.D. Sorensen

JOURNAL Engineering in Medicine and Biology Society (EMBC), 2012 Annual International Conference of the IEEE

PUBLICATION HISTORY Submission date: 02-03-2012

Evaluation of novel algorithm embedded in a wearable sEMG device for seizure detection

Isa Conradsen^{abc}, Sándor Beniczky^{bd}, Peter Wolf^b, Poul Jennum^{ef} and Helge B.D. Sorensen^a

Abstract—We implemented a modified version of a previously published algorithm for detection of generalized tonic-clonic seizures into a prototype wireless surface electromyography (sEMG) recording device. The method was modified to require minimum computational load, and two parameters were trained on prior sEMG data recorded with the device. Along with the normal sEMG recording, the device is able to set an alarm whenever the implemented algorithm detects a seizure. These alarms are annotated in the data file along with the signal. The device was tested at the Epilepsy Monitoring Unit (EMU) at the Danish Epilepsy Center. Five patients were included in the study and two of them had generalized tonic-clonic seizures. All patients were monitored for 2-5 days. A double-blind study was made on the five patients. The overall result showed that the device detected four of seven seizures and had a false detection rate of 0.003/h or one in twelve days.

Index Terms—Epilepsy, seizure detection, tonic-clonic, GTC, surface Electromyography, sEMG, wireless device.

I. INTRODUCTION

About 1% of the world's population suffers from epilepsy, which is defined as a brain disorder with repetitive seizures due to an abnormal excessive or synchronous neural activity in the brain [1]. If patients are medicated appropriately most become seizure free, but about one third are characterized as medically refractory patients [2], [3]. Most of these patients experience seizures with predominantly motor symptoms such as generalized tonic-clonic (GTC) seizures [4]. Epilepsy causes major societal burden [5]. GTC carries major risk complications as fractures, falls, cardiac complications, cognitive dysfunctions and ultimately sudden unexpected death in epilepsy (SUDEP) [6], [7], [8]. GTC may occur in situations where the patients are unobserved and consequently helpless, e.g. while alone or during sleep. Beside these complications GTC causes major concern to the patients and their relatives.

One way to help the patients is through a simple alarm system, capable of detecting the GTC seizures. Such an alarm

system would then alert relatives and caretakers, whenever a seizure sets in. In a previous study we found that there are significant differences between tonic seizures and the tonic phase of tonic-clonic seizures, when comparing them to simulated tonic activity [9]. Based on this knowledge we proposed an algorithm for the purpose of detecting GTC seizures [10], which seems reliable on conventional sEMG data. This algorithm has been modified and implemented in a small sEMG wireless device developed by DELTA, Denmark, on behalf of IctalCare A/S, Denmark.

Several groups (including ourselves) have attempted to develop an effective alarm system based on accelerometer data [11], [12], [13], [14], [15], but with a performance which could be improved. Our previous results [11] on conventional sEMG data (measured with standard sEMG electrodes) were promising and we expect to achieve even better results with the wireless sEMG data, due to the avoidance of artifacts from wire-pulls. We present the results of an implementation of a novel algorithm into a wireless detection device. It is able to detect most GTC seizures, with a relatively short latency and without too many false alarms. Our approach is generic and based on a single wireless device placed on the tibial muscle. The device with the algorithm implemented has for this study been tested on five patients.

II. METHODOLOGY

A. Patients

Five consecutive patients were included from the Danish Epilepsy Center in Dianalund, Denmark, for diagnostic reasons. All patients included have a history of generalized tonic-clonic seizures. The patients's age, gender, amount of GTC seizures during the recording, duration of the seizures and the recordings are all listed in Table I.

TABLE I
THE PATIENTS'S GENDER, AGE, THE AMOUNT OF SEIZURES, THE LENGTH OF THE ADMISSION AND THE LENGTH OF THE GTC SEIZURES.

Patient	Gender	Age	# GTC	Seizure duration [s]	File length [h]
D207	F	15	0		-
D208	M	34	3	88, 77, 52	68.4
D209	M	48	0		50.1
D210	M	38	0		53.3
D211	M	44	4	100, 105, 98, 102	126

Corresponding author: Isa Conradsen, isaconradsen@gmail.com

Contact information: SB: sbz@filadelfia.dk,

HBDS: hbs@elektro.dtu.dk

^aDTU Electrical Engineering, Ørsteds Plads, building 349, DK-2800 Kgs. Lyngby

^bDanish Epilepsy Center, Kolonivej 1, DK-4293 Dianalund

^cIctalCare, Venlighedsvej 4, DK-2970 Hørsholm

^dUniversity of Southern Denmark, Institute of Regional Health Services Research, Winsløwparken 19, 3, DK-5000 Odense C

^eDepartment of Clinical Neurophysiology, University of Copenhagen, DK-2100 Copenhagen

^fDanish Center for Sleep Medicine and Center for Healthy Aging, Glostrup Hospital, DK-2600 Glostrup

B. Recordings

The normal admission recordings included electroencephalography (EEG), video, electrocardiography (ECG) and sEMG electrodes placed on several, clinically relevant muscles. Along with this our wireless device for measurements of sEMG was placed on a tibial muscle (left/right) as shown in Fig. 1. The choice of side for the placement of the device (left/right) was decided by the physician based on records on where each patient normally have their seizures expressed the most. The device only sets hidden alarms, which means that the staff at the hospital are unaware of the times of the alarms. The admission lasted 2-5 days depending on the patient, thus providing us with a huge amount of data for each patient. The sEMG was sampled with a frequency of 1024Hz. Two of the patients had GTC seizures, while the others had other kinds of seizures or none at all. The times for the beginning and ending of the seizures were annotated by a physician based on the gold standard (video and EEG signals). For the first patient we had some recording problems, which means that unfortunately no data have been recorded from the wireless device placed on the tibial muscle, see table I.



Fig. 1. The wireless sEMG device placed on the tibial muscle.

C. Algorithm implementation

The original algorithm [10] is based on a high pass filtering and a count of zero-crossings above and below a hysteresis of $\pm 50\mu\text{V}$. This count of zero-crossings is calculated for a window of 1 second and every window overlaps the previous and the next by 75%. For the algorithm to detect a seizure the count of zero-crossings should be above a threshold (first parameter) for a certain number of windows (second parameter). The two parameters (*threshold* and *number of windows*) were trained for the data on which it was intended to be used. Even though the algorithm was developed with consideration to a later implementation in a small detection device, small changes had to be made to realize the implementation. The first thing changed was the filter, since the device could not encompass a filter of the size

we used in the off-line algorithm. A new filter was designed, so as it resembles the old one as closely as possible, and at the same time with an order as low as 11 (the maximum number of coefficients allowed for the filter to follow the limitations regarding the capacity of the current version of the wireless device). The off-line filter had an order of 21, which means we have lowered both the summations and multiplications with 10 in the algorithm. The filter in the off-line algorithm was a finite impulse response (FIR) hamming window filter, with the filter characteristics shown in blue in Fig. 2. The new filter was chosen as an FIR equiripple filter with order 11. This filter is shown in red in Fig. 2.

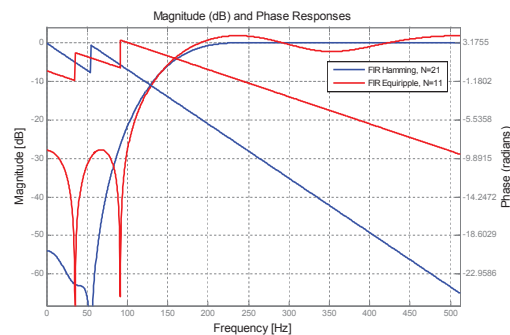


Fig. 2. The filter characteristics for the off-line filter (blue) and the new on-line filter (red) implemented in a wireless detection device.

The frequencies of interest are all above 150 Hz, where the phase is seen to be linear for both filters. For the on-line filter the equiripples make small differences in the suppression of the signal above a frequency of 150 Hz. For the frequencies below 150 Hz, a larger difference is seen, but for both filters, this part of the signal is lowered tremendously. This means, that it will be inconsiderable, when continuing with the count of zero-crossings above and below the hysteresis of $\pm 50\mu\text{V}$. Since the algorithm is to be used on sEMG from our wireless sEMG device, the parameters (*threshold* and *number of windows*) must be fitted to this exact type of data. At the time of implementation we only had data from two patients with GTC seizures. Normally we would record from both the biceps and the tibial muscle, but in the case of these two patients, we unfortunately had some technical problems with the device on the biceps, which meant that we only had sEMG data from the tibial muscle during the seizures. The parameters were trained as described in [10], from which we found the optimal parameters to be *number of windows* = 15 and *threshold* = 300. Thus the number of windows is similar to the one obtained in our off-line study [10] for the conventional sEMG data, whereas the threshold in case of the wireless device data is a bit higher than for the conventional sEMG data.

D. Data evaluation

The data were collected from the recording site and visualized through the free-ware program EDFbrowser [16]. The data files contain one vector featuring the sEMG signal and one holding a notation vector, which contains the alarm times. An example of a GTC seizure and the matching hidden alarms are shown in Fig. 3. Several alarms are shown, but in a final product only the first one will set off an actual alarm. The time for each alarm is annotated and sent to a third party, before the true seizure times are received from the recording site. This is to verify that it is a double-blind study. The results for each patient are shown in Table II.

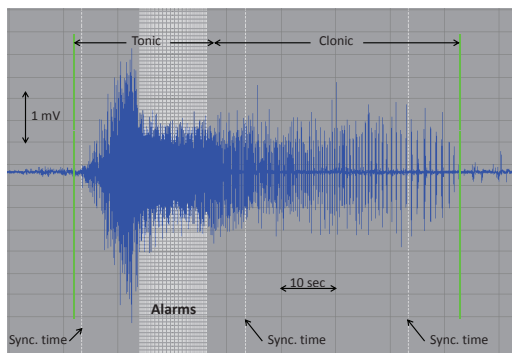


Fig. 3. The sEMG during the second GTC seizure from patient D208. The period is divided into a tonic and a clonic phase. It is seen that all the consecutive alarms are set within the tonic phase. The two green vertical lines mark the beginning and end of the seizure. The three single white vertical lines are as stated synchronization time stamps, which are set by the wireless device to keep track of the time.

For patient D207 no data are recorded on the tibial muscle. Patient D209 and D210 had no seizures, but neither did we detect any false alarms. Patient D208 had three GTC seizures during the admission, while patient D211 had four. For patient D208 we were able to detect all three seizures, and at the same time we did not register any false alarms. For patient D211 we succeeded in detecting one of the four seizures, while the other three were missed. Furthermore, we registered one false alarm for this patient.

TABLE II
THE RESULTS FOR EACH OF THE PATIENTS.

Patient	Sensitivity [%]	Latency [s]	FDR [h]
D207	-	-	-
D208	100	31; 18; 5	0.000
D209	-	-	0.000
D210	-	-	0.000
D211	25	46	0.008
Mean	57	25	0.003

III. DISCUSSION

The device proved to function intentionally for patient D208-D210 with a 100% sensitivity and no false alarms.

Unfortunately, it did not show as well a result for patient D211.

In patient D211, where the algorithm failed to detect three of the seizures, the seizures are quite different from the typical GTC seizures. These seizures consist of more interchanging tonic and clonic phases than the usual two. Furthermore each phase is shorter than during a classical GTC seizure. In Fig. 4 the count of zero-crossings during seizures are plotted for patient D200 (used for training of the parameters), D208 and D211. The features (zero-crossing) for the seizures are very much alike within each patient. It is furthermore seen that the feature for the seizures for patient D208 is very similar to the ones for patient D200, whereas the ones for D211 is seen to be very different. The algorithm detects the peak, which is seen to be both shorter and lower for the seizures for patient D211. Thus the tonic phases for patient D211 may not be long and strong enough for the algorithm to capture them. The many alternating phases of tonic and clonic activity may explain the longer latency, since there is a clonic phase before the tonic phase, where the seizures are detected. In general the latency could be improved, which is the plan for our future device. The used parameters are trained on a very narrow basis, and a modification of the algorithm towards a shorter detection time would be welcome. If the threshold was lowered to 250 (about the value for the conventional sEMG data) six of the seven seizures were captured, but the amount of false positives would also increase to seven.

Comparing the mean results in Table II (sensitivity = 57%, latency = 25s, FDR = 0.003/h) to our results on conventional sEMG data on the tibial muscle (sensitivity = 77%, latency = 14.1s, FDR = 0.2/h) presented in [10], the overall impression is an improvement, especially when taking into account that patient D211 in this study is an outlier. The sensitivity was better for the algorithm on the conventional sEMG data, but the false detection rate was significantly improved in our on-line algorithm.

If we compare our results to Kramer *et al.* [15] they have a higher sensitivity (91%). Our FDR is however slightly lower than theirs (0.004/h). Also Lockman *et al.* [14] have an interesting study with a sensitivity of 88% and 204 false positives. Unfortunately they do not list the number of hours of data which they have analyzed, but they do state, that they have a very high FDR. Our results do show a too low sensitivity compared to these studies, but if we exclude the outlier patient (D211), we would have shown a 100% sensitivity, which we expect to do for future patients with typical GTC seizures as well. Our false detection rate is the lowest of all the studies, which make our system the most reliable regarding false alarms. Since the other two methods are based on a detection in the clonic phase, compared to ours in the tonic phase, we expect to have a lower latency period.

In our previous study on the conventional sEMG data, the results showed to be significantly better for the data recorded on deltoid, compared to those recorded from the tibial muscle. In an unpublished study we obtained the same

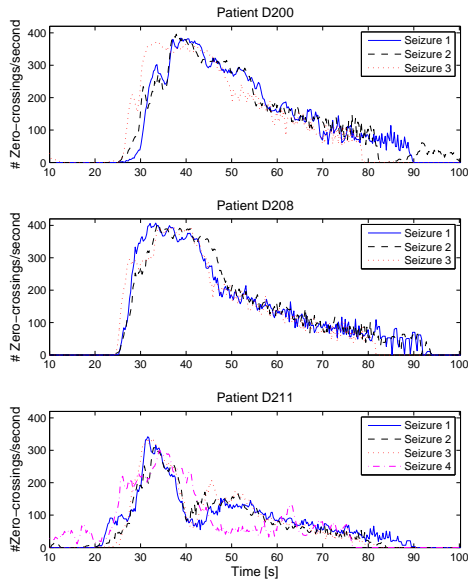


Fig. 4. The zero-crossing counts for each seizure for patient D200, D208 and D211, respectively.

promising results for data recorded from biceps. We therefore expect to get a better result when testing the algorithm on data from our wireless device recorded from the biceps, however firstly we need to train parameters for this, since there are differences between the two muscles with respect to using the algorithm.

The missing data for the first patient imply that we have some recording problems, which need to be clarified. It should be noticed that the used wireless device is only a prototype and the next version is in preparation. Thus the complications are expected to be corrected.

IV. CONCLUSION

Our wireless device with an implemented generic algorithm is the first device developed towards detection of generalized tonic-clonic seizures based on a single sEMG channel. The algorithm detects whenever a GTC seizure starts. The results showed that the device performed as intended for three of the five patients. For one patient it failed to record any data and for another it only managed to register one of four GTC seizures. However, the FDR has proven to be extremely low, despite our huge amount of data for each patient. Furthermore we have an explanation towards

the three missing detections, so we find that the results are very promising. We expect to achieve an even better result, when we test our device on sEMG data from the biceps.

V. ACKNOWLEDGEMENTS

This work was supported by the Peter & Jytte Wolf Foundation for Epilepsy, the Danish Epilepsy Centre, the Danish Agency of Science Technology and Innovation, the Technical University of Denmark, and the Danish National Advanced Technology foundation.

REFERENCES

- [1] R. Fisher, W. Boas, W. Blume, C. Elger, P. Genton, P. Lee, and J. Engel Jr, "Epileptic seizures and epilepsy: definitions proposed by the International League Against Epilepsy (ILAE) and the International Bureau for Epilepsy (IBE)," *Epilepsia*, vol. 46, no. 4, pp. 470–472, 2005.
- [2] L. Rudzinski and K. Meador, "Epilepsy: Five new things," *Neurology*, vol. 76, Suppl 2, no. 7, pp. S20–S25, 2011.
- [3] J. French, "Refractory epilepsy: one size does not fit all," *Epilepsy Currents*, vol. 6, no. 6, pp. 177–180, 2006.
- [4] W. Blume, H. Lüders, E. Mizrahi, C. Tassinari, W. van Emde Boas, E. Engel Jr, *et al.*, "Glossary of descriptive terminology for ictal semiology: report of the ilae task force on classification and terminology," *Epilepsia*, vol. 42, no. 9, pp. 1212–1218, 2001.
- [5] P. Jennum, J. Gyllenberg, and J. Kjellberg, "The social and economic consequences of epilepsy: A controlled national study," *Epilepsia*, vol. 52, no. 5, pp. 949–956, 2011.
- [6] S. Shorvon and T. Tomson, "Sudden unexpected death in epilepsy," *The Lancet*, vol. 378, pp. 2028–2038, 2011.
- [7] D. Hesdorffer, T. Tomson, E. Benn, J. Sander, L. Nilsson, Y. Langan, T. Walczak, E. Beghi, M. Brodie, and A. Hauser, "Combined analysis of risk factors for sudep," *Epilepsia*, vol. 52, no. 6, pp. 1150–1159, 2011.
- [8] D. Hesdorffer, T. Tomson, E. Benn, J. Sander, L. Nilsson, Y. Langan, T. Walczak, E. Beghi, M. Brodie, and W. Hauser, "Do antiepileptic drugs or generalized tonic-clonic seizure frequency increase sudep risk? a combined analysis," *Epilepsia*, 2011.
- [9] I. Conradsen, P. Wolf, T. Sams, H. Sorensen, and S. Beniczky, "Patterns of muscle activation during generalized tonic and tonic-clonic epileptic seizures," *Epilepsia*, vol. 52, no. 11, pp. 2125–2132, 2011.
- [10] I. Conradsen, S. Beniczky, K. Hoppe, P. Wolf, and H. Sorensen, "Automated algorithm for generalised tonic-clonic epileptic seizure onset detection based on semg zero-crossing rate," *Biomedical Engineering, IEEE Transactions on*, vol. 59, no. 2, pp. 579–585, 2012.
- [11] I. Conradsen, S. Beniczky, P. Wolf, T. Kjaer, T. Sams, and H. Sorensen, "Automatic multi-modal intelligent seizure acquisition (misa) system for detection of motor seizures from electromyographic data and motion data," *Computer Methods and Programs in Biomedicine*, 2011. Published online.
- [12] I. Conradsen, S. Beniczky, P. Wolf, J. Henriksen, T. Sams, and H. Sorensen, "Seizure onset detection based on a Uni-or Multi-modal Intelligent Seizure Acquisition (UISA/MISA) system," in *Engineering in Medicine and Biology Society (EMBC), 2010 Annual International Conference of the IEEE*, pp. 3269–3272, IEEE, 2010.
- [13] K. Cuppens, L. Lagae, B. Ceulemans, S. Van Huffel, and B. Vanrumste, "Detection of nocturnal frontal lobe seizures in pediatric patients by means of accelerometers: A first study," in *Conference proceedings: 31st Annual International Conference of the IEEE Engineering in Medicine and Biology Society*, vol. 1, pp. 6608–6611, 2009.
- [14] J. Lockman, R. Fisher, and D. Olson, "Detection of seizure-like movements using a wrist accelerometer," *Epilepsy & Behavior*, 2011.
- [15] U. Kramer, S. Kipervasser, A. Shlitner, and R. Kuzniecky, "A novel portable seizure detection alarm system: Preliminary results," *Journal of Clinical Neurophysiology*, vol. 28, no. 1, p. 36, 2011.
- [16] T. van Beelen, "Edfbrowser." www.teuniz.net/edfbrowser/.